Welsh School of Pharmacy

Cardiff University

TOWARDS A NANOMEDICINE-BASED BROAD-SPECTRUM TOPICAL VIRUCIDAL THERAPEUTIC SYSTEM

By

DAVID MALCOLM JOHN HOUSTON

A thesis submitted to Cardiff University in

accordance with the requirements for the degree

of

Doctor of Philosophy

September 2011

THESIS DECLARATION AND STATEMENTS PAGE

DECLARATION

This work has not previously been accepted in substance for any degree and is not concurrently submitted in candidature for any degree.

Signed  **(candidate) Date 26-01-2012**

STATEMENT 1

This thesis is being submitted in partial fulfilment of the requirements for the degree of Ph D.

Signed  **(candidate) Date 26-01-2012**

STATEMENT 2

This thesis is the result of my own independent work/investigation, except where otherwise stated. Other sources are acknowledged by explicit references.

Signed  **(candidate) Date 26-01-2012**

STATEMENT 3 PREVIOUSLY APPROVED BAR ON ACCESS

I hereby give consent for my thesis, if accepted, to be available for photocopying and for interlibrary loans after expiry of a bar on access previously approved by the Graduate Development Committee.

Signed  **(candidate) Date 26-01-2012**

ACKNOWLEDGEMENTS

The support of the Welsh Office of Research and Development in funding this study and my studentship is greatly appreciated.

I am very grateful for the help and support given to me by my supervisors – Dr Charles Heard, Prof Stephen Denyer and Dr Joachim Bugert. Their help and support, and particularly their relevant challenges and expectations have been invaluable to me during the period of study. Charles has not only been a superb supervisor – he has inspired me to pursue an academic career, and has become a great friend.

I would like to thank Dr I McDonald and Dr N Buurmer for the use of their equipment and expertise.

Many thanks to fellow doctorate students Nor, Nassima, Hanif, Wing and Caroline, who have helped to encourage me, and with whom it has been a pleasure to learn, and a thankyou to the masters students Beth, Oliver and Jon.

Thank you to my family who have given me their full support, help with transport/printing, and kept faith in me to succeed. I am so grateful to Jane, Phil and Rachel who have been so generous with their time. Thanks to my friends who are always there for me (Harry).

And finally a special thanks to my mother who has inspired me not only in academia but also in life.

ABBREVIATIONS

24 WP	24 well plate
96 WP	96 well plate
AA	Aachiodonic acid
APS	Ammonium persulphate
COX	Cyclooxygenase
CTEM	Cyclopore Track Etched Membrane
DI	Deionised
DMEM	Dulbecco`s minimum essential medium
DMSO	Dimethyl sulphoxide
DPBS	Dulbecco`s phosphate-buffered saline
DPX	Di-butylpthalatexylene
DTT	Dithreitol
EDTA	Ethylene diamine tetraacetic acid
EtOH	Ethanol
FBS	Foetal bovine serum
FDC	Franz diffusion cell
$FeSO_4$	Ferrous sulphate
HBSBS	Hanks balanced salt buffer solution
HEPES	4-(2-hydroxyethyl)-1-4piperazineethanesulfonic acid
HIV	Human immunodeficiency virus
HPLC	High performance liquid chromatography
HRP	Horse radish peroxidase
HSBM	Heat separated buccal membrane
HSE	Heat separated epidermis
HSV	*Herpes simplex* virus
HSV-2 ACR	Aciclovir resistant *Herpes simplex* virus type 2
ICC	Immunocytochemistry
ICP MS	Inductively Coupled Plasma Mass Spectrometry
IHC	Immunohystochemistry
ITC	Isothermal Titration Calorimetry
Jss	Pseudo-steady state flow
LOD	Limit of detection
LOX	Lipooxygenase
MTT	3-(4, 5-dimethylthiazol-2yl)-2,5-diphenyl tetra bromide
NSAIDs	Non-steroidal anti inflammatory drugs
PAGE	Polyacrylamide gel electrophoresis
Pb	Phthalate buffer
PBS	Phosphate buffered saline
PMSF	Phenylmethyl sulphonyl fluoride

PRE	Pomegranate rind extract
RIPA	Radio immune precipitation assay
RK13	Rabbit kidney epithelial cell line 13
SC	Stratum corneum
SDS	Sodium dodecyl sulfate
SDVM	Scalpel dissected porcine vaginal mucosal membrane
TBS	Tris-buffered saline
TDF	Tannin devoid fraction
TEMED	N,N,N`,N-Tetramethylethylenediamine
TFA	Trifluoroacetic acid
TPT	Total pomegranate tannins
US	United states
Vero	Green monkey kidney epithelial cells
$ZnSO_4$	Zinc sulphate heptahydrate

SUMMARY

The health benefits of the fruit of *Punica granatum* (pomegranate) have been recognised for many centuries. This thesis tested the hypothesis that a potent novel antimicrobial system could be developed based upon the activity of pomegranate rind extract (PRE), particularly when combined with a potentiating agent, and focussed on studying activity against *Herpes simplex* virus, types 1 and 2 (HSV-1 and HSV-2). High potentiated virucidal action of PRE against HSV-1 was observed when ferrous sulphate ($FeSO_4$) was added; however, this activity diminished rapidly and also gave rise to an unsightly black byproduct. Data was obtained suggesting this was linked to the rapid oxidation of ferrous to ferric (Fe (II) to Fe (III)); however, no such oxidation was indicated when zinc sulphate ($ZnSO_4$) was added instead, prompting an exploration of the effects of PRE + $ZnSO_4$ combination on HSV. The potentiation of PRE by $ZnSO_4$ in *virucidal* mode was comparable to that observed with $FeSO_4$ (at the concentration examined for both metal salts). More in-depth investigation of the potentiation of PRE and $ZnSO_4$ achieved over a 9000 fold increase in viral destruction in comparison to either agent alone. This activity was not transient and did not produce a (black) byproduct. Other salts of Zn (II) generally performed similarly to $ZnSO_4$, with the main exception of ZnO which was too insoluble in water to test. When the *antiviral* properties of PRE were examined, the results were again potent and comparable to Aciclovir, the established treatment for *Herpes simplex* infections. Furthermore, PRE demonstrated even greater potency against Aciclovir-resistant HSV-2. When applied to *ex vivo* skin, PRE produced a 66% reduction in the level of cyclooxygenase-2 (COX–2) - an important inflammatory mediator - with the presence of $ZnSO_4$ having no effect. PRE and $ZnSO_4$ were formulated as a stable hydrogel, which was able to effectively deliver the biologically active compounds through the epidermal, buccal and vaginal membranes to the epidermal/dermal interface - the major sites of HSV-1 and HSV-2 vesicular clusters during a clinical infection.

TABLE OF CONTENTS

LIST OF FIGURES

LIST OF TABLES

Chapter 1 **General Introduction**

1.1. Overview

Funded by a Welsh Office of Research and Development (WORD) studentship, this thesis explored the potential for developing a new therapeutic antimicrobial system based on extracts of the fruit rind of *Punica granatum*, or pomegranate, referred to as PRE. In particular, the work built upon previous observations that potent antimicrobial activity occurred when PRE was combined with a potentiating or synergising agent. Although the health and antimicrobial benefits of the pomegranate have been known for many centuries, it had more recently been found that the addition of ferrous sulphate dramatically increased activity against bacteriophages. For reasons outlined, the focus of this work shifted to PRE and zinc sulphate, and this combination was probed in numerous multi-disciplinary scientific areas, particularly against *Herpes simplex* virus, but always with translation to a viable commercial topical product as a key goal, in line with the WORD award.

This thesis will explore the virucidal, antiviral and anti-inflammatory properties of PRE, with the use of a number of virucidal potentiators, and will aim to develop a resultant topical therapeutic system for use in *Herpes simplex* viral type 1 and 2 infections. This introduction includes the relevant background knowledge of PRE, viruses, particularly *Herpes simplex* virus, its clinical pictures and treatments currently available, and the structure of skin as it pertains to the topical delivery of therapeutic agents.

1.2. Historical Summary of *Punica Granatum L.*

The fruit of the *Punica granatum* (the pomegranate) has been known throughout recorded human history; it has not only been eaten as a fruit, but extracts rich in tannins have been used in tanning leather. The fruit was agriculturally grown in ancient Egypt; in Greek mythology the pomegranate is key to the story of Persephone and Hades and in many various mythological beliefs it is thought to be the fruit of the underworld. In Judaism its seeds represent the 613 commandments in the Torah, and Spanish conquistadors introduced it to the Americas where the fruit now grows in abundance.

Punica granatum, a relatively small tree originating in the Orient, belongs to the *Punicaceae* family and at present is mainly grown in the USA, India and Far Eastern

countries. The main use of pomegranate is as table fruit, although large amounts are used in the beverage and liquor industries(Patel, et al. 2008). The pomegranate is classified as a family of one genus and two species, one species in the wild form with a smaller fruit (5-8cm diameter) in comparison to the cultivated form (6-12cm diameter), the other species being a dwarf form grown as an ornamental plant (Ward 2003). The pomegranate tree/fruit can be divided into distinct components; the seed, juice, rind, flowers, leaf, bark and root.

In Greek, Arabic and Chinese history the pomegranate was representative of wealth, fertility and the afterlife. The pomegranate has also been used to treat a wide range of ailments throughout history. In De Materia Medica written by Dioscorides, in the first century A.D. the use of pomegranate flower, rind and seed for medicinal purposes has four main entries. The document describes the use of these extracts for the treatment of ulcers of the mouth and genitals, pains in the ears, bleeding gums and loose teeth. It was also used to kill *latas tineas ventris* (tape worm) (Gunther 1934). According to Unani Tibb medicine, with its roots in Greek, Egyptian, Arabic and Indian Medicine and mentioned in the Koran, pomegranates are used medicinally for diarrhoea, earache, bad vision, fevers, teeth and gum disorders and indigestion.

In Cairo (circa 11th century) it was discovered that pomegranates were used for the treatment of eye diseases, inflammatory conditions of the tongue and gums, fevers, heptic and septic fevers, cancer, erysipelas, soft and hard inflammatory swellings and elephantiasis (Lev 2007). 16th century Cypriote monastery prescriptions detailed the topical use of pomegranate for the treatment of skin wounds and *Herpes* type infections (Lardos 2006).

1.2.1. Phytochemical review of *Punica granatum L*

Over 120 different phytochemicals have been identified in the juice, seed, peel and rind of the pomegranate (N. P. Seeram 2006). There has been a substantial amount of research conducted upon different components and chemical extracts of the pomegranate. Punica granatum rind extracts (PRE) have been shown to possess significant antioxidant activity in various *in vitro* models (Kotamballi 2002). PRE contains a large proportion of polyphenols e.g. ellagic acid, gallotannins, anthocyanidins such as delphinidin, cyanidin and pelargonidin, proanthocyananidins

and various flavonoids. Of specific interest are the hydrolysable tannins; punicalin, pedunicalin, punicalagin as well as gallic and ellagic acid esters of glucose (Mustafa, Yaşar and Gökhan 2009). Punicalagin is the most abundant, constituting 80-85% w/w of total pomegranate tannins. Other bioactivities have been described for PRE and punicalagin, including antiproliferation, apoptopic and antibacterial properties (Seeram, et al. 2005) (Negi and Jayaprakasha 2003). The antibacterial bioactivity of PRE has been attributed mainly to fractions extracted with acetone and MeOH. The antibacterial effect was observed against both gram-positive and gram-negative bacteria. 100 percent growth inhibition of *B. cereus, B. subtilis, B. coagulens, S. aureus, E. coli* and *P. aeruginosa* was shown at 300 ppm (Negi and Jayaprakasha 2003).

The punicalagin is a large polyphenolic compound, the molecular formula is $C_{48}H_{28}O_{30}$ and it has a molecular mass of 1084.718 amu. The compound consists of 11 rings with ester bridging groups. Punicalagin exists in two anomers punicalagin α and β with a ratio of roughly 1:2 respectively. The structure of the molecule is shown in Figure 1-1. The hydrolysis of punicalagin to its breakdown products, ellagic acid and Punicalin, is shown in Figure 1-2. Punicalagin and its major degradation compounds are thought to be the main bioactive extracts present in PRE (Seeram, et al. 2005), analysis of the PRE research with respect to permeation and penetration will be quantified through the detection of the two punicalagin anomers.

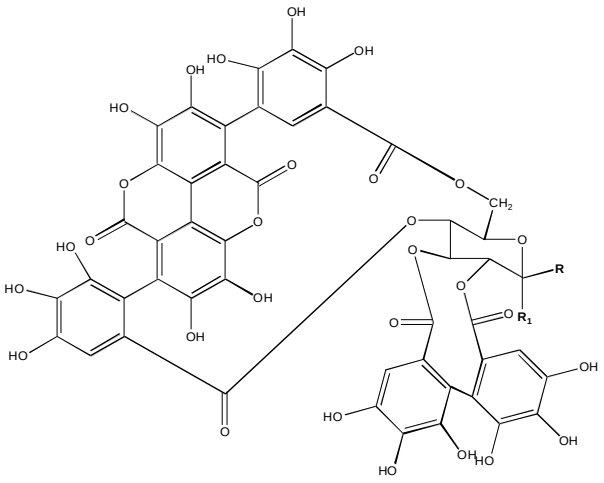

Figure 1-1 Structure of the abundant hydrolysable tannin, Punicalagin.

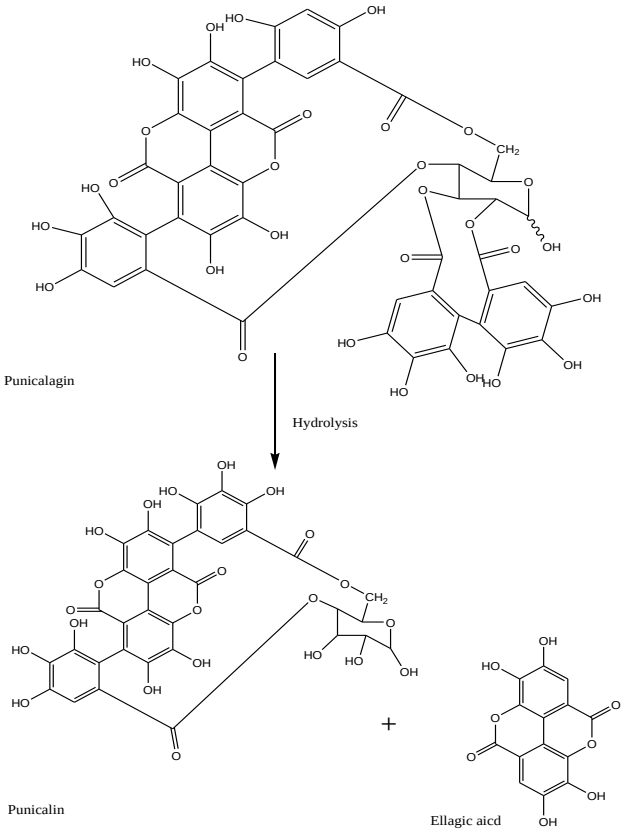

Figure 1-2 Hydrolysis of Punicalagin yielding Punicalin and Ellagic acid.

1.2.2. Radical Scavenging and Antioxidant Capacity of *Punica granatum*.

An antioxidant is a substance that when present at low concentration, compared to that of an oxidisable substrate, significantly delays or prevents oxidation of that substrate (Gil, et al. 1996). Antioxidants may act in various ways, by scavenging free radicals or by decomposing peroxides and by chelating metal ions (Kulkarni, Aradhya and Divakar 2004). Antioxidant properties extracted from plant species play an important part in human health care. The protective effects of antioxidants in biological systems are ascribed mainly to their capacity to scavenge free radicals, chelate metal catalysts, activate antioxidant enzymes and inhibit oxidization.

The antioxidant activity of the pomegranate is largely attributed to the presence of the ellagitannin, punicalagin (Slusarczyk, et al. 2009). The ability of punicalagin to act as an antioxidant, with the potential to reduce free radicals involved in chain reactions that damage cells, has been well established with differing materials and methods (Turk, et al. 2008). Punicalagin anomers α and β are the main active phytochemicals for this type of cytoprotection, accounting for 92% of the antioxidant activity (Sestili, Chiara and

Vilberto 2007). It is also important to note that gallic acid and ellagic acid, which although are only in small quantity, are also potent antioxidants. Therefore when punicalagin breaks down, the total antioxidant capacity is not greatly decreased.

1.2.3. Antiviral and Virucidal Action

The potential virucidal activity of the pomegranate rind extract is shown in the research on phage reduction assays (Stewart, et al. 1998), specifically the combination of pomegranate rind extract and Ferrous Sulphate ($FeSO_4$) in an acid buffer (phthalate buffer at pH 4.5).

The use of bacteriophages as suitable surrogates for mammalian viruses in both medical and environmental virology applications has been reported in a number of studies. A current review stated that there is a considerable body of evidence to suggest and support the use of bacteriophages as surrogates for mammalian viruses. "The use of appropriately sized bacteriophages provides an innocuous, efficacious and expeditious method for economical testing and validation of viral clearance capabilities" (Aranha-Creado and Brandwein 1999).

This combination of PRE and $FeSO_4$ was reported to be extremely potent, producing an eleven-log reduction in plaque forming ability of phage within two minutes of application of an aqueous mixture at room temperature (Stewart, et al. 1998). The two bacteriophages *Pseudomonas aeruginosa* and *Escherichia coli* phage were used in Stewart's study. They displayed significant and detrimental damage to their head and tail regions as well as to their overall integrity, following treatment with pomegranate rind extract and Ferrous Sulphate solution combined. The use of an acidic buffer was believed to help protect the hydroxyl groups. Although this level of acidity would be expected to demonstrate a phagicidal effect, it is negligible when compared to that of the PRE and $FeSO_4$.

Research has been conducted to assess the antiviral effect of pomegranate juice by applied *in vitro* methods, and demonstrated that pomegranate juice extracts had antiviral effects against HIV; the mechanism of action appeared to inhibit the binding of the HIV-1 envelope glycoprotein gp 120, preventing the interaction of HIV-1 with the CD4 receptor, and thus reducing the infectivity of the virus (Neurath, et al. 2004).

Corao reported an inhibition in α-glucosidase and Human Leukocyte Elastase activity by pomegranate rind extract (Corao 2001). This action impedes viral attachment and penetration via disruption of the glycosylation of viral glycoproteins and is also observed with an extract of *Hamamelis virginiana* bark, which displays significant antiviral activity against HSV type 1.

1.3. **General Virology**

Viruses are sub-microscopic particles unable to reproduce outside a host cell. Their size varies between 30-400 nm. Each virion is composed of genetic material (RNA or DNA) within a capsid core of protein material and the shapes of viruses are very diverse. The replication process of viruses vary according to their specific make up but there are six basic stages of virus life cycles in the living cell: attachment, penetration, un-coating, replication, assembly and release – as shown in Figure 1-3.

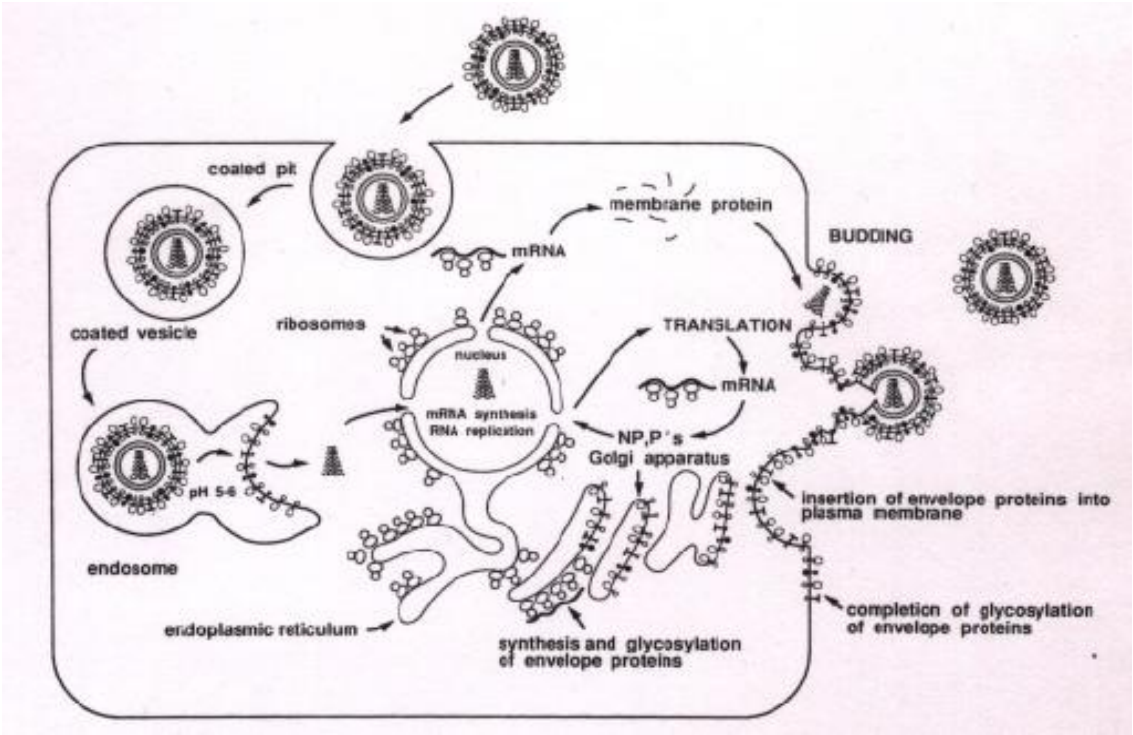

Figure 1-3 A Diagrammatic Representation of Viral Replication (Lamb and Krug 1996).

1.3.1. Attachment

A prerequisite for this step is the collision between the virion and the cell. Viruses do not have the capacity for locomotion and so the collision event is a random process determined by diffusion (Sherris 1990) and Brownian motion. In some cases there is specific binding between the viral envelope and specific receptors on the host's cellular surface. This attachment can induce the viral protein receptor to change so that it fuses with the host cellular membrane. Once a virus has penetrated to the inside of the cell it is effectively hidden from the immune system.

1.3.2. Penetration

Following attachment the virus can enter the host cell in two main ways. Receptor mediated endocytosis which is when the virus binds to receptors on the surface and is surrounded and contained within a vacuole that fuses with cellular endosomes. The other main entry technique of viruses is fusion: where an enveloped virus can directly fuse with the cell membrane, which results in release of the viral capsid into the cytoplasm (rarely the whole virus particle can pass directly into the cytoplasm (Ojala, et al. 2000).

1.3.3. Un-coating

Un-coating refers to the process where the capsid core is degraded by viral and or host enzymes and the viral genome is exposed for transcription and replication. Removal of the capsid core from the virus can occur in two ways: upon entry or, for virions that replicate inside the nucleus, the genome must penetrate through the nuclear membrane or the virus un-coats in the cytoplasm. This process is enabled by interactions between the viral capsid and nuclear pore complexes, which results in the release of the viral genome into the nucleoplasm (Dimmock and Primrose 2007).

1.3.4. Replication

The process of replication is to synthesise viral mRNA (transcription) and protein synthesis. David Baltimore and Howard Temin discovered the reverse transcriptase in retrovirus and identified the key molecule for viral replication as mRNA (Flint 2000).

The Baltimore classification system identifies seven classes based upon the strategies used by virus mRNAs for replication. The initial stages of replication are very cell dependent, the late stages tend to be more virus led. Once uncoated the nucleic acids are revealed so that replication can take place.

Class I: double stranded DNA (ds DNA) viruses e.g. Adenovirus, Herpes virus, and Poxvirus. These viruses are dependent upon the cell cycle, as they must enter the host nucleus to replicate and require host cell polymerization. In this class the designation of plus and minus is not meaningful since different mRNA species may come from either strand.

Class II: e.g. parvoviruses, viruses which have a single stranded DNA genome of the same sense as mRNA. They replicate in the nucleus and form a double stranded DNA intermediate during replication.

Class III: e.g. reoviruses. Consist of viruses with a double stranded RNA. This class replicates in the cytoplasm.

Class IV: e.g. picornaviruses, togaviruses. Consists of viruses of a single stranded RNA genome of the same sense of mRNA (positive strand RNA viruses). Replication is mainly in the cytoplasm and does not rely upon the cell cycle in comparison to DNA viruses.

Class V: e.g. orthomyxoviruses, rhabdoviruses. Consists of viruses that have a single stranded RNA genome that is complementary in base sequence to the mRNA (negative strand RNA viruses). Replication is mainly in the cytoplasm and does not rely upon the cell cycle as much as other viruses.

Class VI: e.g. retrovirus. Consists of viruses that have a single stranded positive sense RNA genome and which have a DNA intermediate during replication. One of the defining features of this is the use of reverse transcriptase to convert the positive sense RNA into DNA.

Class VII: e.g. hepadnaviruses. Consists of viruses with double stranded DNA that replicate through a single stranded RNA intermediate (Baltimore 1971).

1.3.5. Assembly and Release

Virus assembly involves a process in which the chemically distinct macromolecules are transported, often through different pathways, to a point within the cell where they are assembled into a viral particle (Fields, Knipe and Howley 2007). The assembly process divides viruses into two distinct groups. This is based on the presence or absence of a lipid bi-layer envelope. For non-enveloped viruses the assembly takes place in the cytoplasm or nucleus. They exit from the cell by breaking through the cell membrane and causing lysis. Enveloped viruses must obtain a lipid bilayer in their assembly from one of the cells membranes. The nucleocapsids exit from the nucleus and pass out of the cell by a process known as budding where the virus acquires the lipoprotein envelope.

1.3.6. Viruses Possibly Suitable for Topical Virucidal and Antiviral Treatment

There are three main virus types responsible for the majority of viral skin infections poxviruses, papilloma viruses and herpes simplex virus. Pox viruses are a very large family of viruses that are always enveloped. They vary in shape and size but are up to 250nm in diameter and 350nm in length. They are classified as a dsDNA virus and follow this route of replication. The papilloma viruses are a diverse group of non-enveloped viruses. Over 100 different types of human papilloma viruses (HPV) have been identified. Each different virus is numbered as HPV 1, HPV 2 and so on. They replicate exclusively in the skin and mucosal surfaces of the genitalia, anus, airways and mouth. Some of these viruses have been linked to cancers that kill thousands of people each year, with the following being high risk - HPV 16, 18, 31, 33, 35, 39, 45, 51, 52, 56, 58, 59, and 68 (Smith, et al. 2008). This is an interesting area for the possible use of transdermal and topically applied drugs.

Examples of human pathogenic *Herpes*-viridae include Varicella-Zoster virus responsible for chicken pox and shingles, cytomegalovirus and *Herpes simplex* virus. Latency is a characteristic property of *Herpes* virus (Garner 2003).

The mode of action of a drug used to combat a viral based infection can be placed into two main groups, anti viral and virucidal. Anti viral drugs work on the principle of

preventing one or more of the six basic stages of the virus life cycle in the living cell. Virucidal drugs effectively kill the virus by destroying a part or all of the viral structure, usually the viral capsid.

1.3.7. Evaluating treatment efficacy

From an efficacy standpoint, the most appropriate way to test the hypothesis of PRE with the combination of a metal salt either as a virucidal, or an antiviral, or both, would be via a controlled clinical investigation, involving an adequate number of human test subjects. Such evaluations are very costly, involve a great deal of coordination and necessitate the obtaining of full ethical approval (MHRA 2011). A crucial prerequisite is a series of *in vitro* tests performed to determine the potential of various treatments, prior to clinical evaluation.

The activity of potential treatments against viruses can be determined in 2 modes, depending on the activity against the virus.

1.3.7.1. Antiviral

Antiviral activity occurs when a test agent acts to inhibit the replication of the virus, without actually destroying it. Most topical antivirals, including Aciclovir (a thymidine kinase inhibitor) competitively inhibit viral DNA polymerase (Whitley and Gnann 1992). Although efficacious, this type of product cannot destroy the viral load near the point of application, which may be associated with viral latency, the re-emergence of cold sores and transfer. Furthermore continual use of stereosymetrical compounds can facilitate drug-resistance, for example the increasing prevalence of Aciclovir resistant HSV-1 and 2 strains due to continual/overuse of Aciclovir and similar derivatives (Erlich, et al. 1989) (Whitley and Gnann 1992) (Bacon, et al. 2003). To quantify the antiviral activity a plaque reduction assay was used to quantify the infectious HSV-1 and HSV-ACR virions (Matrosovich, et al. 2006).

1.3.7.2. Virucidal

Virucidal activity may be described as one in which the viruses are destroyed by the presence of the test agent. Many compounds, given high enough concentration, are capable of destroying viruses. However these tend to be powerful biocides such as Dettol (chemical) and bleach (sodium hypochlorite). Such materials should not be

applied directly to skin in view of toxicity, inflammation and injury. The virucidal activity can be tested via a plaque reduction assay due to the ability of HSV-1 to form plaques within the vero cell host, each plaque representative of one HSV-1 virion (Schuhmacher, Reichling and Schnitzler 2003).

1.4. *Herpes simplex* virus

The *Herpes simplex* virus is a member of the *Herpes viridae* family. The virus frequently infects humans, causing a range of diseases from mild uncomplicated mucocutaneous infection to life threatening illness. From this family the strains HSV-1 and -2 are the most prevalent pathogens. HSV-1 is normally associated with orofacial infections and encephalitis, HSV-2 is normally associated with genital infections, and can transfer from mothers to neonates. After primary infection, HSV-1 and HSV-2 can cause latent infections, the virus resides in neurones of dorsal root ganglia and the autonomic nervous systems. However, it is now clear that HSV can also remain latent elsewhere, e.g. in the superior cervical and vagal ganglia. The suspicion that the virus might also remain latent in the cells of the skin or mucous membranes has never been proven in human infection (Topley and Wilson 1990). The virus resides in latently infected ganglia in a non-replicating state with a very low level of virus gene expression. Infective HSV grows rapidly in cell culture which has led to the speculative theory that the latent virus is not present as virions but as viral DNA integrated into cellular genomes. The viral latency lasts for the lifetime of the host.

Recurrent oral facial infections of HSV-1 and -2 are generally referred to as cold sores, *Herpes* labialis and fever blisters. The lesions usually occur on the skin by the cutanneous branches of the maxillary and mandibular branches of the trigeminal nerve (Weatherall, Gledingham and Warrell 1996). Vesicles are most common on the lips or skin around the mouth and often recur in the same place. Recurrence only occurs in around 30% of people with only 10% being affected once a month. Recurrent herpetic eruptions are precipitated by overexposure to sunlight, febrile illnesses, physical or emotional stress, immunosuppression, or unknown stimuli.

1.4.1. Classification

Herpes simplex virus 1 and 2 are two closely related viruses of the *Herpes* virus family. They are double stranded DNA viruses of the *Herpes viridae* family and are classified within a sub-family as alpha *Herpes virinae* of the *simplex* virus genus.

1.4.2. Structure

The structure of HSV-1 and HSV-2 are very similar, both encapsulated within an envelope as shown in Figure 1-4. They contain a large double stranded DNA molecule. The HSV virion is roughly 110-130 nm in diameter and consist of four main parts

- an electron dense core containing viral DNA
- an icosapentahedral capsid composed of 6 proteins
- the tegument -an amorphous layer of at least 15-20 proteins, which is in contact with both the capsid and the envelope
- the envelope containing at least 8 glycoproteins.

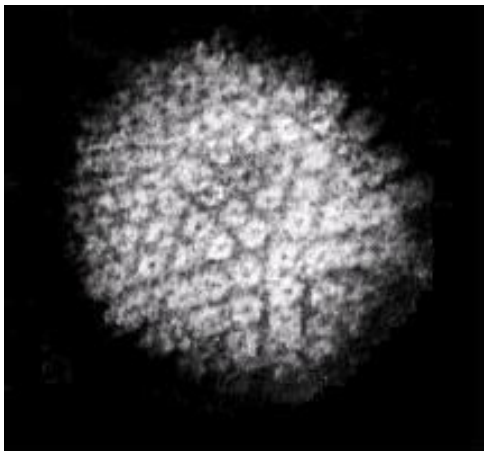

Figure 1-4 TEM micrograph of a *Herpes simplex* virus (NASA 2009).

1.4.3. Binding

The entry of HSV-1 and -2 requires the binding of the virus to receptors on the cell surface for fusion of the envelope and the cell plasma membrane to occur. The

envelope glycoproteins that are known to be involved in the binding process are gB, gC, gD and gH-L(Heldwein and Krummenacher 2008). The proteins gB, gD and gH-L are indispensable as deletion of these proteins results in an entry defective phenotype (Browne, Bruun and Minson 2001) (Subramanian and Geraghty 2007).

1.4.4. Nuclear Import, Replication and Transcription

Upon entry to the host cell the HSV neucleocapsid is transported to the nuclear pores, where viral DNA is released onto the nucleus (Newcomb and Brown 2007). The immediate-early (α) phase of viral transcription occurs when the viral genome is accompanied by the α-TIF protein. The transcription of RNA occurs when DNA is transcribed to RNA, by DNA dependent RNA polymerase.

The control of mRNA to: synthesize new virus particles causing cell death; synthesize new virus particles constantly shedding virus; and remain latent is dependent on the nuclear factors of the cell and proteins encoded by the virus. The formation of latent infection is due to the properties of the host cell preventing progression beyond the immediate early genes. DNA replication, the formation of capsids, and packing of viral DNA occur in the nucleus (Roizman 2007).

1.4.5. Assembly and Budding

The envelopment of alpha herpes viruses is a complex process. An outline of this process is shown in Figure 1-5 and a brief description is given below. The egress of the HSV-1 virion requires a budding process from the inner nuclear membrane that contains viral glycoproteins (Mettenleiter 2002). A mature capsid surrounded by the tegument protein U_L31 directs the process of budding through the nuclear membrane into which the U_L31 and U_L34 phosphorylated membrane protein has been inserted (Wagner 2003). The primary envelope is then lost as the capsid buds through the outer nuclear membrane after which the tegument proteins (α-tif and vhs given in diagram) encapsulate the capsid (Enquist, et al. 1999). The mature capsids and tegument protein acquire the full envelope by budding into exocytotic vesicles (Gil, et al. 2002). The virion is now complete and can remain within the cell or be released as an infectious virion (Wagner 2003).

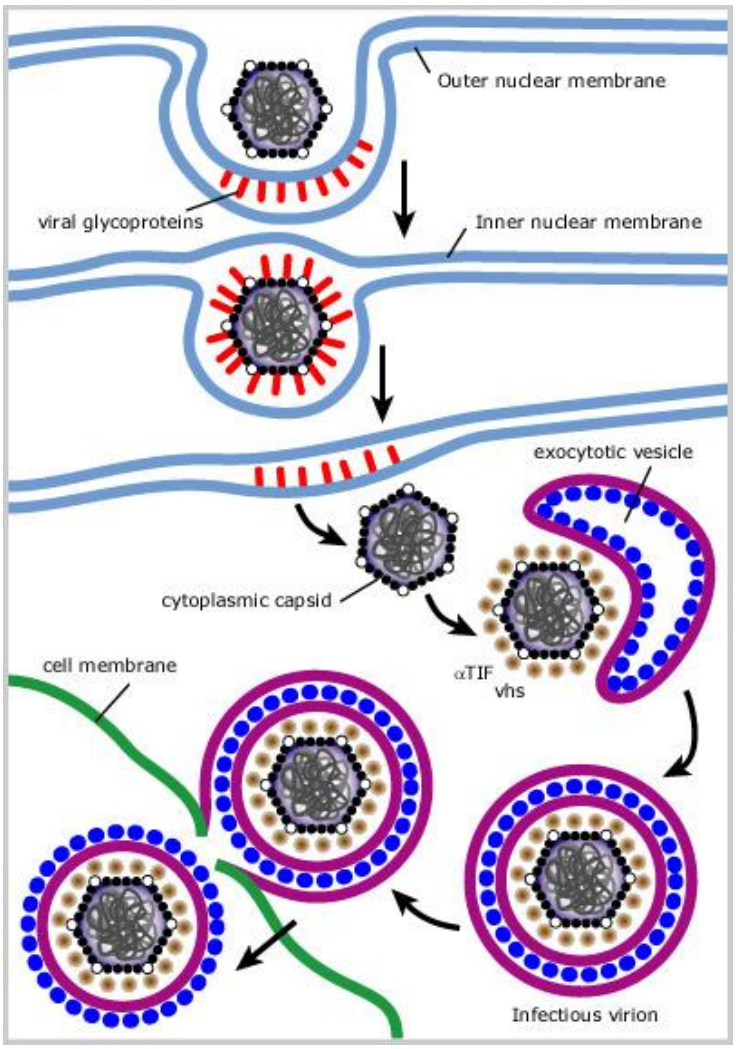

Figure 1-5 A diagrammatic representation of the Assembly and budding of HSV-1 within epithelial cells (Wagner 2003).

1.4.6. Pathology and the Clinical Picture

Irrespective of the viral type, HSV-1 or HSV-2 primarily affects skin and mucous membranes. The classic perspective on perioral and genital herpetic infections describe peri-oral infection as caused by HSV-1 and anogenital infection as caused by HSV-2. However, these distinctions are imprecise as HSV-1 or HSV-2 can be associated with any of the syndromes and their symptoms listed in Table 1-1.

Herpetic infection	Characterising Symptoms
Primary Herpetic Gingivostomatitis	Wisespread painful oral/perioral vesiculo-ulcerative lesions
Reccurrent Orofacial Herpes	Single painful lesions on skin of lip or face
Genital Herpes	Ulcerative lesions on the penis, vulvae and vagina
Eczema Herpeticum	Widespread infection of skin in someone with eczema
Herpes Gladiatorum (Scrumpox)	Painful vesicular rash of face, chest etc with fever and lymphadenopathy. Due to direct abrasive contact.
Herpetic Whitlow	A pustular lesion close to the nail, usually finger
Ocular Herpes	Infection of the cornea and conjunctivae
Neonatal Herpes	Widespread vesicular rash contracted during birth. Very serious.

Table 1-1 Symptoms of the different clinical diseases caused by HSV-1 and HSV-2.

HSV-1 and -2 replication occurs at the epidermal/dermal interface with the establishment of vesicular clusters, culminating in the destruction of the overlying epidermal membrane and the formation of the clinical lesion. HSV -1 and -2 virus are therefore present in the vesicles, and transmission occurs via skin to surface (skin) contact.

1.4.7. HSV-1 and -2 specific treatment

Current treatment is with Aciclovir, a guanine analogue antiviral drug. ValAciclovir and famciclovir, derivatives of Aciclovir, are also used as they have better oral bioavailability (Balfou 1999). Table 1-2 is a representation for the prescription of antiviral therapy to combat various HSV infections.

Type of infection	Route and dose	Comments
Genital HSV		
Initial episode		
Aciclovir	**200 mg by mouth 5 times/day for 7–10 days**	**Preferred route in normal host**
	5 mg/kg intravenous every 8 h for 5–7 days	**Severe cases only**
	400 mg by mouth 3 times/day	
ValAciclovir	**1 g by mouth twice daily for 7–10 days**	
Famciclovir	**250 mg by mouth 3 times, i.e. 3 times/day for 5–10 days**	
Recurrent episode		
Aciclovir	**400 mg by mouth twice daily for 5 days**	**Limited clinical benefit**
ValAciclovir	**500 mg by mouth twice daily for 5 days**	
Famciclovir	**125–250 mg by mouth twice daily for 5 days**	
Suppression		
Aciclovir	**400 mg by mouth twice daily**	**Titrate dose as required**
ValAciclovir	**500 or 1000 mg by mouth once daily**	
Famciclovir	**250 mg by mouth twice daily**	
Mucocutaneous HSV in immunocompromised patients		
Aciclovir	**200–400 mg by mouth 5 times/day for 10 days**	**For minor lesions only**
	5 mg/kg intravenously every 8 h for 7–14 days	
	400 mg by mouth 5 times/day for 7–14 days	
ValAciclovir	**500 mg twice daily by mouth**	
Famciclovir	**250 mg 3 times/day by mouth**	
HSV encephalitis		
Aciclovir	**10–15 mg/kg intravenously every 8 h for 14–21 days**	
Neonatal HSV		
Aciclovir	**20 mg/kg intravenously every 8 h for 14–21 days**	

Table 1-2 Indication for therapy among patients with herpes simplex virus infections (Whitley and Roizman 2001).

The current topical therapeutic treatment of HSV-1 and 2 infections is much less effective than oral treatment; the topical therapy of penciclovir will accelerate healing by about one day (Whitley and Roizman 2001). Oral Aciclovir reduces the time to loss of crust by up to seven days, but does not alter duration of pain or time to complete healing (Clercq 2004).

1.5. **The Skin**

1.5.1. Function and Structure of Human Skin

The skin is the main interface between the body and the external environment in which we live. It is the largest organ in the human body constituting almost 10% of the total body mass of an average person (Williams 2003). The skin is made up of multiple layers of epithelial tissues that cover the underlying muscles and organs.

1.5.1.1. Skin Function

The skin performs many functions and is an anatomical barrier to the environment protecting the host from pathogens and the external environment; it is a sensory organ with many nerve endings which react to heat, pressure and other stimuli. The skin is involved in the process of homeostasis (keeping different aspects of the body constant i.e. temperature). It controls evaporation from the body and a small amount of oxygen, nitrogen and carbon dioxide can diffuse into the epidermis. All these functions play a pivotal role when considering the creation of a topically applied drug. The skin comprises of three main layers: the epidermis, the dermis, and the hypodermis - as shown in Figure 1-6.

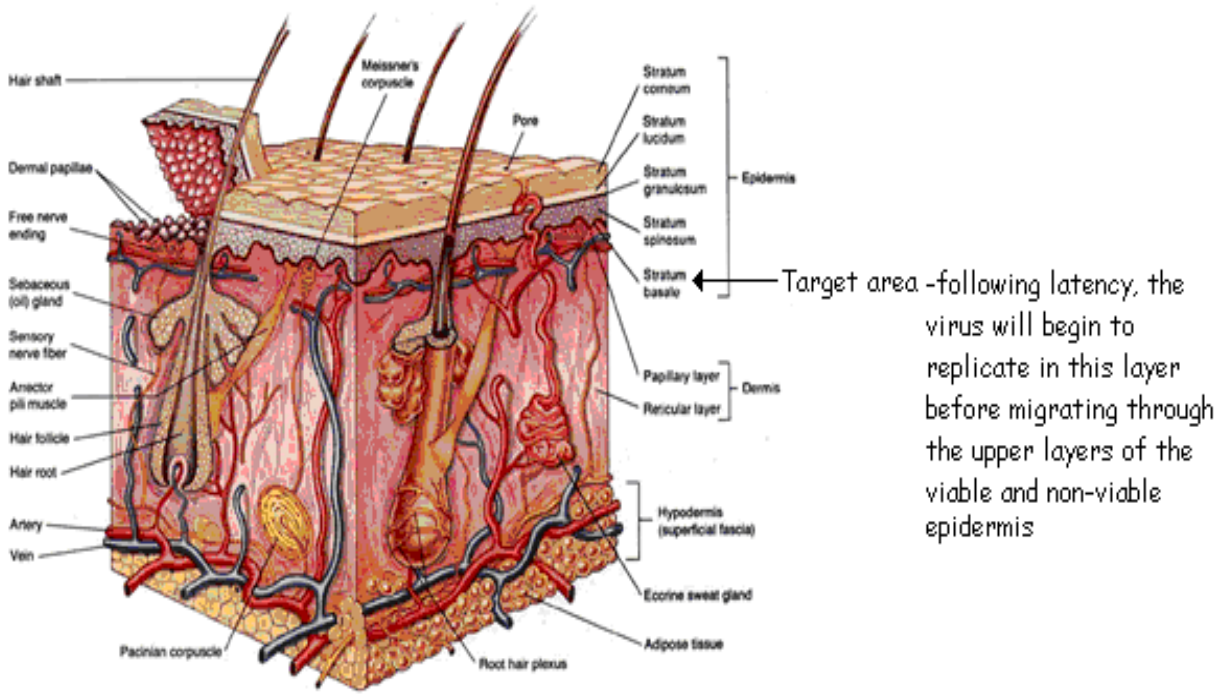

Figure 1-6 A Cross Sectional Diagram of Human Skin (London Health Sciences Centre 2003).

1.5.1.2. The Epidermis

The epidermis is never more than 0.1 cm thick in normal skin. The thickness varies depending on the age and specific area of the body. It is thickest on the palms and the soles of the feet, and thinnest on the eyelids. The epidermis contains no blood vessels and consists mainly of the cells keratinocytes, melanocytes Langerhans cells and Merkels cells. These are found in five main sub-layers of the epidermis called the Stratum Corneum (SC), Stratum Lucidum, Stratum Granulosum, Stratum Spinosom and Stratum Basale, shown in Figure 1-7.

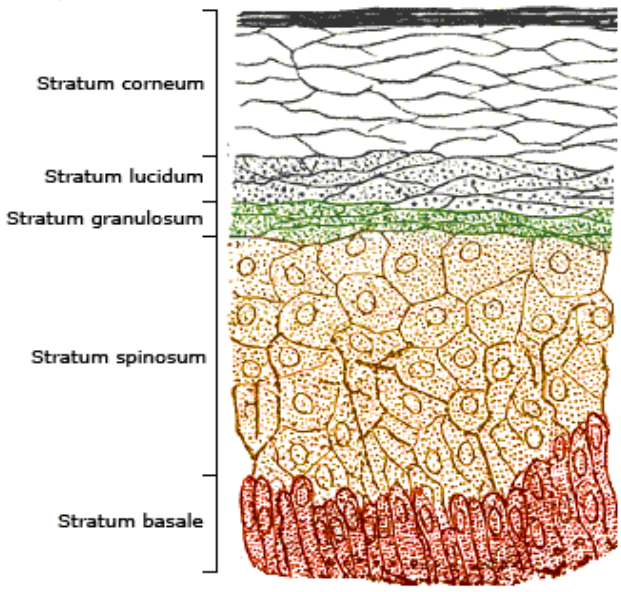

Figure 1-7 A cross sectional diagram to show layers of the epidermis (London Health Sciences Centre 2003).

1.5.1.3. Stratum Corneum (SC)

The skin's function as a barrier, specifically to permeation, is due to the characteristic architecture of the SC. The SC is created by keratinocytes and an understanding of their life cycle enables us to understand the SC.

The creation of new keratinocytes from stem cells is an exclusive feature of the stratum basale, the proliferation in this area forces the bulk of the cells to migrate upwards and to differentiate into the corneocytes. Cornification of the keratinocytes starts in the stratum spinosum but is more pronounced in the stratum granulosum (Houben 2007). The completely cornified cells now called corneocytes are embedded in an intercellular lipid (ICL) matrix in the SC (Weerheim and Ponec 2001). ICLs are considered to be an essential component of an adequate permeability barrier function. A "sandwich" model has been proposed where a narrow fluid lipid phase is interspersed between two broad crystalline lattices. The terminal differentiation of keratinocytes results in cell death. This is not, however, exactly the same as normal cell death, apoptosis. Keratinocyte cornification is considered to be distinct from apoptosis, despite the fact that cell death is programmed from the moment the basal keratinocyte leaves the basal compartment, corneocytes are not phagocytised and the cytoskeleton is reorganized, also apoptotic caspases are not activated during cornification (Eckhart, et al. 2000). They do still play

an important role in the epidermal barrier function until they detach, desquamation is the final detachment of the corneocytes.

It is obvious that the SC and the keratinocytes in all their forms are a very important part of the skin to understand when designing a topically applied drug. Other cell types found in the SC are melanocytes, which inject granules of pigment into the neighbouring cells. Melanin, the dark pigment produced, protects the skin by absorbing ultraviolet radiation, and visibly darkens skin exposed to sunlight.

Langerhans cells are also found in the epidermis, they are dendritic cells and their main function is to process antigen and present it to other cells of the immune system.

Merkel cells are cells found in the stratum basale and are associated with sensory nerve endings. The exact function of this cell is not fully understood.

There are certain aspects of the skin that break the continuity of the SC and are pathways for drug delivery (hair follicles, sweat glands, sebaceous glands and apocrine glands). These routes supply a negligible amount of net flux.

1.5.1.4. The Dermis

The dermis comprises the largest fraction of the skin, about 90%, and is responsible for its structural strength. The dermis is connected to the epidermis via the basement membrane; the basement lamina consists of an electron-dense membrane called the lamina densa, which consists of different types of collagen. The dermis contains hair follicles, the previously stated glands and also provides an environment for nerve and vascular networks. The main cell types of the dermis are fibroblasts, macrophages, and mast cells. The blood vessels not only provide nourishment and waste disposal to this area but also to the stratum basale above.

The dermis does not prove a hindering point for the permeation of most drugs. Only the most highly lipophilic drugs are likely to encounter resistance in this area after traversing the epidermis. The blood supply removes those molecules rapidly *in vivo* that have successfully penetrated the outer layer, however this blood uptake does provide a concentration gradient, which is considered the driving force behind effective transdermal absorbance. The concentration gradient is largely produced via the

lymphatic draining system which also facilitates immunological responses to foreign bodies.

1.5.1.5. The Hypodermis

Depending on the region of the body, the hypodermis, composed of fibroblasts, macrophages and adipocytes, is of varying thickness. The hypodermis provides insulation and energy storage in the form of fat, attachment of the skin to the underlying muscle, and supplies the skin with blood vessels and nerves.

1.5.2. Topical Drug Delivery

Pharmaceutical drug delivery is generally based upon the administration of oral or intravenous compounds. However for the treatment of skin diseases and afflictions both methods are often affected by issues such as first pass metabolism whereby the concentration of a drug is greatly reduced before it reaches the systemic circulation and therefore the target organ (the skin). The reduction is due to metabolism by the liver and it reduces the drug's bioavailability. The purpose of a vast range of research is to enhance drug targeting specificity, lower systemic drug toxicity, improving treatment absorption rates, and to prevent the biochemical degradation of active compounds. Delivery directly to or near the site intended especially for skin afflictions presents a possible mode of drug delivery which overcomes many of the previously stated goals. The delivery of drugs which uses the skin as a mode of transport can be categorized into three groups based upon the intended site of delivery, the topical transdermal, and transcutaneous routes.

1.5.2.1. Topical

Topical drug delivery is used to specifically target the local area of application with minimal absorption into systemic circulation.

1.5.2.2. Transcutaneous

The transcutaneous delivery system is intended to deliver drugs to tissues underlying the skin such as muscle or joints tissues. The drug must penetrate all layers of the skin but not be removed by the circulatory system. Topically applied non-steroidal anti-

inflammatory drugs (NSAID`s) such as Ibugel Forte (ibuprofen) and Powergel (ketoprofen) utilise the transcutaneous mode of drug delivery.

1.5.2.3. Transdermal

A transdermal drug delivery system is intended to deliver the drug into the general circulation. The use of this system requires that a drug has to successfully penetrate the SC and epidermis. The drug must then be taken up by the circulatory or lymphatic system and transported to the intended site. Transdermal therapeutic systems have been designed to provide controlled and sustained drug delivery across the skin barrier. Two effective examples of drugs that utilize this are the nicotine replacement Exelon Patch (rivastigmine) and the hormonal replacement therapy Testoderm (Testosterone)

1.5.2.4. Routes of Drug Permeation across the Skin

Topically applied drugs have to permeate the skin to be effective. The stratum corneum is the primary barrier and the rate of permeation is governed by its affect. Three main routes of permeation have been identified - appendageal, intercellular and transcellular. It is important to note that these pathways are not mutually exclusive and depending upon the nature of the molecule permeation is often via a mixture of these pathways.

1.5.2.4.1. *Transappendageal (shunt route)*

The transappendageal route involves the transport of molecules across the stratum corneum via hair follicles and sweat ducts. Although these appendages have a relatively small surface area (approximately 0.1%) they contribute to a large percentage of the total permeation. The shunt pathway is the major contributor to the initial phase of skin permeation (Scheuplein and Blank 1971).

1.5.2.4.2. *Intercellular route*

The intercellular route is the mode in which non-polar molecules transverse the SC. It is often represented with a simple brick and mortar model, but the lipid matrix is a very tortuous pathway. This route provides the principal pathway by which most small uncharged molecules permeate the SC.

1.5.2.4.3. *Transcellular Route*

The Transcellular route is often regarded as the pathway for polar molecules. Diffusion is predominately through hydrated keratinocytes, a quick process for polar molecules. Generally, this route is slowed due to the lipid bilayers either side of the keratinocyte.

1.5.2.5. Factors Affecting the Absorption of Topically Applied Drugs

Ficks Law of diffusion describes the permeability of intact stratum corneum "the speed of movement of substances across a membrane is proportional to the concentration differences across that membrane". This appears to be a concise and succinct explanation to the permeability of the stratum corneum, however the law only applies to the uppermost layer of skin, which can accumulate a limited amount of drug with its saturated state being readily reached. The level of percutaneous absorbtion of a substance is affected by many contributing factors.

-*Thickness of skin*	-Site of absorption
-Type of skin	-Age
-Hydration	-Application variables
-Partition coefficient	-Co-permeation
-Particle size	

1.6. **Aims and Objective**

The thesis aimed to develop a therapeutic system for the treatment of *Herpes simplex* virus type 1 and 2 infections, which could be administred topically.

The objectives are:

- To investigate the virucidal, antiviral and inflammatory properties of PRE with the inclusion of a potentiating metal salt
- To identify the optimal combination of PRE and potentiating agent

- To formulate any proposed biologically active combination so that the topical application of any combination will deliver the actives so that it is effective at the site specific regions of HSV-1 and -2 replication

Chapter 2 **Materials and Methods**

2.1. **Materials**

All the materials used in this project are listed alphabetically in Table 2-1:

24 well plates (24wp)	Fisher Scientific (Loughborough, UK)
3-(N-mopholino) propanesulfonic acid (MOPS)	Fisher Scientific (Loughborough, UK)
50 mL sterile Blue cap	(Greiner Bio-One Ltd. (Stonehouse, UK)
96 well plates (96 wp)	Fisher Scientific (Loughborough, UK)
Acetic acid	Sigma-Aldrich Company Ltd. (Poole, UK)
Aciclovir	Gifted by Dr J J Bugert (Medical Microbiology, UHW, Cardiff)
Acrylamide/bis-acrylamide 29:1 (30%, v/v solution)	Sigma-Aldrich Company Ltd. (Poole, UK)
Ammonium persulphate (APS ≥98%)	Sigma-Aldrich Company Ltd. (Poole, UK)
Anti-mouse primary antibody	Amersham Biosciences Ltd (Amersham, UK)
Aprotinin	Sigma-Aldrich Company Ltd. (Poole, UK)
Avicel	Sigma-Aldrich Company Ltd. (Poole, UK)
Bio-Rad protein assay reagents	Bio-Rad Laboratories Ltd. (Hertfordshire, UK)
Bovine serum albumin (BSA)	Sigma-Aldrich Company Ltd. (Poole, UK)
Bromophenol blue (99% UV-VIS)	Fisher Scientific (Loughborough, UK)
Cab-o-sil M5	Sigma-Aldrich Company Ltd. (Poole, UK)
Carbopol 942 P	Fisher Scientific (Loughborough, UK)
Carbopol 971 PNF	Fisher Scientific (Loughborough, UK)
Cell Scraper (sterile) (Corning®)	Sigma-Aldrich Company Ltd. (Poole, UK)
CellTiter 96® Aqueous solution	Promega (Southampton, UK)
Cetyl alcohol	Fisher Scientific (Loughborough, UK)
Chemiluminescent Supersignal® West HRP substrate (pico, dura and femto)	Pierce and Warriner Ltd. (Cheshire, UK)
Chloroform	Fisher Scientific (Loughborough, UK)
COX-2 primary antibody	Cell Signalling Technology, New England Biolabs (Hitchin, UK)
Crystal violet	Sigma-Aldrich Company Ltd. (Poole, UK)
Cyclopore track etched membranes (CTEM)	Fisher Scientific (Loughborough, UK)
DAB liquid substrate chromagen system	Dako (Ely, UK)
De-ionised and phosphate buffered saline (DPBS, PBS)	Sigma-Aldrich Company Ltd. (Poole, UK)
Di-butylpthalatexylene (DPX)	Raymond A Lamb Ltd. (Eastbourne, UK)
Dimethyl sulfoxide (DMSO)	Fisher Scientific (Loughborough, UK)
Di-thiothreitol (DTT),	Sigma-Aldrich Company Ltd. (Poole, UK)
Dulbecco's Modified Eagle Medium	Fisher Scientific (Loughborough, UK)

(DMEM) (with L-Glutamine, 4500 mg L^{-1} D-glucose, without sodium pyruvate).	
Ellagic acid	Fisher Scientific (Loughborough, UK)
Eppendorf tubes (1.8 mL)	Sigma-Aldrich Company Ltd. (Poole, UK)
Ethanol (HPLC grade)	Fisher Scientific (Loughborough, UK)
Ethylene diamine	Sigma-Aldrich Company Ltd. (Poole, UK)
Ethylene glycol-bis(2-amino-ethylether)-N,N,N',-tetraacetic acid (EGTA)	Sigma-Aldrich Company Ltd. (Poole, UK)
Ferrous sulphate ($FeSO_4$)	Fisher Scientific (Loughborough, UK)
Foetal bovine berum (FBS)	Fisher Scientific (Loughborough, UK)
Formaldehyde	Fisher Scientific (Loughborough, UK)
Gentamycin sulphate	Fisher Scientific (Loughborough, UK)
Glycerine	Fisher Scientific (Loughborough, UK)
Glycerol	Sigma-Aldrich Company Ltd. (Poole, UK)
Glycine	Sigma-Aldrich Company Ltd. (Poole, UK)
Hanks balanced buffered salt solution (HBBSS)	Sigma-Aldrich Company Ltd. (Poole, UK)
HEPES (n-[2-hydroxyethyl] piperazine-N'-[2-ethanesulfonic acid])	Sigma-Aldrich Company Ltd. (Poole, UK)
High vacuum grease	Dow Corning (Barry, UK)
Horseradish peroxidase (HRP)-labelled anti-rabbit polymer EnVision™ system	Dako (Ely, UK)
HRP-linked secondary antibody	Amersham Biosciences Ltd (Amersham, UK)
HSV-1 17+	ECACC (Salisbury, UK, ECACC No 0104151)
HSV-2-ACR	ECACC (Salisbury, UK, ECACC No 513)
HSV-2-HG32	ECACC (Salisbury, UK, ECACC No 618)
Hydrochloric acid (HCl)	Sigma-Aldrich Company Ltd. (Poole, UK)
Hydrogen Flouride	Sigma-Aldrich Company Ltd. (Poole, UK)
Hydrogen peroxide	Sigma-Aldrich Company Ltd. (Poole, UK)
Hydroxymethylcellulose	Sigma-Aldrich Company Ltd. (Poole, UK)
Kodak MXB autoradiography film (blue sensitive)	Genetic Research Instrumentation (GRI) (Rayne, UK)
Lauric acid	Fisher Scientific (Loughborough, UK)
Leupeptin	Sigma-Aldrich Company Ltd. (Poole, UK)
Methanol (HPLC grade)	Fisher Scientific (Loughborough, UK)
Methocel 856N	Fisher Scientific (Loughborough, UK)
Methyl green	Sigma-Aldrich Company Ltd. (Poole, UK)
Methylparaben	Fisher Scientific (Loughborough, UK)
Micro stirrer bars (2x5 mm)	Fisher Scientific (Loughborough, UK)
Microscope slides	Surgipath (Cambridgeshire, UK)
Milk (Marvel™ original dried skimmed milk)	Sainsburys (Cardiff)

Millex®HA syringe-driven filter unit	Millipore (Watford, UK)
Monoclonal Anti-β-Actin antibody (clone AC-74, ascites fluid, A 5316)	Sigma-Aldrich Company Ltd. (Poole, UK)
N,N,N',N'-tetramethylene-diamine (TEMED)	Sigma-Aldrich Company Ltd. (Poole, UK)
Nitrocellulose transfer membrane (Protran® BA85) 0.45µm pore size	Schleicher and Schuell (Dassel, Germany)
Pasteur pipettes	Sigma-Aldrich Company Ltd. (Poole, UK)
PBS + 0.02% Tween	Sigma-Aldrich Company Ltd. (Poole, UK)
Phenylmethyl sulphonyl fluoride (PMSF)	Sigma-Aldrich Company Ltd. (Poole, UK)
Phosphoric acid	Fisher Scientific (Loughborough, UK)
Pluronic F 127	Sigma-Aldrich Company Ltd. (Poole, UK)
Pluronic F-127	Sigma-Aldrich Company Ltd. (Poole, UK)
Polyetheylene glycol sorbitan bees wax	Fisher Scientific (Loughborough, UK)
Polyethylene glycol 400 (PEG 400)	Sigma-Aldrich Company Ltd. (Poole, UK)
Polyethyleneglycol (100) stearate	Fisher Scientific (Loughborough, UK)
Polyoxyethylene-sorbitan monolaurate (Tween 20)	Sigma-Aldrich Company Ltd. (Poole, UK)
Pomegranate	Sainsburys (Cardiff)
Ponceau S solution (0.1%, w/v in 5% acetic acid)	Sigma-Aldrich Company Ltd. (Poole, UK)
Potassium hydrogen phthalate	Fisher Scientific (Loughborough, UK)
Potassium hydroxide	Fisher Scientific (Loughborough, UK)
Propylparaben	Fisher Scientific (Loughborough, UK)
Punicalagin	Phytolab (Vestenbergsgreuth, Germany)
Radioimmunoprecipitation assay (RIPA) buffer	Sigma-Aldrich Company Ltd. (Poole, UK)
Rainbow Marker (12-225 kDA)	GE Healthcare Life Sciences (Buckingham, UK)
RK13 cells	ECACC, (Salisbury, UK, ECACC No 88062427)
SDS-PAGE lower buffer (tris 1.5M pH 8.8)	Bio-Rad Laboratories Ltd. (Hertfordshire, UK)
SDS-page upper buffer (tris 0.5M pH 6.8),	Bio-Rad Laboratories Ltd. (Hertfordshire, UK)
Sellotape	Sainsbury's (Cardiff)
Sephadex LH-20	Sigma-Aldrich Company Ltd. (Poole, UK)
Sodium azide	Sigma-Aldrich Company Ltd. (Poole, UK)
Sodium bicarbonate	Sigma-Aldrich Company Ltd. (Poole, UK)
Sodium chloride (NaCl)	Sigma-Aldrich Company Ltd. (Poole, UK)
Sodium citrate	Sigma-Aldrich Company Ltd. (Poole, UK)
Sodium dodecyl sulphate (SDS)	Sigma-Aldrich Company Ltd. (Poole, UK)
Sodium hydroxide,	Sigma-Aldrich Company Ltd. (Poole, UK)
Spectrophotometer micro-cuvettes	Bio-Rad Laboratories Ltd. (Hertfordshire, UK)

Stearic acid	Fisher Scientific (Loughborough, UK)
Stearyl alcohol	Fisher Scientific (Loughborough, UK)
Sterile pipettes 10 mL and 25 mL	Greiner Bio-One Ltd. (Stonehouse, UK)
Super glue	Sainsburys (Cardiff)
Syringe (5 mL, Sterile)	Sigma-Aldrich Company Ltd. (Poole, UK)
Syringe needles	Sherwood-Davies and Geck (Gosport, UK)
T 75, T 25 and T150 TPP tissue culture flasks	(Greiner Bio-One Ltd. (Stonehouse, UK)
Tetraacetic acid (EDTA),	Sigma-Aldrich Company Ltd. (Poole, UK)
Triflouroacetic acid (TFA)	Sigma-Aldrich Company Ltd. (Poole, UK).
Tris(hydroxymethyl) aminomethane (TRIS)	Sigma-Aldrich Company Ltd. (Poole, UK)
Trizma® base	Sigma-Aldrich Company Ltd. (Poole, UK)
TrypLE™ Express trypsin solution	Invitrogen (Paisley,UK)
Uranyl acetate	Sigma-Aldrich Company Ltd. (Poole, UK)
Vero cells (green monkey kidney epithelial cells)	ECACC, (UK , ECACC No 85020205)
Wax pen	Dako (Ely, UK)
Western blocking reagent	Roche Diagnostics, Gmbh (Mannheim, Germany)
Whatman filter paper	Fisher Scientific (Loughborough, UK)
White paraffin wax pellets	Sigma-Aldrich Company Ltd. (Poole, UK)
X-ray film developer and film fixative solutions	X-O-graph Imaging System (Tetbury, UK)
Xylene	Fisher Scientific (Loughborough, UK)
Zinc citrate	Fisher Scientific (Loughborough, UK)
Zinc gluconate	Fisher Scientific (Loughborough, UK)
Zinc iodide	Fisher Scientific (Loughborough, UK)
Zinc nitrate	Fisher Scientific (Loughborough, UK)
Zinc oxide	Fisher Scientific (Loughborough, UK)
Zinc stearate	Fisher Scientific (Loughborough, UK)
Zinc sulphate ($ZnSO_4$)	Fisher Scientific (Loughborough, UK)
β-actin primary antibody	Sigma-Aldrich Company Ltd. (Poole, UK)

Table 2-1 Alphabetised list of the chemicals and materials and their sources used in this thesis.

2.2. **Methods**

2.2.1. Preparation of Solutions

2.2.1.1. Pomegranate Rind Extract (PRE)

The primary extraction method of pomegranate rind (PRE) was derived from a published method which favoured the extraction of polyphenols (Stewart, et al. 1998). Six fresh pomegranates were peeled; the rinds cut into thin strips approximately 2 cm in length, blended in DI H_2O (25% w/v) and boiled for approximately 10 minutes. The crude solution was then transferred into centrifuge tubes and centrifuged at 10,400g at 4°C for 30 min using a Beckman Coulter Avanti J25 Ultracentrifuge and vacuum filtered through a Whatman 0.45μm nylon membrane filter. The solution was then freeze dried, occluded from light and stored at -20°C until required. The punicalagin concentration of each extract was analysed, and consisted of 20% w/w of PRE.

2.2.1.2. Phthalate Buffer

Solutions of potassium hydrogen phthalate (0.1 M) and sodium hydroxide (0.1 M) were prepared in DI H_2O. Potassium hydrogen phthalate solution (250 mL) was added to Sodium Hydroxide solution (87 mL) in a 1litre bottle. The volume was adjusted to 1 L with DI H_2O and sonicated (5 min). The pH of the final solution was adjusted to pH 4.5 with Phosphoric acid

2.2.1.3. Reconstitution of Freeze-Dried PRE

Freeze dried PRE (2 mg) was added to phthalate buffer (10 mL, pH 4.5). The solution was sonicated for 10 min at 50-60 Hz. Once fully dissolved the solution was subsequently filtered through a 0.45 μm Millex®-FG syringe driven filter unit and frozen at -20°C until further use.

2.2.1.4. $FeSO_4$

Ferrous sulphate heptahydrate (0.0533g) was added to phthalate buffer (10 mL, pH 4.5). The solution was sonicated for 10 min at 50-60 Hz. Once fully dissolved the solution was filtered through a 0.45 μm Millex®-FG syringe driven filter unit.

2.2.1.5. $ZnSO_4$

Zinc sulphate heptahydrate (2.875g) was added to phthalate buffer (10 mL, pH 4.5) (1M solution). The solution was sonicated for 10 min at 50-60 Hz. Once fully dissolved the solution was subsequently filtered through a 0.45 μm Millex®-FG syringe driven filter unit. The preparation of other zinc salts followed that for $ZnSO_4$ above; however the stock solutions were made to the concentrations stated in Table 2-2.

Salt	Stock solution Concentration (M)
Zinc oxide	0.00004
Zinc nitrate	0.002
Zinc citrate	0.002
Zinc Iodide	0.002
Zinc Stearate	0.002
Zinc Gluconate	0.002

Table 2-2 Concentration of zinc salt stock solutions. Note: solution of ZnO lower due to low solubility.

2.2.1.6. Punicalagin

Punicalagin (10 mg) was added to phthalate buffer (10 mL, pH 4.5) and sonicated for 10min at 50-60 Hz. Once fully dissolved accurate dilutions were made from this solution using phthalate buffer (pH 4.5).

2.2.1.7. Ellagic acid

Ellagic acid (50 μg) was added to phthalate buffer (10 mL, pH 4.5) and sonicated for 10min at 50-60 Hz. Once fully dissolved accurate dilutions were made from this solution using phthalate buffer (pH 4.5).

2.2.1.8. HEPES-Buffered Hanks' Balanced Salt (HBHBS)

The solution was made up of Hanks' balanced salt buffer (9.7 g), HEPES (6 mg), and sodium bicarbonate (0.35 g) in 1L DI H_2O

2.2.1.9. Running Buffer I (10 x stock solution)

Tris base (30.35 g) was added to glycine (144 g) and 10 mL SDS and made up to 1 L with DI H_2O.

2.2.1.10. Running Buffer II

Tris base (36.42 g) was added to glycine (180 g) and 10 mL SDS and made up to 1 L with DI H_2O.

2.2.1.11. Transfer Buffer

Immediately before use 40 mL of running buffer II was added to 200 mL EtOH and 760 mL DI H_2O. The solution was mechanically mixed for 15 min before use.

2.2.1.12. TBS-Tween (10 x stock solution)

A stock solution of tris buffered saline tween-20 solution was prepared by the addition of 10 mL Tween-20, 24.2 g Trizam base and 80 g NaCl made up to 1 L with DI H_2O. The solution was mechanically stirred until complete dissolution was obtained, then stored at 2 - 4 °C.

2.2.1.13. Citrate Buffer

The citrate buffer used for the recovery of antigen within skin samples after the fixation process was made by dissolving 2.94 g of sodium citrate in DI H_2O and sonicated for 10 min at 50-60 Hz. The solution was adjusted to pH 6 by the dropwise addition of hydrochloric acid.

2.2.1.14. LaemmLi Buffer

A double-strength LaemmLi buffer was made by the addition of 1.2 mL of 1 M Tris-HCl pH 6.8, 4 mL of 10% w/v SDS, 2 mL glycerol and 0.01% w/v bromophenol blue in DI H_2O to make up a total volume of 10 mL.

2.2.2. Porcine Membrane Preparations

The porcine ears, vagina and cheeks were collected from a local abattoir as soon as possible after they were excised, then transported to the lab immersed in iced HEPES-buffered Hanks balanced salt solution (HBHBS), generally arriving in the laboratory

within 1h. Only freshly excised skin was used throughout this thesis, application of test materials began at a maximum of three hours after excision.

2.2.2.1. Full Thickness Ear Skin

The ears were gently washed under cool running water and full thickness skin removed from the dorsal cartilage by blunt dissection, using a scalpel. The skin was further sectioned into 2 x 2 cm squares and used straight away.

2.2.2.2. Heat-Separated Epidermis (HSE)

The skin samples were prepared as previously reported (Kligman and Christophers 1963). After they were cut into 2 x 2 cm squares (section 2.2.2.1) they were immersed in DI H_2O at a temperature of 55 °C for a period of 1 min. The epidermis was then manually separated from the dermis using gloves by slowly peeling one away from the other. Each separated epidermis was visually assessed for holes and defects etc, and any damaged epidermis was discarded.

2.2.2.3. Buccal Mucosal Membrane

The porcine cheeks were washed under DI H_2O, the full thickness membrane was excised from the inner cheek region via blunt dissection and placed in DI H_2O at 80 °C for 60 s. The epithelial mucosal membrane was then peeled away carefully using forceps. Each peace was cut into 2 x 2 cm^2 sections and visually assessed under a microscope, then used immediately.

2.2.2.4. Vaginal Mucosal Membrane

Excess fat and muscle was cut away from the porcine inner vaginal wall via scalpel dissection. The vaginal cavity was opened by cutting one vaginal wall from the vaginal opening to the cervix. The vaginal mucosal membrane was then trimmed down carefully by hand using a scalpel until only the top epithelial mucosal membrane remained, this was sectioned into 2 x 2 cm^2 pieces and used immediately.

2.2.3. Franz Diffusion Cell (FDC)

For membrane permeation and penetration studies, all-glass FDCs were used (Sartorelli, et al. 2008) with nominal diffusional area of 1 cm diameter (0.88 cm^2) and

nominal receptor phase volume of 3 mL. These were custom fabricated by retired glass-blower, Mr DW Jones, Loughborough, UK. The membrane was mounted on the lightly pre-greased flanges of the receptor compartment of a Franz cell shown in Figure 2-1. The donor chamber was placed on top of the membrane and clamped in position. A micro-stirrer bar was added to the receptor compartment, filled with temperature equilibrated (37^{o}C) solution and the sampling arm capped. The cells were placed on a multiple stirrer plate in a thermostatically controlled water bath set at 37 °C for 15 min to allow the temperature to reach equilibrium. The receptor fluid used was DI H_2O to provide a sink for the water-soluble compounds of interest in this work. The donor cells and sampling arm were occluded.

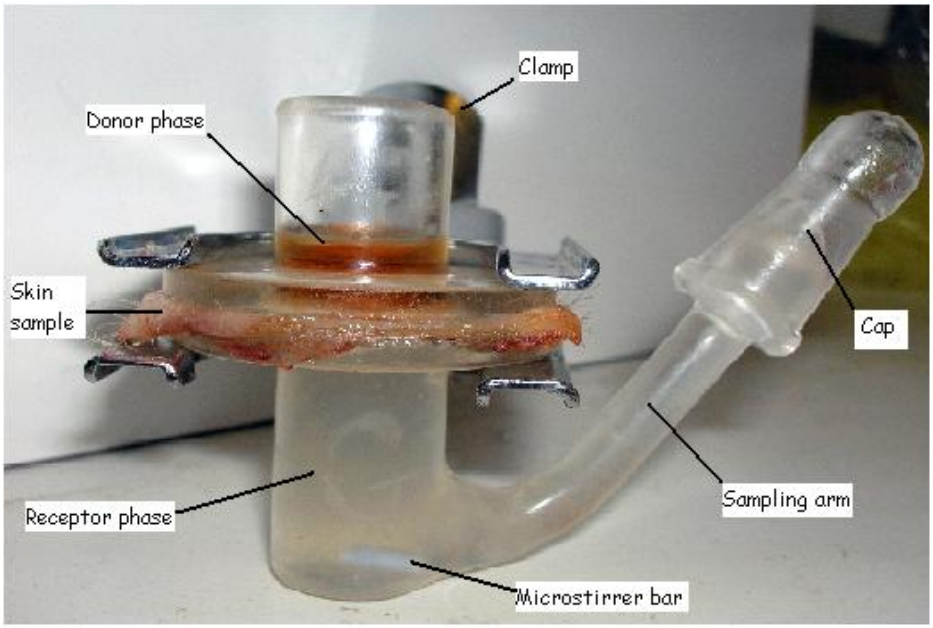

Figure 2-1 A typical Franz diffusion cell (FDC) assembly as used throughout the work in this thesis.

2.2.3.1. Penetration Through Epidermal Membrane

This technique is used to assess the cumulative drug permeation over time. Using heat separated (porcine) epidermis as a model for the permeation of drugs through human epidermis is qualitatively and quantitatively similar to dermatomed skin and circumvents complications from the presence of the dermis. Depending on the penetration study the use of heat separated epidermis, heat separated buccal membrane or vaginal mucosal membrane (following the methodology of Section 2.2.2.) which had been sectioned into 2 cm^2 sections were placed onto the pre-greased flanges of the

Franz type diffusion cell (Section 2.2.3.), the receptor phase filled with DI H_2O, placed in an incubator at 37°C for 15 min before the application of test materials.

2.2.3.1.1. *Finite Dose Application*

The application of a 40 µL, representative of a finite dose of test material, is done via pipette onto the centre of the membrane. The sample chamber was occluded after application. The entire receptor phase was removed using Pasteur pipettes at pre defined time points 3, 6, 12, 18 and 24 h and replaced with fresh receptor phase stored at 37°C. The removed receptor phase was transferred into Eppendorf tubes and frozen at -20°C for analysis at a later time.

2.2.3.1.2. *Infinite Dose Application*

Sterile syringes, 5 mL, were used for the application of 300 mg of hydrogel/emulsion formulation, representative of maximal delivery. A separate sterile 5 mL syringe was used for each gel and these were filled with the formulation (hydrogel or emulsion) slowly. The syringe was then weighed prior to and after application to ensure the exact weight of applied formulation. A sterile glass rod (0.7 cm diameter, with a rounded bottom) was placed into the donor chamber and twisted slowly 10 times with a small but constant level of pressure. The glass rod was weighed prior to and after application, the amount of hydrogel dosed to each FDC was then determined by difference. For every hydrogel, a dedicated sterile syringe was used. Sampling was as above.

2.2.3.2. Spontaneous Release

Spontaneous release of the active ingredients from a formulation matrix was determined by the use of a minimal resistance membrane, Cyclopore Track Etched Membrane (CTEM), mounted in FDCs. Section 2.2.3. The CTEM was soaked in receptor phase (DI H_2O) prior to fixing between the pre-greased flanges and being clamped. A micro stirrer bar was added via the sampling arm. The complete cells were placed onto the magnetic stirrer base set up in a water bath set at 37 ºC. A replication of n=4 cells were used per application. After 15 min, the donor phases were dosed with 1 mL of formulation. Receptor phase samples were taken at 0.5 h to replicate a maximal application end point, and 24 h as a maximal release end point. The receptor phase was completely removed using a sterile pipette and 0.5 mL aliquots stored at -20 °C until analysis. The receptor chamber was refilled using another sterile pipette. Thawed

samples were analysed for punicalagin and zinc content by HPLC and ICPMS respectively, as outlined in Sections 2.2.4.1. and 2.2.4.2.

2.2.3.3. Stability

The stability analysis of the hydrogel formulation was determined in terms of the concentration of the spontaneous release of both the $ZnSO_4$ and punicalagin from the Methocel 856N matrix after a designated period of storage. Due to the breakdown of PRE constituents after long term exposure to light all proposed formulations would remain occluded from light at all times prior to use or evaluation. Therefore formulations were stored at ambient temperature within sealed containers, which were occluded from light and air. Samples of the formulations were taken at 0, 3, 6 and 12 months and subjugated to analysis via spontaneous release (Section 2.2.3.2). These storage conditions of the test materials adhere to the basic guidelines for preliminary analysis into the stability of a product (Food and Drug Administration 2009).

2.2.3.4. Tape Stripping of Full Thickness Skin

At 24 h the skin was removed from the Franz cell and placed on a clean, dry surface. Excess formulation was removed from the skin surface using a cotton bud. The pressure applied and number of strokes was kept uniform between samples. Twenty strips are taken from the skin by applying the tape with constant pressure, and removal at a constant velocity. The first two strips were discarded as they usually contain excess formulation. The 20 strips were then grouped 2 per vial containing 4mL ethanol and rocked on an electronic rocker for no less than 24 h. The remaining skin sample was placed in ethanol and agitated over night using a laboratory rocker. The solution was evaporated to dryness then 1mL aliquots of DI H_2O was added to each vial and centrifuged at 15000 *g* for 15 min. The supernatant was then transferred to auto sampler vials and analysed by reverse phase HPLC (Escobar-Chávez, et al. 2008) (Weerheim and Ponec 2001).

2.2.3.5. Reverse Tape Stripping

Reverse tape stripping was conducted after a 24 hr epidermal membrane penetration study was completed. The same methodology followed that in Section 2.2.3.4; however, instead of starting from the top layer of the membrane which is in contact with the donor phase, the bottom side was the starting point (which is in contact with

the receptor fluid). This allows the analysis of the amount of analyte that has localised within the basal layer, i.e. adjacent to site of HSV replication.

The epidermal membrane was removed from the FDC using sterile plastic tweezers and dabbed clean of formulation very carefully and trimmed to the area of application. Superglue was applied to a ceramic tile, the membrane was placed on the superglue, donor application side down. Regular adhesive tape strips were placed on to the membrane and a small amount of pressure applied. The tape was then carefully removed using tweezers and is placed in a vial containing 2 mL of methanol and rocked over night (0 °C and occluded from light). This was repeated twice for each porcine membrane. The tape was removed from the vials and he methanol was evaporate under vacuum at less than 0 °C and occluded from light. The vials were filled with 2 mL of DI H_2O and rocked until all solid was re-dissolved. The samples were then stored at -20 °C and occluded from light until the point of analysis.

2.2.4. Analytical Methods

2.2.4.1. HPLC Analysis of PRE and Punicalagin

The analysis was performed using an Agilent series 1100 HPLC system at 258 nm fitted with a Phenomex Gemini NX C18 110A 250 X 2.6 mm column. Gradient elution was used, involving A: MeOH with 0.1% trifluoroacetic acid (TFA) and B: DI H_2O with 0.1% TFA. The gradient timetable and percentage composition of mobile phase is shown in Table 2-3.

Time (min)	A. % MeOH + 0.1% TFA	B. % H_2O + 0.1% TFA
0	5	95
15	20	80
30	60	40
40	60	40

Table 2-3 Gradient timetable for the HPLC analysis of PRE

2.2.4.1.1. *Punicalagin Standard*

The punicalagin standard was analysed over a range of concentrations so that a calibration curve could accurately be produced (Figure 2-2) to incorporate all sample data throughout the project. Punicalagin was dissolved in DI H_2O, analysed following the HPLC method outlined above, and is found to exist as two natural anomers: punicalagin α and β as stated in Chapter 1 and within the chromatogram in Figure 2-3. A calibration curve representative of peak area vs total punicalagin concentration of each anomer is shown in Figure 2-2.

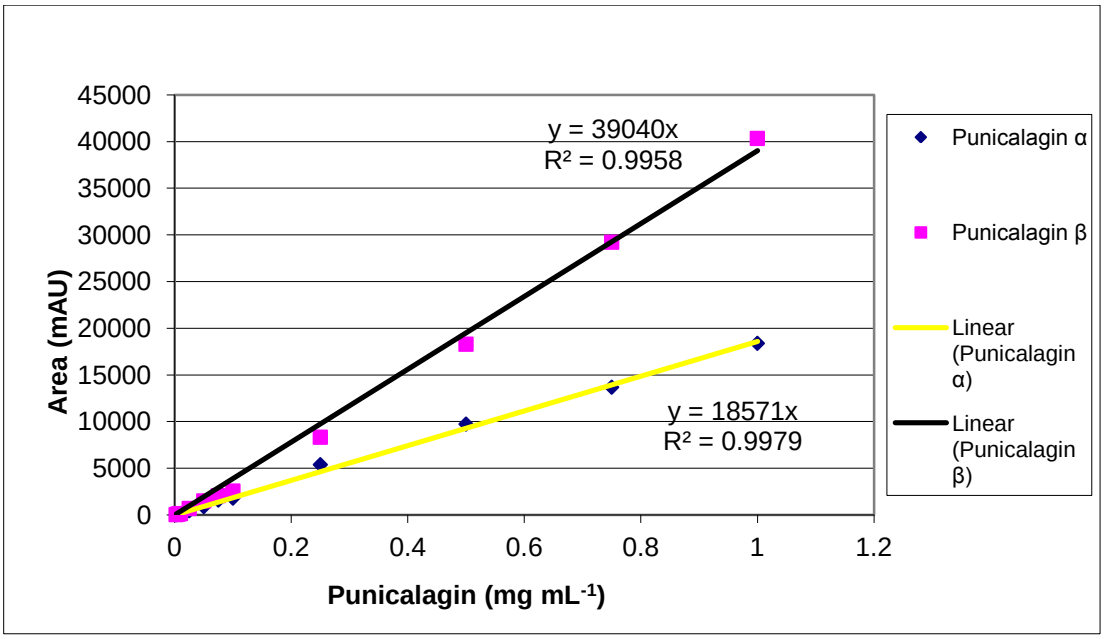

Figure 2-2 HPLC calibration curve for punicalagin anomers α and β (n=3 ± s.d.)

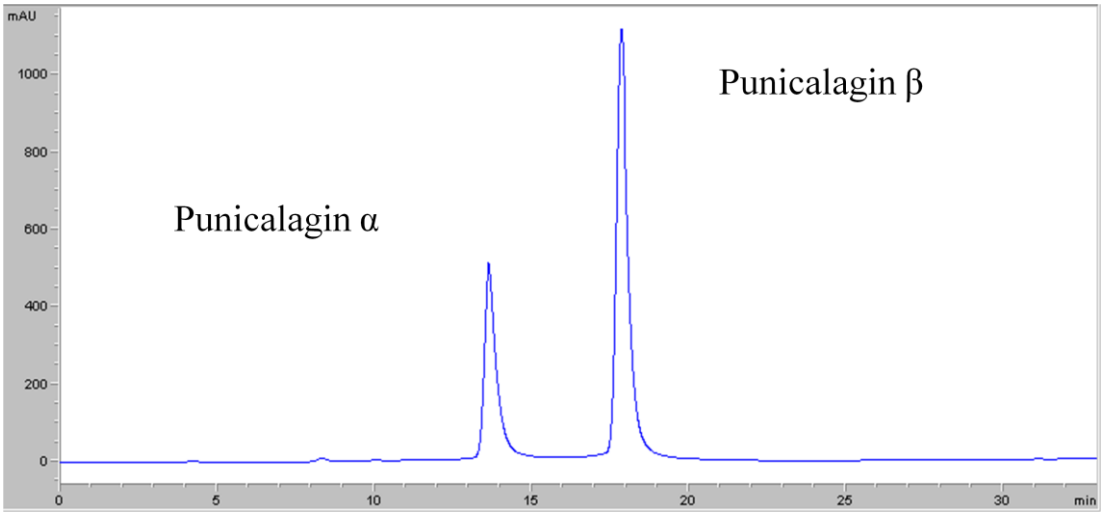

Figure 2-3 A sample HPLC chromatogram of punicalagin anomers α and β.

It was determined that the punicalagin anomers in the standard were at all times in the ratio of punicalagin α : β is approximately 1 : 2, which is similar to that described for other PRE extracts (Satomi, et al. 1993) (Nigrisa, et al. 2011). The consistent ratio of punicalagin anomers within PRE, as stated previously (Seeram 2006) and shown by Figure 2-4, allows for the analysis of punicalagin to be drawn from the peak area values of just one anomer. Due to the increased concentration of punicalagin β this anomer was used for quantification of total punicalagin concentration.

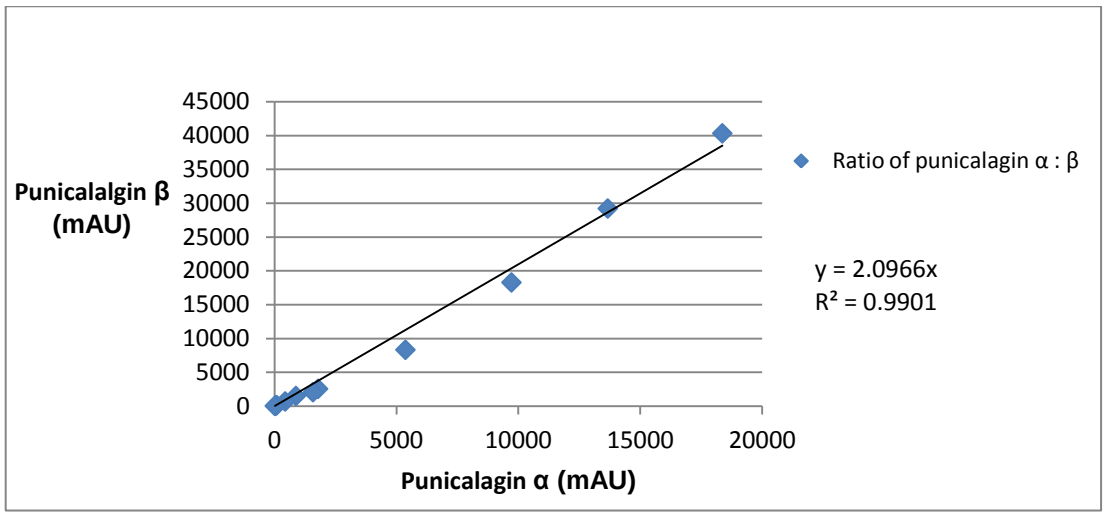

Figure 2-4 The ratio of the area of absorbance via HPLC analysis between the anomers of punicalagin: α and β. (n=3 ± s.d.).

Figure 2-5 shows that the concentration of punicalagin within the freeze dried pomegranate rind extract is one fifth the total mass extracted.

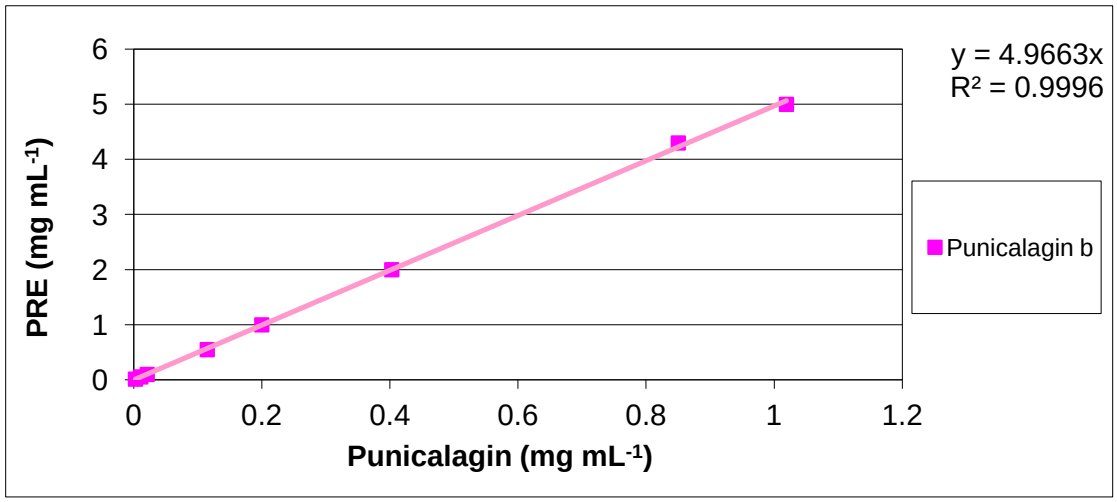

Figure 2-5 Concentration of punicalagin within freeze dried PRE (n=3 ± SD).

2.2.4.2. Inductively Coupled Plasma Mass Spectrometry (ICPMS)

The levels of zinc were determined by ICPMS analysis in the laboratories of Dr. I MacDonald, School of Earth Sciences, Cardiff University. Analysis was performed using a Thermo Elemental X Series 2 ICP-MS system equipped with a Plasma Screen. Analysis was performed in triplicate on each solution using ^{66}Zn as the analytical mass. Calibration was carried out using synthetic standard solutions prepared from single element stock standards. Periodic checks for accuracy were performed by analysis of a solution of the international rock standard JB1a as an unknown. This standard was prepared by digesting a sample in HF/HNO_3 and then HNO_3 procedures described previously (Parkinson and Pearce 1998).

2.2.4.3. Isothermal Titration Calorimetry (ITC)

Binding interactions were probed by ITC in the laboratories of Professor Niek Buurma, School of Chemistry, Cardiff University. Figure 2-6 is an illustration of an ITC instrument. When the reference cell and titrate cells have equilibrated, the titrant ($FeSO_4$) is injected into the ITC cell containing the titrate (PRE). The enthalpy change due to the introduction of the titrant is measured, the cell re-equilibrates leading to a slower drift back to the baseline. This peak is then integrated which gives the enthalpy change of that experiment. The subsequent enthalpy changes of each injection are added until there is no further heat change, which allows the measurement of ΔH. The series of several injections can lead to the calculation of free energy, enthalpy, entropy, Kd, and stoichiometry of binding. The ITC instrument used was the Microcal VP-ITC (Amersham, UK).

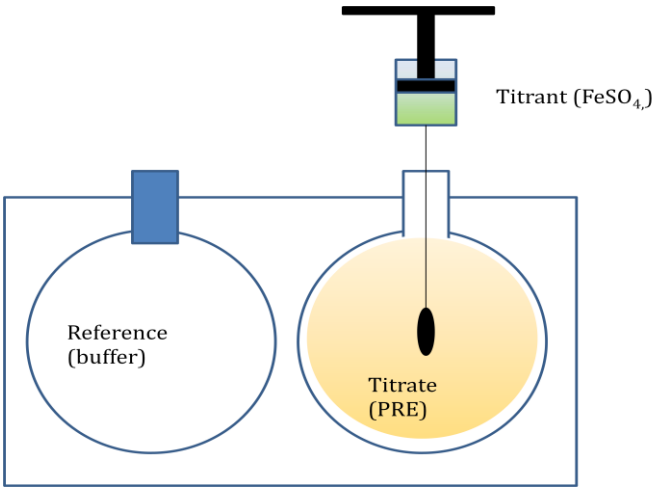

Figure 2-6 Representation of Isothermal Titrated Calorimetry (ITC) with PRE as the titrate and $FeSO_4$ as the titrant.

Each cell was washed and emptied twice with a solution of 50% 3-(N-morpholino) propanesulfonic acid (MOPS) buffer and 50% DI H_2O. A preliminary titration was run with DI H_2O and the buffer solution being titrated in to note any underlying heat effects. This involved injecting an aliquot of 15 µL into the cell over a period of 15 sec with 420 sec between each injection (n=18) to note any heat changes. Each cell was washed and emptied twice with a solution of 50% MOPS buffer and 50 % DI H_2O before the addition of PRE 0.6 mg mL^{-1} which equilibrated to 25˚C. An aliquot of 15 µL of the $FeSO_4$ (2.5 mM) solution was injected into the cell over a period of 15 seconds with 420 sec between each injection (n = 36). The first in the series of 18 injections is always discarded due to heat irregularities that occur with the first injection. To account for varying pH in calculating the binding constant a further experiment was run using an acetate buffer pH 4.5, all other factors remained the same. All solutions were degassed before analysis.

2.2.4.4. Protein Analysis and Western Blotting

The process of western blotting is to detect proteins extracted from the lysis of cells or tissue homogenate. The separation of proteins, in order to probe for specific proteins of interest (i.e. COX-2), was done via gel electrophoresis. The analysis of the inflammatory marker protein, COX-2, has been established by the use of Western blotting techniques (Abdalla, Sanderson and Fitzgerald 2005)(Laouini, et al. 2005), and used as a standard model in our laboratory (Zulfakar, Abdelouahab and Heard 2010)

2.2.4.4.1. *Preparation of Skin Lysates*

Porcine full thickness skin sections were prepared and set up in Franz diffusion cells following the methods outlined in sections 2.2.2.1 and 2.2.3, with a receptor phase comprised of Hanks buffer. After a 6 h application time the FDC assemblies were dismantled, the membranes recovered and test materials carefully removed then gently cleaned with PBS. The area of application was excised by scalpel dissection and homogenised using a Silverson homogeniser (Chesham, UK) in 1 mL RIPA lysis buffer (1 mM EDTA, 150 mM NaCl, 0.1% SDS, 1 mM PMSF, 1% sodium deoxycholate, 50 mM Tris-HCl (pH 7.4), 1% Triton x-100, 5 μg mL^{-1} aprotinin and 5 μg mL^{-1} leupeptin), the protease inhibitors were added immediately prior to homogenising. The homogeniser was cleaned after each skin section with PBS. The lysates were incubated for 15 min on ice then pelleted by centrifugation at 1400 *g* for 2 x 15 min at 4°C. The supernatant was stored at -20°C.

2.2.4.4.2. *Protein Assay*

The total protein concentration of each supernatant sample was determined via spectrophotometric analysis by the use of BIO-RAD protein assay kit, following the instructions given with the kit (BIO-RAD laboratories Hercules, California). A calibration curve was produced between 0 and 50 μg mL^{-1} BSA in DI H_2O. The sample supernatant (5 μL) was diluted to 1/200 in DI H_2O (1000 μL). 200 μL of the BIO-RAD reagent was added to 800 μL of the diluted sample. Samples were left for a 15 min development time before optical density was read at 595 nm using a Cecil CE2041 series 2000 spectrophotometer (Cecil Instruments, Cambridge, UK). The volume needed for 30 μg of protein for each sample was calculated from the calibration curve.

2.2.4.4.3. *Protein Denaturation*

Skin lysates containing 30 μg of soluble proteins were aliquoted diluted in a 1:1 ratio with 2 x LaemmLi buffer containing 0.1 M DTT within Eppendorf tubes. The mixtures were mixed gently on Eppendorf Mixer 5432 (Eppendorf®-Netheler-Hinz GmbH, Germany) for 5 min. The lids of the tubes were pierced with a syringe needle before heating at 100 °C for 5 min, to denaturise the tertiary form of the proteins, after which they were left to cool for 5 min. The samples were mixed as before on an eppendorf mixer at room temperature and centrifuged (14,000 *g* at 4°C for 1 min, Heraeus

Multifuge *3 S-R*). The denatured samples were then stored at -20°C or used straight away for Sodium dodecyl sulphate-polyacrylamide gel electrophoresis (SDS-PAGE).

2.2.4.4.4. *Sodium Dodecyl-Sulphate Polyacrylamide Gel Electrophoresis (SDS-PAGE)*

The SDS-PAGE protein separation was carried out using the Xcell SureLock 1-d electrophoresis system (Invitrogen, Paisley UK) shown in Figure 2-7. The separating gel (3.3 mL 30 % acrylamide, 2.5 mL 1.5 M tris HCl (pH8.8), 4 mL DI H_2O, 0.1 mL 10 % SDS, 0.1 mL 10% APS and 10 µL TEMED) was pipetted into disposable plastic cassettes, DI H_2O was carefully pipetted on top and the gel was allowed to set for 30 min. Once set the H_2O was poured of the top of the gel and the stacking gel solution (1.7 mL 30% acrylamide, 2.5 mL 1.5 M tris HCl (pH6.8), 5.8 mL DI H_2O, 0.1 mL 10% SDS, 0.1 mL 10% APS and 10 µL TEMED) was pipetted on top of the separating gel, with a well-casting comb and left to set for 20 min. Once set the comb was removed, the wells were washed with DI H_2O and the cassette was locked into position within the Xcell SureLock case. The wells were carefully filled with 1 x running buffer (100 m L running buffer I was added to 1 L DI H_2O) via pipette after which the tank was slowly filled with 1 x running buffer I. The samples were applied via pipette to the bottom of each well, in one well 5 µL of the rainbow marker was applied. The proteins were separated via electrophoresis at 125 V for between 1.5 - 2 h. The cassette was removed once adequate separation had taken place and carefully broken apart for the removal of the gel.

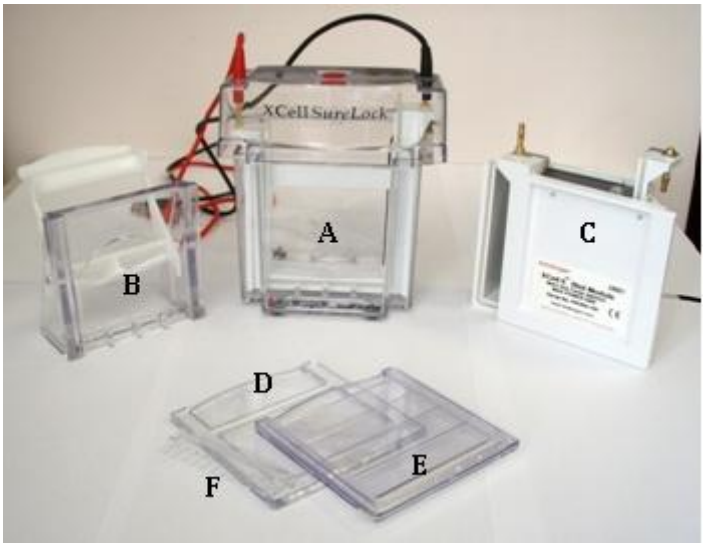

Figure 2-7 Components of XCell SureLock™: (A) electrophoresis module consists of a running tank, buffer core, and lid; (B) gel tension wedge; (C) Xcell™ Blot Module; (D) buffer dam; (E) plastic cassette; and (F) comb.

2.2.4.4.5. *Blotting (Transfer of Proteins)*

Prior to blotting, filter paper and sponge pads were soaked in transfer buffer. Nitrocellulose blotting membrane (0.45 µm pore size) was wetted with methanol and shaken in DI H_2O. The sponge pads filter paper gel and blotting membrane were assembled as shown by Figure 2-8 and placed in the Xcell blotting module. The module was filled with transfer buffer and placed inside the Xcell Sure Lock case which was subsequently filled with DI H_2O. The transfer was run at 25 V for 1.5 h.

Figure 2-8 Assembly of the sponges, filter papers, nitrocellulose blotting membrane and gel for Western blotting of proteins.

2.2.4.4.6. *Immunohistochemistry for Western Blot (IHC)*

The completion of protein transfer to the nitrocellulose membrane was assessed by removing the membrane from the blotting module assembly with tweezers and placing it in a solution of Ponceau S (0.1% w/v Ponceau S in 5% acetic acid) briefly followed by washing with 1 x TBS-Tween and visual assessment of the protein bands was carried out, washing resumed until the blot was cleared.

2.2.4.4.7. *Membrane Blocking*

To prevent the non specific binding of protein the blot was blocked using 5% milk in 1 x TBS tween for 1 h at room temperature with constant rocking. After blocking, the milk solution was discarded and the blot was rinsed with TBS-Tween (3 x 10 min, 10 mL per blot).

2.2.4.4.8. *Primary and Secondary Antibody Conjugation*

The blot was incubated in the diluted primary antibody (COX-2, 1/1,000 dilution, 5 mL per blot) at 4°C overnight with constant rocking. After the overnight incubation the blot was washed with TBS-Tween (3 x 10 min, 10 mL each blot). The blot was incubated with the secondary HRP-linked antibody at a 1/10,000 dilution in TBS-Tween with 1% w/v Marvel milk (a total volume of 5 mL per blot), for 1 h under constant rocking, at room temperature. The membrane was washed in PBS-Tween (3 x 10 min, 10 mL each blot) prior to chemiluminescence signal detection.

2.2.4.4.9. *Detection of Protein*

The chemiluminescence detection of the protein was carried out by the transfer of the blot into a light-proof x-ray cassette with the protein side facing up. The blot was evenly covered with 300 µL of freshly prepared SuperSignal West Dura Substrate working solution. It was incubated in the reagent for 2 min at room temperature. A clear plastic wrap was carefully placed on the cassette to cover the blot, to prevent air pocket formation, and the excess reagent was drained with a soft tissue. The exposure of the blot to autoradiography film varied between experiments until a plot specific exposure time was achieved. The film was developed using X-ray developer (X-O-graph Compact X2, X-O-graph Imaging System, Tetbury, UK). The resulting dark

bands corresponded to the protein of interest. Membranes were subsequently washed in TBS-Tween (3 x 10 min, each) and stored in the fridge for up to 14 days.

The bands were scanned and analysed using Scion Image software for Macintosh, version alpha 4.0.3.2 (National Institute of Health Image, U.S.). β-actin served as a loading control. Histograms represent the ratio of the protein of interest against β-actin and the control is 100%.

2.2.4.4.10. *Loading Control*

β-actin, a 42kDa ubiquitous protein, was used as the loading control to account for any pre experimental variations within the excised skin. The blot was probed with 1/50,000 β-actin primary mouse antibody for 45 min followed by conjugation with Anti-rabbit IgG, secondary HRP-linked antibody for 1 h. Both incubations were done at room temperature with constant rocking. After each incubation the blots were subjected to 3 x 10 min washes in TBS-Tween.

2.2.4.5. Immunohistochemistry (IHC)

IHC is a standard technique used to qualitatively assess the localization and relative levels of proteins within a tissue (Lia, et al. 2005). The specific binding of an antigen to a fluorescently linked antibody, with subsequent staining, allows for the visual assessment of a protein specific colouration of a tissue sample.

2.2.4.5.1. *Application to, and Fixation of, Full Thickness Porcine Skin*

Full thickness porcine skin were set up within a Franz diffusion cell as stated in sections 2.2.2.1 and 2.2.3. The application of 1 mL of test solution to the skin was done via pipette, the receptor solution was HBSS. The porcine skin was removed from the FDC at 0, 3, and 6 h. The application and diffusional area was sectioned into 1 x 0.1 cm^2 strips, placed in disposable cassettes and fixed in 4 % formaldehyde over night.

2.2.4.5.2. *Dehydration and Wax Embedment of Tissues*

The cassettes were passaged through increasing concentrations of EtOH and then chloroform, following Table 2-4, to dehydrate the skin sections.

Solution	Time
70 % Ethanol	2 x 30 min
90 % Ethanol	2 x 30 min
100 % Ethanol	2 x 30 min
Chloroform	1 x 1 h, followed by 2 x 30 min

Table 2-4 Protocol for the dehydration of excised porcine skin sections.

The wax used for embedding the skin samples was de-gassed following the vacuum protocol outlined in Table 2-5.

Wax bath	Vacuum timings
1	Vacuum off 15 min Vacuum on 10 min Vacuum off 5 min
2	Vacuum off 10 min Vacuum on 15 min Vacuum off 5 min
3	Vacuum off 10 min Vacuum on 15 min Vacuum off 25 min

Table 2-5 Protocol for de-gassing embedding wax.

The skin samples were then embedded within the degassed wax by placing the skin sections in moulds so that the skin layers were perpendicular to the mould surface. Molten degassed wax was then carefully poured into the moulds, the cassette lid was placed on top and left to solidify over night. The wax blocks were then removed from the mould so that they could be sectioned.

2.2.4.5.3. *Microtoming*

The wax blocks were mounted on a Shandon Finesse microtome and 5 µm sections were taken. Each section was flattened by floating on 40 °C DI H_2O and mounted on Surgipath microscope slides.

2.2.4.5.4. *Dewaxing and Rehydration*

The dewaxing and rehydration of the skin sections, required prior to staining, was done by heating the slides within an oven at 60 °C then passaging of the slides through solutions following Table 2-6.

Solution	Time
Chloroform	2 x 7 min
Ethanol 100 %	2 x 3 min
Ethanol 90 %	2 x 3 min
Ethanol 70 %	2 x 3 min

Table 2-6 Dewaxing and rehydration protocol for microtomed, wax embedded, skin sections on microscope slides.

2.2.4.5.5. *Peroxidase Blocking*

The use of a HRP conjugated antibody may result in high non-specific background staining. It is therefore important to block the staining caused by the endogenous peroxides. A 3% hydrogen peroxide solution was applied to the skin sections for 5 min, excess hydrogen peroxide was removed by passaging the slides through PBS (2 x 3 min).

2.2.4.5.6. *Antigen Recovery*

To recover any antigen which is masked by the fixation process the samples were microwaved in 1 L citrate buffer for 15 min, followed by cooling *In situ* for 35 min. The slides were washed with running tap water for 15 min and then rinsed with PBS. Each skin section was outlined with a wax pen and were then blocked by the incubation of the slides in PBS-Tween, for 20 min, within a humidity chamber.

2.2.4.5.7. *Primary Antibody*

The primary antibody COX-2, at a 1 in 50 dilution (PBS), was added via pipette onto each section and left over night at room temperature. The slides were then washed by PBS and then PBS-Tween.

2.2.4.5.8. *Detection, Staining and Counter Staining*

The Dako Envision+ system horse radish peroxidise labelled polymer anti rabbit (HRP) was used as the detection system. The HRP linked secondary antibody was applied to the skin sections and left at room temperature for 2 h. The sections were rinsed in PBS and PBS-Tween. The application of the Dako Chromogen system enables the binding of three 3 Diaminobenzidine to the HRP, if binding occurs then a brown colour is observed. One drop of stock solution was added to 1 mL DI H_2O and was applied to the skin sections for a period of 10 min, after which the slides were rinsed in DI H_2O. Each sample was then counterstained by the application of 0.5% methyl green for 2 min, followed by rinsing in DI H_2O. After drying the slides were covered with DPX and a cover slip. The skin sections were imaged under a microscope (Optihop, Nikon Corporation, Tokyo, Japan) equipped with a camera (Axiovision LE, Carl Zeiss Ltd., Welwyn Garden City, UK).

2.2.4.6. Rheology

Hydrogel formulations were subjected to rheological examination in order to obtain the shear strain, shear rate and viscosity parameters, using a Bohlin CS10 Rheometer (Malvern, UK). Viscoelastic measurements were taken shortly after the formulation of the hydrogel. For this specific analysis the rheometer was fitted with a cone and plate assembly. A mass of 300 mg of gel was placed on the plate and the cone was lowered onto the matrix so that the gap between cone and plate was 0.5 mm, this gap and the temperature (32.5 ± 0.1 °C) was maintained throughout the experiment. The cone was spun with at incremental speed and the force required for the maintenance and increase in revolutions was measured. The mechanical analysis of these factors on the increase and decrease of the shear stress from 30 Pa to 300 Pa back to 30 Pa enabled the calculation of shear rate, strain and viscosity (Barbucci, et al. 2008). The technique was repeated twice for each sample and the averages plotted graphically. The interpretations of the graphs were done in respect to the illustrations of flow curves for typical Newtonian, plastic, pseudoplastic and dilatant flow (Barry 1983).

2.2.5. Cell Culture Techniques

2.2.5.1. Cell Culturing

As already mentioned, viruses are unable to replicate without a host. Therefore cultures of cells were used to act as host cells and allow the replication of the virus. All cell culture experiments were performed in an Envair class II unidirectional laminar-down flow microbiology safety cabinet (Haslingden, UK). These were kept at 37°C and 5%CO_2. The cell types used within this thesis are green monkey kidney epithelial Vero cells, and rabbit kidney 13 (RK13) cell line, which was initiated from the kidney of a 5-week-old rabbit (*Oryctolagus cuniculus*) (Nikon 2011).

2.2.5.2. Sterile Technique

Sterile manipulation was used in cell culture as any bacterial contamination can cause bacterial over growth resulting in competition for nutrients in the media, and possible cell death, and it will also alter the behaviour of the cells to any test conditions. Antibiotics can be used to prevent any growth; however good aseptic technique is often the best practice to adopt. In all of the work antibiotics were not used as one cannot always fully distinguish the role in which they are playing in the tests and the effect of their interaction with any drug added. In this study, a class II cabinet was used for all cell culture manipulation.

2.2.5.3. Isolation of Cells

The cells are isolated from soft tissue, such as monkey kidney epithelial tissue, by enzymatic degradation. The enzyme used is trypsin, which is a protein digestive enzyme that releases the cells from the extra cellular matrix to produce a suspension of cells, however this enzyme will kill the cells if left on for an extended period of time. The cells are left to settle in a bottle containing a nutrient rich media as described below.

2.2.5.4. Cell Media

Cells need to be grown in an environment that mimics physiological conditions, therefore the cells were grown in a nutrient rich medium and incubated at 37^{o}C, 5% CO_2 in an incubator. The type of nutrient rich medium used was Dulbecco Modified Eagles Medium (DMEM) which contains +glucose, +glutamine and -pyruvate. For

cells to grow effectively Foetal Bovine Serum (FBS) was also added at a concentration of 10%. The environment of the cells was kept at a neutral pH, DMEM is a bicarbonate buffer but the pH of added drugs and other media was taken into careful consideration. Media changes were required to avoid a build up of metabolic by-products and dead cells, and to replace nutrients.

2.2.5.5. Passaging of Cells

Passaging or splitting of the cells was done on a regular basis when the cells become 90-100% confluent as shown by Figure 2- 9. If this is done regularly the health of the cells is maintained. If not done regularly the cells will no longer grow in a monolayer upon the bottom of the container and they may morphologically change. A high density can cause death of cells due to depletion of nutrients or arrest of replication due to contact inhibition. Although the number of times a particular cell line is able to be passaged is around 50 times, after this many passages the cells will degrade and morphologically change and no longer act normally.

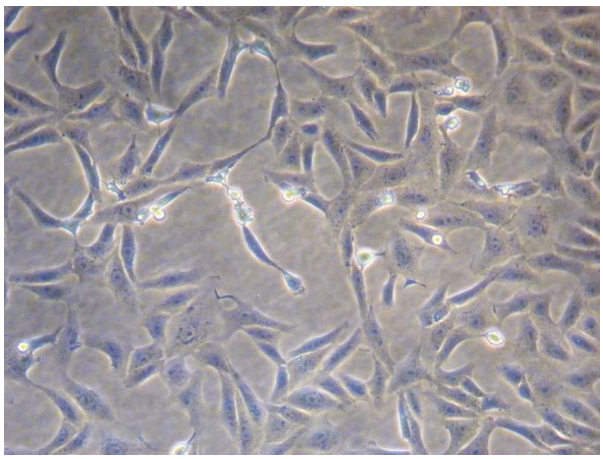

Figure 2-9 An inverted phase contrast microscope image of Vero cells.

To passage Vero cells from a T75 following sterile technique the cell media was removed and discarded, 2 mL of trypsin was added to the T75 and washed over the cells 5 times, then removed and discarded. 1 mL of trypsin was added to the cells and spread over the bottom of the container the container which was then incubated for 5-7 min at 37°C, 5% CO_2 until all cells were freely moving in the liquid. This was microscopically assessed before any further action. The Trypsin containing cells was then removed and either discarded, used or stored in an Eppendorf tube for further use.

The T25 was then refilled with 10 mL DMEM With 10% FBS and replaced in the Incubator.

2.2.5.6. Plating Vero Cells in a 24wp

The Vero cell trypsin solution obtained following the passaging of a confluent T75 (section 2.2.5.5.) was added to 50 mL of DMEM containing 10% FBS. This was thoroughly mixed and pipetted in 1 mL portions to each well. The 24WP was incubated overnight and microscopically analysed for confluency before use.

2.2.5.7. Cell Titer 96® AQueous Assay

A cytotoxic assay allows the evaluation of the effect a drug or foreign body has upon cells. The assay was done in a 96 WP with a known concentration of cells in each well, which allowed for the quantification of viable cells. To do this after a pre-defined incubation period Cell Titer 96® was added. Cell Titer 96® AQueous assay is a colorimetric test for determining the living cells. It consists of a tetrazolium compound [3-(4,5-dimethylthiazol-2-yl)-5-(3-carboxymethoxyphenyl)-2-(4-sulfophenyl)-2H-tetrazolium, inner salt] (MTS) and an electron transfer reagent phenazine methosulphate (PMS). Cells which are still metabolically active convert MTS into a water soluble Formazan product through dehydrogenase enzymes, these enzymes generate the reducing agents NADH and NADPH which are thought to play an important role in converting MTS into Formazan. Formazan is a coloured compound so therefore the absorbance measured at 490nm is directly proportional to the amount of viable cells (Berridge and Tan 1993).

A concentration of 2.5 x 10^3 cells per well for each plate was used, by the trypsinisation of 80% Vero cells within a T75 container and reconstituted in fresh media. Cells were seeded onto 96-well plates and incubated for 24 h at 37°C, 5% CO_2. The medium was removed by aspiration, washed 3 times with DPBS then immediately replaced with the dilutions of test materials. Cells were incubated for 6, 24, 48 and 72 h. Cell Titer 96® AQueous solution was used to detect cell viability. It was added to each well and the plates were incubated for 1 h at 37°C, 5% CO_2. The optical density was then determined at 492 nm. The reading from the blank sample was subtracted from each sample reading and the means of density for the control cells were arbitrarily assigned a value of 100%.

2.2.5.8. HSV-1 -2 and ACR Growth Kinetic

The growth conditions required for the propagation of high titre HSV-1 and HSV-2 ACR (Aciclovir resistant) was investigated by assessing the optimum container size and host cell.

2.2.5.8.1. *Viral Growth:*

For the viral stock Growth kinetic an MOI (multiplicity of infection) of 0.01 was used (Balfou 1999) (Clercq 2004). Each confluent T25 of Vero cells and RK-13 cells contained approximately 3 x 10^6 cells so the viral titre must equal 3 x 10^4.

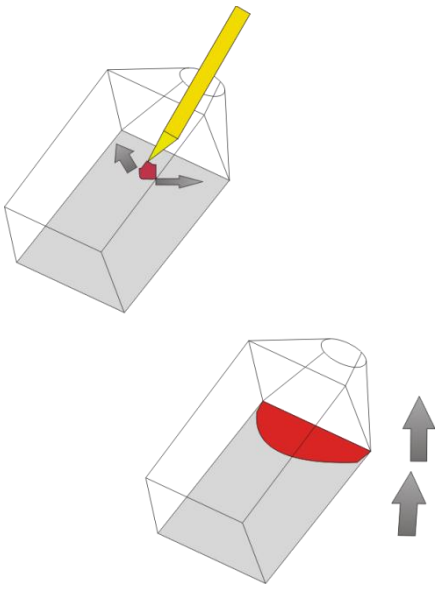

Figure 2-10 A diagrammatic representation of the viral infection in confluent T25 flasks

In confluent T25s the medium was removed and discarded, the cells were washed 3 times with 10 mL PBS. 300 µL of virus (moi 0.01) was added to each T25, the virus was pipetted into one area at the top of the T25 and spread from left to right to form a solution front, the T25 was slowly tipped so that the virus solution front flows over all the cells. This process takes 2-3 min and is illustrated in Figure 2-10.

After infection, cell medium was replaced with DMEM and 2.5% FBS. The T25s were then incubated at 35 °C and 5% CO_2 for as many days as desired before collection.

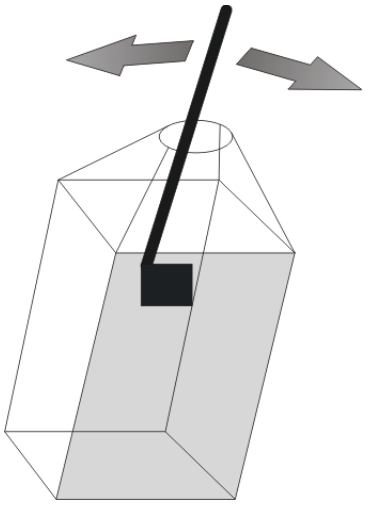

Figure 2-11 Cell removal from a T25 flask using a cell scraper.

2.2.5.8.2. *Collection of Virus*

After incubation, the supernatant was mixed and removed from the T25 via a pipette then frozen in 1 mL aliquots at -70 °C. The cells were removed from each bottle using a sterile cell scraper in an oscillatory fashion, slightly rocking the bottle so that all the cells were floating in the medium. This motion was repeated until

no cells were visible on the bottom of the tissue culture flask**,** as shown in Figure 2-11.The suspension was then washed over the base of the culture flask, 1 mL of this was frozen at -70°C.

2.2.5.8.3. *Viral titre analysis*

The analysis of the supernatant titre was carried out on Vero cells in 24 well plates (24WP) following the same method as that used for virucidal titre analysis below.

2.2.5.9. Plaque reduction assay

A plaque reduction assay uses titration of a known concentration of a virus to infect a cell culture monolayer in a number of different wells of the same size. This was performed in a 24WP. Each virion resulted in a localized area of infection known as a plaque. From this the number of plaque forming units (pfu) was quantified representative of the number of virions present. A crystal violet stain distinguished between healthy or damaged and destroyed cells. The number of plaques was then counted. Figure 2-12 shows an example of an individual experiment in a 24WP.

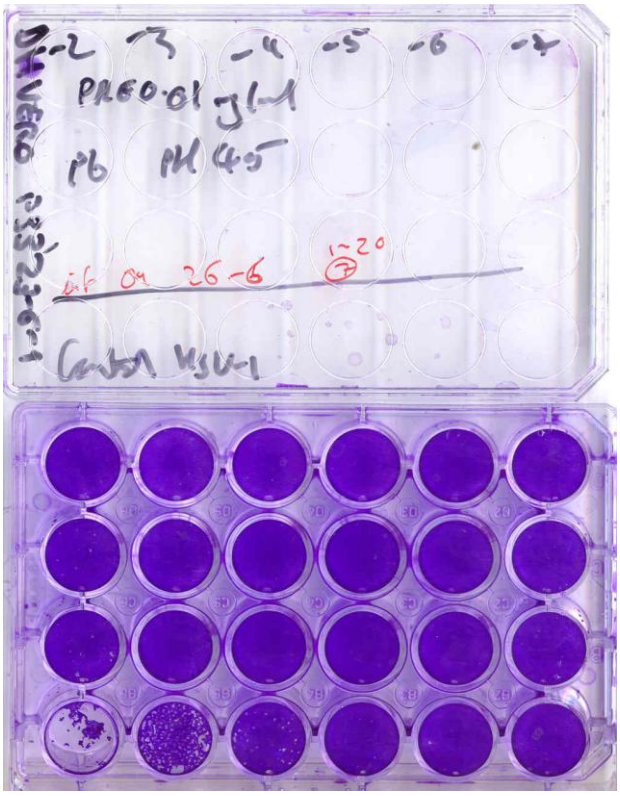

Figure 2-12 An example experimental 24 well plate of the number of plaque forming units (pfu) observed after the 3 day incubation of HSV-1 on confluent vero cells. The HSV-1 was introduced to PRE 0.01 mg mL^{-1} for 30 min prior to incubation, the control HSV-1 was not.

The annotations to the top plate are: 'Inf' refers to infection, followed by the date (09) day and month (26-6), the circled number represents the numbered infection on this day, eg 7, then a brief description of the drug used i.e. PRE 0.01 mg mL^{-1} + pb (phthalate buffer pH4.5), the virus strain used was HSV-1. The untreated control HSV-1 dilutions are the lower row of 6 wells. DH refers to the initials of the experimenter and the host cells are Vero cells with the passage number (P33) and the date of that passage (23-06-09).

2.2.5.10. Antiviral Plaque Assay

Antiviral activity was analysed by the application of drug and then virus (after an incubation period) to confluent Vero cells in a 24WP (section 2.2.5.6.). For each confluent 24WP one drug was analysed in 5 different concentrations i.e. 100 µM, 50 µM, 10 µM, 5 µM and 1 µM and a control. Each dilution was replicated in 4 wells. Using suction, media was removed from the first row of four cells and application of 400 µL of drug was applied. This was repeated until all medium was removed and

replaced. Once the last well was filled the time was noted, and the plates incubated for 30 min to allow for any cellular absorption or reaction.

After the 30 min incubation period, 100 µL of virus (ca 150 pfu mL^{-1}) was added to each well. Each plate was rocked / swirled to ensure an even spread of the virus. The plate was then incubated at 37°C for 45 min with rocking/swirling every 5 min, to ensure potential viral entry into the cells. After the incubation period, 300 µL of 1.2 % Avicel overlay was applied to each well and the plate was incubated for three days. The plates were then stained using crystal violet. A plaque assay was used to assess the antiviral activity of a compound by quantifying infectious viruses (Matrosovich, et al. 2006).

2.2.5.10.1. *IC_{50} Calculation*

Antiviral results are normally presented as an IC_{50} value, IC_{50} is an abbreviation for the half maximal inhibitory concentration. This is a measure of the effectiveness of a compound in inhibiting biological or biochemical function. In this case the inhibitory effect was in respect to HSV-1 infection. When an IC_{50} value was not present due to incomplete results or when testing a vehicle (i.e. phthalate buffer) an IC_{50} was either taken from the curve or the greatest antiviral response was stated.

The IC_{50} was calculated from the equation given by the application of a special logistic function producing a sigmoid curve. This was always done in respect to the log of the drug concentration, and as a percentage of the control. Graph Pad Prism 5 (GraphPad Software Inc, California, USA) was used to analyse the data.

2.2.5.11. Avicel Overlay Medium

An overlay medium is added to all plaque assays in order to stop the virus becoming detached from the infected cells and thus spreading over the cell monolayer. If the overlay is not applied then plaques would become too large and merge, the virus could also replicate within the cells and produce secondary plaques giving a false result. Avicel microcrystalline cellulose that had been partially hydrolysed with acid and reduced to a fine powder was the overlay medium used for this study. Avicel is a relatively new medium that is a colloidal form of water insoluble cellulose microparticles blended with sodium carboxymethylcellulose to facilitate dispersion.

The Avicel particles are readily dispersed in water to form suspensions and thixotropic gels and it also has a relatively low viscosity.

2.2.5.12. Recovery of Penetrants in FDC Receptor Phases

The methodology for the penetration of test compounds through HSE for maximal delivery was given in sections 2.2.2.1. and 2.2.3, however the receptor phase was only removed once after 24 h and was freeze dried. This was reconstituted in 100 µL of DI H_2O and passed through a 0.45 µm pore size Whatman syringe filter for sterilisation. The solution was retained and stored in a sterile Eppendorf tube, after which it was used as the test material for virucidal analysis following that stated in section 2.2.5.9.

2.2.6. Fractionation of PRE by Column Chromatography

Fractionation of PRE was achieved in a 2-step process, generally following the method of Seeram et al (2005).

2.2.6.1. Amberlite XAD-16

All H_2O was degassed and deionised prior to use. All MeOH was degassed prior to use. The column was slurry packed using 75g of Amberlite XAD-16 resin in H_2O with 2cm sand protecting layers above and below the resin, using a glass wool plug. The resin was washed with 300 mL MeOH then 100 mL H_2O and left for 12 h to equilibrate. PRE was adsorbed onto the column, the optimal loading volume 40 ± 5 mL per 75g of preconditioned XAD-16 resin per column. The column was eluted with 300 mL of H_2O until the tannin devoid pale yellow eluent (fraction1) shown in Figure 2-13 was fully removed. The remaining tannins were eluted with 100 mL MeOH to yield a dark red solution (fraction 2). The time taken to produce one cycle <30 min.

Figure 2-13 XAD-16 Column with adsorbed PRE. Using H_20 to fraction the yellow tannin devoid solution being collected, leaving the red total pomegranate tannins (TPT) on the column.

2.2.6.2. Sephadex LH-20 Column

The fractionation of TPT was done following an established method for purifying punicalagin from total pomegranate tannins (TPT) (Seeram et al., 2005). The precise solvents used were solvent A (H_2O 80 : 20 MeOH) and solvent B (H_2O 20 : 80 MeOH). Each solvent was filtered through a Whatman 0.45µm filter before use to protect the column from large insoluble particles, bacteria and reduce the risk of gas bubbles forming. The solvents were introduced to the column via two automatic syringe drivers. Non-return valves were fitted at the point of solvent mixture.

A 35 cm^3 column (0.75 cm radius) was slurry packed with 8.8g of Sephadex LH-20 in 40 mL MeOH with a glass wool filter. The slurry was left to expand for 3 h prior to

packing. The gradient elution timetable with the two solvent systems running in unison (combined total of 18 cm^3 h^{-1}) followed that stated in Table 2-7 with collection of each fraction after 1 h (fractions 1-8) with the last fraction collected over 3 h (fraction 9).

Solvent A (mL h^{-1})	Solvent B (mL h^{-1})	H_2O %	MeOH%
18	0.00	80	20
16.5	1.44	75.2	24.8
15.12	2.88	70.4	29.6
13.50	4.50	65.0	35.0
11.88	6.12	59.6	40.4
10.44	7.56	54.8	45.2
9.00	9.00	50.0	50.0
7.38	10.62	44.6	55.4
5.94	12.06	39.8	60.2
4.50	13.50	35.0	65.0
2.88	15.12	29.6	70.4
1.44	16.56	24.8	75.2
0.00	18.00	20	80

Table 2-7 Gradient elution timetable for the fractionation of TPT with solvent A and solvent B through a Sephadex LH-20 column

2.2.6.2.1. *Removal of Solvents from the Fractions*

After column chromatography all fractions were occluded from light and cooled to -20°C. MeOH was removed under vacuum at less than 0°C and occluded from light, using two liquid nitrogen cold traps. After which the samples were frozen at -20°C so that the remaining H_2O could be removed by freeze drying. The residue of each fraction was weighed, occluded from light and stored at -20°C until further use.

2.2.7. Hydrogel Formulation

The 'hot/cold' technique involved heating 1/5th to 1/3rd of the desired overall volume to approximately 80°C and then dispersing the required amount of thickening agent to the heated liquid. The solution was mixed continuously until all particles were thoroughly wetted (DOW Chemical Company 2002). To complete the solubilisation process the remainder of the liquid required to make the total volume was added to the heated solution. This liquid was cooled or iced to ensure the thickening agent becomes solubilised in water, and therefore result in the powder hydrating and the hydrogel becoming more viscous. Agitation of the hydrogel continued for 30 minutes after the

addition of the cooled water to guarantee a uniform and evenly dispersed hydrogel. All formulations were refrigerated for a minimum of four hours after agitation so that a uniform hydrogel was formed (Tonic-Ribarska, et al. 2005).

In the formulation process of Methocel 856N with PRE it was observed that black dots appeared within the hydrogels, Figure 2-14 shows examples of this phenomenon. After the application of a strong magnetic field to the Hydrogel the coloured dots migrated towards the source of the magnetic field leaving a dark streak behind. Due to the migration of the dots and the aforementioned blackening of PRE upon the addition of $FeSO_4$ it was hypothesised that the dots were due to iron flakes attached to the magnetic stirrer bars, used for continuous agitation, which were removed from the magnet as the gel thickened. Therefore it was decided to use a glass rod for all agitation and stirring, after which no black dots appeared. Therefore to prevent Fe contamination the formulation process used no magnetic stirrers.

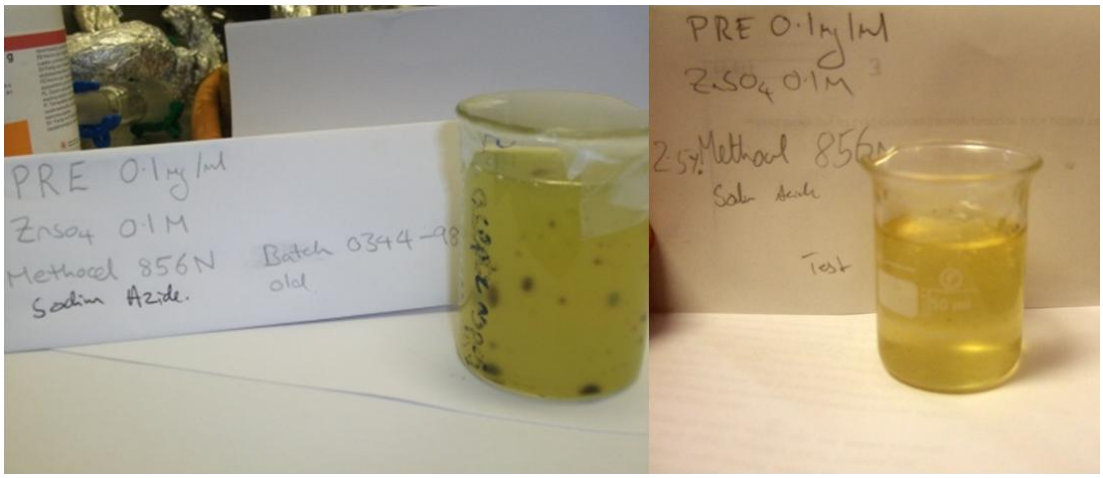

Figure 2-14 Comparison of hydrogels containing 2.5% Methocel 856N, 0.1 mg mL^{-1} PRE and 0.1M $ZnSO_4$ after formulation with (left) and without (right) the use of a magnetic stirrer, (formulation using a magnet displaying "black dots" due to contamination with iron particulates).

2.2.7.1. Aesthetic tests

Generally, 3 tests were carried out to determine formulation aesthetics:

- Appearance was determined visually under normal light. The gels were examined for obvious properties including hue, clarity and homogeneity. Additionally, approximately 50 µL of formulation was applied to porcine

epidermis and a clean round bottomed glass rod used to apply pressure and was twisted 20 times. A visual inspection of the dermis was then conducted to assess the appearance on skin.

- Formulations were also probed by the author, for any discernible odour.
- Tactile properties were determined by rubbing a small amount (approx 50 μL) of formulation between thumb and index finger, where obvious greasiness, grittiness and sensitivity were noted.

2.2.8. Statistical Analysis

Data are expressed as means ± s.d. unless otherwise stated. One way analysis of variance (ANOVA) with either Tukey's post test (to identify statistical significances between groups) or Dunnett post test (to compare groups against the control) and $p < 0.05$ and $p < 0.01$ were defined as significant and very significant respectively. the analysis was carried out using InStat for Macintosh, version 3.0 (GraphPad Software Inc, San Diego, CA).

Chapter 3 **HSV Growth Kinetic and the Virucidal Activity of PRE and Ferrous Sulfate against Herpes Simplex Virus**

3.1. **Introduction**

As described in Chapter 1 the combination of PRE + $FeSO_4$ has been shown to exhibit potent synergistic (potentiated) phagicidal activity. Within the patent (Jassim, Stewart and Denyer 1995) it was further stated that synergistic HSV-1 virucidal activity had been observed, although no data was provided. It was hypothesised that the synergistic phagicidal action observed with respect to a range of bacteriophage [*Staphylococcus* NCIMB 9563, *Salmonella* Felix O-1, *Pseudomonas* NCIMB 10884 and *Pseudomonas* NCIMB 10116 (Stewart, et al. 1998)] was due to modulation of the bacteriophage envelope and that this action may also be observed with other microorganisms with similar envelopes, for example enveloped viruses such as Herpes simplex virus. This is due to the similarities between the bacteriophage protein envelope and the protein envelope encapsulating the HSV-1 virion. The phagicidal activity of PRE and $FeSO_4$ was shown to be transient in nature and inactive after a 3 minute reaction time between PRE and $FeSO_4$. The reaction of PRE and $FeSO_4$ also created a black precipitate (Stewart, et al. 1998).

Possible modes of action for the phagicidal activity have been attributed to the reaction of compounds within PRE and Fe^{2+} resulting in both the destruction of the bacteriophage envelope and the creation of a black precipitate (Stewart, et al. 1998). An alternative hypothesis was that the phagicidal action of one or more compounds within the PRE mixture and the Fe^{2+} ion acted synergistically whilst the ion is in free solution. After the ion had undergone reaction it had bound with the phagicidal compounds within PRE thus inactivating the mixture. Another theorised mode of action is the creation of free radicals, the addition of the ferrous ion enabling a cascade effect of electrons, the transient nature of the observed bioactive state occurring within this window of free radical production before the known ability of punicalagin to act as an antioxidant, with the potential to reduce free radicals involved in chain reactions that damage cells. This protective effect of punicalagin has been well established with differing materials and methods (Slusarczyk, et al. 2009) (Turk, et al. 2008) (Seeram, et al. 2005).

The objective of this Chapter was to determine whether the previously reported activity of PRE and $FeSO_4$ against bacteriophage and Herpes simplex virus type one (HSV-1) could be replicated. In particular, similarities to the previously reported work, in terms

of the kinetics of antimicrobial activity, were probed and the implications of the black by-product considered.

3.1.1. Objective and Aims

To establish the optimum growth parameters for HSV-1 and HSV-2 ACR and evaluate the virucidal activity of PRE and $FeSO_4$ against Herpes simplex virus and consider its practical complications.

-Optimise the growth conditions for HSV-1 and HSV-ACR

-Analyse the cytotoxic effect of all formulations

-Probe the kinetics of virucidal activity of PRE + $FeSO_4$ against HSV-1 and HSV-ACR

-Consider the implications of any black by-product

3.2. **Materials and Methods**

3.2.1. Materials

The materials used within this Chapter are given in Chapter 2 section 2.1.

3.2.2. Methods

The methodology for general cellular microbiology and the formulation of solutions extracts and buffers follows that described in Chapter 2 section 2.2.1. unless otherwise stated.

3.2.2.1. Growth Kinetics of HSV-1, HSV-2 and HSV-ACR

In order that high stocks of HSV-1 and -2 ACR (Aciclovir resistant HSV-2) can be grown, it was important to investigate the specific growth kinetics of each virus type. Titres up to or greater than 1×10^7 are needed in order to carry out both antiviral and virucidal studies. For the purpose of viral growth kinetics Vero cells (Brant, Coakley and Grau 1992) and the rabbit kidney 13 (RK13) cell line, which was initiated from the kidney of a 5-week-old rabbit (*Oryctolagus cuniculus*) (Nikon 2011), were evaluated as

host cell lines (Epstein, Yvonne and Jacquemont 1990) (Rigby and Johnson 1972). The methodology for this is stated in Chapter 2 section 2.2.5.8.

3.2.2.2. Viral Titre Determination

The titre of the supernatant was established on Vero cells in 24 well plates following the same methodology as that used for virucidal titre determination (section 2.2.5.8.3.).

3.2.2.3. Virucidal Assessment

To establish the virucidal activity of PRE and $FeSO_4$ against HSV-1 the virucidal plaque reduction assay was used and followed the procedure detailed in section 2.2.5.9. HSV-1 was retrieved from storage in a freezer at -80°C. The materials tested were PRE, $FeSO_4$ and phthalate buffer alone and in combination. The virucidal analysis of the combination of PRE, $FeSO_4$ and phthalate buffer was indicated by introducing HSV-1 to the combination immediately upon mixture. To assess the time dependant nature of activity, samples of mixture were held occluded from light and at room temperature for 3, 12 and 24 h after which they were introduced to the virus beginning the virucidal plaque reduction assay.

3.2.2.4. Cell Titre 96 Aqueous Cell Proliferation Assay

The metabolic viability of green monkey epithelial kidney cells (Vero cells) treated with PRE, $FeSO_4$ and phthalate buffer (pH4.5) was assessed using the cell titre 96 aqueous one solution assay as described in section 2.2.5.7. 96-well plates were prepared, the medium was removed by aspiration and 10-fold dilutions of PRE (1mg mL^{-1}), $FeSO_4$ (1M) and phthalate buffer (pH 4.5) in DMEM were added onto sub-confluent Vero cells in 4 replicates for each concentration. 12 sub-confluent wells containing 100 µL DMEM were used as a control and 12 wells containing only DMEM in the absence of cells was used as a blank. After an incubation time of 6, 24, 48 and 72 h the growth medium was removed via aspiration and the cells were washed three times with DPBS. Following this 20 µL of cell titre 96 one solution (containing MTS and PES) and 100 µL of DMEM was added to each well. After an incubation of 1 h (37°C, 5% CO_2) optical density measurements at 490nm were taken and the results plotted graphically.

3.2.2.5. Statistical Analysis

The statistical analysis of data followed that stated in Chapter 2 section 2.2.8.

3.3. **Results**

3.3.1. Optimizing Viral Growth Conditions for HSV-1 and HSV-ACR

Figure 3-1 displays the viral titre retrieved after the incubation of HSV-1 in two types of container (T25 and T150) using vero cells as the host. It can be seen that throughout all time points analysed the greatest viral titre retrieved was following incubation within the T25 container. A generally linear growth pattern was observed with time of incubation and viral titre from the T150 container; this trend was not so apparent within the T25 flask, which increased over 48 h, followed by a slight decrease at 72 h with a linear response to time after this point.

An incubation time of 5 days as expected resulted in the largest titre of HSV-1 retrieved from the T150 at $3.0 \times 10^6 \pm 1.9 \times 10^6$ and T25 $4.3 \times 10^7 \pm 1.8 \times 10^6$. However the smaller container (T25) produced a higher titre at each time point, this was an unexpected result due to the use of the same multiplicity of infection (MOI).

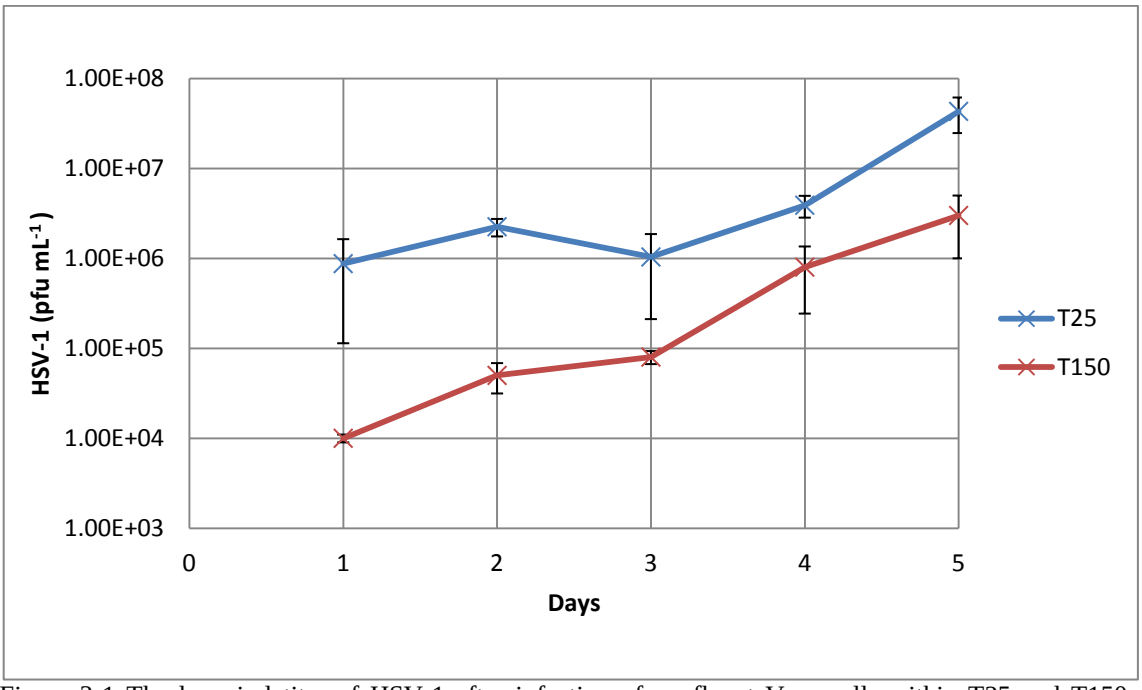

Figure 3-1 The log viral titre of HSV-1 after infection of confluent Vero cells within T25 and T150 containers over 5 days (MOI 0.01) (n=4, ± S.D.)

Figure 3-2 shows that the growth kinetics of HSV-1 with an MOI of 0.01 in Vero cells and RK-13 cells is similar within both types of host cell. A slight decrease is observed at 72 h however the titre reaches a maximum after a 5-day incubation period within the host RK-13 and Vero cells resulting in a maximum titre of 3.7 x 10^7 and 4.3 x 10^7 respectively.

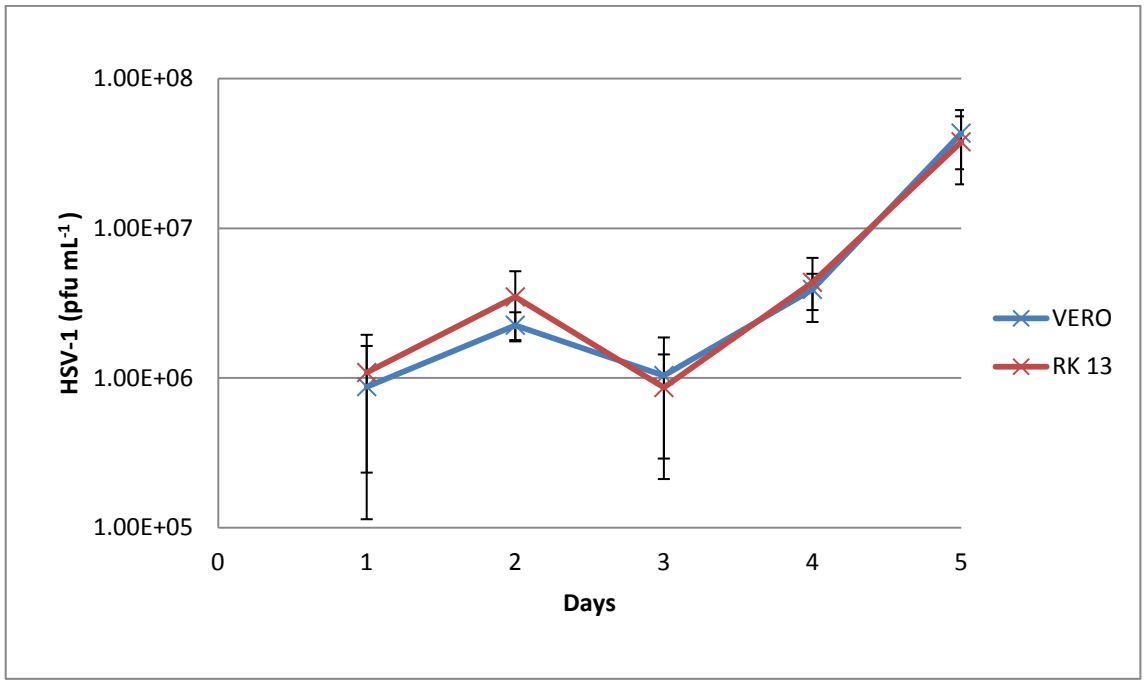

Figure 3-2 The log viral titre for the growth of HSV-1 after infection of confluent T25 with Vero and RK-13 host cells over 5 days (MOI 0.01) (n =3, ± s.d.)

The growth kinetics in Figure 3-3 of HSV-2 ACR with Vero and RK13 as the host cells within a T25 container shows a similar trend with respect to the time of incubation. However the titre obtained using a Vero cell host was greater with maximum levels of 1.74 x 10^8 ± 1.5 x 10^6 and 1.79 x 10^8 ± 1.2 x 10^6 after 2 and 4 day incubation periods respectively. After 4 days of incubation full lysis of the cells was observed this resulted in a decrease in viable HSV-2 ACR.

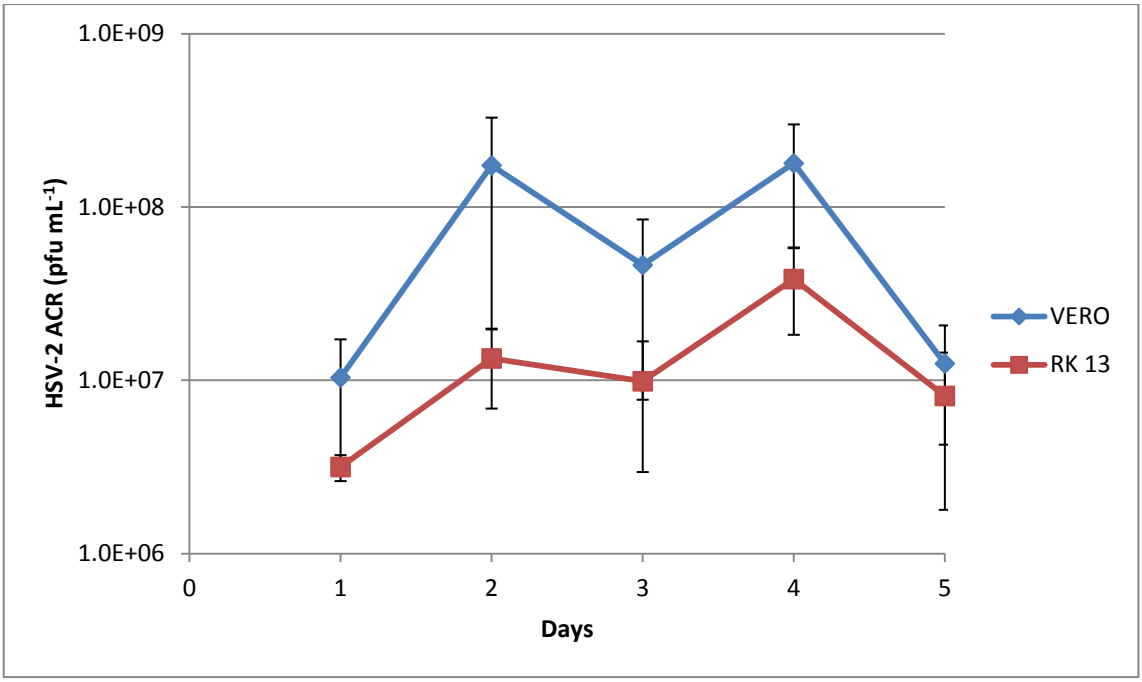

Figure 3-3 The log viral titre for the growth of HSV-2 ACR after infection of confluent T25 containers with Vero and RK-13 as the host cells over 5 days (MOI 0.01) (n=3, ± s.d).

The viral growth of HSV-2 ACR, with Vero and RK 13 as host cells within the T150 container is displayed in Figure 3-4, this shows that viral growth is maximised after 24 h in Vero and RK-13 cells with titres of $4.2 \times 10^7 \pm 8.4 \times 10^5$ and $2.6 \times 10^7 \pm 7.2 \times 10^5$ respectively. There was a general decrease in titre within both cell lines with respect to time. The viral titre retrieved was not significantly different between the host cells except after an incubation of 4 days, in which a greater titre was retrieved from the Vero cell host.

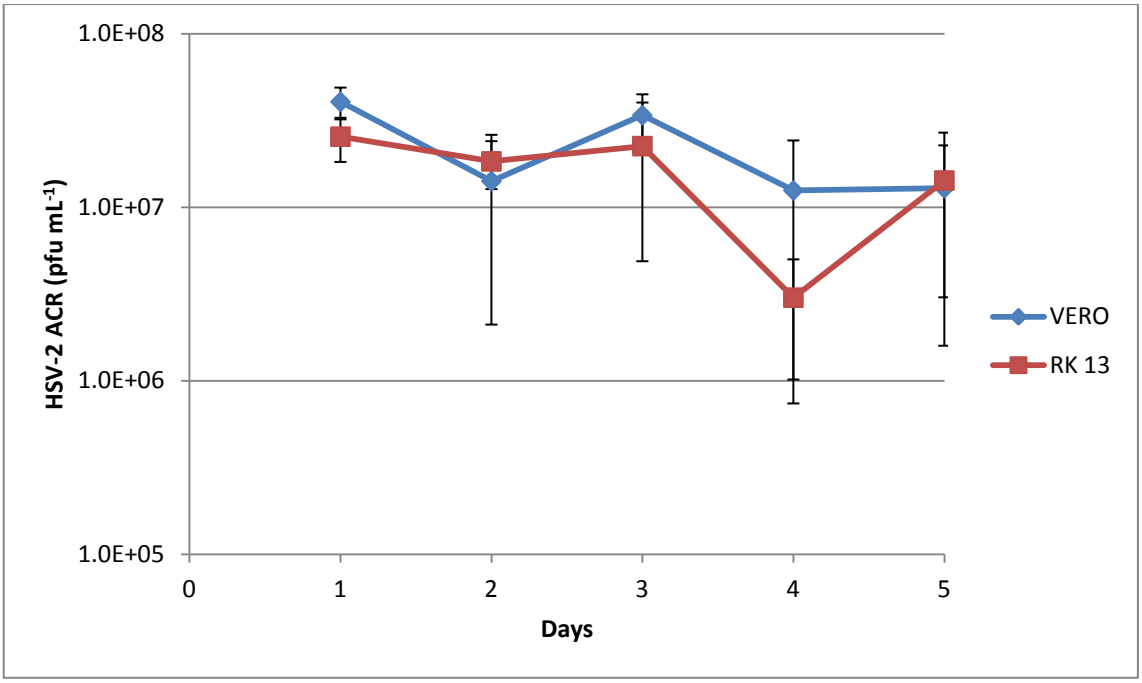

Figure 3-4 The log viral titre for the growth of HSV-ACR after infection of confluent T150 with Vero and RK-13 host cells over 5 days (MOI 0.01)

The optimal growth conditions for HSV-1 and HSV-2 ACR was observed using Vero cells as the host cell and within the T25 container after an incubation of 5 and 2 days respectively.

3.3.2. Cytotoxicity of PRE, Ferrous Sulphate and Phthalate Buffer

Figure 3-5 shows the cell proliferation of Vero cells after application of the test materials over a 72 h period. It was observed that after this period of exposure Phthalate buffer and $FeSO_4$ (1M) caused no significant decrease $P>0.05$ in cell viability. Application of PRE (1 mg ml^{-1}) led to a decrease of cell viability by 14% ± 0.14 and 47% ± 0.183 after 48 and 72 h respectively; it was therefore necessary to examine the effect of PRE at lower concentrations, to determine whether the *in-vitro* application of PRE to Vero cells would affect the cells during virucidal or antiviral testing via plaque assays. The highest applied concentration used within this project was PRE 0.1 mg mL^{-1}. Figure 3.5 shows that after 48 h incubation no significant decrease in viable Vero cells was observed at this concentration. Therefore the concentrations employed in all testing during this project do not affect cell viability and the compounds used are proven to have a low cytotoxicity.

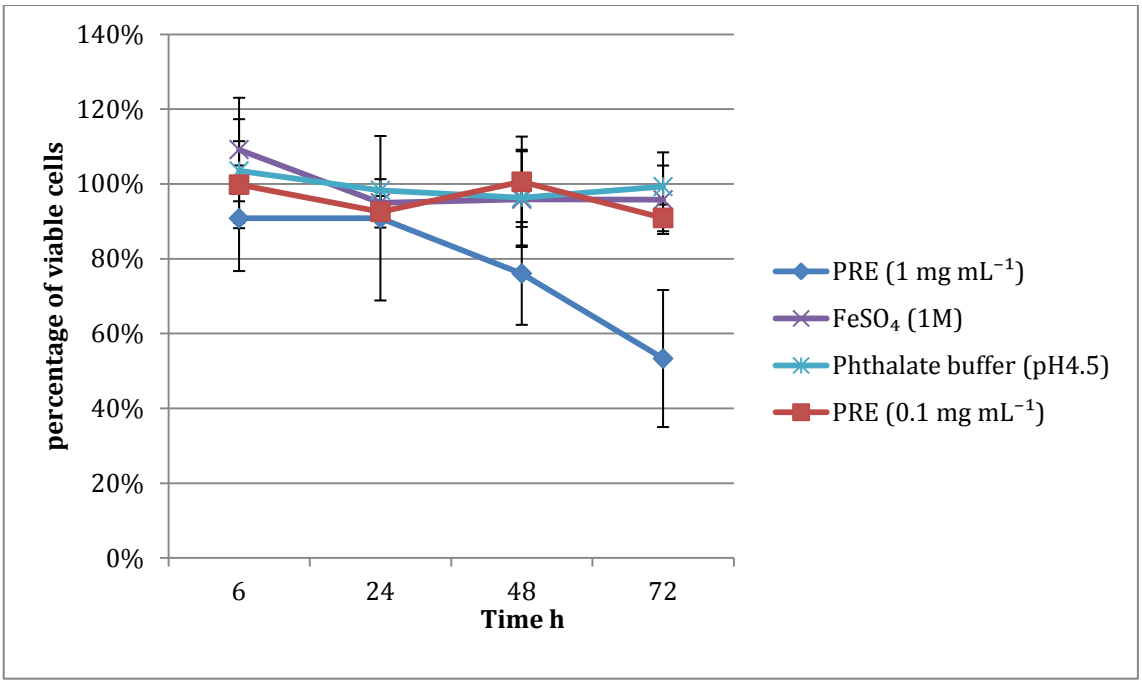

Figure 3-5 Proliferation of Vero cells at 6, 24, 48 and 72 h after the application of PRE (1 mg mL^{-1}), PRE (0.1 mg mL^{-1}), $FeSO_4$ and Phthalate buffer.

3.3.3. Virucidal Activity of PRE and $FeSO_4$

Figure 3-6 shows the virucidal activity of PRE against HSV-1 in the absence and presence of $FeSO_4$. PRE alone exhibited a 0.49 ± 0.02 log reduction, whereas $FeSO_4$ gave a log reduction of 0.24 ± 0.38; and the reduction caused by the control phthalate buffer was negligible. However, when all components were used in combination a log reduction of 3.27 ± 0.74 was achieved. As this value was much greater than the resultant addition of the log reduction of the components, this result was evidence of a synergistic or potentiated effect of the addition of $FeSO_4$ to PRE.

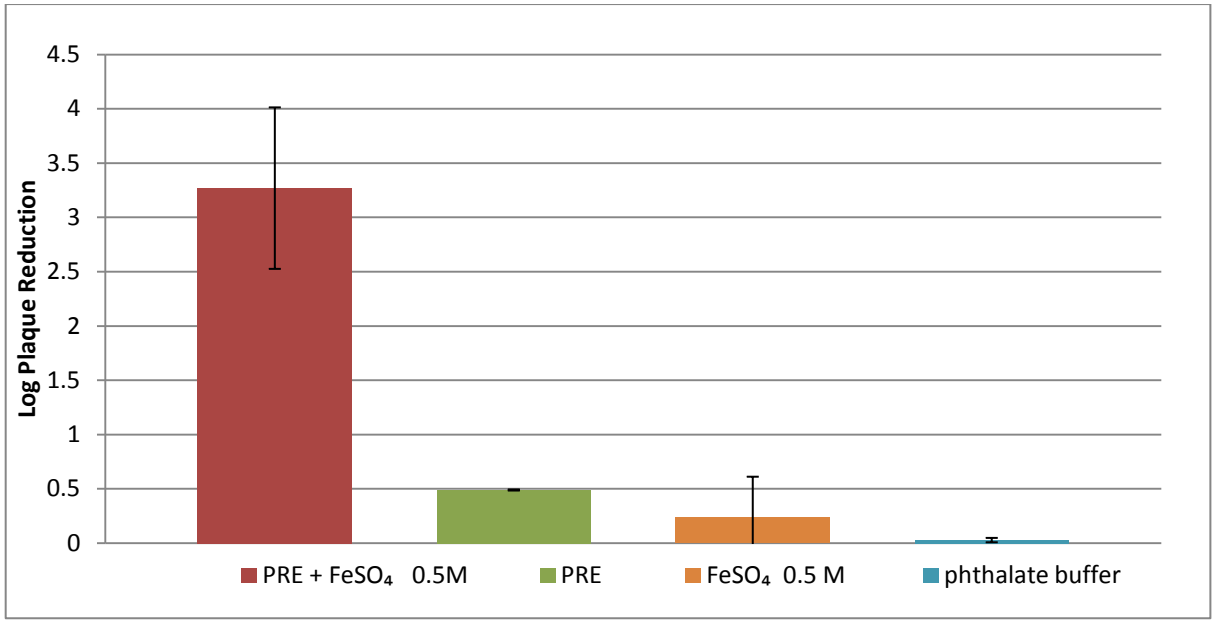

Figure 3-6 The virucidal log reduction of PRE, $FeSO_4$ and phthalate buffer following their immediate combination (n=4 ±SD).

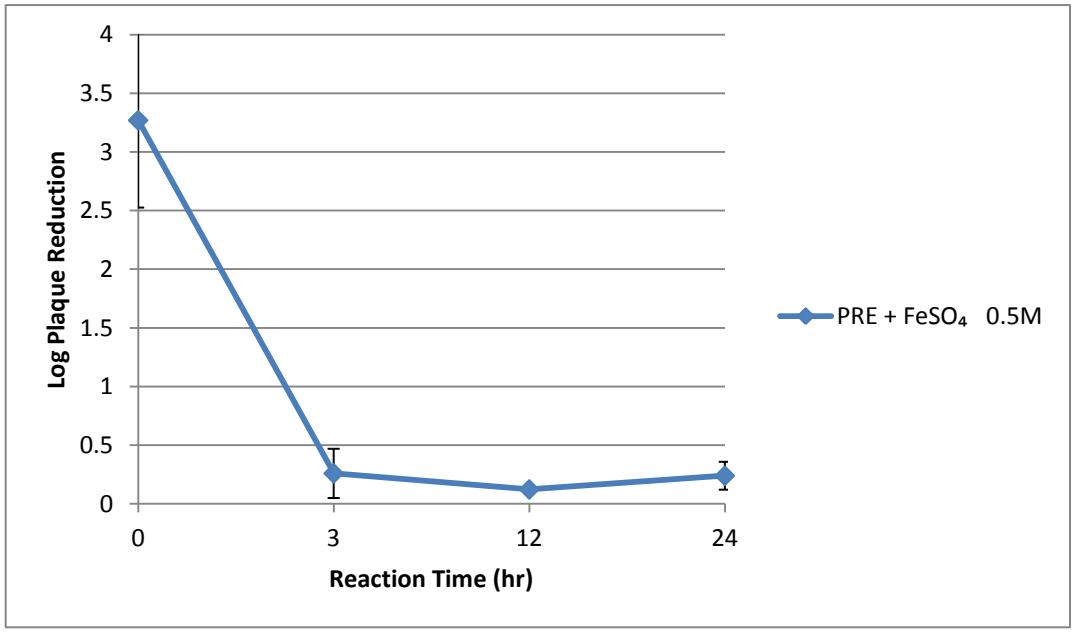

Figure 3-7 The virucidal log reduction of HSV-1 after addition of PRE + $FeSO_4$. The combination was added after the PRE/FeSO4 mixture was allowed to react at room temperature and occluded from light for a period of 0, 3, 12 and 24 h (n=3 ±SD).

It is apparent from Figure 3-7 that the formulation loses its synergism and almost all of the virucidal activity after a three hour reaction time between PRE and $FeSO_4$. The log reduction of HSV-1 drops from 3.27 ± 0.74 to 0.26 ± 0.21 and remains at this level for all other reaction times, a level similar to that of $FeSO_4$ alone.

3.3.4. The Black By-Product

It was apparent that very soon after PRE came into contact with $FeSO_4$ a black by-product appeared in the test solutions, confirming earlier observations. Figure 3-8 illustrates the colour change observed on the addition of $FeSO_4$ (0.05 mg mL^{-1}) to PRE (0.05 mg mL^{-1}) 3 min after addition a strong black by-product has formed. Neither $FeSO_4$ nor PRE in solution alone have a discernable colour.

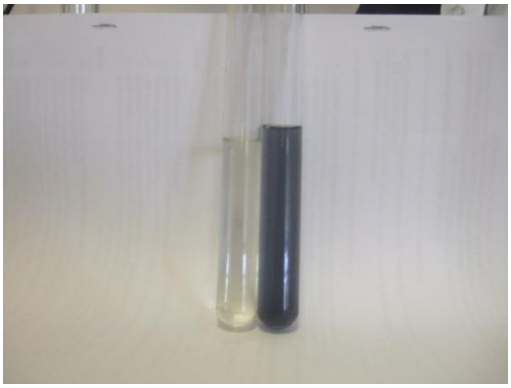

Figure 3-8 The colour change associated with the addition of $FeSO_4$ to PRE after three minutes at room temperature. From left to right PRE 0.05 mg mL^{-1} and PRE 0.05 mg mL^{-1} +$FeSO_4$ 1 M. All are dissolved in phthalate buffer pH 4.5 and DI H_2O.

Figure 3.9 shows the sequential addition of $FeSO_4$ to PRE. Immediately on addition the black colour and precipitate begins to form. After a 3 min reaction time at room temperature the whole solution is filled with an opaque black solution.

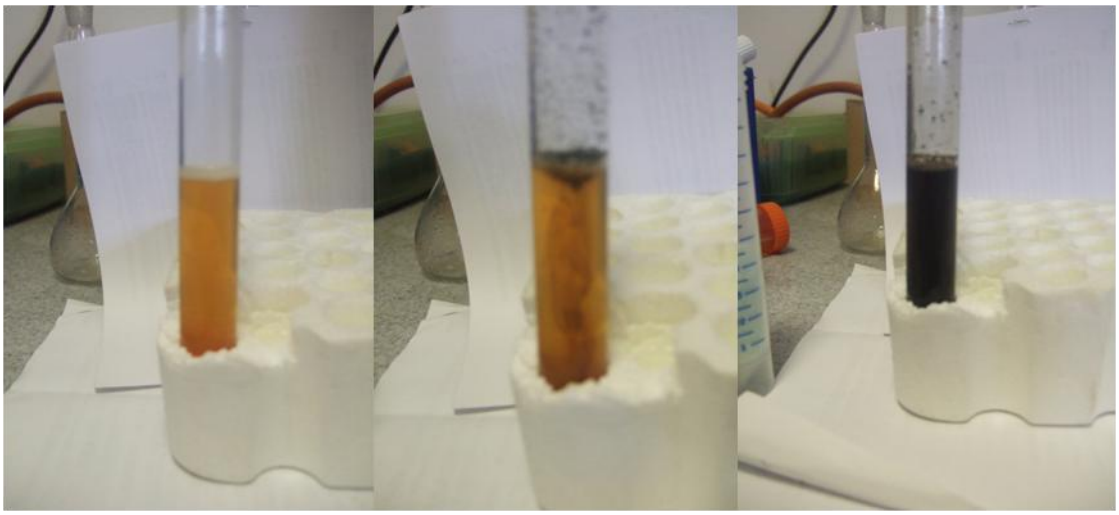

Figure 3-9 The sequential addition of $FeSO_4$ 1 M to PRE 5 mg mL^{-1}. From left to right before addition, upon addition of $FeSO_4$ and 3 minutes after addition.

Figure 3.10 shows the solution when applied to the lower arm. This clearly shows unsightly colouration.

Figure 3-10 The black stain left on human forearm skin after a 20 second application of the fully reacted solution of PRE 0.05 mg mL^{-1} + $FeSO_4$ 1 M (The forearm belongs to the author Mr D. Houston).

3.4 Discussion

A definition of potentiation is that activity exceeds the additive effects of combining two substances. In this work, the log reduction for PRE and $FeSO_4$ individually were 0.49 and 0.24 respectively, with an additive activity value of 0.73, whereas the combination resulted in a potentiated log reduction far in excess of this, namely 3.27, thereby confirming potentiation. However, this potentiation was only apparent soon after mixing, and diminished rapidly thereafter – a feature also observed previously in

experiments involving bacteriophage. After 3 h, the activity had reduced to non-potentiated levels, as shown in Figure 3-7.

It is clear that there are two major problems with any potential commercial product based upon a combination of PRE and $FeSO_4$. Firstly, the diminishing virucidal activity observed when the two components are combined gives rise to major stability problems in a proposed formulation. A patented single compartment formulation strategy had been developed (Heard, Bowen and Denyer 2008), where the potentiating agent ($FeSO_4$) was entrapped within liposomes overcame this to a certain extent, although stability issues remained a problem. A 2-compartment solution might be viable, although this would not resolve the second problematic issue.

The second problem is the generation of the very insoluble black by-product. As outlined in Chapter 1, PRE is rich in ellagitannins. Apart from issues relating microbicidal activity, the addition of $FeSO_4$ to Tannin/ tannic acid rich solutions producing a black precipitate is well known, and the process for and use of pomegranate 'gall ink' has been used since the early sixth century (Carvalho 2008). These were widely used up until the early 20^{th} century: JS Bach used this to notate his music; Rembrandt used it for his sketches; while Thomas Jefferson used this type of ink to write the Declaration of Independence (Kolara, et al. 2006). "The ink was used due to the difficulties in removing the stain, however the ink's corrosive properties, identified already at a Conference at St. Gallen in 1898, inflict severe damage to numerous artefacts"(Bundar, et al. 2006).

3.5 Conclusion

The potentiated activity of PRE and $FeSO_4$, as observed in earlier work has been confirmed against HSV-1 and the combination of PRE and $FeSO_4$ has also proven to be non-cytotoxic. However, also consistent with previous work are the phenomena of a short window of virucidal activity and the generation of a black by-product.

Overall, it is unlikely that patients would accept a product that would 1. Have such a narrow window of efficacy and 2. Leave behind such an obvious post-application stain to the skin, as shown in Figure 3-7. However, the high potentiated virucidal activity would appear to have potential as an anti-HSV therapeutic, if these problems can be resolved.

Chapter 4 **Probing Aqueous-Based Interactions Between PRE And Ferrous Sulphate or Zinc Sulphate**

4.1. Introduction

Chapter 3 confirmed three major features concerning the combination of PRE and $FeSO_4$, namely:

1. Potent synergistic virucidal activity
2. The short-lived transient nature of this activity
3. The development of a black by-product that accompanied the decrease in activity

The studies in Chapter 3 sought to probe the basis of this activity, in particular the transient nature and colour change. Furthermore, as the development of a commercial product would be compromised by features '2' and '3' the potential for alternative potentiating agents was explored.

4.1.1 Redox Reactions and PRE Potentiation

Redox reactions describe all chemical reactions in which there is a change in oxidation number/state. As previously stated it was hypothesised that the virucidal nature of PRE and $FeSO_4$ was due to the interaction of compounds within PRE and the Fe (II) ion, and that the transient nature of the activity was due to the conversion of free Fe (II) ions to bound Fe (III) ions, following a similar reaction to that of tannic acid and Fe (II). Such redox processes are very likely to be behind the depletion of both antimicrobial activity and associated colour change. Iron is a transition metal with an atomic mass of 26. Other transition metals have previously demonstrated activity against microorganisms (Nagar 1990) (Singh and Katiyar 2008).

PRE has been used with the addition of copper sulphate and has shown moderate synergistic bactericidal properties (Naughton 2007) (Gould, et al. 2009); however Cu^{2+} as well as Fe^{2+} and Pb^{2+} readily form complexes with tannins within the PRE mixture (Stewart, Jassim and Denyer 1998) (El-Ashtoukhya, Amina and Abdelwahabb 2008) (McCarrell, et al. 2008) (Gould, et al. 2009). Changing the oxidation state and the formation of highly coloured solutions is a characteristic of transition metals. However, as the change from Fe (II) to Fe (III) is associated with diminishing antimicrobial activity, then it can be hypothesised that similar behaviour would arise in redox reactions involving these other transition metals. Furthermore, from a patient

perspective, colouration and colour change is likely to remain unacceptable in a commercial product. The salts of alternative transition metals with similar d orbital e-, yet able to remain in the 2+ state without colour change upon addition to PRE were considered and zinc identified as a suitable candidate.

4.1.1. Rationale for Examining Zn^{2+} as an Alternative Potentiating Agent

Initially, the electronic configuration of zinc was considered. Most transition metals readily form two or more ions due to the free space within the 3d-orbital. The electron orbital filling for iron is $1s^2$, $2s^2$, $3s^2$, $3p^6$, $3d^6$, $4s^2$, Fe 2+ ([Ar] $3d^6$), enabling the transfer of electrons to and from the unfilled 3d orbital requiring relatively low energy, a characteristic of most transition metals. However, due to the specific sub d orbital filling of zinc it only forms one ion Zn^{2+} as it has a completely full 3d sub-orbital losing the $4s^2$ electrons first, giving the following configuration: $1s^2$ $2s^2$ $3s^2$ $3p^6$ $3d^{10}$. With this configuration the Zn^{2+} ion is in a thermodynamically stable and favourable state as Zn^{2+}. This is available in many water soluble salt forms which are typically white (uncoloured).

In the current chapter the solution chemistry of zinc sulphate ($ZnSO_4$) was compared with that of ferrous sulphate ($FeSO_4$). Zinc sulphate, having the same sulphate counterion, would thus provide a direct comparison with ferrous sulphate. Furthermore, $ZnSO_4$ has high water solubility, low toxicity (Poires, et al. 1967) (Hoogenraad, Van Hattum and Van den Hamer 1987) and, as stated, no discernible colouration.

4.1.2. Methods for Probing Interactions

Evidence for solution interactions following the combination of metal ion with PRE can be either spectroscopic (where shifts of specific absorbances may be determined) or calorimetric (where enthalpy changes are determined).

4.1.3. Aims

The aim is to seek evidence for the transient nature of PRE and ferrous sulphate activity in comparison to zinc sulphate. Three different approaches were taken:

1. Comparative Ultra violet-visual spectroscopy (UV)

2. Comparative High Pressure Liquid Chromatography (HPLC)
3. Comparative Isothermal Titration Calorimetry (ITC)

4.2. **Material and Methods**

4.2.1. Materials

The materials used in this chapter are given in Chapter 2.1

4.2.2. Methods

The preparation of the extracts, buffers and solutions are stated in Chapter 2 section 2.2.1. unless otherwise stated.

4.2.2.1. Ultra Violet (UV) Visual Spectroscopy

UV spectroscopy analyses the absorbance of UV light waves by a compound (Watson 2005). The addition of compound into a solution of another can affect the UV absorbance spectrum, a change (shift) of the UV spectrum is indicative of electron transfer and suggests the formation of an intermolecular interaction, or the formation of a new complex - this is a common and sensitive method for the indication of metal chelation (Andjelkovic, et al. 2006). Alternatively, interactions can result in solvatochromic effects, a hypsochromic blue shift or bathochromic red shift can be observed depending on solvent polarity.

For the UV spectroscopy determinations, all solutions were prepared using a phthalate buffer at pH 7.4. PRE was used at a concentration of 0.05 mg mL^{-1}, and to establish the effect of $FeSO_4$ addition to PRE the concentration range of 1, 2, 3, 4, 5, and 6 x 10^{-4} M was used. This follows on from previous work where it was stated that the reaction between PRE and $FeSO_4$ was completed within this range (Kulkarni, et al. 2007). The range of $ZnSO_4$ concentration analysed was 1.6, 3.1, 6.3, 12.5, 25, and 50 x10^{-4} M. PRE and each salt was analysed individually, and in combination after a 1h reaction period at room temperature and under occlusion from light. Due to the spectral shift analysed on the addition of $FeSO_4$ at low concentrations and the absence of any change on the addition of $ZnSO_4$ it was deemed pertinent to analyse the addition of $ZnSO_4$ over a

greater concentration range. Samples were centrifuged for 10 min at 10000 *g* prior to the supernatant being sampled and analysed.

Each sample was analysed in a silica cuvette (L 0.1cm) placed into a Cary 50 UV Spectrophotometer. UV scans were run at 960 nm min^{-1} between 300-600 nm using the phthalate buffer as the baseline UV absorbance.

4.2.2.2. High Pressure Liquid Chromatography (HPLC)

HPLC is routinely and widely used to quantitatively analyse compounds using absorption spectrophotometry; the method can be used to specifically identify compounds i.e. punicalagin within a complex solution such as PRE. Chromatographic information can be used to determine the amount of compounds within PRE and upon addition of metal ions any changes to compound levels or the formation of new compounds. However, a limiting factor for HPLC is that during analyses the analytes are dissolved within a variety of solvents; this can lead to the breakdown or dissolution of unstable products.

Quantitative determinations were carried out on a HP series II 1090 liquid chromatograph, fitted with a Phenomex Gemini NX 5µ C18 110A 250 X 2.60 mm column. Gradient elution was used, involving, A, MeOH with 0.1% Triflouroacetic acid (TFA) and, B, DI H_2O with 0.1% TFA. The gradient timetable and percentage composition of mobile phase is shown in Chapter 2 section 2.2.4.1. Analysis was carried out using an UV detector at 258 nm, injection volume 20µL and a flow rate of 1 mL min^{-1}. Samples were prepared according to section Chapter 2 section 2.2.4.1. The concentration range of PRE used varied between 0.05, 0.1 and 1 mg mL^{-1}.

4.2.2.3. Isothermal Titration Calorimetry (ITC)

ITC is used to measure interactions between ligands and substrates, and is ideal for the analysis of the addition of one material ($FeSO_4$) to another (PRE) and elucidating any interactions which may take place within a system place based on any observed change in enthalpy (Grolier and Rio 2009). The sample preparation and machine methodology followed that described in Chapter 2 section 2.2.4.3. 2.4 mL of PRE 0.6 mg mL^{-1} was used as the titrate within the titrate cell and $FeSO_4$ 2.5 mM in a 50% MOPS and 50% DI buffer was used as the titrant. To account for varying pH in calculating the binding

constant a further experiment was run using an acetate buffer pH 4.5; all other conditions remained the same.

4.3. **Results**

4.3.1. UV Spectroscopy

The UV spectra for punicalagin produced a λ_{max} at 379 nm (Figure 4-1) for each concentration of $FeSO_4$. When the absorbances were measured at 379 nm significant dose dependent increases were found ($p<0.0001$), which when plotted against the concentration of $FeSO_4$, produced a linear relationship (Figure 4-2)

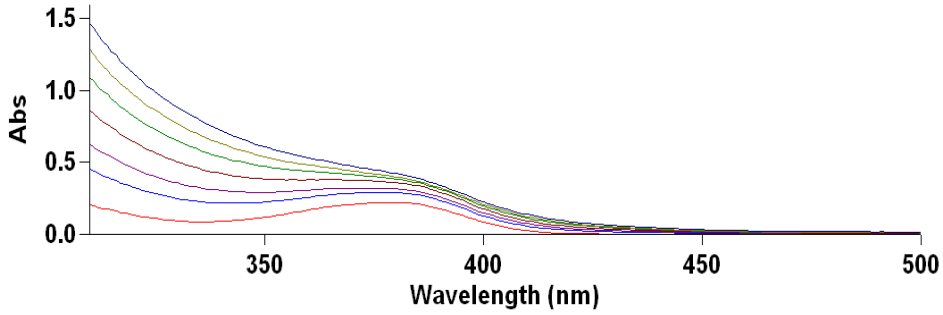

Figure 4-1 Punicalagin 0.03 mg mL^{-1} plus $FeSO_4$ (0-6 $x10^{-1}$mM) in pH 4.5. Punicalagin alone (red) with increasing concentration of $FeSO_4$.

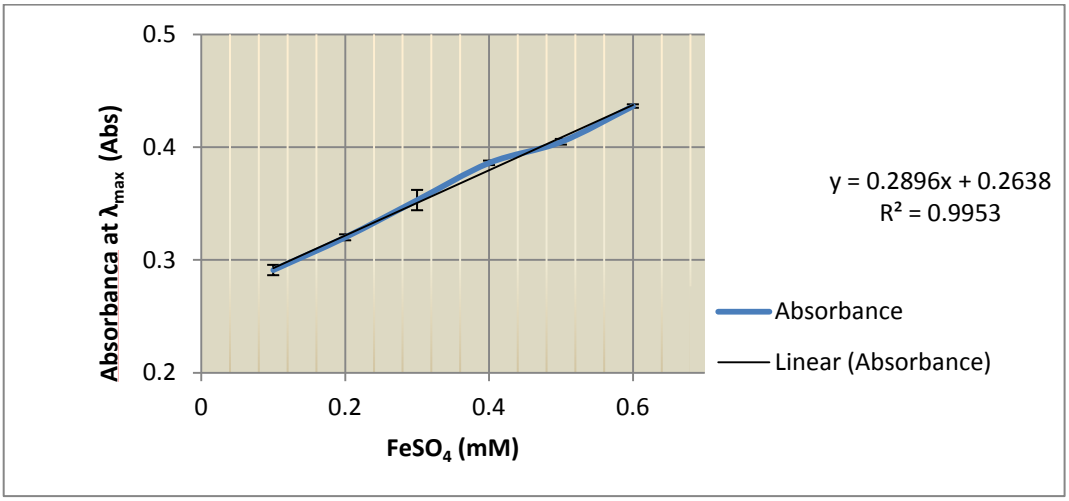

Figure 4-2 Plot to show change in absorbance at 379 nm for punicalagin 0.03 mg mL^{-1} with increasing concentrations of $FeSO_4$ (0.1 – 0.6 mM) (n=3, ± SD).

According to (Andjelkovic, et al. 2006) the binding constant can be determined from the gradient and the y intercept of a double reciprocal plot of concentration vs absorbance for $FeSO_4$ for the linear portion: This is shown in Figure 4-3.

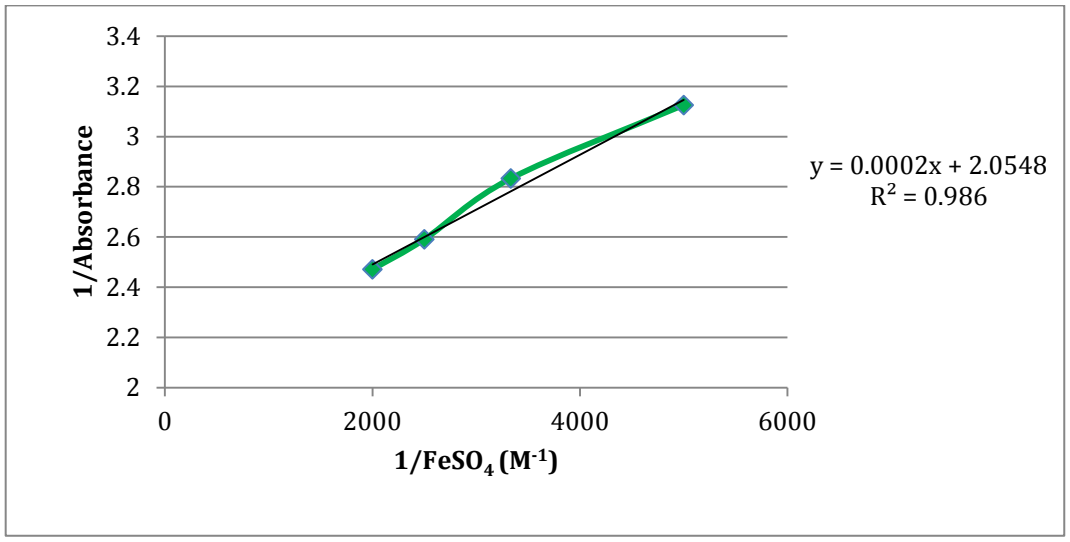

Figure 4-3 A double reciprocal plot of $FeSO_4$ on addition to punicalagin mg mL^{-1} verses absorbance (linear portion only).

Therefore, by substituting in the numbers from Figure 4-3 k_a for $FeSO_4$ and punicalagin can be calculated as:

$$k = \frac{intercept}{gradient}$$

$$k = \frac{2.0548}{0.0002}$$

$$k = 1.02 * 10^4 M^{-1}$$

In contrast to $FeSO_4$, on addition of $ZnSO_4$ to punicalagin no significant changes in absorbance were apparent. The average absorption at 379 nm for PRE and on the addition of $ZnSO_4$, was found to be statistically the same ($p > 0.05$) at 0.250 ± 0.006 (Figure 4-4). Figure 4-5 re-affirms this and shows there was no correlation between increased concentration and absorption at this wavelength.

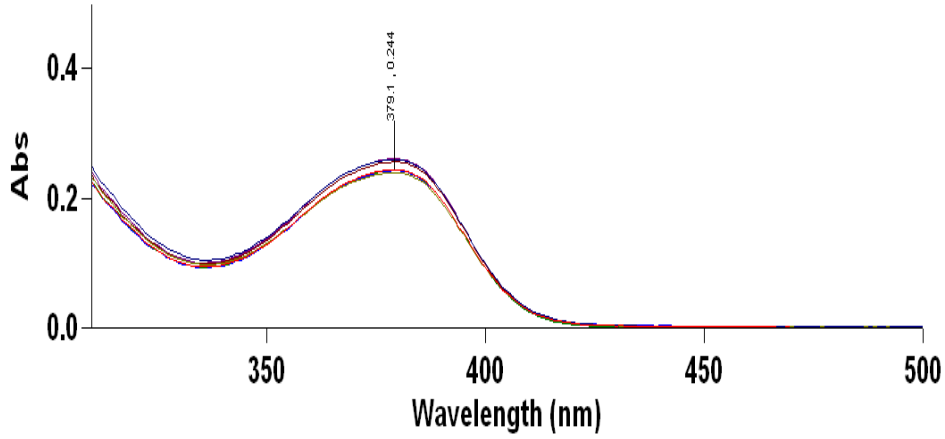

Figure 4-4 The UV-vis absorbance spectra of punicalagin 0.03 mg mL^{-1} with the addition of $ZnSO_4$ (0-5 mM).

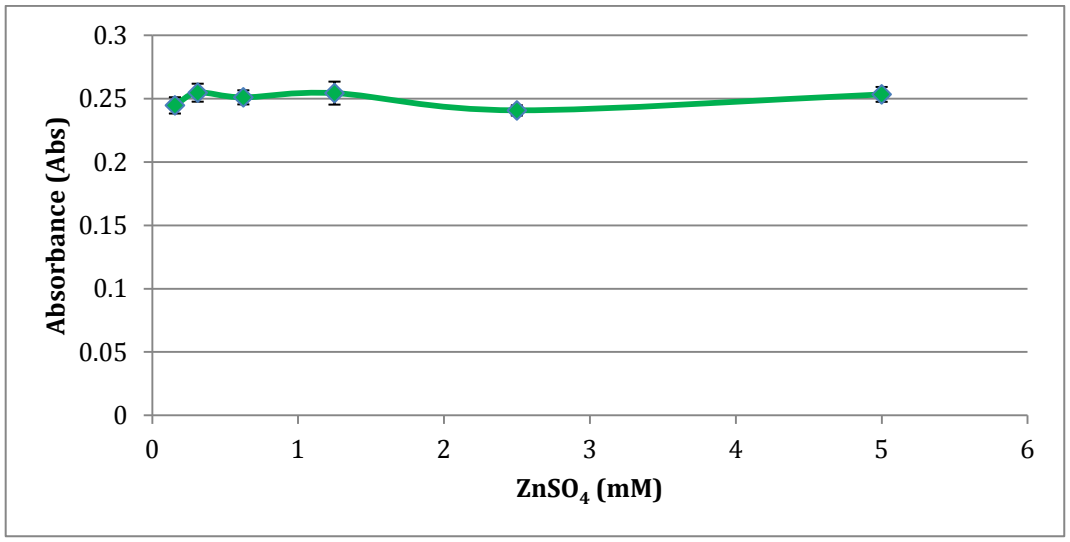

Figure 4-5 The absorbance of punicalagin 0.03 mg mL-1 following the addition of increasing concentrations of $ZnSO_4$ (0.16-5 mM) at 379 nm (n=3 ± S.D).

It should be noted that no absorbance increase was observed with either $ZnSO_4$ or $FeSO_4$ alone at 379 nm. Therefore any increase at ≈ 379 nm or deviation from the punicalagin spectra can be entirely attributed to the chelation of $FeSO_4$ with punicalagin.

It was then pertinent to investigate the UV absorbance spectra following the addition of the two metal sulphates PRE to examine whether similar UV spectra would be observed to that seen with punicalagin.

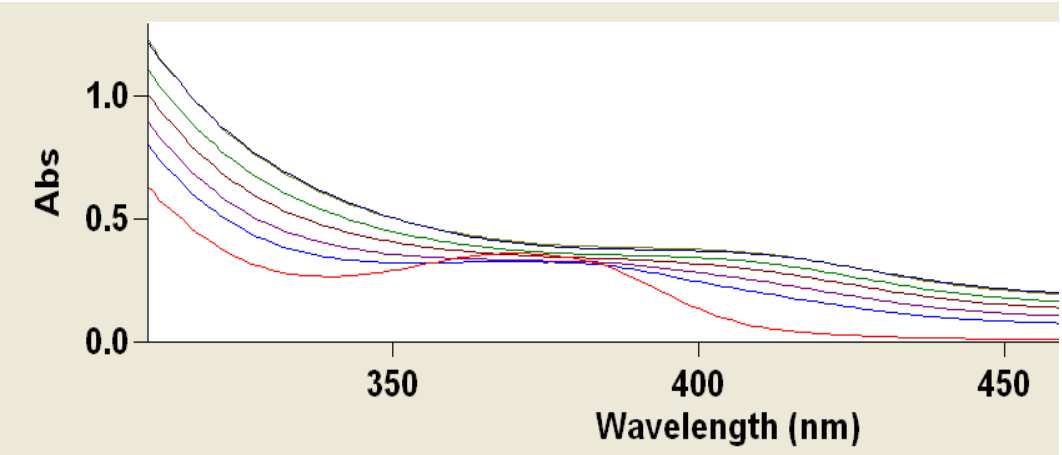

Figure 4-6 The UV-vis spectra for PRE 0.2 mg mL^{-1} and the addition of $FeSO_4$ (0-0.6 mM). PRE alone (red), and the addition of $FeSO_4$ 0.1 mM (blue), 0.2 mM (purple), 0.3 mM (brown), 0.4 mM (green) and 0.5 mM (navy) overlapping with 0.6 mM (black).

From Figure 4-6 it is clear that $FeSO_4$ does indeed change the spectra from PRE alone (as shown in red) shifting the λ_{max}. At higher concentrations there is no clear λ_{max} for PRE and a plateau is observed. However, PRE at 0.2 mg mL^{-1} gave a λ_{max} of 371 nm, which was shifted to 379 nm on the addition of $FeSO_4$. This is compelling evidence of electron transfer probably resulting from a redox reaction (Neudeck, Petr and Dunsch 1999).

The plot of absorbance at λ_{max} against $FeSO_4$ concentration (Figure 4-7) confirms the dose response relationship as shown with punicalagin. However, it is clear that the standard deviation is larger. This could be due to variations within the PRE formulation and specific concentrations of polyphenols present; it could also be due to a variation in the binding of $FeSO_4$ to different molecules within the PRE mixture. The difference in the gradient between the Figure 4-7 and Figure 4-1 (the plot of absorbances of the addition of $FeSO_4$ to punicalagin against the concentration of $FeSO_4$) eludes to the binding of $FeSO_4$ to more than one compound within PRE.

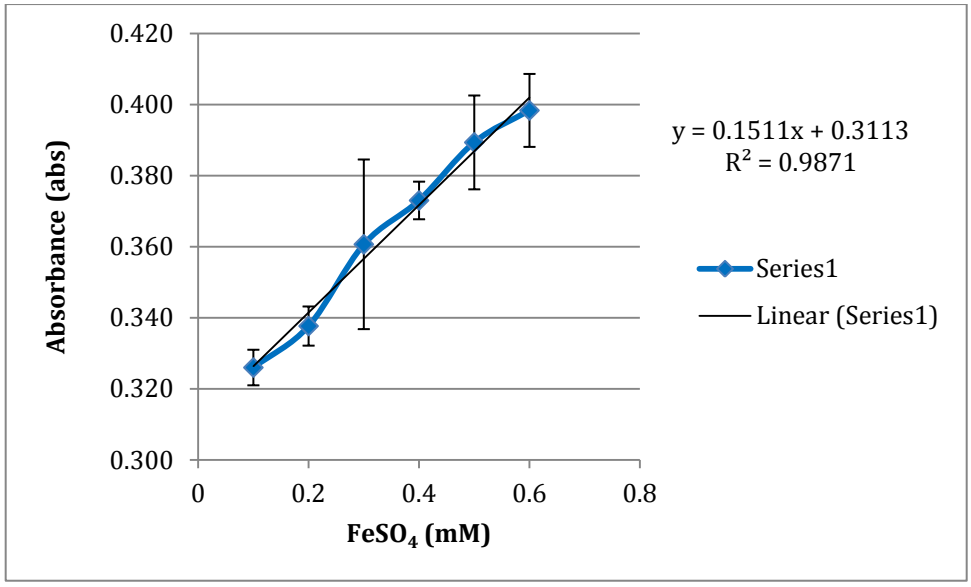

Figure 4-7 The relationship between increasing $FeSO_4$ concentration and absorbance at $\lambda_{max.}$

Similarly, then compared with punicalagin, a binding constant K_a can be determined by plotting a double reciprocal plot of concentration against absorbance. (Figure 4-8)

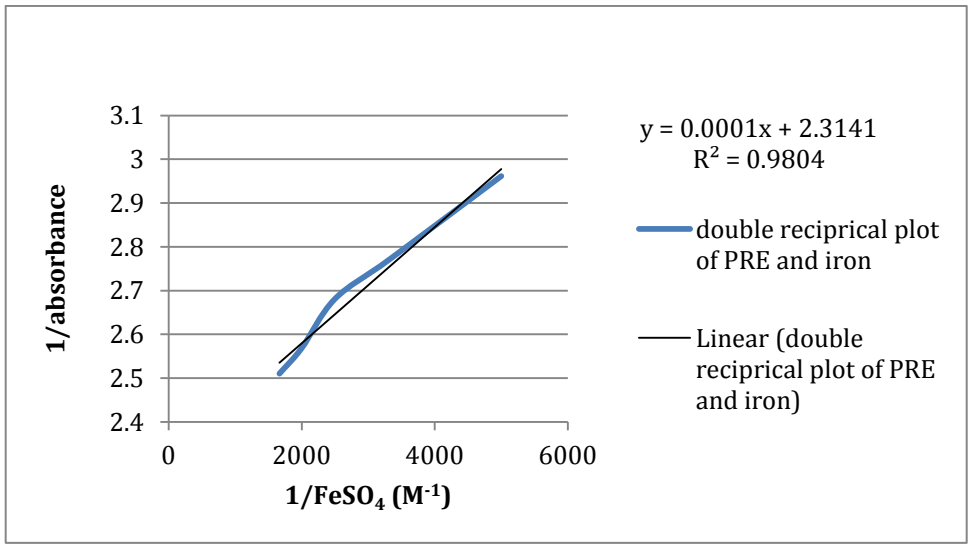

Figure 4-8 Double reciprocal plot of $FeSO_4$ concentration against absorbance.

$$k = \frac{2.3141}{0.0001}$$

$$k = 2.31 * 10^4 M^{-1}$$

This further shows the complexation of Fe with punicalagin and/or other components within PRE. The k value of 1.02 x 10^4 M^{-1} given for the interaction between $FeSO_4$ and punicalagin is half of the value for the addition of $FeSO_4$ to PRE suggesting that the binding of the Fe^{2+} is stronger when added to the pure extract of punicalagin as opposed to the mixture of PRE. This is likely due to the Fe^{2+} ion binding with more than one polyphenol within the PRE mixture. The large mixture of polyphenols and the resulting competition for chelation could also account for the decrease in binding strength by creating a scenario in which two or three binding events occur.

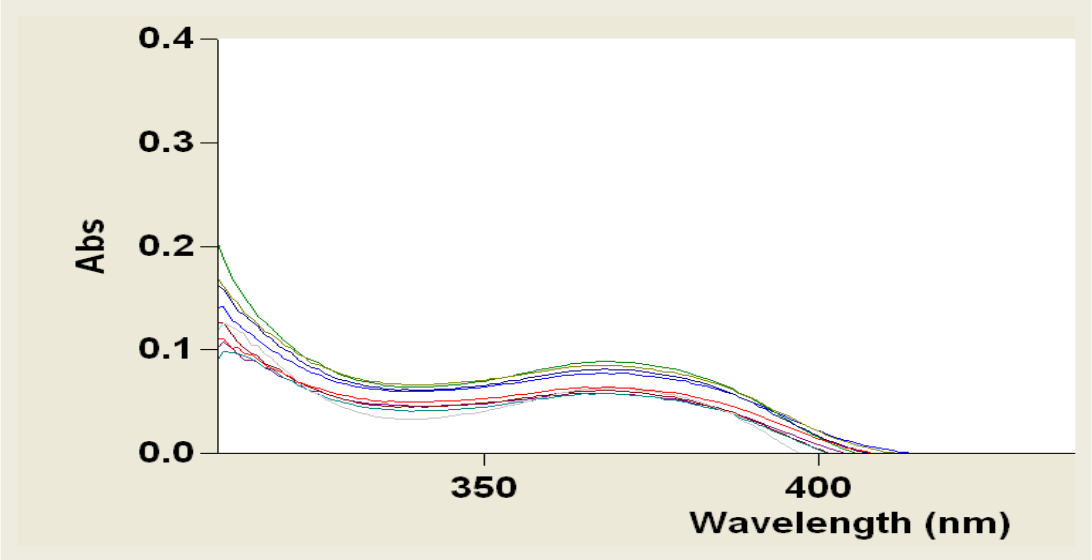

Figure 4-9 The UV-vis absorption spectra for 0.05 mg mL^{-1} PRE with the addition of $ZnSO_4$ (0-5 x 10^{-3} M). PRE (red) the repeat absorptions of the additions of $ZnSO_4$ (0-5 x 10^{-3} M) are given (range of colours).

Figure 4-9 shows the Uv-vis absorbance spectra for PRE alone and the addition of $ZnSO_4$ (0-5 x 10^{-3} M). It is clear that there was no change in the λ_{max} (371 nm), which is demonstrative of no correlation in increased absorbance or any change in λ_{max} with the addition of $ZnSO_4$. As the data shows no effect on absorption when $ZnSO_4$ is added to PRE there is no complexation occurring.

4.3.2. HPLC

HPLC analysis was used to study the interaction of punicalagin with the transition metals. Figure 4-10 shows the HPLC trace at 258 nm for punicalagin (0.03 mg mL^{-1}) with punicalagin α eluting at 12.21 min with an AUC 782.4 ± 6.78 (n=3) and punicalagin β eluting at 17.58 min with an AUC 1503.8 ± 7.21 (n=3).

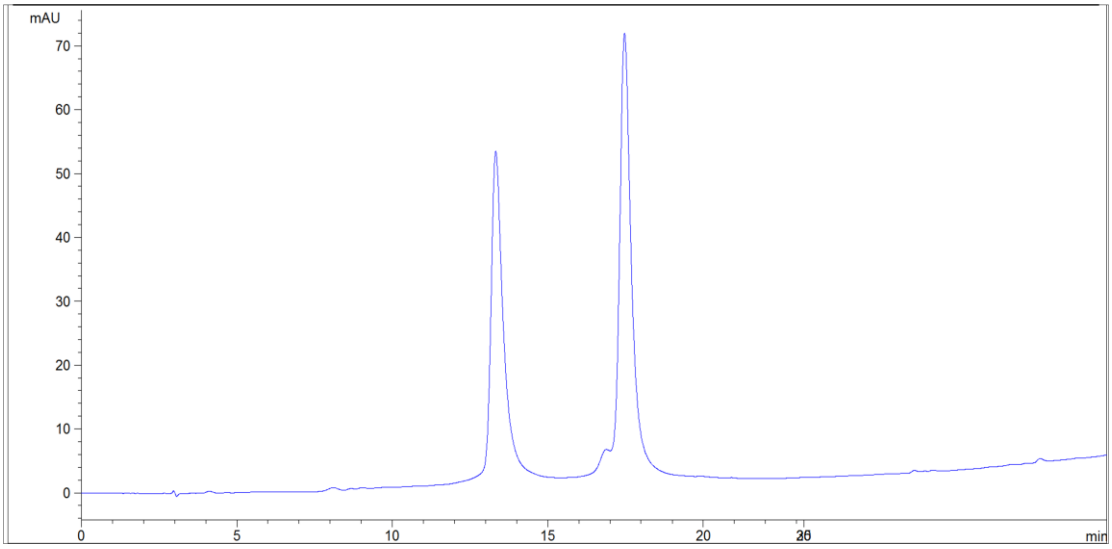

Figure 4-10 Typical HPLC chromatogram of punicalagin 0.03 mg mL^{-1}

However, on addition of 0.1 M $FeSO_4$ to 0.03 mg mL^{-1} punicalagin a new peak appeared at 5.3 min. This was accompanied with depletion of both punicalagin peaks (Figure 4-11).

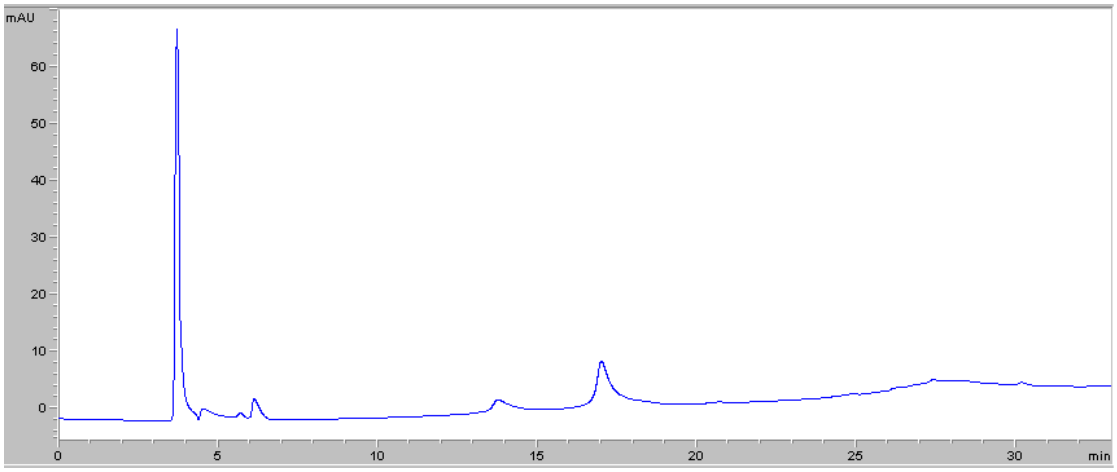

Figure 4-11 A typical HPLC chromatogram of punicalagin 0.03 mg mL^{-1} with $FeSO_4$ (0.1 mM).

The relationship between the formation of the new peak and the depletion of both punicalagin α and β anomers over time is shown in Figure 4-12. The appearance of the new compound was clearly based on the consumption and was therefore a derivative of punicalagin (no peak was seen with $FeSO_4$ alone).

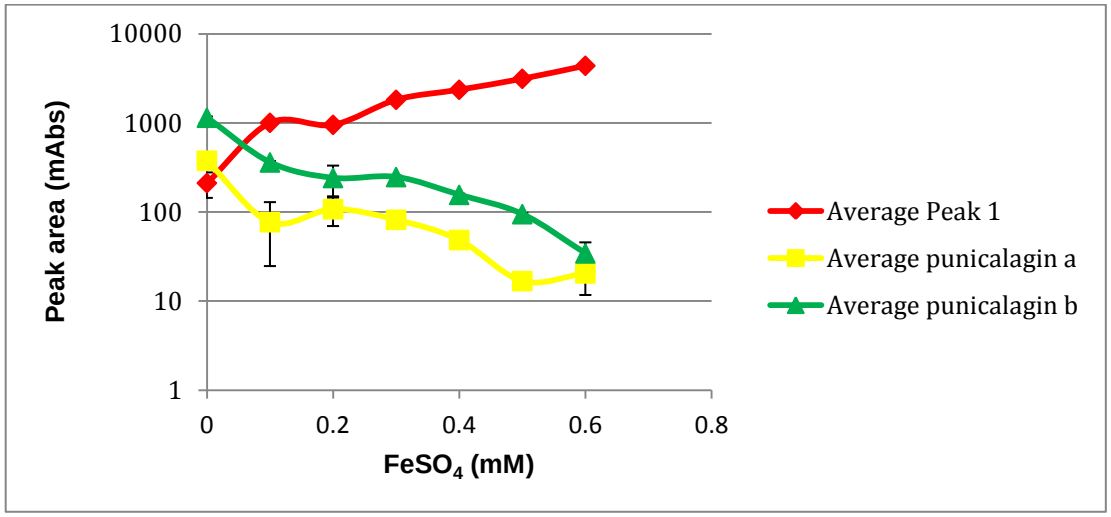

Figure 4-12 The decrease in absorbance of punicalagin anomer peaks and increase in the area of new unidentified peak (Figure 4-14) (red) following the addition of varying concentrations of $FeSO_4$ (n=3 ±SD).

Figure 4-13 shows a linear response to the decrease of punicalagin by the addition of increasing $FeSO_4$, and a strong correlation is shown by the R^2 value of 0.99.

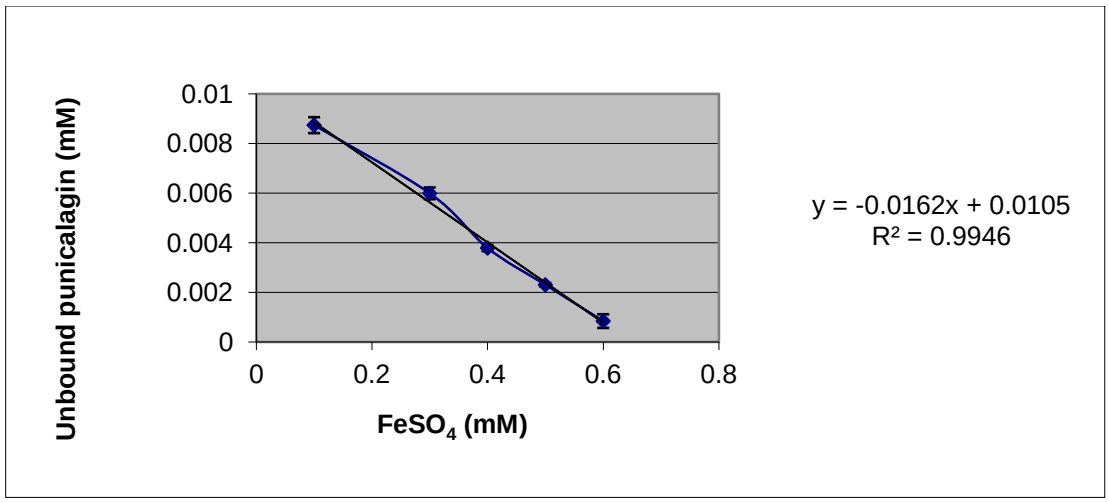

Figure 4-13 Unbound punicalagin concentration versus $FeSO_4$ concentration (n = 3 ± SD).

In contrast to $FeSO_4$, the addition of $ZnSO_4$ to punicalagin exhibited no significant change ($p > 0.05$) in either peak area for punicalagin α and β or the concentration of punicalagin shown in Figure 4-14; a sample chromatogram of punicalagin 0.03 mg mL^{-1} + $ZnSO_4$ 5mM is provided in Figure 4-15 showing the two punicalagin peaks and the absence of new peaks.

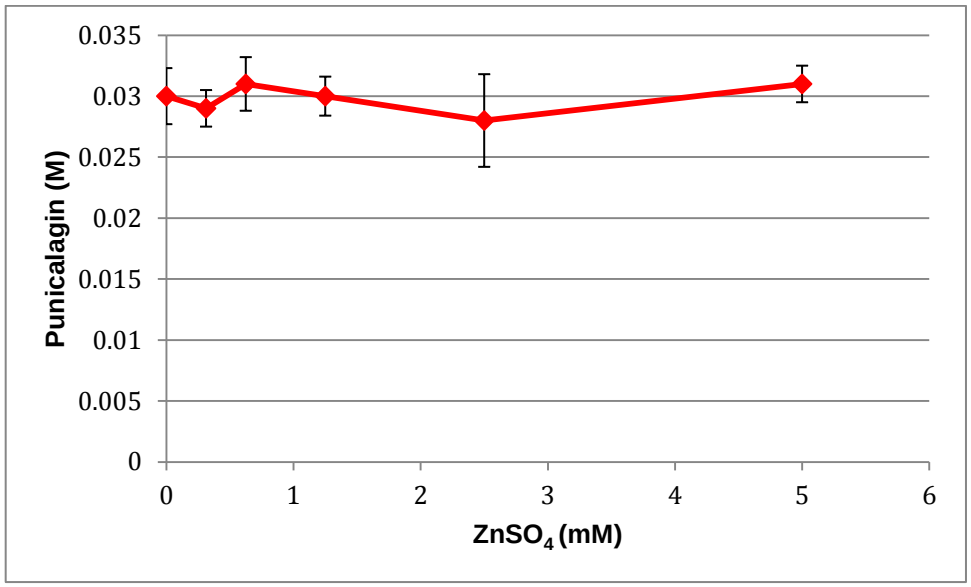

Figure 4-14 Absence of depletion in the concentration of punicalagin following the addition of different concentrations of $ZnSO_4$ (n = 3 ± SD).

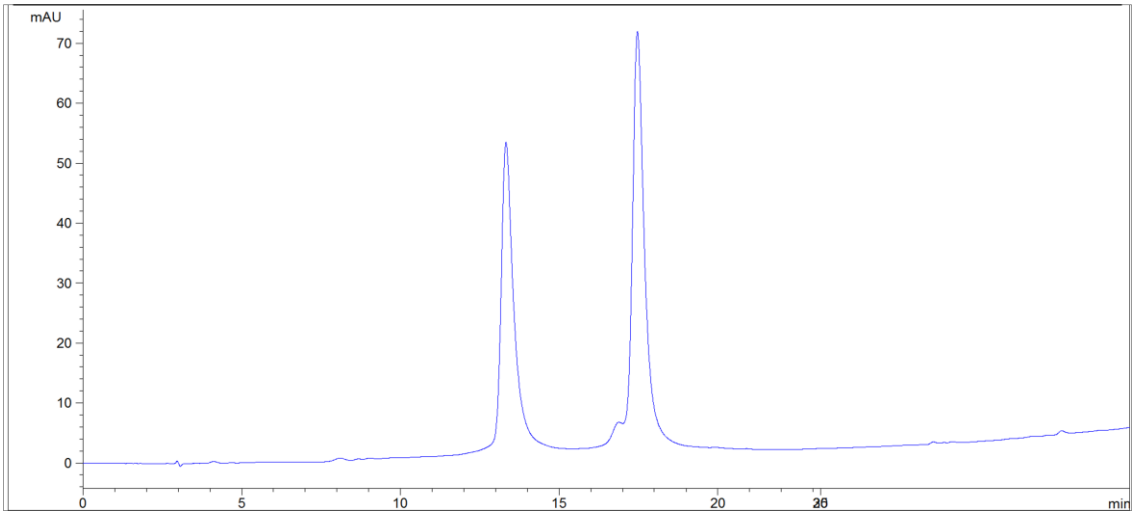

Figure 4-15: Typical HPLC chromatogram at 258 nm of 0.03 mg mL^{-1} punicalagin with $ZnSO_4$ (5 mM).

4.3.3. Isothermal calorimetry (ITC)

ITC can determine binding constants, stoichiometry and enthalpy change. Results can either be obtained directly from Figure 4-16 or derived from the data using computational fit. Enthalpy change was determined by integrating the peaks formed by each injection. ΔH can then be determined directly from the experimental data by taking the sum of the integrals of the enthalpy change as shown in the bottom portion of Figure 4-16, ΔH_{a1} = 1019.25 kcal M^{-1}, which is considered a fairly small enthalpy change.

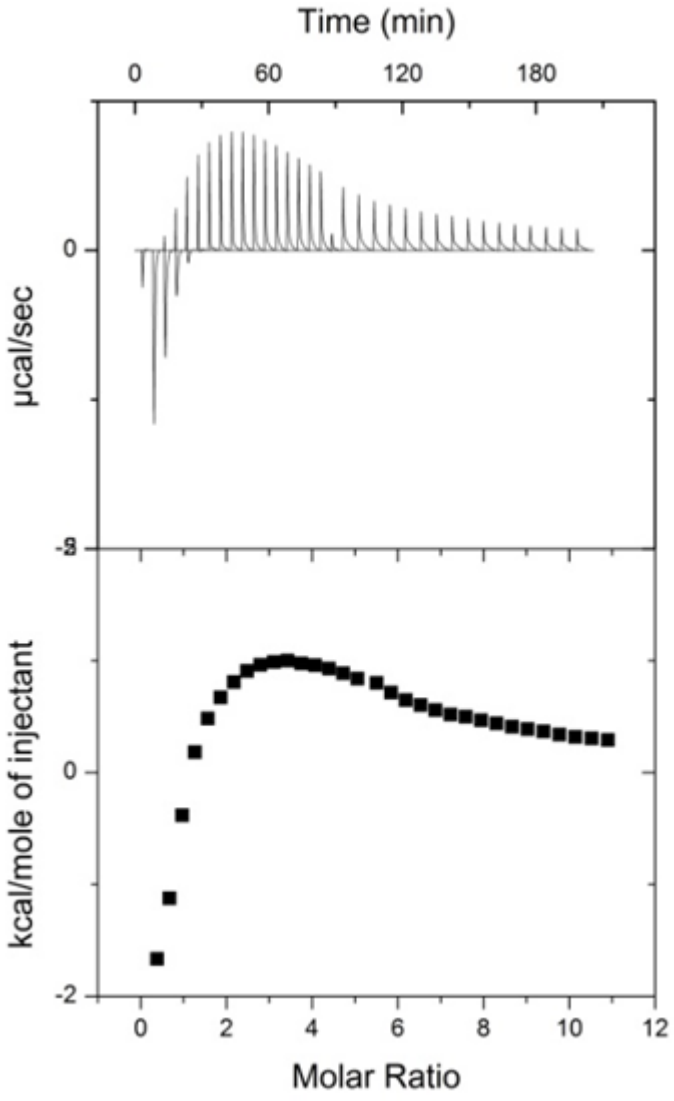

Figure 4-16 The plot of enthalpy change measured via ITC of the injection of $FeSO_4$ into PRE given as ucla s^{-1} against time (min) and kcal M^{-1} of injectant against the molar ratio.

Other thermodynamic parameters can be calculated from this data such as the binding constants (K_{A1}, K_{B1}) and the stoichiometry of binding by considering how they would thermodynamically react.

$$[pun - Fe(II)] \underset{K_{A1.}}{\overset{\Delta H_a}{\rightleftarrows}} [pun]\,[Fe\ (II)] + [lagins] \underset{\Delta H_b}{\overset{K_{B1}}{\rightleftarrows}} [\ lagins - Fe(II)]$$

Therefore K_{A1} can be derived in the following equation where N_{a1} = the stoichiometry of the binding site.

$$K_{a1} = \frac{[PunFe]}{N_{a1} \times [Pun] \times [\mathrm{Fe}]}$$

Similarly then a secondary binding constant can be determined

$$K_{b1} = \frac{[LaginsFe]}{N_{b1} \times [lagins] \times [\mathrm{Fe}]}$$

From the data obtained two K values for Fe have been calculated, which have indicated that two binding events were occurring as the graph Figure 4-16 was not sigmoidal. It has been assumed that as the majority of the extract is punicalagin the major K_a value (K_{a1}) is related to punicalagin and the secondary enthalpy change is as a result of the other components within the solution. To be confident in the true value, a pure sample of punicalagin would need to be run. However, due to time and cost limitations this was not possible.

For the addition of Fe it was determined that K_{a1} was 3.97×10^5 M^{-1}. The stoichiometry (N_{A1}) of this reaction was however shown to be specific with a value of (0.811); for practical reasons this is assumed to be 1. This is approximately 50 x less in comparison to the binding constant with Fe (II) with punicalagin determined by (Kulkarni, et al. 2007), which is quoted as 1.8×10^7 M^{-1}. However, this binding constant was determined using a different technique and done with pure punicalagin therefore no interaction of other polyphenols present in PRE was accounted for. No other binding constant between iron and extracts of pomegranate are quoted in the literature.

The secondary binding event was determined to have a weaker K_a again with 1.56 x 10^4 M^{-1}. This event was much less specific with an N_{b1} of 5.42.

Another test was run at a lower pH using an acetate buffer.

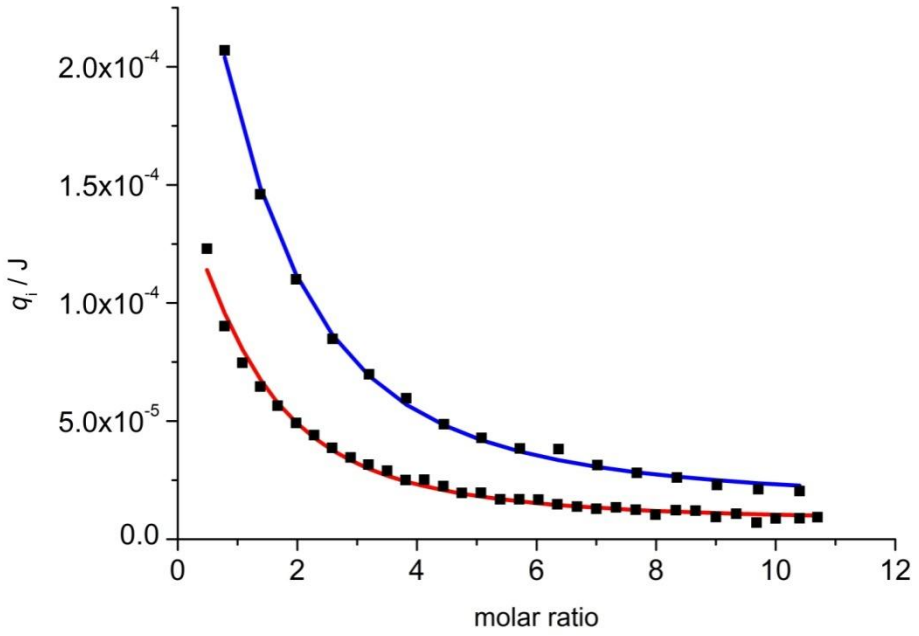

Figure 4-17: graph to show two titrations of PRE 0.6 mg mL^{-1} with $FeSO_4$ at pH 4.5 (blue) in acetate buffer (red).

It was determined from the data (Figure 4-17) that the K_a of this reaction was weaker again compared with Figure 4-16 (3.90 x 10^3 ± 566 dm^3 mol^{-1}) and the enthalpy change was similar ΔH (1.15 x 10^3 kcal mol^{-1} ±) (n = 2 ± 67.6 kcal S.D).

4.4. Discussion

It is a well-known phenomenon that the addition of $FeSO_4$ to PRE leads to the formation of a dark black precipitate, and a black coloured solution; this has also been observed on addition to punicalagin, the main phytochemical within PRE. The addition of $ZnSO_4$ to either solution does not result in any precipitate or colour change. It was theorised that the production of the black precipitate was due to the oxidation of Fe^{2+} to Fe^{3+} following a similar reaction between Fe^{2+} and tannic acid, and the formation of gall ink. From the results obtained it is apparent that the addition of $FeSO_4$ to PRE

results in the formation of a new compound and this also occurs on addition to punicalagin. The UV-vis spectra showed no shift of λ_{max} on the addition of $FeSO_4$ to punicalagin, however a dose dependant increase in absorbance was observed, however a shift in the plateau of λ_{max} on addition to PRE was shown. The binding constant obtained from this data was $k=1.02 \times 10^{-4} M^{-1}$ for the addition to punicalagin and $k = 2.31 \times 10^{-4} M^{-1}$ on addition to PRE, suggesting the $FeSO_4$ is bound less strongly when added to PRE. The doubling of k could be due to the binding of Fe^{2+} with various polyphenols within the PRE mixture, or that the binding to punicalagin within PRE is less stable due to molecular interactions within the PRE mixture. The shifts observed are indicative of electron transfer and thus a redox reaction, which is likely to be due to the chelation of the metal ion and the change in ionic state from Fe^{2+} to Fe^{3+}. The lack of spectral change on the addition of $ZnSO_4$ suggests that there was no formation of new molecules and no reaction was occurring.

The analysis of $FeSO_4$ and $ZnSO_4$ reaction to punicalagin concurred with the UV-vis data by the depletion of the punicalagin peaks and the formation of a new peak. The correlation between the addition of $FeSO_4$ and the decrease in punicalagin concentration and increase in the new peak formation shows that a new compound is formed supporting the theory that the metal ion is chelating with punicalagin. Once again there was no change to punicalagin on the addition of $ZnSO_4$.

Isothermal titration calorimetry alluded to a double binding reaction on the addition of $FeSO_4$ to PRE, with a binding affinity of k_{a1} $3.97 \times 10^5 M^{-1}$ and K_{a2} $1.56 \times 10^4 M^{-1}$. The double binding scenario is likely due to the interaction of $FeSO_4$ and punicalagin, k_{a1}, and to other phytochemicals k_{a2}. This once again supports the previous data and the original theory that the addition of $FeSO_4$ to PRE results in the formation of a new compound likely arising from the chelation of iron to punicalagin.

If the oxidation of Fe^{2+} to Fe^{3+} *and* the concomitant loss of punicalagin in the formation of a new complex is detrimental to microbiological activity, then it can be hypothesised that substituting Fe^{2+} with more stable Zn^{2+} will not result in the loss of punicalagin, and therefore maintain antimicrobial activity.

4.5. **Conclusion**

The results demonstrated that the addition of $FeSO_4$ to PRE resulted in a redox reaction of Fe^{2+} + punicalagin → Fe^{3+}, with a new, as yet unidentified, compound being formed. The formation of this new compound and oxidation of the iron appears to coincide with the loss of virucidal activity (Chapter 3) and phagocidal activity (Jassim, Stewart and Denyer 1995) previously described. The results also proved that no such redox change occurred and no new compound was formed using $ZnSO_4$. This is presumably due to the stability of the Zn^{2+} ion, in terms of its resistance to further oxidation.

Based on these results it was decided that $ZnSO_4$ (and potentially other zinc salts) was deemed a good candidate for further microbiological examination, due to its longevity within the +2 state and thus hypothesised sustained antimicrobial activity.

Chapter 5 **Microbiological Effects of PRE and Zn^{2+}**

5.1. **Introduction**

In Chapter 2, plaque assays confirmed that the combination of PRE and $FeSO_4$ provided potentiated virucidal activity against HSV-1, ACR HSV-2. Chapter 3 found evidence for the mechanism behind the short-lived and unsightly black by-product of the PRE/$FeSO_4$ combination, based upon redox chemistry. Chapter 3 also provided a candidate alternative potentiating agent, namely Zn^{2+}, which is resistant to further oxidation in the presence of PRE. This, theoretically, should provide potentiated virucidal activity over an extended period of time, whilst not developing the black by-product.

The current chapter examines both the virucidal and anti-viral activities of PRE/Zn^{2+} against HSV-1 infected Vero cells. The work concentrated on zinc sulphate ($ZnSO_4$) for consistency with the previous work involving $FeSO_4$. However, in order to probe the effects of alternative counterions, a variety of other zinc salts were also examined. Metal salts are combinations of the metal cation and non-metal anion that bind according their association/dissociation constants. Strongly bound salts tend to dissociate to a lesser degree and be less water soluble than weakly bound salts. This may affect the efficacy of a salt in anti-viral and virucidal tests.

The distinction between virucidal (viral destruction) and anti-viral (viral inhibition) properties of a compound or product was outlined in Chapter 1. Currently available topically-applied medications that work against viruses are anti-viral; virucidal disinfection products would presumably be detrimental when applied to the skin. However, a product that possessed both virucidal and anti-viral properties would have a distinct advantage. Consequently, the activity of the PRE and $ZnSO_4$ combination was studied in both modes.

5.1.1. Objective and Aims

To investigate the virucidal and anti-viral effects of $ZnSO_4$, and other zinc salts, against HSV-1:

- the virucidal activities of a range of zinc (II) salts in combination with PRE against HSV-1;
- the optimal potentiation ratio between PRE and $ZnSO_4$;

- the virucidal activity of the major phytochemicals within PRE (punicalagin and ellagic acid);
- the potentiation in activity between $ZnSO_4$ and punicalagin;
- the anti-viral properties of PRE and its main polyphenols (punicalagin and ellagic acid) with and without the addition of $ZnSO_4$ against HSV-1 and ACR-HSV.

5.2. Materials and Methods

5.2.1. Materials

Materials used in this section are detailed in Chapter 2 section 2.1.

5.2.2. Methods

The methodology for general cellular microbiology and the formulation of solutions extracts and buffers follows that described in Chapter 2 unless otherwise stated.

5.2.2.1. Cytotoxicity

The methodology for the cytotoxicity analyses followed that described in Chapter 2 section 2.2.7.5., and further discussed in Chapter 3 section 3.2.2.4.

PRE 0.1 mg mL^{-1}, $ZnSO_4$ 0.1M and phthalate buffer alone and in combination were analysed using the Cell Titer 96® AQueous assay method. All formulations were made using the phthalate buffer at pH 4.5.

5.2.2.2. Virucidal Plaque Reduction Assay

The virucidal analyses followed the method outlined in Chapter 2 section 2.2.5.9. and further discussed in Chapter 3 section 3.2.2.3. The concentrations and combinations of the materials which were investigated using the plaque reduction assay are shown in Table 5-1.

Compound	Extract
Zinc oxide 0.00001M	± PRE 0.05 mg mL^{-1}
Zinc nitrate 0.0005M	± PRE 0.05 mg mL^{-1}
Zinc citrate 0.0005M	± PRE 0.05 mg mL^{-1}
Zinc iodide 0.0005M	± PRE 0.05 mg mL^{-1}
Zinc stearate 0.0005M	± PRE 0.05 mg mL^{-1}
Zinc gluconate 0.0005M	± PRE 0.05 mg mL^{-1}
$ZnSO_4$ 0.5M (143.77 mg mL^{-1}) 0.1M (28.75 mg mL^{-1}) 0.05M (14.37 mg mL^{-1}) 0.01M (2.88 mg mL^{-1}) 0.005M (1.44 mg mL^{-1}) 0.001M (0.29 mg mL^{-1}) 0.0005M (0.14 mg mL^{-1})	± PRE 0.05 mg mL^{-1} ± Punicalagin 0.01 mg mL^{-1}
No addition	PRE 0.05 and 0.01 mg mL^{-1}
No addition	Punicalagin 0.05 and 0.01 mg mL^{-1}
No addition	Ellagic acid 1 mM

Table 5-1 Mixtures employed in virucidal studies.

5.2.2.3. Antiviral Plaque Assay

Antiviral activity was determined by the application of test solution and then virus (after an incubation period) to confluent Vero cells in a 24 well plate (24wp). The methodology followed that stated in Chapter 2 section 2.2.5.10.

The test substances used with this method were PRE, $ZnSO_4$, their combination, punicalagin, ellagic acid phthalate buffer and Aciclovir. The antiviral studies did not test above 100 µM of any compound.

5.2.2.4. IC_{50} Calculation

Antiviral results are typically presented as IC_{50} values, which refer to half the maximal inhibitory concentration, and are a measure of the effectiveness of a compound for inhibiting biological or biochemical function (Wilson and Walker 2010), following the methodology stated in Chapter 2 section 2.2.5.10.1.

5.2.2.5. Avicel Overlay Media

An overlay medium is added to the plaque assay in order to stop the virus becoming detached from the infected cells and spreading over the cell monolayer. The methodology for the use of this is stated in Chapter 2 section 2.2.5.11.

5.3. **Results**

5.3.1. Virucidal Activity of PRE and Various Zinc Salts

Although the earlier work involved ferrous ions with a sulphate counterion, in this part of the work a range of different counterions for Zn^{2+} were examined. There were 2 main objectives:

1. to provide an indication of a mode of action, by probing whether it was the zinc cation (Zn^{2+}), rather than the sulphate counterion (SO_4^-) that provided the potentiation effect with PRE

2. to determine which counterion may facilitate maximal potentiation

To achieve this, the range of zinc salts shown in Table 5-1 was evaluated for virucidal activity, at the same molar levels unless otherwise stated. Figure 5-1 shows the virucidal action of PRE ± Zn^{2+} with a range of anions.

Salt added to PRE (0.05 mg mL^{-1})	Salt concentration (mM)	Virucidal pfu log reduction
Zinc sulphate ($ZnSO_4$)	0.5	3.18 ± 0.076
Zinc oxide (ZnO)	0.01*	1.21 ± 0.21
Zinc nitrate ($Zn(NO_3)_2$)	0.5	1.59 ± 0.51
Zinc citrate ($Zn_3(C_6H_5O_7)_2$)	0.5	3.19 ± 0.62
Zinc iodide (ZnI_2)	0.5	1.65 ± 0.1
Zinc stearate ($Zn(C_{18}H_{35}O_2)_2$)	0.5	2.94 ± 0.35
Zinc gluconate ($C_{12}H_{22}O_{14}Zn.xH_2O$)	0.5	3.26 ± 0.42

Table 5-2 The range of zinc salts analysed for potentiated virucidal activity with respect to HSV-1 on addition to PRE (0.05 mg mL^{-1}) (n=4 ± SD). *lower concentration used due to low aqueous solubility.

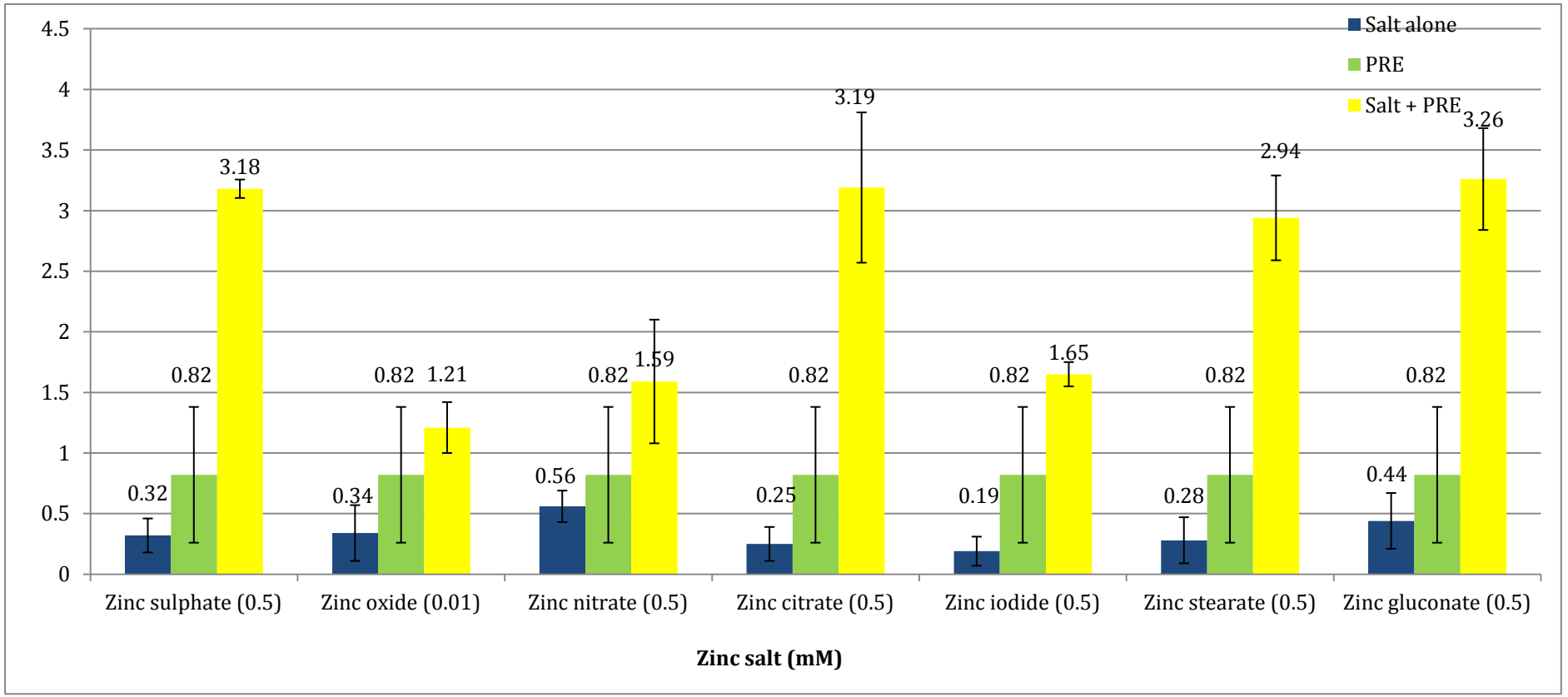

Figure 5-1 Virucidal log reduction data for the addition of PRE (0.05 mg mL^{-1}) and a range of Zn^{2+} salts to HSV-1 (n = 3 ± SD). Blue = salt alone, green = PRE alone, yellow = salt + PRE.

The results in Figure 5.1 show that the salts alone provided generally low activity. There were some small variations that could be related to the varying solubilities, and dissociation constants. However, across the range there was no statistically significant difference ($p > 0.05$).

The salts zinc oxide, zinc nitrate and zinc iodide failed to demonstrate potentiation. In the case of zinc oxide, the solubility was very low and had to be evaluated at 10^{-5} M, rather than 10^{-4} M as for the other zinc salts. Zinc nitrate and zinc iodide each in combination with PRE are represented as having low log reductions due to the high cytotoxicity of the mixture limiting the analysis at these concentrations. The iodide ion is a known biocide and it is believed application of zinc iodide was cytotoxic to the host Vero cells. This was apparent visually during the experiment by the full lysis of Vero cells and therefore lack of crystal violet staining. In a similar manner, it can be concluded that the nitrate ion was also cytotoxic to the Vero cells.

However, the remaining salts were water soluble (≥ 0.0005 M) and did not result in cell cytotoxicity. Thus potentiated activity was successfully displayed by zinc sulphate, zinc citrate, zinc stearate and by zinc gluconate, with log reduction values of approximately 3. Although there was some apparent variation, the differences were not statistically significant ($p > 0.05$).

There were no colour changes with any of the zinc salts upon the addition of PRE, although zinc iodide was intrinsically a brown-coloured solution and remained so throughout the experiment. These observations supported the chemical analyses carried out in Chapter 4, in particular the absence of any evidence for a redox reaction involving Zn^{2+}.

It was decided to proceed further with the examination of the sulphate salt ($ZnSO_4$). The reasons were:

- high aqueous solubility
- lack of colour change
- the level of potentiated virucidal action
- biocompatibility

5.3.2. Cytotoxicity of PRE, $ZnSO_4$ and Phthalate Buffer

Figure 5-2 shows the percentage of viable cells after application of PRE 0.1 mg mL^{-1}, $ZnSO_4$ 0.1 M and phthalate buffer pH 4.5, alone and in combination. Each formulation was made in the phthalate buffer at pH 4.5. There was no significant difference ($p > 0.05$) between the applied formulations at any time point over the 72 h period resulting in no decrease in the percentage of viable cells in comparison to the control. There was no cytotoxic effect observed on the application of PRE and $ZnSO_4$ at any concentration analysed throughout this project.

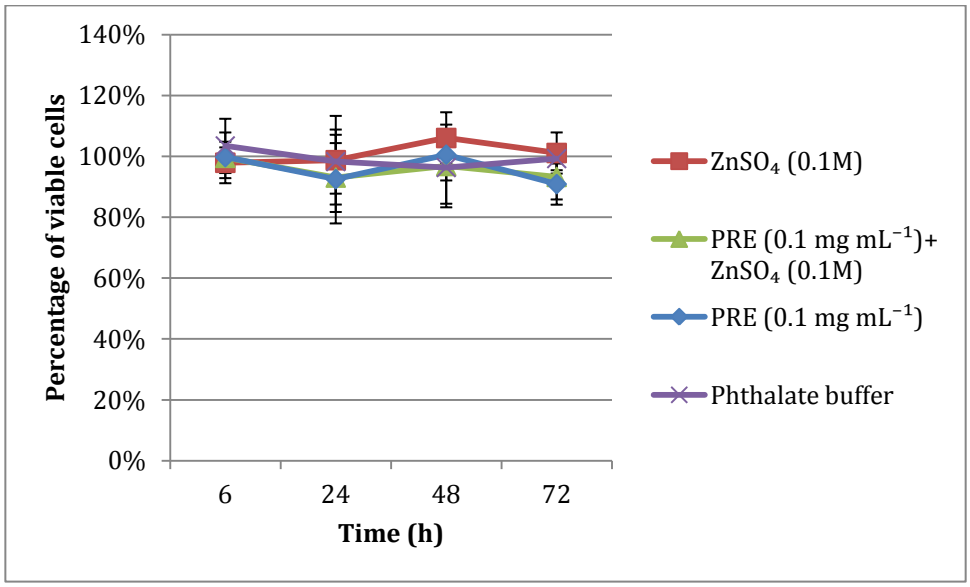

Figure 5-2 The percentage of viable cells after application of PRE 0.1 mg mL^{-1}, $ZnSO_4$ 0.1 M and phthalate buffer pH 4.5, alone and in combination, after 6, 24, 48 and 72 h (n = 3 ± SD).

5.3.3. Virucidal and Antiviral Analysis

5.3.3.1. Virucidal Activity of PRE and Different Concentrations of $ZnSO_4$

Having selected $ZnSO_4$ for further study, the next part of the work involved a study of the effects of $ZnSO_4$ concentration on the potentiation of PRE virucidal activity. This would provide important information on the relative proportions of the two components that could usefully be combined in a potential product to achieve optimal virucidal activity.

Figure 5-3 shows the log reduction of HSV-1 pfus with increasing levels of $ZnSO_4$. As the level of $ZnSO_4$ increased so did the log reduction of HSV-1 pfu, with maximal log reduction of 4.47 ± 0.11 and 4.56 ± 0.11 after the addition of 1.44 and 14.38 mg mL^{-1} of $ZnSO_4$. After this point a decrease in virucidal activity was observed. It is important to note that between the two maximal points a statistically significant decrease in the virucidal activity was observed, at a $ZnSO_4$ concentration of 2.88 mg mL^{-1} the log reduction decreased to 3.11 ± 0.57.

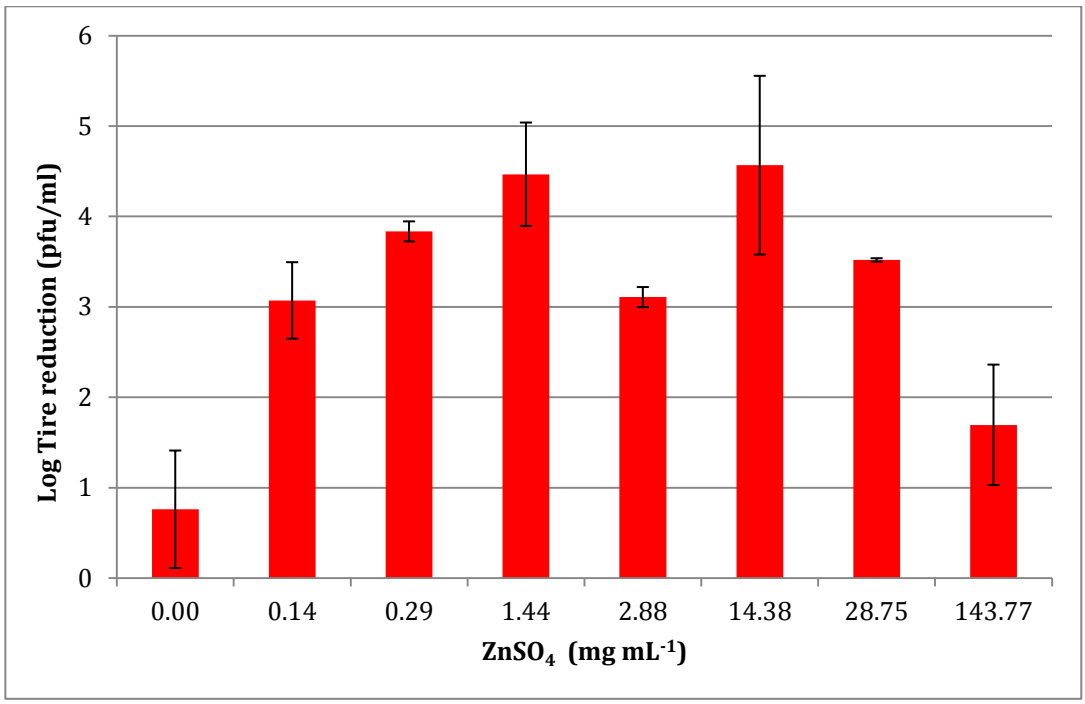

Figure 5-3 Effect of $ZnSO_4$ concentration on the potentiated virucidal activity upon addition to PRE (0.05 mg mL^{-1}) (n = 4 ± SD).

5.3.3.2. Virucidal Activity of $ZnSO_4$ and Different Concentrations of Punicalagin

As outlined in the introduction, the major phytochemical present in PRE is the ellagitannin, punicalagin (Jingjing, Yun and Qipeng 2007), at approximately 20%, which has reported microbicidal activity (Seeram, et al. 2005). It was therefore determined to examine the effect of this compound in isolation from the other components of PRE. A product based upon a single phytochemical such a punicalagin would be easier to standardise, with less liability to show batch-to-batch variation regarding the overall composition. Whether PRE or punicalagin was the more efficacious in terms of virucidal activity was not easy to determine, as a pure

compound (such as punicalagin) cannot be directly compared to a chemically diverse mixture (as is PRE). Notwithstanding, a comparison was made by evaluating both as equal mass mL^{-1}.

The virucidal log reduction of punicalagin in comparison to PRE (weight-to-weight) is represented in Figure 5-4. The results show that the log reduction of HSV-1 pfu due to the isolated punicalagin (0.05 mg mL^{-1}) was 5.93 ± 0.35, significantly greater than the log reduction due to PRE (0.05 mg mL^{-1}) of 0.76 ± 0.66 ($p < 0.05$). *It is important to note that a log reduction of 5.93 is the maximal limit of the test due to viral titer, however the marked difference between the activities of PRE and punicalagin was again observed at the lower concentration of 0.01 mg* ml^{-1}.

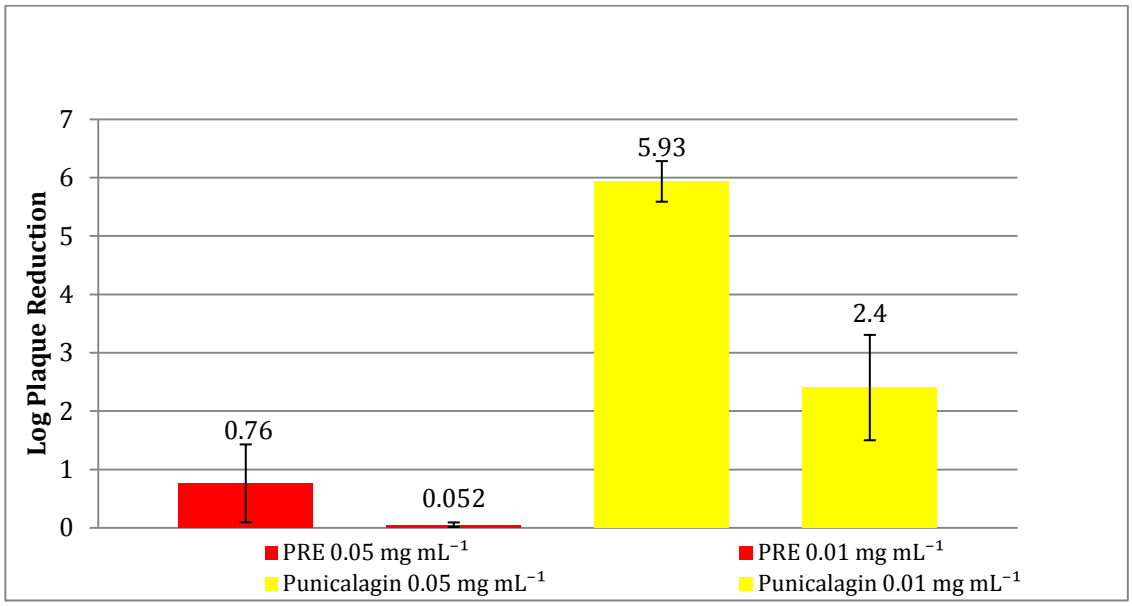

Figure 5-4 Comparison of the virucidal log reduction of HSV-1 by PRE and punicalagin on a mass-to-mass basis at both 0.05 mg mL^{-1} and 0.01 mg mL^{-1} (n=4 ± SD).

Punicalagin 0.01 mg mL^{-1} is representative of the concentration of punicalagin within 0.05 mg mL^{-1} PRE (i.e. punicalagin accounts for approximately 20% of the dry mass of PRE). The log reduction data of HSV-1 in Figure 5-4 shows that the virucidal log reduction due to PRE and punicalagin decreased from 0.76 ± 0.66 and 5.93 to 0.05 and 2.4 ± 0.9 respectively. These results demonstrate the greatly enhanced virucidal activity of punicalagin on a mass-to-mass basis relative to PRE. The virucidal activity of PRE, if it is to be mainly attributed to the punicalagin

content with the extract, appears partially compromised by other components of the extract.

5.3.3.3. Virucidal Activity of PRE and Ellagic Acid in Isolation

Punicalagin, although in greatest proportion, is by no means the only phytochemical constituent of PRE. In this section, we examined the effect of another ellagitannin, ellagic acid (EA), a direct breakdown product of the esterification of punicalagin. However, obtaining a direct comparison with punicalagin proved problematic due to the extremely low aqueous solubility of EA. An alternative solvent was needed in which both species were soluble, and preliminary experiments to the use of 10% DMSO in DI H_2O. Figure 5-5 shows that the virucidal activity of EA provided no statistical difference in comparison to DMSO solution ($p > 0.05$); however, punicalagin showed significantly greater virucidal action than either the control or ellagic acid ($p < 0.05$).

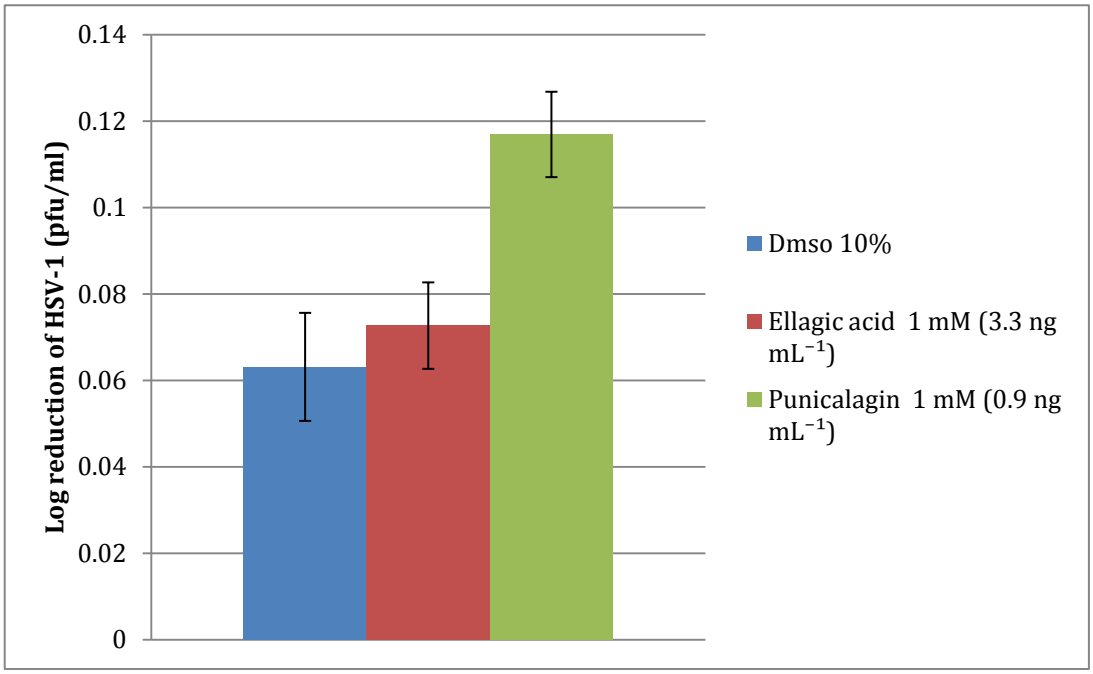

Figure 5-5 Virucidal log reduction due to the main phytochemicals within PRE; ellagic acid and punicalagin solubilised in 10% aqueous DMSO (n = 4 ± SD).

5.3.3.4. Virucidal Activity of Punicalagin with Different Concentrations of $ZnSO_4$

Having demonstrated that punicalagin is active against HSV-1, the next part of the study examines the potentiation of activity by different concentrations of $ZnSO_4$. Figure 5-6 shows the potentiation of different $ZnSO_4$ concentrations on the virucidal activity of 0.01 mg mL^{-1} aqueous punicalagin. As previously shown in Figure 5-4 punicalagin has a high innate virucidal effect resulting in a log reduction of 2.4 ± 0.9 (note: 0.01 mg mL^{-1} used here rather than 0.05 mg mL^{-1}).

Addition of $ZnSO_4$ (0.14 mg mL^{-1}) caused a marked increase in potentiated virucidal action to 4.6 ± 0.16. However, in the PRE experiment (Figure 5-3), the addition of greater amounts of $ZnSO_4$ caused a decrease in the virucidal activity below that of punicalagin alone. A biphasic trend was again observed, as at the higher concentrations of $ZnSO_4$ (14.38, 28.75 and 143.77 mg mL^{-1}) higher log reductions of 3.01, 2.56 and 2.22 were observed.

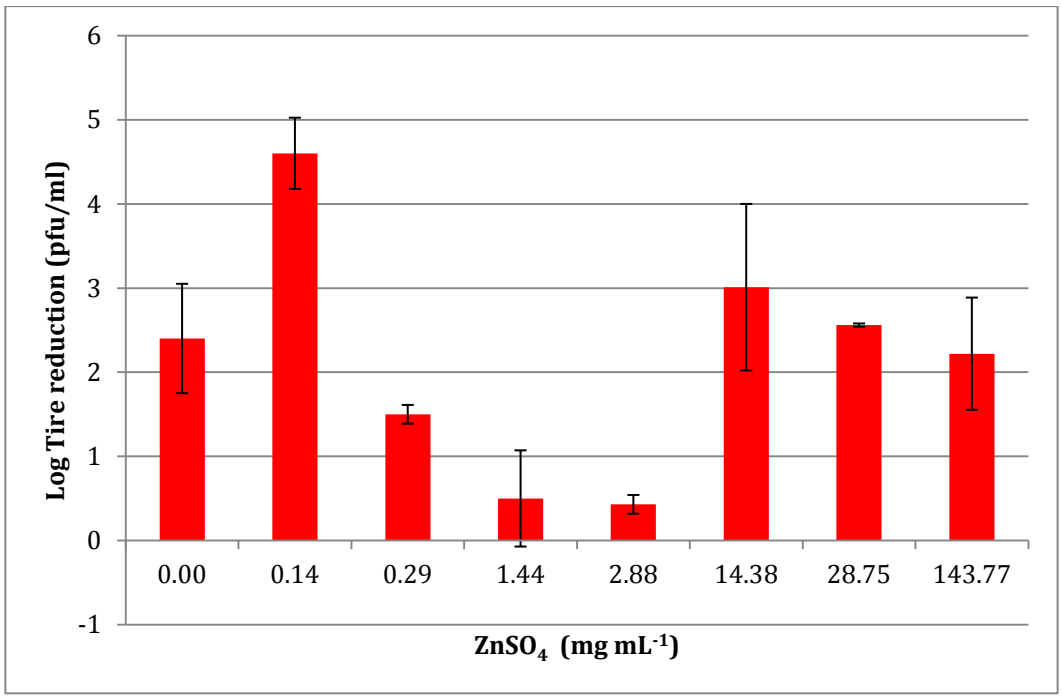

Figure 5-6 Effect of $ZnSO_4$ concentration on the potentiated virucidal activity of punicalagin (0.01 mg mL^{-1}) (n =4 ±SD).

5.3.3.5. Antiviral Activity of PRE, Punicalagin, Ellagic Acid and Aciclovir Against HSV-1 and Aciclovir-Resistant HSV-2

As outlined in Chapter 1, most topical treatments for skin viral infections exploit an antiviral mechanism, where the active compound inhibits viral replication. In this section, the viral replication inhibitory activities of PRE, punicalagin and ellagic acid were determined alongside the established topical antiviral drug, Aciclovir. Two strains of Herpes simplex virus were used: HSV-1 and HSV-2 Aciclovir resistant (ACR). Table 5-3 shows that the IC_{50} of Aciclovir against HSV-1 was 0.81 µM (which is equivalent to 182 µg mL^{-1}), agreeing with literature (Sarisky, et al. 2001) (Hobden, et al. 2011) and experimental findings of Dr JJ Bugert (personal communication).

Compound	Virus	IC_{50}
PRE	HSV-1	0.560 ± 0.039 µg mL^{-1}
	HSV-ACR	0.016 ± 0.009 µg mL^{-1}
PRE + $ZnSO_4$ (1:1)	HSV-1	0.550 ± 0.062 (PRE=µg mL^{-1}) ($ZnSO_4$= µM)
Punicalagin	HSV-1	≥100µM
	HSV-ACR	≥100µM
Ellagic Acid	HSV-1	≥100µM
	HSV-ACR	≥100µM
$ZnSO_4$	HSV-1	≥100µM
	HSV-ACR	≥100µM
Aciclovir	HSV-1	0.809 ± 0.030 µM (182 µg mL^{-1})
	HSV-ACR	≥100 µM

Table 5-3 The antiviral IC_{50} against HSV-1 and HSV-ACR of PRE, punicalagin and ellagic acid in comparison to Aciclovir (n=3 ± SD) Note: concentration of PRE is in mass mL^{-1} rather than moles.

The PRE extract exhibited strong antiviral properties against HSV-1 0.556 ± 0.39 μg mL^{-1}. On a mass-to-mass basis PRE is over 1000 times more potent than Aciclovir. PRE demonstrated an even greater antiviral response against HSV-ACR with an IC_{50} of 0.016 ± 0.009 μg mL^{-1}, whereas Aciclovir showed no effect (≥100 μM).

Surprisingly neither punicalagin nor ellagic acid elicited any antiviral activity at the concentrations tested ($IC_{50} \geq 100$ μM). This result indicates that, unlike in the earlier tests where punicalagin was clearly involved in virucidal activity, the anti-viral activity of PRE *cannot* be attributed to this compound. Thus antiviral activity is due to another phytochemical constituent of PRE or, more likely, a combination of compounds.

The addition of $ZnSO_4$ was not found to increase the anti-replicative potential of the extracts.

The concentration dependant antiviral profile from selected experiments is displayed in Figures 5-7 (PRE and HSV-1), 5-8 (PRE and HSV-2 ACR), 5-9 (PRE + $ZnSO_4$ and HSV-1) and 5-10 (Aciclovir and HSV-1). It is interesting to note the shape of these graphs, the sharp decline in viral activity over a small concentration gradient implies that PRE ± $ZnSO_4$ requires a threshold concentration to have any antiviral effect. The shape of the IC_{50} curve for Aciclovir exhibits a gradual decline in antiviral activity over a wide concentration range (Figure 5-10); this, and the antiviral activity of against HSV-2 ACR which is resistant to Aciclovir suggests that the antiviral activity of PRE is exercised by a different mode of action to that of Aciclovir.

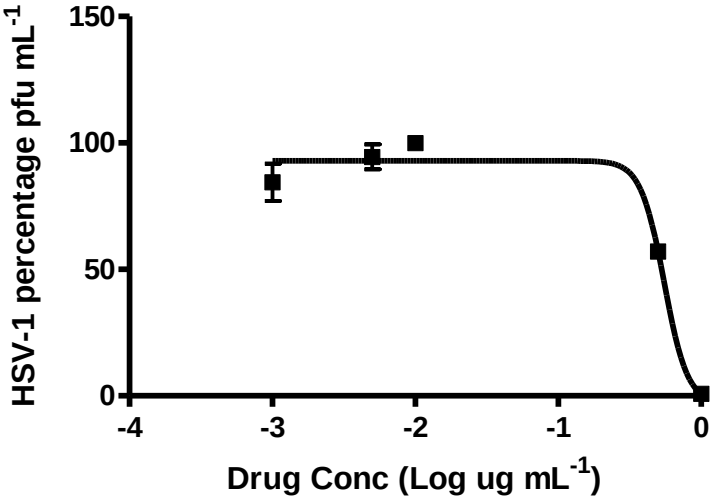

Figure 5-7 The IC_{50} curve arising from the antiviral activity of PRE against HSV-1 (n=3, ± SD).

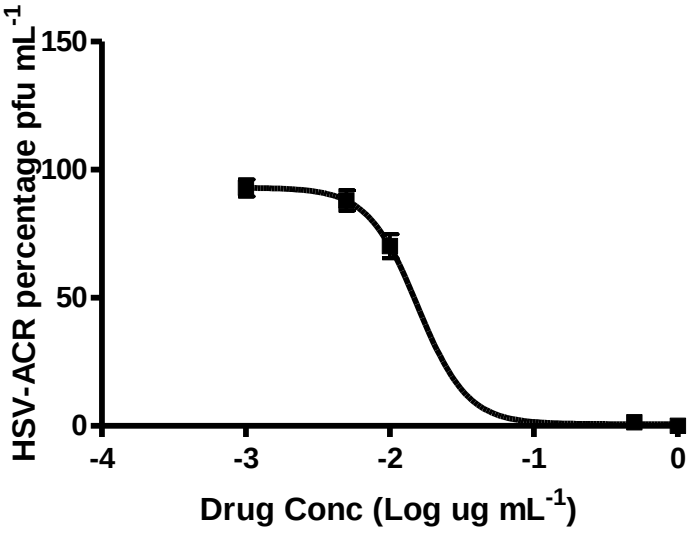

Figure 5-8 The IC50 arising from the antiviral activity of PRE with against to HSV-2 ACR (n=3, ± SD).

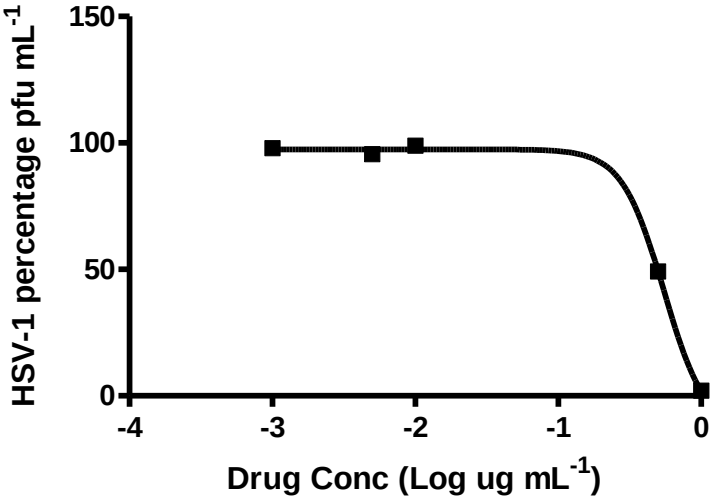

Figure 5-9 The IC50 curve arising from the antiviral activity of PRE and $ZnSO_4$ against HSV-1 (n=3, ± SD).

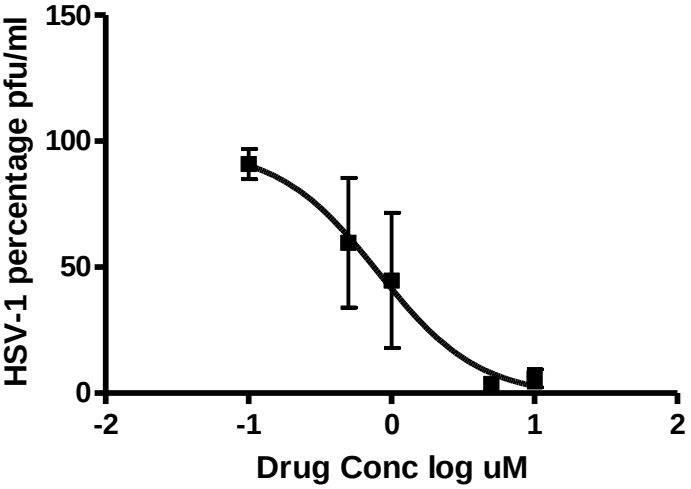

Figure 5-10 The IC_{50} curve arising from the antiviral activity of Aciclovir against to HSV-1 (n=3, ± SD).

5.4. **Discussion**

Examination of a range of zinc salts showed that comparable potentiation was achieved to $ZnSO_4$ when equal concentrations were employed and the counterion had no adverse effect on the host vero cells. This is strong evidence that the Zn^{2+} ion in solution is principally responsible for the potentiating effect.

The biphasic concentration-dependant response to $ZnSO_4$ of both PRE and punicalagin is surprising, although the experiments were performed four times. Potentiation increases up to 1.44 mg mL^{-1}, after which it dips before again reaching a maximum, thereafter steadily diminishing. PRE is a complex mixture of phytochemicals and the addition of $ZnSO_4$ adds to the complex interplay between constituents.

To speculate, similarities between the virucidal effects of the higher concentrations of $ZnSO_4$ combined with PRE and punicalagin can be observed and may indicate that a dual effect is occurring. Thus far the combination of $ZnSO_4$ plus punicalagin at the lower concentrations of $ZnSO_4$ (0.14 mg mL^{-1}): the viral envelope is first compromised by the punicalagin and then bound by the free Zn^{2+} ions, however, at higher concentrations of $ZnSO_4$, the Zn^{2+} ions may act first allowing for the punicalagin to then combine with the protein envelope thus destroying it. A similar level of viral destruction is observed within the PRE + $ZnSO_4$ system, however, due to the protective nature of a natural product upon its constituent parts, the virucidal activity of punicalagin remains active and thus potentiation is maintained over a greater concentration range of $ZnSO_4$ addition (0.14 and 28.75 mg mL^{-1}). The decrease in virucidal activity at $ZnSO_4$ concentrations 0.29, 0.144 and 0.288 mg mL^{-1} to punicalagin (shown in Figure 5-6) and 2.88 to PRE (shown in Figure 5-3) may indicate competitiveness for a specific protein and or binding site, hindering potentiation. Previous studies have not elucidated the virucidal mode of action of polyphenols found in pomegranate however a growing body of research has indicated the interaction between polyphenols, such as punicalagin and ellagic acid, with envelope viral glycol proteins in respect to varying strains of influenza (Nagai, et al. 1993); (Neurath, et al. 2004); (Song, Lee and Seong 2005).

It is interesting to note the apparent equivalence in antiviral activity between PRE and the established antiviral Aciclovir (Table 5-3). Even more interesting is the fact that PRE demonstrated an even greater activity against ACR-HSV – the implication is that PRE could have a role in future HSV strategies, when Aciclovir has become obsolete. The addition of $ZnSO_4$ was found not to provide enhanced activity in any case, and therefore is not involved in a potentiating mechanism during the viral replication stage.

In a practical context, the topical application of PRE and $ZnSO_4$ might be expected to result in virucidal kill outside of the host cell post-budding and help eliminate the viral vesicles. This would have important beneficial consequences for preventing viral transfer by a number of mechanisms, eg human mouth-to-mouth, mouth-to-genital, mouth-to-drinking vessel, mouth-to-joint (shared smoking), vagina-to-neonate (herpes infected mother). Additionally, PRE (alone) would inhibit viral replication within adjacent cells preventing formation of a viral cluster, which in turn would prevent a cold sore outbreak i.e., formation of a cold sore.

5.5. **Conclusion**

The activities of PRE and punicalagin with added $ZnSO_4$ has been determined against HSV-1 and HSV-ACR in both virucidal and antiviral modes. Very encouraging data has been obtained in both cases that indicate therapeutic potential as anti-cold sore and herpes treatment, provided that the main chemical constituents are able to adequately penetrate skin. This is considered in Chapter 6.

Chapter 6 **Penetration of Punicalagin and Zinc across Full Thickness and Heat Separated Epidermal Membranes from Solution**

6.1. **Introduction**

In Chapter 5 it was found that the combination of PRE and zinc salts provided significantly higher virucidal activity than either alone, thus providing the basis for a potential new product against HSV infections. HSV is a virus that generally affects perioral skin (cold sores) and the ano-genital area (herpes). The location of the viral load in each case is generally the stratum basale, particularly prior to eruption. Therefore, for a treatment based on PRE and zinc to be efficacious, it is necessary that the active compounds are able to penetrate across the skin to these areas. This is not straightforward given the barrier function of the skin, particularly in the early stages of an outbreak, where the stratum corneum is still intact. As outlined in Chapter 1 section 1.5.2., there are certain ground-rules that typically apply to the uptake and permeation of chemical compounds across skin. Most notably these relate to lipophilicity and molecular weight (Williams and Barry 1991). However, in the later stages of an outbreak, where the stratum corneum is breached, such parameters are of less importance.

In this chapter the focus is on the penetration of punicalagin from PRE and Zn^{2+} from simple liquid solutions, separately and in combination, across excised skin membranes *in vitro*. It was of great interest to establish that the main active compounds penetrate the skin at the same time and with the ratio of concentrations required to maintain virucidal potentiation. The *in vitro* examination of the permeation and penetration would suggest a similar result *in vivo* and, in particular, that antiviral and virucidal effects would be observed in lesion outbreak.

Membrane permeation, referring to the transport of molecules across the skin, is depicted in permeation profiles (cumulative mass or moles per area vs time), from which skin permeability parameters may be taken, including steady state flux and lag time. However, in order to determine the amount of a compound resident within skin after a certain time, it is conventional to use the technique of tape stripping, where adhesive tape is used to sequentially remove layers of skin tissue from the diffused area when removed from an FDC. The compounds are then extracted from the strips and analysed to yield relative depth versus concentration information (Escobar-Chávez, et al. 2008).

The membranes examined in the current work were porcine ear skin, which has been used extensively as a model for human skin in recent years. Porcine ear skin has been widely used for *in vitro* skin permeation studies and has shown to be the best alternative model for human skin (Meyera, et al. 2007) (Sekkat, Kalia and Guy 2004) (Simon and Maibach 2000). Full thickness skin is typically used in such experiments; although heat separated epidermal (HSE) membranes are also used, where the dermis is separated from the epidermis by heat action. Both were examined in this work, and were mounted in all-glass Franz diffusion cells, as described in Chapter 2 section 2.2.3.

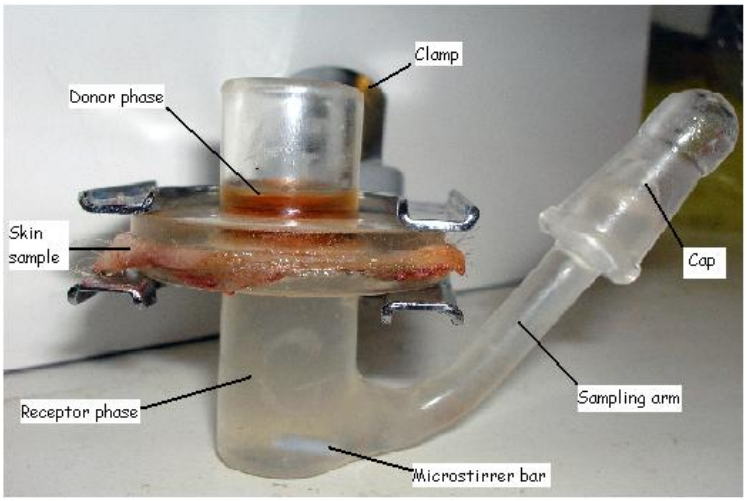

Figure 6-1 Glass Franz diffusion cell with Skin membrane *in situ.*

Test solutions were prepared in pH 4.5 phthalate buffer for consistency with the microbiology work of Chapters 4 and 5. Furthermore, this is within the range of the natural pH of the PRE as stated in (Akbarpour, Hemmati and Sharifani 2009), and studies have shown that PRE stability is greatest under such conditions (Panichayupakaranant, Itsuriya and Sirikatitham 2010). In addition, the skin surface is acidic with a general pH of 5.5, so the use of this buffer was considered appropriate. Single finite doses (40 μL) of the test solutions were applied to the membranes to approximate to *in vivo* use conditions.

6.1.1. Objective and Aims

To determine the potential for delivering punicalagin and Zn^{2+} into and across skin.

1. Determination of the cumulative permeation of punicalagin and Zn^{2+} across skin membranes following the administration of a simple liquid dose.

2. Determine the levels of punicalagin and Zn^{2+} in the skin by depth profiling, following the administration of a simple liquid dose.

6.2. **Materials & Methods**

6.2.1. Materials

The preparation of extracts and buffers used throughout this chapter are detailed in Chapter 2 section 2.2.1. unless otherwise stated

6.2.2. Preparation of test solutions

The procedures for the preparation of solutions of PRE, phthalate buffer at pH 4.5, $ZnSO_4$ and their various combinations was outlined in Chapter 2 Section 2.2.1. Table 6-1 outlines the test solutions used for each method of investigation. Prior to application all formulations were kept at 4°C and occluded from light.

Solution	Contents	Test/membrane	Volume Applied
PRE	Freeze dried PRE 1mg mL^{-1}in pH 4.5 phthalate buffer	HSE penetration FT penetration FT permeation	40 µL 40 µL 40 µL
PRE + $ZnSO_4$	Freeze dried PRE 1mg mL^{-1} and $ZnSO_4$ 1M in pH 4.5 phthalate buffer	HSE penetration FT penetration FT permeation	40 µL 40 µL 40 µL
$ZnSO_4$	$ZnSO_4$ 1M in pH 4.5 phthalate buffer	HSE penetration FT penetration FT permeation	40 µL 40 µL 40 µL
Blank	pH 4.5 phthalate buffer	HSE penetration FT penetration FT permeation	40 µL 40 µL 40 µL

Table 6-1 Experimental conditions for the determination of penetration and permeation across heat separated membranes (HSE) and full thickness skin membranes (FT).

6.2.3. Preparation of Porcine Ear Skin Membranes

The preparation of both full thickness and HSE membranes from freshly excised porcine ears were detailed in Chapter 2 section 2.2.2.

6.2.4. In-vitro Skin Permeation

The general procedure for determination of *in vitro* skin permeation using Franz diffusion cells with DI water as donor phase was outlined in Chapter 2 section 2.2.3. Single finite doses of 40 µL were applied to mimic in use conditions as shown in

Table 6-1, with replication of n=3 and without massage. The entire receptor phase was removed using Pasteur pipettes at 3, 6, 12, 24 and 36 h and replaced with fresh receptor phase at 37°C.

6.2.5. *In-vitro* Depth Profile Analysis by Tape Stripping

The general method for tape stripping was detailed in Chapter 2 section 2.2.3.4. After 24h post application, the membranes were recovered and 20 strips taken from the diffused areas, with constant pressure applied for each strips The first two strips were discarded to account for remaining test solution; each subsequent 2 strips were combined, dissolved in 2 mL MeOH, the strips were removed manually and the solvent was removed under vacuum. The residue was reconstituted in DI H_2O and stored at - 20°C before analysis.

6.2.6. Quantitative Analysis

The punicalagin content of samples were analysed via reverse phase HPLC using an Agilent 1100 HPLC system following the method set out in Chapter 2 section 2.2.4.1. Zinc analysis was conducted using Inductively Coupled Plasma Mass Spectrometry (ICP-MS) following the methods described in Chapter 2 section 2.2.4.2. Samples ranging between 0.1 and 10 µM of zinc were analysed using ICP-MS following standard calibration of the machine. Cumulative moles per area are presented to allow numerical comparison between punicalagin and zinc quantities.

6.3. **Results**

6.3.1. Permeation across Heat Separated Epidermis

Figure 6-2 shows the permeation profile of punicalagin that permeated porcine HSE following the application of a 40 µL dose of test solution. The results show that punicalagin permeated rapidly, with pseudo steady state permeation during the first 6 h of application. After this the trend was towards a plateau; there was no lag phase apparent. At 24h the permeation of punicalagin from the application of PRE and PRE

+ $ZnSO_4$ was 3.64 ± 0.11 nM cm^{-2} and 4.13 ± 0.1 nM cm^{-2}. This difference was statistically significant (p<0.05).

No punicalagin peaks were observed when the HSE was dosed with either control sample or $ZnSO_4$.

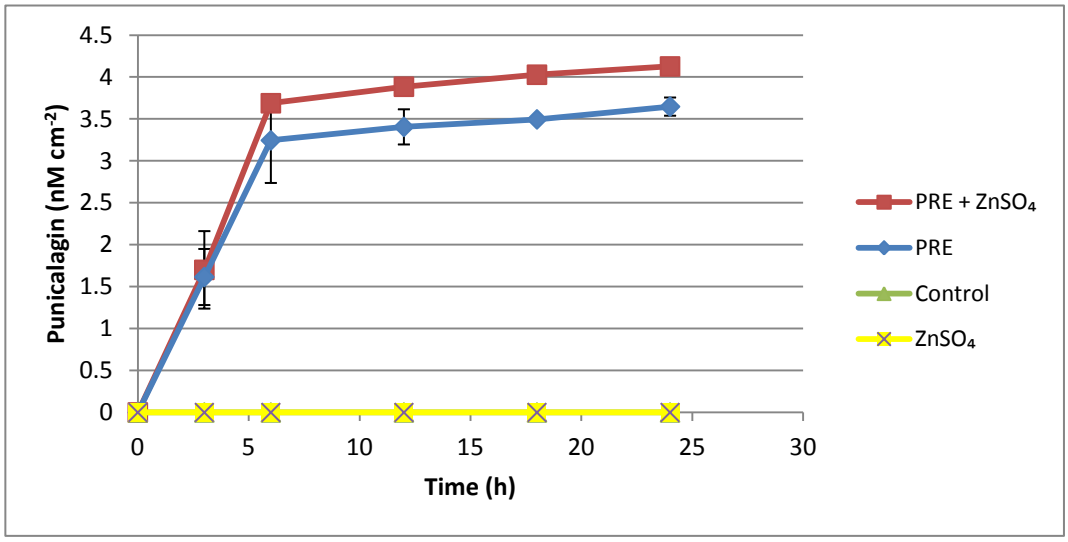

Figure 6-2 Cumulative permeation of punicalagin across HSE over 24 h (n=3, ± SD). The plot correspond to: PRE 1mg mL^{-1} + $ZnSO_4$ 1 M (red), PRE 1 mg mL^{-1} (blue), $ZnSO_4$ 1 M (yellow) and phthalate buffer control (green). 40 uL of each formulation was applied.

Figure 6-3 shows the cumulative permeation of zinc across HSE. Firstly, it is clear that the same levels of zinc were detected in the control and PRE-dosed cells. This demonstrates that an amount of endogenous zinc leached from the skin; however, this level was the same as that from PRE, indicating no additional presence of zinc from the PRE.

Similar to Figure 6-2, pseudo steady state permeation of zinc from skin dosed with $ZnSO_4$ and PRE + $ZnSO_4$ occurred within the first 6 h of application; after which point the permeation profile plateaued upon reaching equilibrium.

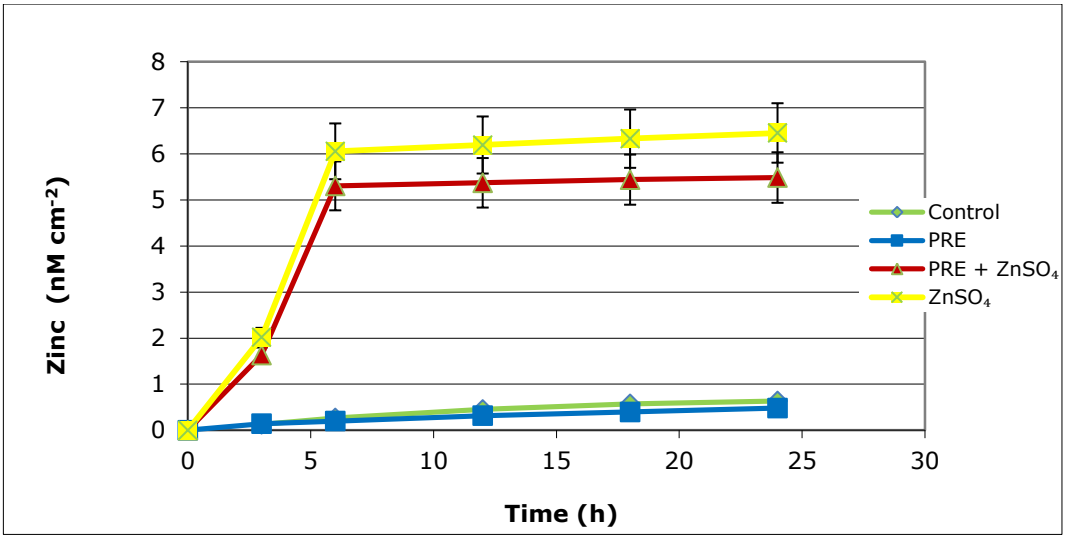

Figure 6-3 The permeation of zinc across HSE over 24 h (n=3 ± SD). The plot colours correspond to: PRE 1mg mL^{-1} + $ZnSO_4$ 1 M (red), PRE 1 mg mL^{-1} (blue), $ZnSO_4$ 1 M (yellow) and phthalate

Figure 6-4 shows the permeation of the analytes, punicalagin and zinc, through the epidermal membrane after application of 40 µL of PRE (1 mg mL^{-1}) + $ZnSO_4$ (1M). This is the equivalent of applying 7.38 nM of punicalagin. It is apparent that after 3 h both punicalagin and zinc permeate at similar concentrations, 1.7 ± 0.46 nM cm^2 and 1.6 ± 0.16 nM cm^2. After 6 h there is greater permeation of Zn (5.3 ± 0.49 nM cm^2) in comparison to that of punicalagin (3.69 ± 0.09 nM cm^2), after this time the permeation of both analytes reaches equilibrium.

This data shows that the finite dosing of 40 µL of PRE (1 mg mL^{-1}) + $ZnSO_4$ (1M) to the epidermis resulted in the simultaneous permeation of zinc and punicalagin to the site specific area of HSV-1 vesicles at the epidermal dermal interface. The concentration of permeated zinc and punicalagin at both 3 h and 6 h were at a ratio for which potentiated virucidal activity was observed in Chapter 5.

The results from the control and PRE treated epidermis were not statistically different ($p>0.05$) and in agreement with previous work that stated the penetration of zinc into the receptor phase from untreated epidermal membranes over 24 h was 0.09 ± 0.04 ug cm^{-2} (1.3 ± 0.6 nM cm^{-2}) (Cross, et al. 2007).

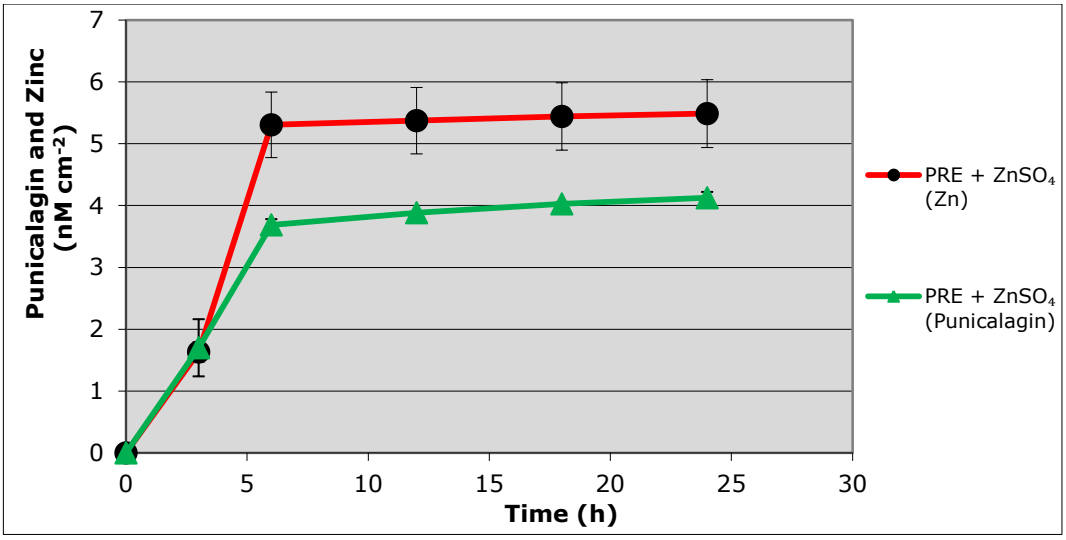

Figure 6-4 The permeation of punicalagin and zinc across HSE over 24 h after application of 40 uL of PRE (1 mg mL^{-1}) + $ZnSO_4$ (1M) (n=3 ± SD). The plot colours correspond to the analyte: red = Zn and green = punicalagin.

A review of the literature has found no reports of $ZnSO_4$ permeation through the epidermis. However, there has been a number of papers on the permeation and penetration of zinc in the form of ZnO. These generally concur that there was no permeation of zinc through the epidermis (Lansdown and Taylor 1997). Studies with microfine and nano sized particles have also drawn the same conclusion that no zinc penetrates the epidermis (Gamer, Leibold and Ravenzwaay 2006) (Cross, et al. 2007).

Figure 6-5 shows that the permeation of zinc occurred within the first six hours, the quantity of zinc detected after this is statistically similar to the values of the control and PRE alone. The quantity of zinc observed after 6 h and throughout the control and PRE treated epidermis is due to the leaching of zinc from the skin, which is relatively constant over the 24hr time period.

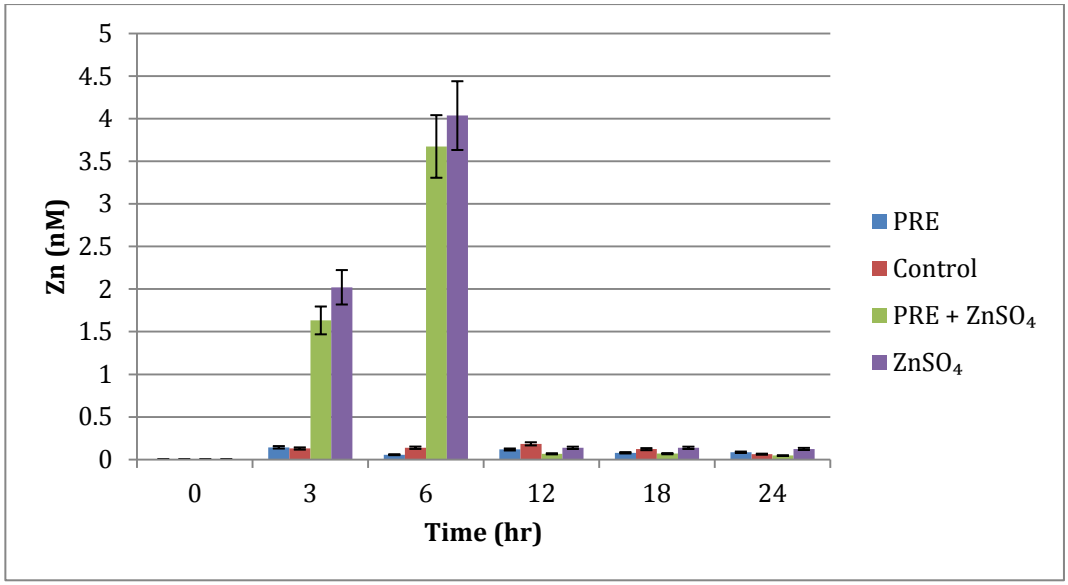

Figure 6-5 Permeation of Zn^{2+} through HSE at the specific time points 3, 6, 12, 18 and 24 h.

On the assumption that freely soluble zinc as $ZnSO_4$ behaves differently to insoluble zinc as ZnO, it may be expected for the zinc to permeate in the first few hours as there was a limited amount applied. This is similar to the permeation of punicalagin and it is clear that zinc permeation was unaffected by the presence of PRE.

The mixture of $ZnSO_4$ and PRE as a topically applied drug was able to permeate the epidermis to an acceptable level (as indicated by virucidal data in Chapter 5.3.3.1.) so that it would still be effective in combination to target a skin virus under or in the epidermis. It is important to note that punicalagin permeation may have been affected due to ester hydrolysis; however, the concentration of porcine esterase within the epidermis is very low (Lau, White and Heard 2010). If ester hydrolysis occurred, there would be an expected increase of the breakdown products of punicalagin, but this was not observed in the HPLC chromatograms.

6.3.2. Tape Stripping

Figure 6-6 shows the punicalagin amounts retrieved from each layer of the stratum corneum after 24h. The penetration of punicalagin is relatively constant throughout each layer of the epidermis, with higher amounts in the upper layers, as typically observed. However, by far the greatest recovery was from the dermis.

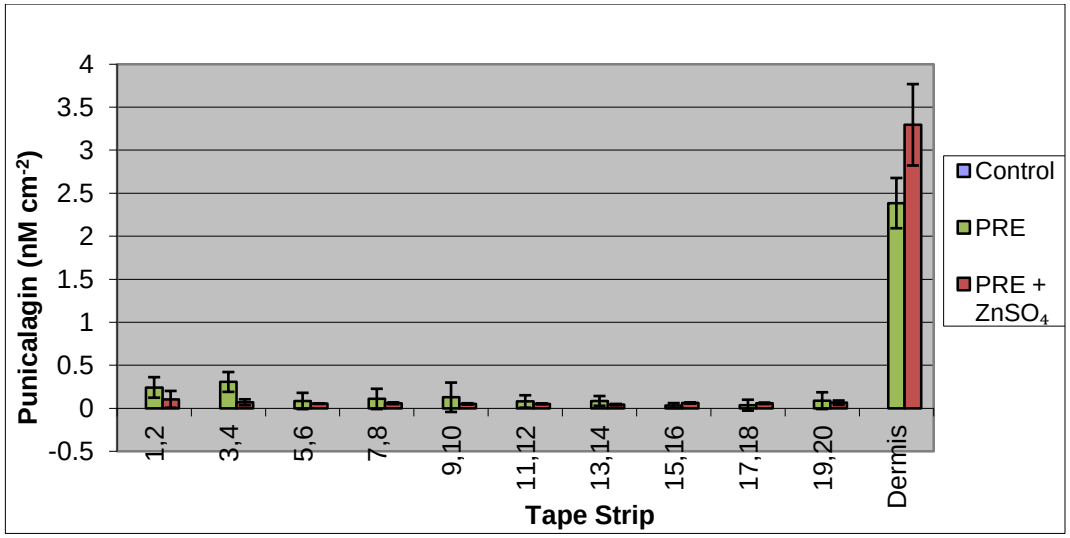

Figure 6-6 Depth profile of punicalagin in porcine skin after application of PRE (green), PRE + $ZnSO_4$ (red) and control (blue) (n=3 ±SD).

The amount of punicalagin recovered in each layer of the epidermis after application of PRE and application of PRE + $ZnSO_4$ was in the region of 0.1- 0.2 nM cm^{-2} and 0.05 - 0.1 nM cm^{-2} respectively. No peaks were identified at the specific time points for the control.

The largest recovery of punicalagin after tape stripping was from the dermis. The level of punicalagin after the application of PRE was 2.39 ± 0.29 nM cm^{-2}. After application of PRE and $ZnSO_4$ the concentration of punicalagin was somewhat lower at 3.3 ± 0.47 nM cm^{-2} ($p < 0.05$). The total recovery of punicalagin after application of PRE and PRE + $ZnSO_4$ from the tape strips and the dermis was not statistically different ($p>0.05$) at 3.58 ± 0.1 nM cm^{-2} and 3.91 ± 0.62 nM cm^{-2} respectively. These results are consistent with the permeation of punicalagin through the epidermis after application of 40 µL of PRE (1 mg mL^{-1}) and PRE (1 mg mL^{-1}) + $ZnSO_4$ (1M).

As shown in the previous permeation experiment, punicalagin permeation occurred rapidly, within the first three to six hours after application. Therefore it is reasonable to conclude that the punicalagin recovered in each of these layers after 24h application time has reached a point of equilibrium. The permeation profiles of punicalagin from both solutions shows that a greater concentration of punicalagin remains within the dermis when PRE is applied in combination with $ZnS0_4$ and that punicalagin has a more evenly distributed permeation through the stratum corneum

and dermis after the application of PRE alone, the difference in the profiles is unknown.

The maintenance of the ratio of punicalagin anomers after permeation and throughout the stratum corneum and dermis was expected, as the reversal or degradation of the concentration of the punicalagin anomers has only occurred in stability studies of pomegranate extracts at a basic pH10. The punicalagin anomers α and β are inverted or degraded at pH 10, at room temperature after reflux, or being microwaved (N. P. Seeram, Pomegranates Ancient Roots to Modern Medicine 2006).

Figure 6-7 shows the cumulative concentration of zinc recovered from the tape stripping of full thickness porcine skin after the topical application of 40 µL PRE (1 mg mL^{-1}) + $ZnSO_4$ (1 M), $ZnSO_4$ (1 M) and control *in vitro*. The concentration of zinc recovered was greatest and not significantly different (p>0.05) after the application of $ZnSO_4$ and PRE + $ZnSO_4$, this remained true at all layers of the stratum corneum and dermis. As expected zinc was recovered from the porcine skin within each layer of the stratum corneum and within the dermis the total quantity recovered was 68.03 ± 5.6 nM cm^{-2} - this value is simlar to that stated previously (Gamer, Leibold and Ravenzwaay 2006).

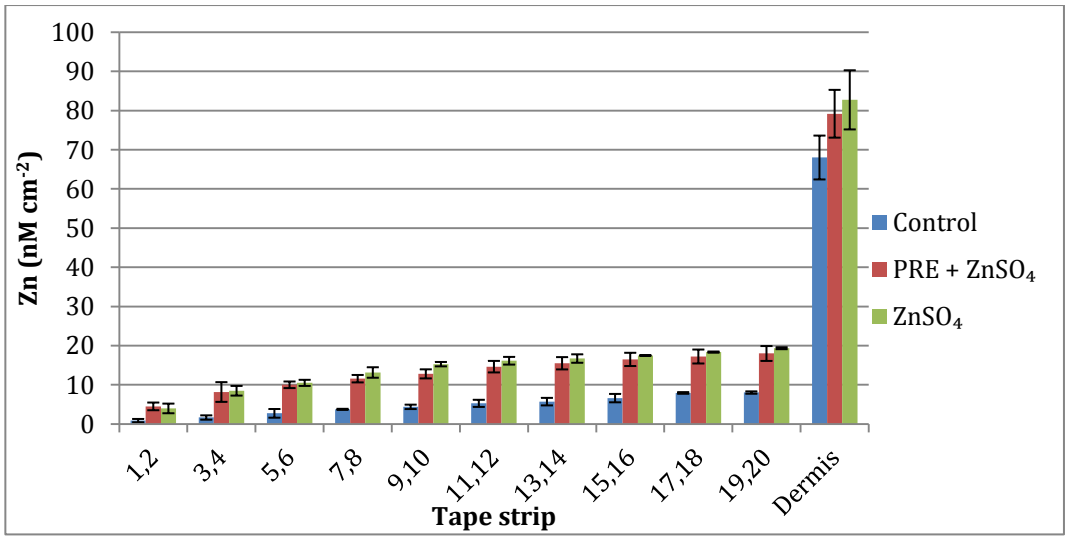

Figure 6-7 The cumulative concentration of Zn recovered from the tape stripping of full thickness porcine skin after 24h application of 40 µL PRE (1mg mL^{-1}) + $ZnSO_4$ (1M), $ZnSO_4$ (1M) and control (n=3 ± SD).

6.4. **Conclusion**

The finite dosing of PRE and $ZnSO_4$ to porcine epidermal membranes shows that punicalagin, the virucidally active compound within PRE, and $ZnSO_4$ all penetrate the epidermis at levels within the concentration ratio required so that a potentiated virucidal action will occur. The tape stripping of full thickness skin confirmed that both agents permeated all levels of the stratum corneum. However, it is apparent that Zn^{2+} permeates through the epidermis but does not permeate the dermis, as the zinc concentration found in this region was not statistically significantly different to the control.

The results show that from a finite liquid dosing, both punicalagin and $ZnSO_4$ are able to permeate in combination at the potentiated virucidal ratio to the epidermal dermal interface where HSV-1 and HSV-2 vesicular clusters form, this therefore shows that a therapeutic system based upon PRE and $ZnSO_4$ has the potential to effectively kill virion at the site of reproduction.

Chapter 7 **Probing the Anti-Inflammatory Effects of Topically Applied PRE and Zinc Sulphate Combination on Epidermal COX-2 Enzyme Activity**

7.1. **Introduction**

Herpes simplex virus type 1 and 2 lesion eruptions cause a significant level of inflammation to the localised area, resulting in erythema, swelling and pain particularly in the later stages. Although challenging the viral load is of primary importance when treating such lesions, there would be distinct advantages if a medication could also address this discomfort and discolouration. By the same token, it is clear that a topical treatment must not be pro-inflammatory as this would exacerbate discomfort. It is therefore pertinent to investigate the inflammatory effects of topically applied PRE and $ZnSO_4$.

Extracts from various parts of *Punica granatum* have been used for centuries to abate inflammation due to a wide range of diseases and afflictions (Aggarwal, et al. 2006). Dietary supplements containing various pomegranate extracts are currently popular in Western society for the treatment and prevention of arthritis and other inflammatory diseases. Anti-atherosclerotic and anti-inflammatory studies have shown the positive effect of consumption of pomegranate extracts and juice *in vivo* (Aviram and Dornfeld 2001)(Larrosa, et al. 2010). Anti-inflammatory effects using *Punica granatum* extracts have been shown *in vitro* by cellular biology, and excised porcine rat and human skin to decrease the inflammatory markers COX-2, LOX-5 and iNOS (Lee, et al. 2010). The evidence of this research has led to the development of a commercial anti-inflammatory, antioxidant and vasodilating product containing pomegranate extract, IGNITE®, produced by ZANAGEN.

The use of topically applied preparations containing zinc in order to accelerate the healing of wounds is well documented within the literature, and the use of gauze impregnated with zinc is known to decrease inflammation. However, much of the work on the anti-inflammatory properties of zinc has focussed on zinc oxide; indeed it has been reported that $ZnSO_4$ has no positive or negative effect on wound healing *in vivo* involving porcine, rat and human subjects. It has also been stated that topically applied $ZnSO_4$ to full thickness intact skin had no effect on the level of inflammation *in vitro* via analysis of the inflammatory markers cyclooxygenase-2 (COX-2) and lipoxygenase (LOX) (Roselli, et al. 2003), and *in vivo*(Agren, Chvapil and Franzen 1991).

The processes involved in skin inflammation occur in the viable epidermis, which is composed of living cells (keratinocytes). During inflammatory challenge to the skin the keratinocytes respond by cytokine release and activation of arachidonic acid metabolism along the COX-2 and LOX pathways. Upon chemical or mechanical tissue injury COX-2 is rapidly upregulated, channelling the arachidonic pathway to produce the inflammatory mediators, prostaglandins. The upregulation of COX-2 and LOX is transient with a short half life and therefore can be analysed as a marker for the level of inflammation within the skin at particular time points. Analysis of the level of COX-2 expression in skin can provide a comparative model for the dermatological activity of topically-applied formulations on inflammation, the probing of COX-2 modulation in *ex vivo* porcine ear skin and determination of the pro- or anti-inflammatory effects of topically applied N-3 fatty acids, betamethasone dipropionate and an extract of *Harpagophytum procumbens* showed this (Thomas, Davidson and Heard 2007) (Zulfakar, Abdelouahab and Heard 2010).

7.1.1. Objective and Aims

The objective of this study was to probe the effect on the inflammatory marker COX-2 expression following the application of individual or combined PRE and $ZnSO_4$ on porcine skin, *ex vivo*. The molecular biology techniques of immunocytochemistry (ICC) and Western blotting were used to determine relative protein (COX-2) levels.

Aims

1. to confirm or otherwise the previously reported downregulation of COX-2 expression within excised porcine epidermis following the topical application of PRE
2. to determine the modulation of COX-2 after topical application of PRE, $ZnSO_4$ and their combination by ICC and Western blotting.
3. to assess the potential of PRE and $ZnSO_4$ in combination as a topical anti-inflammatory system

7.2. **Materials and Methods**

7.2.1. Materials

The materials used in this work are detailed in Chapter 2 section 2.1.

7.2.2. Methods

The methodology for the formulation of solutions, extracts and buffers follows that described in Chapter 2 section 2.2. unless otherwise stated.

7.2.2.1. Formulation Preparation

The preparation of phthalate buffer, PRE, $ZnSO_4$ and their combinations followed the protocols outlined in section 2.2.1. Table 7-1 shows the concentration and volume of the formulations applied to *ex vivo* porcine epidermis and the method of molecular biological analysis used to probe protein levels.

Test solution	**Formulation**	**Volume applied to skin**	**Molecular biology technique**
PRE	0.1 mg mL^{-1} in Phthalate buffer pH 4.5	1 mL 1 mL	ICC Western Blotting
$ZnSO_4$	0.1 M in Phthalate buffer pH 4.5	1 mL 1 mL	ICC Western Blotting
PRE + $ZnSO_4$	PRE 0.1 mg mL^{-1}, $ZnSO_4$ 0.1 M, Phthalate buffer pH 4.5	1 mL 1 mL	ICC Western Blotting
Control	Phthalate buffer pH 4.5	1 mL 1 mL	ICC Western blotting

Table 7-1 Test solutions, applied volume and molecular biology (MB) techniques employed.

7.2.2.2. *Ex vivo* Porcine Skin Preparation

Ex vivo porcine skin membranes used for western blotting and ICC were prepared and used in a Franz diffusion cell following the approach outlined in Chapter 2 sections 2.2.2. and 2.2.3. respectively. However, in this case the Franz diffusion cells were not occluded and Hanks buffer was used as the receptor phase.

7.2.2.3. Immunocytochemistry (IHC)

Table 7-1 describes the concentrations and volumes of PRE, $ZNSO_4$ and their combination applied to the *ex vivo* skin. The full methodology for (IHC) is described in Chapter 2 section 2.2.4.5.

7.2.2.4. PAGE and Western Blot Analysis

The methodology for sample preparation of skin lysates, protein estimation and denaturation, PAGE and western blot analysis is given in Chapter 2 section 2.2.4.4.

7.2.2.5. Data Analysis

The Western blot bands were scanned and analysed using a densitometer (GS-690 Imaging Densitometer, Bio-Rad Laboratories Ltd, Herts, UK) equipped with Alpha DigiDoc software. The data obtained was recorded and analysed using Excel 2007 (Microsoft office, Microsoft Corp, Redmond, WA). Each experiment was performed in triplicate for each sample and the result expressed as the mean ± S.D. Statistical analysis was carried out with InStat for Macintosh, version 3.0 (GraphPad Software Inc, San Diego, CA).

7.3. **Results**

7.3.1. IHC Staining COX-2

At time zero, within the control and all evaluated skin sections COX-2 was clearly observed, as shown by the dark brown staining (Figures 7-1 and 7-2). As expected, the initiation of the inflammatory metabolic pathway for COX-2 suggests substantial inflammation caused by the trauma inflicted during removal and dissection of the porcine ears.

At 6 h it is apparent that the degree of staining and thus the inflammation within the control is sustained, and after 24 h an increase of COX-2 expression is supported by the increase in the level (area) and darkness of the brown stain suggesting a sustained and increasing inflammatory response over the 24 h test period. Previous work has shown that after 24 h necrosis is initiated in such skin samples, making the determination of further time points impossible (Thomas, Davidson and Heard 2007).

In Chapter 6 it was shown that after 6 h of treatment with PRE and $ZnSO_4$, punicalagin and zinc were both able to permeate the epidermis and dermis. Figure 7-1 shows that after 6 h the permeation of PRE resulted in the obvious reduction of COX-2 expression. A similar reduction was observed after the application of PRE + $ZnSO_4$ (Figure 7-2). The level of COX-2 expression, after application of PRE alone and in combination with $ZnSO_4$, was further reduced over 24 h as shown by the lighter staining observed in Figures 6-1 and 6-2 at this time point.

Application of $ZnSO_4$ was found to have no effect on the level of COX-2 expression, as shown by Figure 7-2. The slight increase in the degree of staining after 24 h reflects that observed in the control.

Overall, ICC analysis has demonstrated qualitatively that the topical application of PRE (with and without $ZnSO_4$) reduced COX-2 expression, which implies a reduction in the inflammatory response of the *ex vivo* skin. The application of $ZnSO_4$ appeared to have no effect on the expression of COX-2. In summary, these data represent a qualitative examination of COX-2 mediation after the topical application of $ZnSO_4$ and PRE alone and in combination.

Control 0h	Control 6h	Control 24h
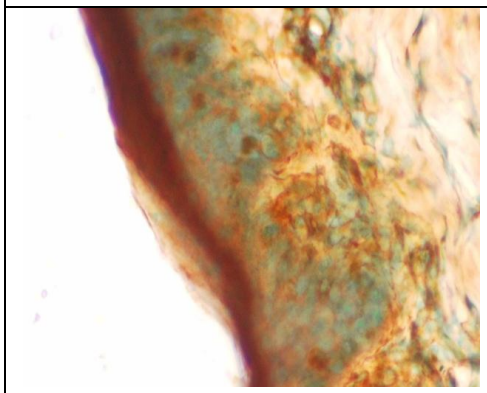	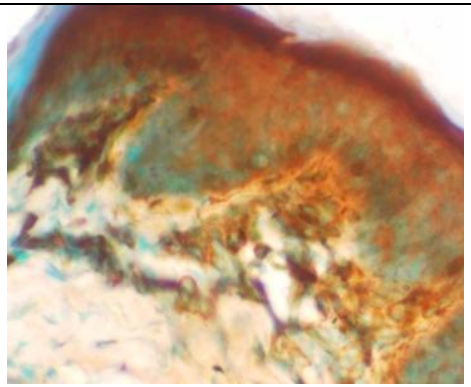	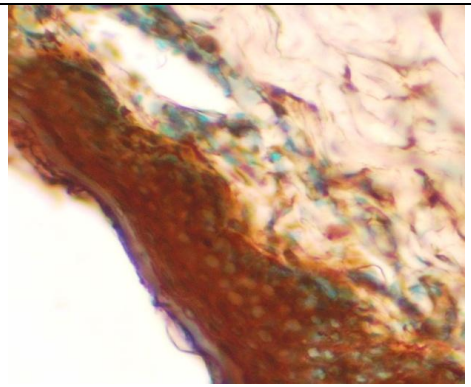
PRE 0h	PRE 6h	PRE 24h
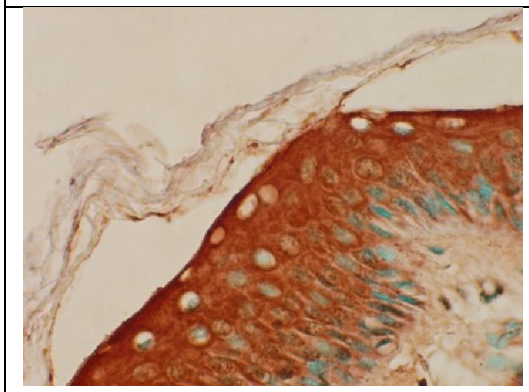	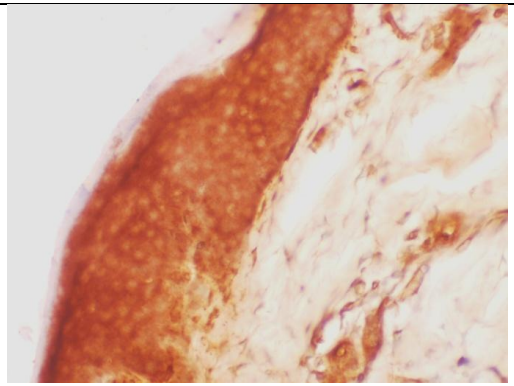	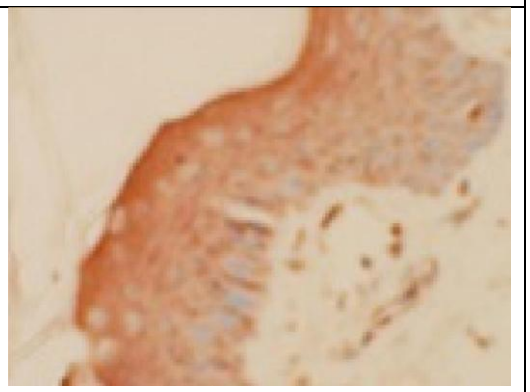

Figure 7-1 COX-2 IHC staining at 0h, 6h, and 24h after the topical application of Control (phthalate buffer pH 4.5) and PRE (1 mg mL^{-1}) (40x magnification).

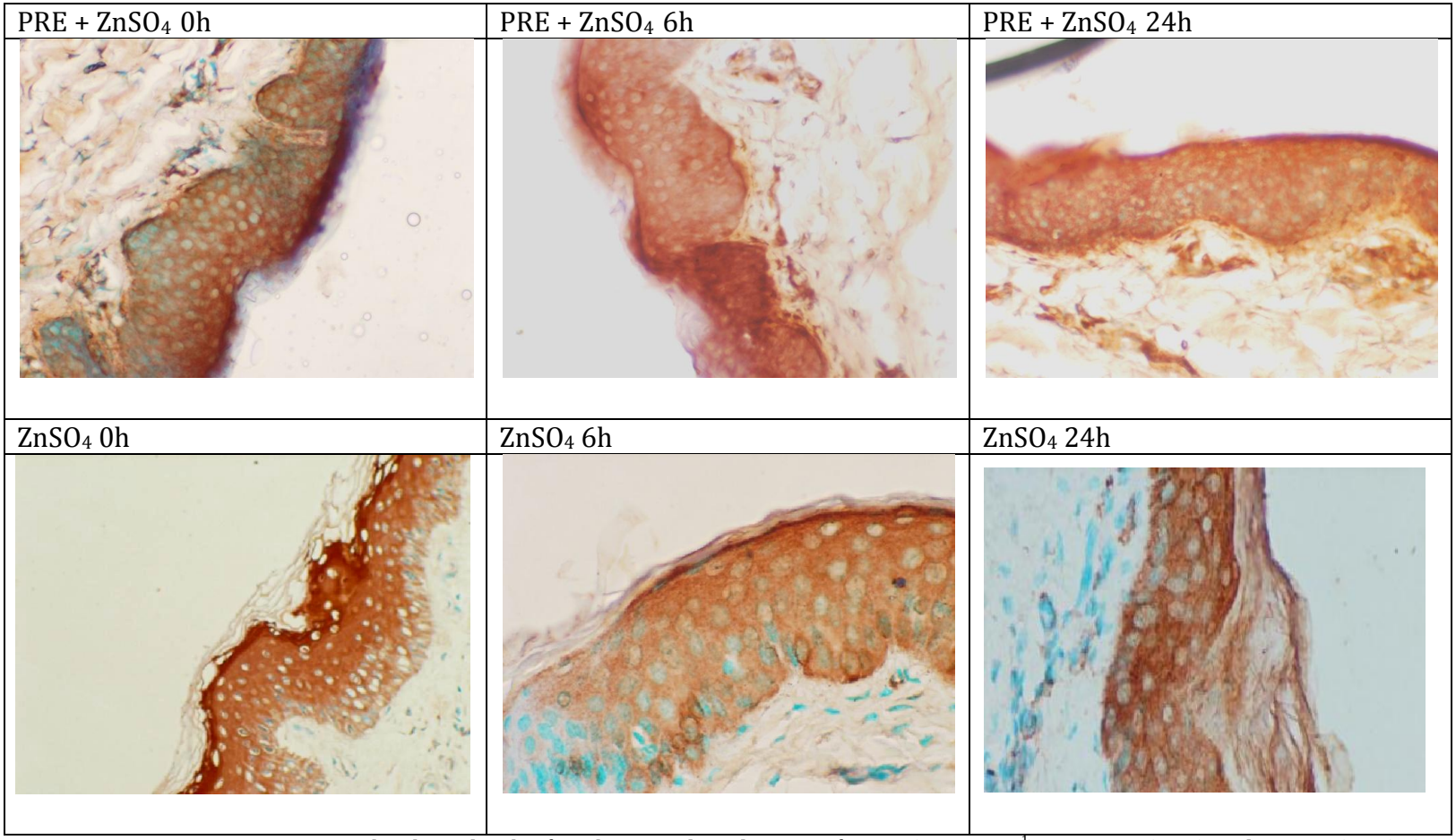

Figure 7-2 COX-2 IHC staining at 0h, 6h, and 24h after the topical application of PRE (1 mg mL^{-1}) + $ZnSO_4$ (1 M) and $ZnSO_4$ (1 M) (40x magnification).

7.3.2. Western Blotting

To further verify and to quantify the qualitative results observed from the IHC COX-2 expression shown above, Western blot analysis was performed. The test materials, formulation and volume stated in Table 7-1 of PRE, PRE + $ZNSO_4$, $ZnSO_4$ and control were applied to *ex vivo* full thickness porcine skin within a Franz diffusion cell for 6 h. After this time SDS PAGE and western blotting was carried out for COX-2, as an inflammatory marker, and β-Actin, as the protein loading control. The variation of COX-2 expression shown by ICC led to a 6 h time point being chosen for experimental comparisons.

Figure 7-3 shows the bands produced by Western blot analysis for COX-2 expression at ~ 72 kDa and the protein loading control of β-actin at ~42 kDa. Densitometric measurements of the bands for COX-2 were normalised using β-actin; levels of COX-2 expression in the control were arbitrarily assigned a value of 100% and test solutions were shown as a percentage of the control and graphically displayed as a histogram in Figure 7-3. The application of PRE and PRE + $ZnSO_4$ led to the statistically significant (p>0.01) reduction of COX-2 expression by 66.5 ± 3.6 % and 64.5 ± 5.1 % respectively. Application of $ZnSO_4$ had no statistically significant (p>0.05) effect on the level of COX-2 expression. Both results were in agreement with those obtained using ICC. The reduction of COX-2 by PRE was similar to that reported by (Adams, et al. 2006) who showed a COX-2 reduction of 79%, and the lack of COX-2 reduction by the application of $ZnSO_4$ at this concentration has also been previously shown (Roselli, et al. 2003).

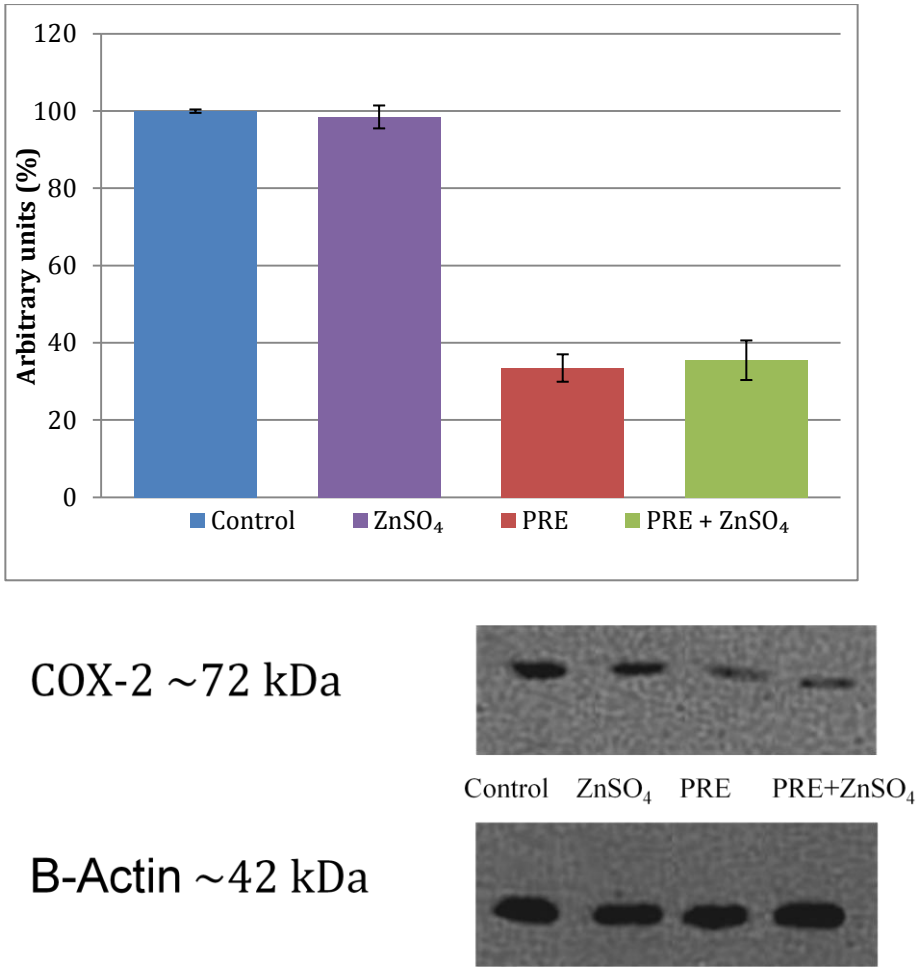

Figure 7-3 Analysis of COX-2 protein expression by Western blot. Full thickness porcine skin was treated with topical $ZnSO_4$ (1 M), PRE (1mg mL^{-1}), PRE (1mg mL^{-1}) + $ZnSO_4$ (1 M) and phthalate buffer as a control for 6 hr, protein was extracted and 30 µg was loaded and separated through SDS-PAGE. The histogram represents COX-2 levels normalised against β-Actin. Levels in control were arbitrarily assigned a value of 100%. (n=3 ± S.D).

7.4. **Conclusion**

It is apparent that the topical application of PRE to full thickness *ex vivo* skin downregulates the expression of COX-2, which was highly significant after just 6 h and which is maintained up to 24 h. There appeared to be no effect following the application of $ZnSO_4$ on the regulation of COX-2 over this time period. When PRE and $ZnSO_4$ were applied in combination a statistically similar downregulation of COX-2 was observed when compared to the application of PRE alone.

As the level of COX-2 present within the skin is a recognised marker for inflammation, the overall conclusion was that the topical application of PRE alone or in combination with $ZnSO_4$ had a substantial anti-inflammatory effect in *ex vivo* skin and that this may be beneficial in ameliorating the inflammation and pain associated with lesions caused by *Herpes simplex* virus.

Chapter 8 **Separation and Analysis of Pomegranate Rind Extract Fractions**

8.1. **Introduction**

In Chapters 3 and 5 the virucidal activity of PRE against HSV-1 was established and attributed to punicalagin, and these results were comparable to findings described for virucidal activity of PRE with respect to HSV-2 (Zhang, et al. 1995). The virucidal activity of punicalagin has further been demonstrated against the Influenza virus (Haidari, et al. 2009). Fractionation and analysis of PRE could elucidate other virucidal fractions or confirm the hypothesis that the virucidal activity is solely due to that of punicalagin.

Conversely, results in Chapter 5 showed that PRE possessed antiviral activity against HSV-1 and HSV-2 ACR, whereas punicalagin and ellagic acid possessed no observable activity. From this it was hypothesized that a complex interplay between the phytochemical constituents was responsible for the antiviral activity. An alternative is that a previously untested fraction of the PRE may have been responsible and if this hypothesis is correct then the fractionation of PRE could lead to the isolation of a new antiviral compound.

Further, the COX-2 modulation results obtained by Western blotting and IHC in Chapter 7 indicated that the total extract reduced the inflammatory response in *ex vivo* skin. This may be related to the total polyphenolic content as stated previously (Adams, et al. 2006) (Aggarwal, et al. 2006) (Larrosa, et al. 2010). Extracts found within PRE were shown to exhibit anti-inflammatory responses (Lee, et al. 2010).

More than 120 phytochemicals have been identified in the juice, seed, peel and rind of *Punica granatum* (Seeram, Schulman and Herber 2006). Pomegranate rind contains a large proportion of polyphenols e.g. ellagic acid, gallotannins, anthocyanidins such as delphinidin, cyanidin and pelargonidin, proanthocyanadins and various flavonoids. Of specific interest are the hydrolysable tannins punicalin, pedunicalin, punicalagin as well as gallic and ellagic acid, esters of glucose (Slusarczyk, et al. 2009), of which punicalagin is the most abundant-constituting 80-85% w/w of total *Punica granatum* tannins (Seeram, et al. 2005). For the PRE used in this study, punicalagin is approximately one fifth of the total dry weight (Chapter 2 section 2.2.4.1.).

Bioactivities described for PRE and punicalagin, include antiproliferative, apoptotic, antiviral, anti-inflammatory and antibacterial (Seeram, Schulman and Herber 2006). The antibacterial activity of various pomegranate rind extracts has been attributed mainly to fractions extracted with acetone and methanol which contained high concentrations of punicalagin. The antibacterial effect was observed against both Gram-positive and Gram-negative bacteria, with complete growth inhibition of *B. cereus, B. subtilis, B. coagulens, S. aureus, E. coli and P. aeruginosa* shown at 300 ppm (Negi and Jayaprakasha 2003). The reduction in COX-2 expression due to PRE has been shown by the inhibition of the TPA-mediated increase in COX-2 expression in a time dependant manner *in vivo* (Afaq, et al. 2005). The downregulation of COX-2 has been attributed to the phenolic content, and some of the activity observed was assigned to punicalagin, however PRE as a whole entity (i.e. without fractionation) resulted in the greatest anti-inflammatory activity (Adams, et al. 2006). Fractionation has also revealed some phytochemicals present in PRE that have HSV, HIV or influenza antiviral effects, these include casuarinin, gallic acid, methyl gallate, and punicalin (Satomi, et al. 1993) (Wang, et al. 2010). It has also been shown that pomegranate extracts which remain as a whole entity are antiviral against a range of enveloped virus; HIV, H5N1, HBV, HCV and HSV (Kotwal 2008) (Sundararajan, et al. 2010).

A greater understanding of the occasionally contradictory data relating to the activity of PRE and components in general may be obtained by isolating individual fractions of PRE and subjecting them to virucidal, antiviral and COX-2 modulation testing.

8.2. **Objective and Aims**

To gain further insight into the phytochemical basis of the virucidal, antiviral and COX-2 modulation activities observed in Chapters 5 and 7, through examination of a range of chromatographically-isolated PRE fractions.

i. To obtain chromatographically separated fractions of PRE

ii. To determine the cytotoxicity of fractions, in comparison to data obtained in 5.3.2.

iii. To determine differences in virucidal activity of each fraction against HSV-1 in comparison to data obtained in 5.3.3.1. and 5.3.3.4.

iv. To determine differences in antiviral activity of each fraction against HSV-1 in comparison to data obtained in 5.3.3.5.

v. To determine differences in COX-2 expression in *ex vivo* skin dosed with each fraction in comparison with the results obtained in Chapter 7

8.3. **Materials and Methods**

8.3.1. Materials

The materials used are given in Chapter 2 section 2.1.

8.3.2. Methods

The general methodology for the preparation of solutions, buffers and extracts are given in Chapter 2 section 2.2.1. unless otherwise stated.

8.3.2.1. Fractionation of PRE

The chromatographic separation of compounds within PRE must follow a logical and structured method. The methodology used to fraction PRE into bands separating total pomegranate tannins (TPT) from the remainder of the extract, a tannin devoid fraction (TDF), used an Amberlite XAD16 stationary phase and followed the method summarised in Chapter 2 section 2.2.6.

8.3.2.2. Fractionation of Total Pomegranate Tannins (TPT)

Further fractionation of the TPT collected via Amberlite XAD 16 stationary phase was achieved using the method reported by Seeram, et al. (2005) involving a Sephadex LH-20 stationary phase, and is detailed in Chapter 2 section 2.2.6.; biological activity was assessed on three of the 9 fractions:

- Fraction 1 containing a small number of tannins including delphinidin 3-glucoside, cyanidin 3-glucoside
- Fraction 2 containing the tannins found in fraction one with the inclusion of ellagic acid and a number of unidentified tannins
- Fraction 9 predominantly comprising of the anomers punicalagin α and β

8.3.3. Cytotoxicity

Followed the Cell Titre 96® AQueous method described in Chapter 2 section 2.2.5.7. With the application of Fraction 1, 2, 9, TPT and TDF as described in Table 8-1.

8.3.4. Virucidal Plaque Reduction Assay

HSV-1was incubated, according to the methods in Chapter 2 section 2.2.5.9., with test solutions of TPT, TDF and Fractions 1, 2, and 9 as shown in Table 8-1 prior to application on vero cells.

8.3.5. Antiviral Plaque Assay

The methodology was the same as that described in Chapter 2 section 2.2.5.10. Vero cells were incubated with the test solutions listed in Table 8-1 being TPT, TDF and Fractions 1, 2, and 9 before application of the HSV-1 virus.

8.3.6. PAGE and Western Blot Analysis.

The analysis of COX-2 expression after the application of TPT, TDF and Fractions 1, 2 and 9 to full thickness porcine skin followed that outlined in Chapter 2 section 2.2.4.4. The data shown in Chapter 7 for PRE was used as a comparison.

8.3.6.1. Test materials

Table 8-1 shows the test fractions, its composition, application volume and analysis method used within this chapter.

Test Material	Composition	Analysis method
TDF	TDF 0.01 mg mL^{-1}, phthalate buffer pH 4.5	Virucidal Plaque reduction assay
	TDF 100 µg mL^{-1}, phthalate buffer pH4.5 (first dilution)	Antiviral plaque assay
	TDF 1mg mL^{-1}, phthalate buffer pH 4.5	PAGE Western Blot
TPT (Total Pomegranate Tannin)	TPT 1mg mL^{-1}, phthalate buffer pH 4.5	Cytotoxicity
	TPT 0.01 mg mL^{-1}, phthalate buffer pH 4.5	Virucidal Plaque reduction assay
	TPT 100 µg mL^{-1}, phthalate buffer pH 4.5 (first dilution)	Antiviral plaque assay
	TPT 1mg mL^{-1}, phthalate buffer pH 4.5	PAGE Western Blot
Fraction 1	Fraction 1, 1mg mL^{-1}, phthalate buffer pH 4.5	Cytotoxicity
	Fraction 1, 0.01 mg mL^{-1}, phthalate buffer pH 4.5	Virucidal Plaque reduction assay
	Fraction 1, 100 µg mL^{-1}, phthalate buffer pH 4.5 (first dilution)	Antiviral plaque assay
	Fraction 1, 1mg mL^{-1}, phthalate buffer pH 4.5	PAGE Western Blot
Fraction 2	Fraction 2, 1mg mL^{-1}, phthalate buffer pH 4.5	Cytotoxicity
	Fraction 2, 0.01 mg mL^{-1}, phthalate buffer pH 4.5	Virucidal Plaque reduction assay
	Fraction 2, 100 µg mL^{-1}, phthalate buffer pH4.5 (first dilution)	Antiviral plaque assay
	Fraction 2, 1mg mL^{-1}, phthalate buffer pH 4.5	PAGE Western Blot
Fraction 9	Fraction 9, 1mg mL^{-1}, phthalate buffer pH 4.5	Cytotoxicity
	Fraction 9, 0.01 mg mL^{-1}, phthalate buffer pH 4.5	Virucidal Plaque reduction assay
	Fraction 9, 100 µg mL^{-1}, phthalate buffer pH4.5 (first dilution)	Antiviral plaque assay
	Fraction 9, 1mg mL^{-1}, phthalate buffer pH 4.5	PAGE Western Blot

Table 8-1 Test solutions and biological analyses carried out: a tannin devoid fraction, TPT, Fraction 1, Fraction 2 and Fraction 9.

8.4. **Results**

8.4.1. PRE Fractionation

8.4.1.1. Separating the Total Pomegranate Tannins (TPT) and a Tannin Devoid Fraction (TDF)

The fractionation of 5 g PRE (dry weight) via an Amberlite XAD 16 packed column to refine the extract into TPT (freeze dried yield 1.3 g, 26%) and TDF (freeze dried yield 3.4 g, 68%). The product red crystals of TPT are shown in Figure 8-3 and HPLC analysis of the TPT fraction provided the chromatogram in Figure 8-1. It can be determined that this fraction contained 1.09 g of punicalagin (84% of the TPT fraction), and 0.009 g of ellagic acid (0.69%). These findings are in accordance with the literature which states that punicalagin was equivalent to 80-85% and ellagic acid 1.3% of the total pomegranate tannin content (Seeram, et al. 2005). There was no presence of tannins within the TDF fraction as shown by the lack of any peaks within chromatogram (Figure 8-2).

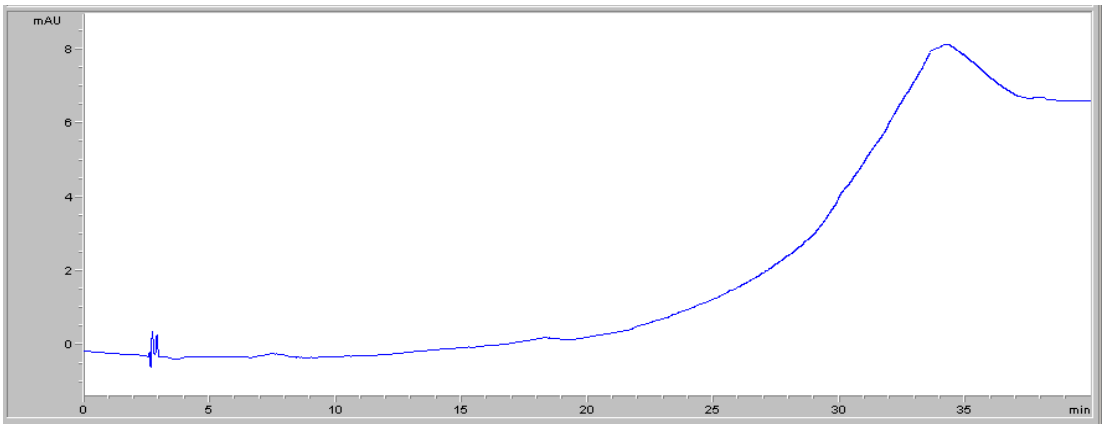

Figure 8-1HPLC chromatogram of the tannin devoid fraction (TDF) collected after XAD 16 column fractionation of PRE. Note: absence of ellagitannins.

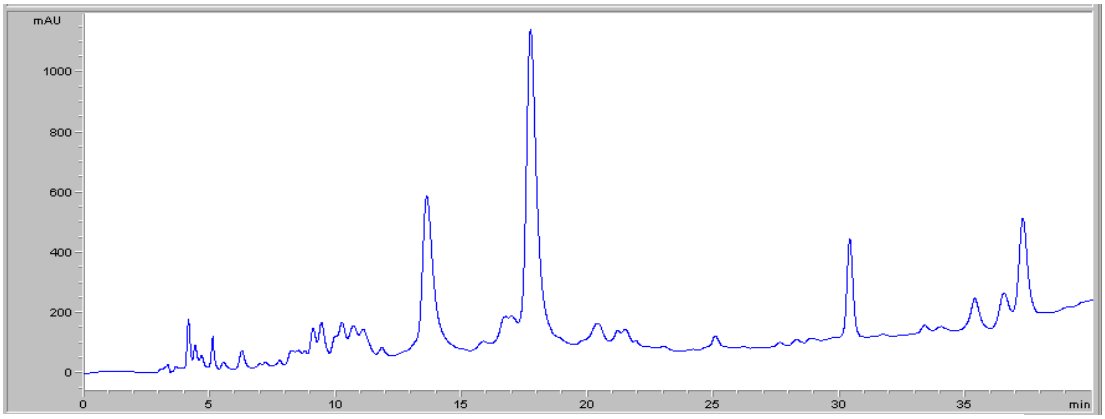

Figure 8-2HPLC chromatogram of the total pomegranate tannin (TPT) fraction collected after XAD 16 column fractionation of PRE.

Figure 8-3 Crystals of TPT isolated and collected after column fractionation.

8.4.1.2. Separating the TPT Fraction

A mass of 500 mg TPT was fractionated using MeOH:H_20 elution through a Sephadex LH-20 packed column, resulting in a total yield of 492 mg separated into 9 fractions. The HPLC chromatographic analysis of each fraction is shown in Figures 8-4 and 8-5. The fractions were dried under vacuum and the total mass of punicalagin, ellagic acid and the remaining unidentified tannins in each sample determined and shown in Table 8-2. The fractions, 1-8, were collected sequentially after each hour of elution, fraction 9 was created by the pooling of the final 3 h of elution, ensuring the full recovery of tannins. The solvent gradient timetable, the collection of fractions and the removal of eluting solvents is given in more detail in Chapter 2 sections 2.2.6.2. and 2.2.6.2.1.

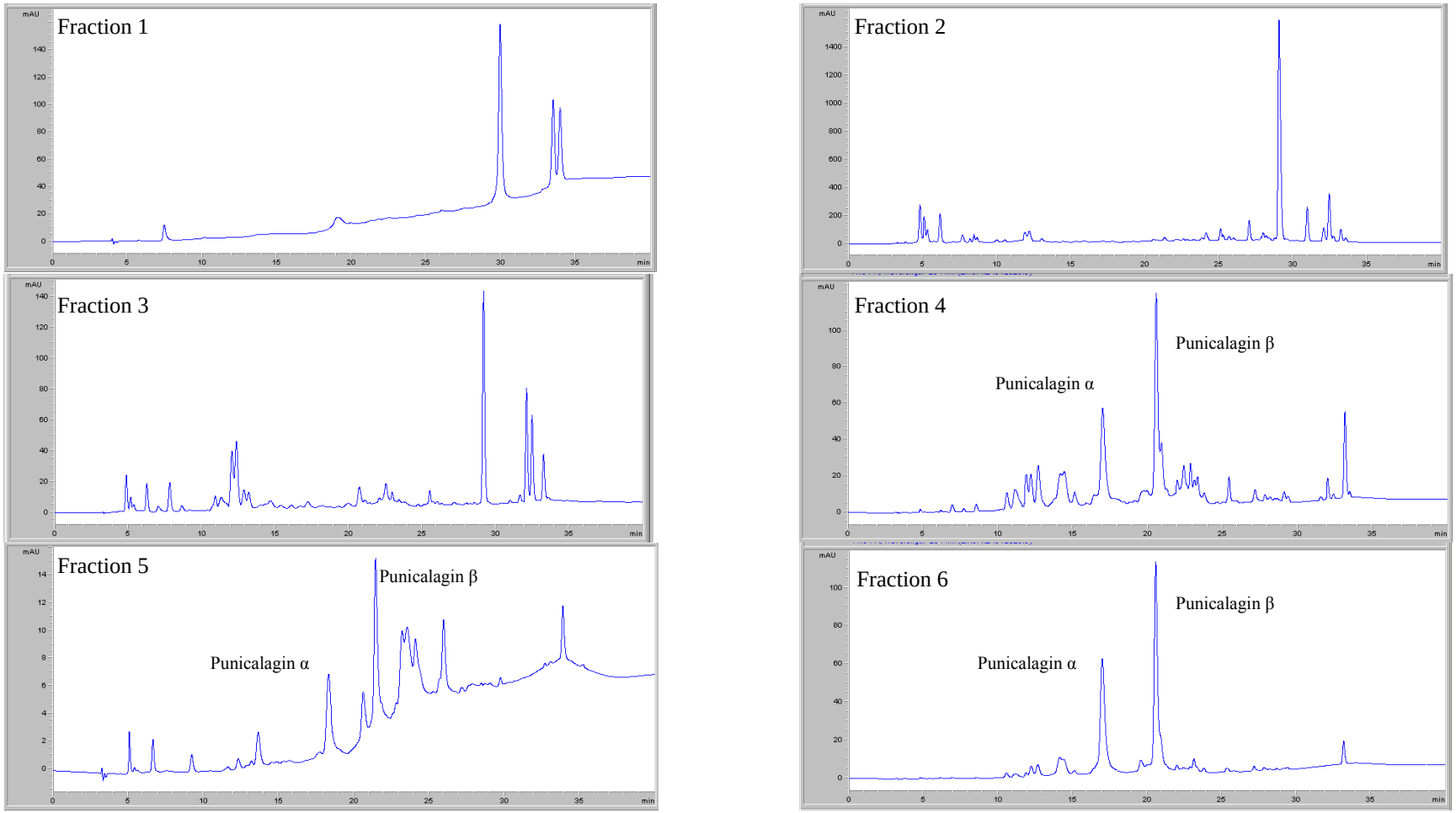

Figure 8-4 HPLC chromatograms of fractionated TPT from PRE through a Sephadex LH-20 column. Fractions taken at 1 h time points following the methods in 2.2.6.2.: Fraction 1-6.

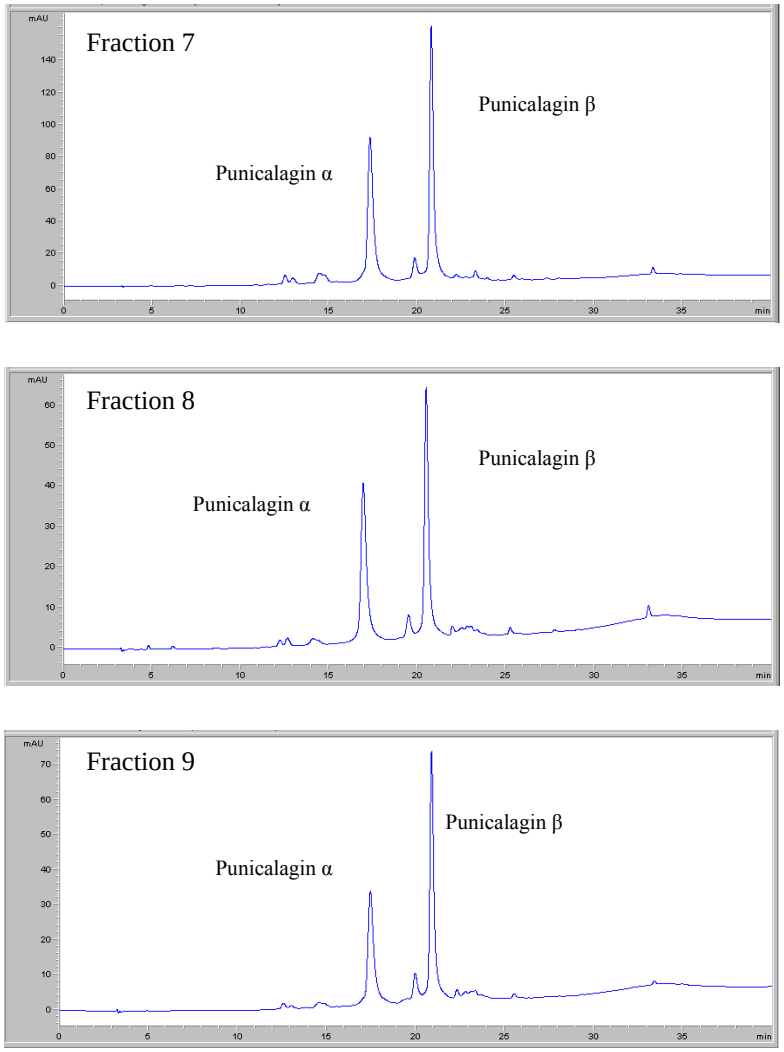

Fraction	Punicalagin (mg)	Ellagic acid (mg)	Unidentified Tannins (mg)	Total mass (mg)
1	0	0	13.47	13.47
2	0	0.97	21.61	22.58
3	1.76	0.02	17.08	18.86
4	79.86	0	12.06	91.92
5	17.86	2.01	5.42	25.29
6	80.72	0	0.90	81.62
7	109.58	0	0.72	110.30
8	62.12	0	0.36	62.48
9	65.30	0	0.18	65.48
Total	417.2	3	74.5	492

Table 8-2 The specific levels of punicalagin, ellagic acid and unidentified tannins within each fraction (1-9) of TPT within PRE after sephedex LH-20 fractionation.

Figure 8-5 HPLC chromatograms of fractionated total pomegranate tannin from PRE through a sephedex LH-20 column. Fractions 7 and 8 taken at 1 h time points and fraction 9 the combination of 3, 1h, time points following the methods in 2.2.6.2.: Fractions 7-9.

The fractionation of PRE into the TPT and TDF fractions via an Amberlite XAD 16 column was successful, as was the further separation of TPT into three fractions, one containing a high concentration of punicalagin using the Sephadex LH-20 column. The results can be summarised as follows:

Fraction 1 contained no punicalagin and comprised solely of other ellagitannins, which remain unidentified in this project; however, comparison to HPLC chromatograms within the literature suggest this fraction probably contained delphinidin 3-glucoside, cyanidin 3-glucoside (Gil, et al. 2000) (Seeram, Schulman and Herber 2006).

Fraction 2 contained a similar mixture of unknown compounds as that of fraction 1, with the inclusion of ellagic acid at 4.2% of the fraction. From the literature, galloylglucose and gallic acid were also likely to be present (Gil, et al. 2000); (Reddy, et al. 2007); (Seeram, et al. 2005).

Fraction 3 contained a very small amount of ellagic acid 0.1% and punicalagin (9%) with a similar mixture of tannins found in fraction 2 at a lower concentration.

Fraction 4 was comprised of all the tannins present within PRE as was fraction 5 this was however at much lower concentration.

Fractions 6, 7, 8, and 9 were comprised almost entirely of punicalagin, with fraction 9 containing the purest sample.

Fractions 1, 2, and 9 were chosen as test fractions to assess the biological activity as they contained between them all of the tannins within PRE at different concentrations, with fractions 1 and 2 not containing punicalagin and fraction 9 comprised almost entirely of punicalagin.

8.4.2. Cytotoxicity

The results of the Cell Titer 96 AQueous assay cytotoxicity tests for TPT, fractions 1, 2 and 9 at 0.1 mg mL^{-1} are shown in Figure 8-6. All fractions were prepared in phthalate buffer at pH 4.5 and demonstrated no cytotoxicity over the 72 h period ($p > 0.05$). This accorded with the lack of cytotoxicity exhibited by PRE, punicalagin and phthalate buffer at 0.01 mg mL^{-1} previously discussed in Chapter 5.

The data also suggests another important outcome. By isolating various compounds from the overall mix, it is conceivable that one fraction might have demonstrated greater cytotoxicity relative to another and the whole extract. Clearly this is not the case and suggests that variations in phytochemical levels, as in batch-to-batch variability, may not result in variable cytotoxicity.

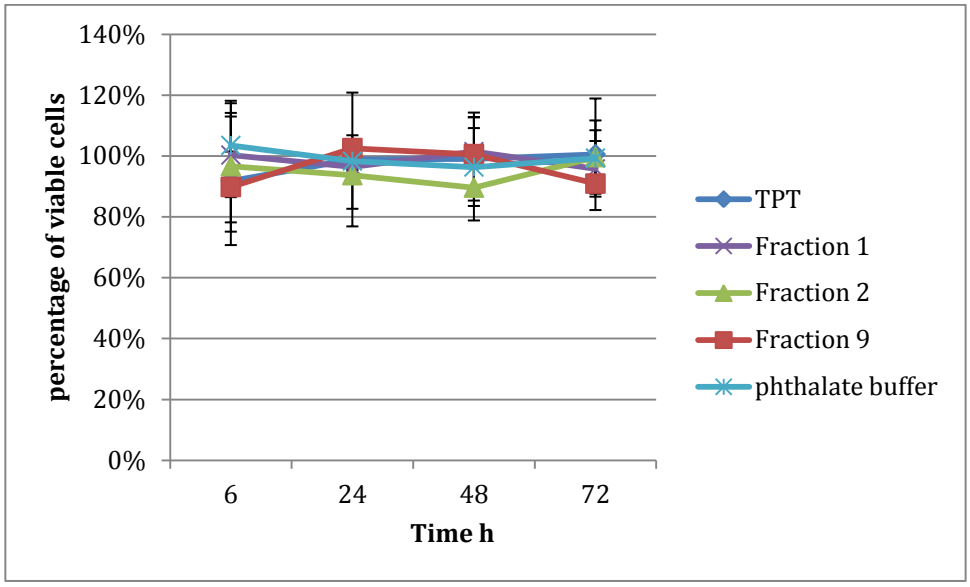

Figure 8-6 Cell Titre 96® AQueous assay cytotoxic evaluation of TPT and fractions 1, 2, and 9 at 0.1 mg mL^{-1}, in phthalate buffer at pH4.5, and expressed as the viable cell percentage of the control (n=3 ± SD).

8.4.3. HSV-1 Virucidal Activity

The log reduction of HSV-1 arising from the incubation with fractionated portions of PRE: (TPT, TDF and Fractions 1, 2 and 9) is shown in figure 8-7. The TDF fraction and fractions 1 and 2 exhibited a virucidal action that was not statistically different from the phthalate buffer in which they were dissolved (p>0.05). The TPT fraction and fraction 9 caused a logarithmic reduction of HSV-1 at 1.89 ± 0.12 pfu and 2.23 ± 0.22 pfu respectively. The observed log reduction can be attributed to the punicalagin content found within the fractions as it is of a similar order to that of punicalagin shown in Chapter 5 of 2.4 ± 0.96 pfu.

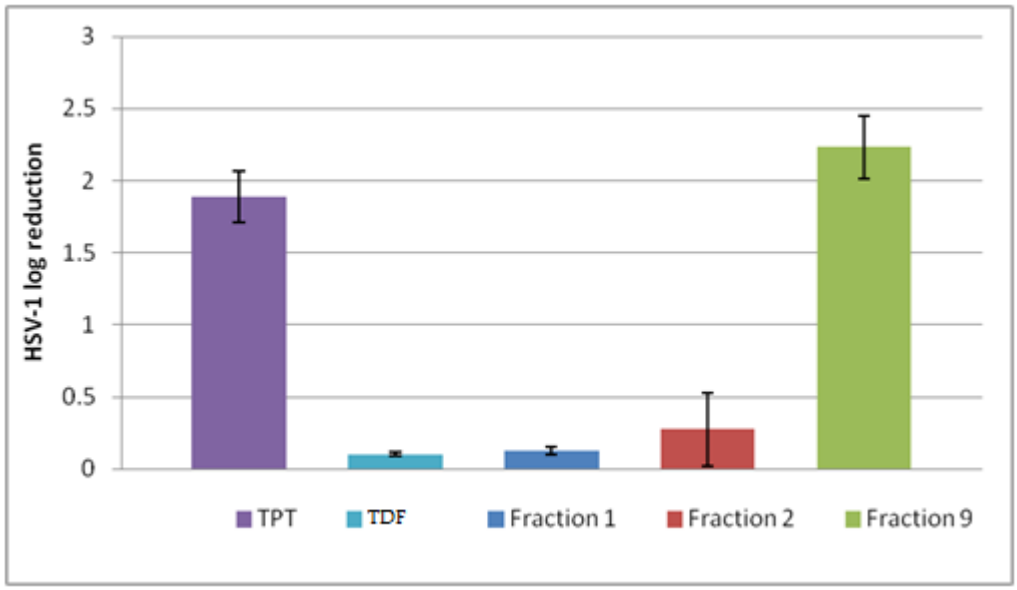

Figure 8-7 The log reduction of HSV-1 after incubation with the pomegranate fractions: TDF, TPT, Fraction 1, Fraction 2 and Fraction 9 at 0.01mg mL^{-1}, pH 4.5 (n=3 ± s.d.).

The two fractions containing punicalagin, TPT (as a component) and Fraction 9 (pure), were the only fractions that exhibited virucidal activity. This provides further evidence that the virucidal activity of PRE is determined by the punicalagin content.

8.4.4. HSV-1 Antiviral activity

The antiviral analyses of TPT, TDF and fractions 1, 2 and 9 are shown in Table 8-3.

Compound	Virus	IC_{50}
TPT	HSV-1	5.48 ± 0.34 µg mL^{-1}
TDF	HSV-1	>100 µg mL^{-1}
Fraction 1	HSV-1	>100 µg mL^{-1}
Fraction 2	HSV-1	>100 µg mL^{-1}
Fraction 9	HSV-1	>100 µg mL^{-1}

Table 8-3 Antiviral IC_{50} against HSV for the fractions of PRE: TPT, TDF, Fraction 1, Fraction 2 and Fraction 3 (n=3 ± s.d.).

The only fraction that showed antiviral activity was TPT, with an IC_{50} of 5.48 ± 0.34 µg mL^{-1}. In Chapter 5 it was found that PRE produced an IC_{50} of 0.556 ± 0.039 µg mL^{-1}. Therefore, although TPT activity was considerable the IC_{50} was significantly higher than that of PRE ($p < 0.05$): i.e. TPT has significantly less antiviral activity than PRE.

It is therefore reasonable to attribute the antiviral activity to the combined tannins within PRE; the removal of the TDF and further fractionation resulted in a significant loss of antiviral activity. This result is similar to that shown by Li *et al.* (2004), who stated that a pomegranate extract devoid of polyphenols did not exhibit antiviral activity and that fractionation led to a decrease in overall antiviral activity.

8.4.5. COX-2 Modulation and Anti-inflammatory Activity

As observed in Chapter 7, COX-2 is significantly downregulated following the application of PRE to full thickness porcine skin *ex vivo* by approximately 66%. In this part of the work, TPT, TDF, fractions 1, 2, and 9 were applied to skin in a similar manner and Figure 8-8 is representative of the bands produced by Western blot analysis for COX-2 expression at ~ 72 kDa with the protein loading control of β-actin at ~42 kDa. Densitometric results of the bands for COX-2 were normalised using β-actin, levels of COX-2 expression in the control were arbitrarily assigned a value of 100%, test solutions were shown as a percentage of the control and graphically displayed as a histogram in Figure 8-8

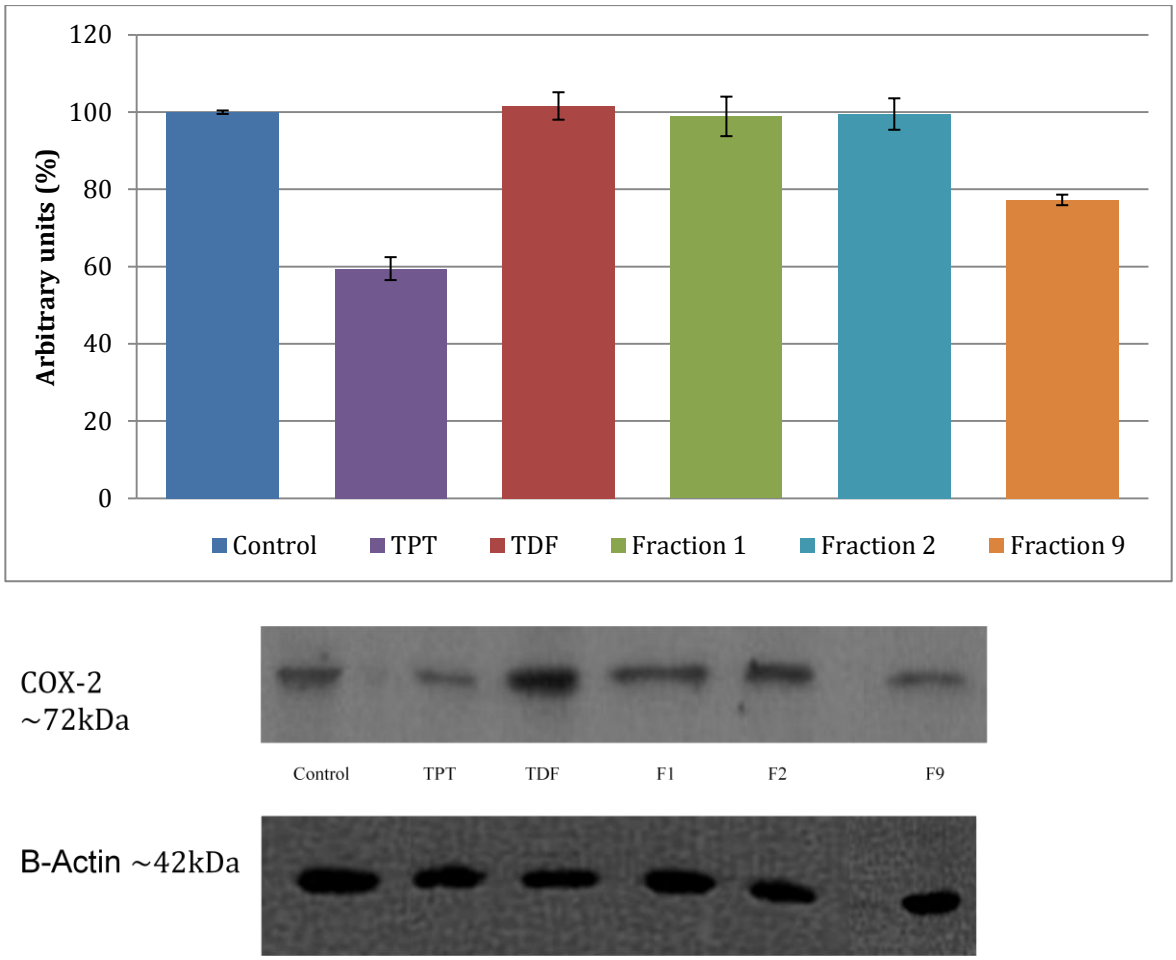

Figure 8-8 Analysis of COX-2 protein expression by Western blot. Full thickness porcine skin was treated with topical TPT 1mg mL^{-1}, TDF 1mg mL^{-1}, Fraction 1 1mg mL^{-1}, Fraction 2 1 mg $mL^{-1}$and Fraction 9 1 mg mL^{-1} and phthalate buffer as a control for 6 h. Protein was extracted and 30 µg was loaded and separated through SDS-PAGE. The histogram represents numerical data of COX-2 normalised against β-actin. Levels in the control were arbitrarily assigned a value of 100%. (n=3 ± SD)

COX-2 expression was only modulated after the application of TPT and fraction 9 with a decrease of 40.5 ± 4.6% and 22.7 ± 1.4% respectively (p<0.05). The application of the TDF and fractions 1 and 2 did not significantly alter the level of COX-2 within the samples in comparison to the control (p>0.05). These results are similar to those stated by Adams *et al* (2006), who showed COX-2 reduction of 55% and 48% after incubation of HT-29 Human colon cancer cells with TPT and punicalagin. The reduction in COX-2 expression is greatest when PRE remained as a whole extract, with TPT and punicalagin exhibiting anti-inflammatory activity,

although to a lesser extent - this is again similar to the findings by Adams *et al* (2006).

8.5. **Conclusion**

None of the fractions analysed exhibited toxic effects on Vero cells at 0.1mg mL^{-1}. The HSV-1 virucidal activity was due to the polyphenolic content within PRE, and can be attributed to punicalagin, as the presence of punicalagin is directly associated with virucidal activity. The antiviral activity of PRE can be attributed to the phenolic content as antiviral activity was observed for the TPT fraction but not for TDF. However, the antiviral activity of PRE is much greater than that of TPT and none of the TPT fractions exhibited any antiviral activity at concentrations less than 100 µg mL^{-1}.

Modulation of the inflammatory marker COX-2 showed that the downregulation of COX-2 by PRE was due to the tannins present within PRE, and a portion of this activity can be attributed to punicalagin. In agreement with the findings of Adams *et al* (2006) the downregulation of COX-2 is greatest when PRE remains as a whole entity with a reduction in downregulation due to fractionation.

Overall, biological activity was undoubtedly compromised or lost as a result of fractionation. This data supports the notion that separation of individual constituents from the PRE extract may decrease overall activity due to unanticipated and unidentified interplay between components.

Chapter 9 **Formulation and Characterisation of a Prototype Hydrogel Product Containing PRE and Zinc Sulphate**

9.1. **Introduction**

Chapter 6 demonstrated that a simple solution of PRE and $ZnSO_4$ enabled the penetration of both punicalagin and Zn^{2+} across freshly excised skin at levels that fulfilled 2 major criteria in the development of a medicinal product:

1. to give high antiviral and virucidal activity against HSV;
2. to confer an anti-inflammatory effect.

In order to facilitate the development of a viable product to treat HSV-induced lesions, PRE and $ZnSO_4$ must be formulated into a form appropriate for topical delivery. A number of different dosage forms are commercially available for treating lesions, for example: the well established Zovirax (Aciclovir) and its generics, are creams; Cymex (Urea, cetrimide) is a cream; Dynamiclear is a liquid containing plant extracts; and Compeed Cold Sore Patch is a hydrocolloid adhesive disc. Creams are generally well accepted, but may leave an unsightly white residue; liquid formulations lack the viscosity that is often needed to retain the actives at the site of application. Although transparent, a hydrocolloid patch applied to a curved moist surface can cause adhesion problems, and users will be conscious of the attachment of a device.

Figure 9-1 Four commercial products currently available for treating cold sores.

In this project it was considered desirable to concentrate on the development of a hydrogel formulation. Not only would this make any product dissimilar to current products, but there are sound reasons based upon biocompatibility (Hoffman 2001)(Li, et al. 2011) that would make preferable a PRE and $ZnSO_4$ formulation within a hydrogel matrix. Hydrogels are colourless and commonly used throughout the pharmaceutical industry for application of drugs and products to various membranes, including epidermal, vaginal, anogenital, oral and ophthalmic (Gulsen and Chauhan 2004); they are also digestible and used readily in the food industry (Guo, Zhank and Yang 2012). No complications would be expected to arise from the use of the hydrogel to treat herpetic lesions within the oral cavity. For comparison purposes, two emulsion formulations were also examined in this work.

Formulation science is a very broad area of research (Osborne and Amann 1990) and a comprehensive study was beyond the scope of this thesis. However, in this chapter we investigated some commonly used excipients to derive a simple prototype formulation, suitable for further study. In the design of a topically-applied formulation the ability to deliver both zinc and punicalagin within the enhanced virucidal ratio (Chapter 3) is of key importance. Furthermore, the formulation must also be stable and of appropriate rheological properties. Other important considerations include aesthetical and tactile acceptability. The formulation should therefore be of a neutral colour, have a smooth feeling whilst being applied to the skin, and should leave minimal residue after application. Given these parameters it was considered that a hydrogel was the most appropriate type of formulation.

9.1.1. Formulations

9.1.1.1. Colloidal Hydrogels

Hydrogels are a type of colloid, where one substance is microscopically dispersed evenly throughout another. A colloid system consists of two phases: an internal phase (the gel matrix) and the continuous phase (water). The use of cross-linked polymers as hydrogels for the topical delivery of drugs was hypothesised in the 1960s (Wichterle and Lim 1960). Hydrogels are generally defined as three-

dimensional polymeric networks containing a high proportion of water when the gel is in the swollen state (Rosiak, et al. 2002) (Hamidi, Azadi and Rafiei 2008). They are often classified into two groups based upon bonding: reversible gels consist of networks that have transient junctions consisting of molecular entanglements, including ionic, H-bonding or hydrophobic forces; permanent gels form covalently cross-linked networks with permanent junctions (Murray and Snowden 1995) (Hoffman 2001).

Hydrogels have many non-biological uses within agriculture and the oil industry. The biological compatibility of hydrogels used in medical and pharmaceutical research and commercial application has satisfied the properties needed in soft contact lenses, wound dressings and drug-delivery systems. Gels can present several advantages over other vaginal drug delivery systems, as in anogenital herpes infections, such as higher bioavailability, safety, versatility, and economic savings (Justin-Temu, et al. 2004).

9.1.2. Emulsions

Emulsions are mixtures of two or more immiscible liquids; for the purpose of this research only simple oil in water (O/W) systems were investigated, however more complex O/W/O, W/O/W and gel emulsions exist. Emulsions have a long history as topical drug delivery vehicles, however, they tend to leave an oily residue after application and do not have the same range of oral and vaginal application which hydrogels possess.

9.1.2.1. Formulation Considerations

While good biocompatibility is a justification for a hydrogel formulation it is important to note, however, that there are several hydrogel polymers which cannot form a colloid gel in the presence of zinc salts. For example, carrageenan a typical hydrogel internal phase is unsuitable for the topical delivery of $ZnSO_4$ (Zn^{2+} ions), because this material naturally binds with Zn^{2+}, the ion establishing a cross-link between the carrageenan polymer chains (Brown and Setloff 1982). Zinc concentration will have a specific effect on the rheology of the gel, since the concentration of Zn^{2+} is proportional to the viscosity of carrageenan in solution

(Keegan, et al. 2007). The formulation of a hydrogel as the carrier for the topical application of PRE and zinc was preferred; however the investigation also assessed a selection of possible emulsion formulations.

Once a prototype formulation had been identified, it was important to characterize it and, in topical products, this typically involves four major considerations:

1. Aesthetic properties.
2. Spontaneous diffusional active release.
3. Rheological properties.
4. Stability.

9.1.3. Aesthetic Properties

The aesthetic properties of a pharmaceutical product are of vital importance in formulation science. Typical properties include an assessment of:

- Appearance – homogeneity, colour, lustre, clarity
- Feel – smoothness, grittiness, lumpiness, oiliness
- Smell – odour, strength of odour, use of odourants/deodourants

Failure in any one of the above may be sufficient to deter a patient from purchasing or using the product (Chadwar and Shaji 2007). Appearance can be determined from examination by eye, or spectrophotometrically. The feel of a formulation can be assessed (e.g. for lumpiness or grittiness) by rubbing between thumb and fingers, although a more scientific approach would involve instruments such as a texture analyser. The smell or taste of a product may appear simple to determine, although an expert panel may be required to discern subtle differences (Buhler 2001).

9.1.4. Rheological Properties

Rheology can be used to study the flow characteristics of topical formulations. Drug delivery from formulations is determined in part by its viscosity and ability to bind to drug molecules (Gallagher and Heard 2005) . The viscosity of a fluid may be described simply as its resistance to flow or movement. Semisolid, eg. gel, formulations can be difficult to characterize and compare rheologically, as they tend

to demonstrate non-Newtonian flow. Figure 6.2 shows typical rheograms or flow curves produced by materials that exhibit Newtonian, and non-Newtonian behaviour.

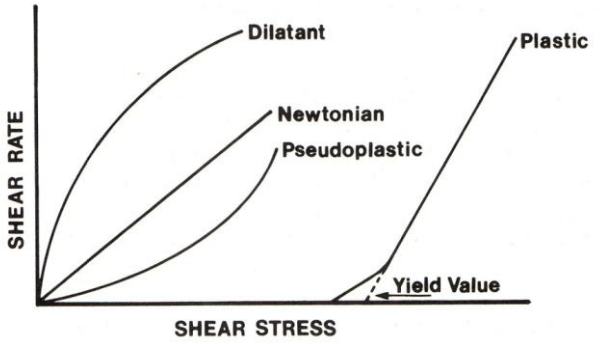

Figure 9-2 Flow curves illustrating typical Newtonian, plastic, pseudoplastic and dilatant flow (Barry 1983).

9.1.4.1. Newtonian Flow

A Newtonian material is one where the relationship between shear rate (γ) and shear stress (σ) is linear, and where the gradient is the viscosity (η). Simple liquids such as water and propylene glycol exhibit Newtonian flow.

9.1.4.2. Non-Newtonian Flow

Non-Newtonian flow can be of several different categories:

Plastic (Bingham flow)

The material flows readily, provided that shear stress is high enough, although below a critical value - the yield stress (σy) - the material will not flow. At lower stresses the substance behaves as a solid or elastic material. The rheogram plot is generally linear, but extrapolation of the linear portion intersects the shear stress axis at the yield value instead of passing through zero.

Pseudoplastic Flow (shear thinning)

The rheogram for a pseudoplastic material begins at the origin and has no yield value, unlike the case with plastic materials. When a shear stress is applied to the material the gradient of the curve gradually decreases with an increasing rate of shear, with no single characteristic value of viscosity observed. Typically, apparent

viscosity data are quoted, in conjunction with the specific shear rate at which the determination was made. Dermatological preparations that typically exhibit pseudoplastic behaviour include natural and synthetic gums.

Dilatant Flow (shear-thickening)

Materials exhibiting dilatant flow properties, produce flow curves opposite to pseudoplastic flow, thus as the rate of shear increases the resistance to flow also increases. There is a corresponding increase in viscosity with increased rate of shear. Suspensions that contain greater than 50% v/v of deflocculated particles typically exhibit dilatant flow, however this type of behaviour is less common than pseudoplastic and plastic flow.

Time Dependent Effects – Continuous Shear

Once the shear stress has been removed, the material may not return to its original rheological ground state instantly. A common feature of these materials, in response to increased shear rate followed by decreased shear rate to zero, is the formation of a hysteresis loop consisting of an up-curve and a down-curve see Figure 9-3. The hysteresis loop is an indication that a breakdown in the structure has occurred, with the area of the loop generally indicative of the extent of this breakdown. This effect is an isothermal and comparatively slow recovery, on standing of a material, of a consistency lost through shearing. Such thixotropy is temperature dependent and can be exhibited by plastic, pseudoplastic and dilatant materials.

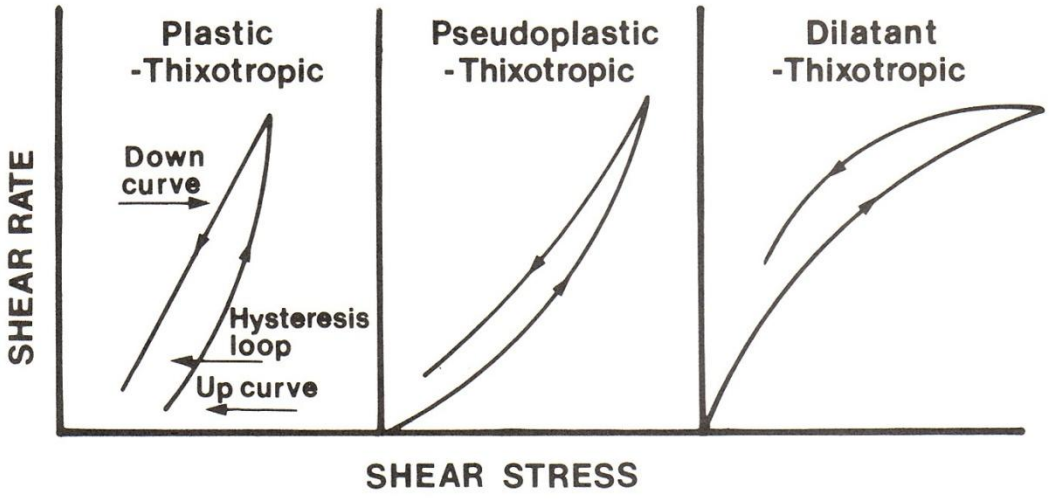

Figure 9-3 Hysteresis loops and different types of thixotropic behaviour (Barnes, Hutton and Walters 1989).

9.1.5. Cone and Plate Rheometer

Rheological measurement of materials generally falls into four main categories: Capillary, Rolling or Falling Sphere, Coaxial and Cone & Plate. The work in this chapter involved using a Bohlin Cone and Plate Rheometer, which operates by shearing the test material between a small angled **cone** and a flat circular **plate** (*Figure 9-4*). Provided the angle is small (< 4 degrees) the shear rate is essentially uniform throughout the sample.

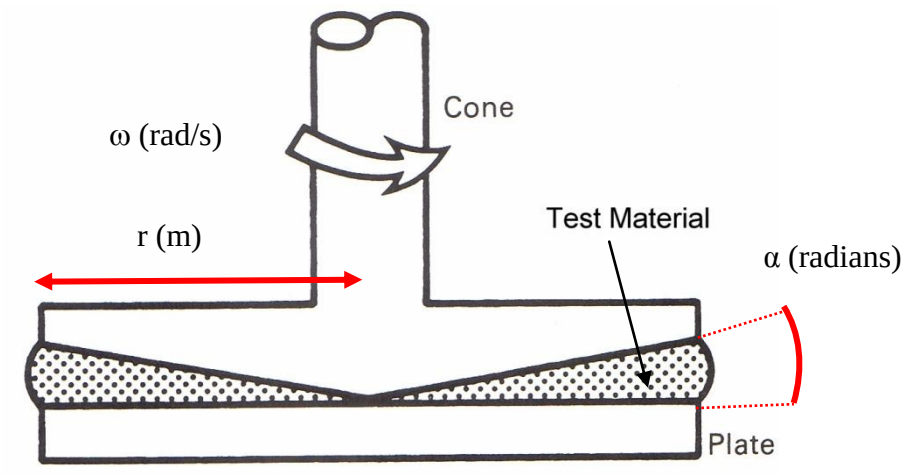

Figure 9-4 Cone and Plate Rheometer (Staniforth 2002).

Where ω is the angular velocity of the plate, r is the radius of the cone and α is the angle between the cone and plate.

A sample of the test material is placed onto the centre of the temperature controlled plate and the cone is lowered so the tip just touches the plate. Typically, the lower plate remains stationary and the upper cone is rotated at a constant speed, with a torque sensor measuring the developed shear stress. Alternatively the cone can be rotated at a constant stress with the shear rate being measured.

Provided the angle is small, viscosity is calculated by:

$$\eta = 3\,\omega T / 2\pi r^3 \alpha \qquad \textbf{(Units of Pa s)} \qquad \textbf{Equation 5.1}$$

where ω is the angular velocity of the plate, T is the torque, r is the radius of the cone and α is the angle between the cone and plate (Barnes, Hutton and Walters 1989) (Figure 5.3).

The shear rate is calculated by:

$$\gamma = \omega/\alpha \qquad \textbf{(Units of } 1s^{-1}\textbf{)} \textbf{ Equation 5.2}$$

And shear stress calculated by:

$$\alpha = 3\,M / 2\,\pi\, r^3 \qquad \textbf{(Units of Pa)} \quad \textbf{Equation 5.3}$$

Where M = Spindle torque.

9.1.6. Spontaneous Diffusional Release

Spontaneous diffusional release can be defined as the tendency of a molecule to dissociate from the bulk of the other excipients within the applied formulation (Wu and Zhou 1999). However, whether release is independent of the solvent is unclear (Aggarwal 2009). It is governed by affinity of attraction for other compounds, for

example Cabosil M5 has been shown to retard release due to binding events between a drug and the silica particles (Gallagher and Heard 2005). The most common way to determine release is to apply the formulation to a minimal resistance barrier membrane mounted in a Franz diffusion cell (Jeans and Heard 1999)(Kros, et al. 2001). The active or active/solvent complex spontaneously exits the formulation passing through the minimal resistance membrane to arrive in the receptor phase, which is then analysed. The information gained can be considered as the maximal amount of active that can be delivered from a given formulation. It is thus highly important that the release membrane used offers minimal resistance to diffusion.

9.1.7. Stability

Stability determinations are an indispensable element in the pre-clinical evaluation of a product. Before a drug product is submitted for regulatory approval, ICH stability testing helps demonstrate it will continue to be safe and efficacious for its stated shelf life. Real-time ICH stability testing is conducted at room temperatures to reproduce actual storage conditions. Launched in 1990, ICH is a unique undertaking that brings together the drug regulatory authorities and the pharmaceutical industry of Europe, Japan and the United States. Harmonisation is achieved through the development of ICH Tripartite Guidelines. Document Q1A (R2) Stability Testing of New Drug Substances and Products (Food and Drug Administration 2009) sets out requirements including temperature, humidity and trial duration.

Over a pre-determined time frame simple laboratory determination can indicate whether: 1. The levels of active remain essentially unchanged and 2. Whether the pharmacological or microbiological activity remains essentially unchanged.

9.1.8. Objective and Aims

To identify and characterise a simple prototype formulation, suitable for further study.

1. Evaluate a range of commonly used excipients in order to derive a suitable prototype

2. Characterise the prototype gel in terms of spontaneous diffusional release

3. Characterise the prototype gel in terms of its macroscopic properties

4. Characterise the prototype gel in terms of its rheological properties

5. Determine the chemical and microbiological stability of the prototype formulation

9.2. **Materials and Methods**

9.2.1. Materials

The materials used within this chapter are listed in Chapter 2 section 2.1.

9.2.2. Formulation of PRE and $ZnSO_4$ Solutions.

The formulation of PRE and $ZnSO_4$ solutions follows the methods described in Chapter 2. The stock solutions of 2 M $ZnSO_4$ and PRE 2 mg mL^{-1} were diluted in DI H_2O to the concentrations required.

9.2.2.1. Emulsion 1

Oleaginous phase and aqueous phases shown in Table 9-1 were heated to 65°C separately in a water bath. Once dissolved, the oleaginous phase was slowly added to the aqueous phase with constant agitation. When the formulation reached 50°C it was homogenised using the homogeniser RW 20 DZM (IKA Works, Asia) for 60s and cooled with continuous stirring until the emulsion turns viscous and reaches room temperature. The emulsion is then cooled to 4°C and stored occluded from light until further use (maximum 24 h).

An example preparation of Emulsion 1 with the final concentration of PRE 5 mg mL^{-1} and $ZnSO_4$ 0.5 M follows the procedure described above. PRE 500 mg and $ZnSO_4$ 28.75 g were diluted in 100 mL of DI H_2O before the addition of the other aqueous phase constituents. The aqueous phase including PRE and $ZnSO_4$ was heated to 65°C, after which the addition of the oleaginous phase was slowly added with constant agitation.

Oleaginous phase	Percentage composition
Stearic acid	13
Stearyl alcohol	1
Cetyl alcohol	1
Aqueous phase	
Glycerine	10
Methylparaben	0.1
Propylparaben	0.05
Potassium hydroxide	0.9
DI H2O	100

Table 9-1 The formulation concentration for Emulsion 1.

9.2.2.2. Emulsion 2

The formulation of Emulsion 2 followed that described in Brown and Setloff (1982) a topical emulsion containing zinc. Lauric acid 11 mg, paraffin wax 3.0 mg, polyethylene glycol (100) stearate 6 mg, polyethylene glycol sorbitan beeswax 4mg was heated to 65°C. Separately water 77 ml was also heated to 65°C. The aqueous phase was slowly added to the oleaginous phase with constant agitation until a thick emulsion was formed. This was left to cool over night to 4°C. $ZnSO_4$ 0.01M and PRE 0.1 mg ml^{-1} were added to the aqueous phase before heating.

9.2.2.3. Preparation of Aqueous Polymer Dispersions and PRE, Zinc Ion Solutions

9.2.2.4.

Hydrogel 1: Carbopol 971 P (C971P)

-Carbopol 971 PNF stock solution

The method used for the preparation of Hydrogel 1 was: 1g of carbopol 971 P was dispersed in 50 ml DI H_2O under magnetic stirring for 4 h. The pH of the solution was adjusted by addition of 0.1M sodium hydroxide or 0.1M HCl and this was then cooled overnight to 4°C.

-Zinc Carbopol 971 PNF

10ml of $ZnSO_4$ solution were slowly added to 10 ml of the C971P stock solution with constant magnetic stirring and continuously stirred for 4 h. This was then cooled to 4°C overnight.

-PRE Carbopol 971PNF.

10ml of PRE solution were added slowly to 10 ml of the C971P stock solution with constant magnetic stirring and continuously stirred for 4 h. This was then cooled to 4°C overnight.

-PRE and Zinc Carbopol 971 P.

10ml of PRE and zinc solution were added slowly to 10 ml of the C971P stock solution with constant magnetic stirring and continuously stirred for 4 h. This was then cooled to 4°C overnight.

-Hydrogel 2: Carbopol 942 P (C942P)

-Carbopol 942 P stock solution

1g of Carbopol was dispersed in 50 ml DI H_2O under magnetic stirring at 350 *g* for 4 h. The pH of the solution was adjusted by addition of 0.1M sodium hydroxide or 0.1M HCl: this was then cooled overnight to 4°C.

-Zinc Carbopol 942 P complexes

10ml of known concentration (0 M, 0.01 M, 0.1 M and 1 M) $ZnSO_4$ phthalate buffer solution was slowly added to 10 ml of the C971P stock solutions with constant magnetic stirring and continuously stirred for 4h: this was then cooled to 4°C overnight.

-Hydrogel 3: Hydroxymethyl cellulose

-Zinc hydroxyl methyl cellulose

Using the cold method described in Chapter 2 section 2.2.7. Hydroxymethyl cellulose (5g) was added to 100 ml of known concentration $ZnSO_4$ solution (0, 0.01, 0.1 and 1M) with constant stirring at 300 *g* for 50 min, pH adjusted via addition of NaOH: this was then cooled to 4°C overnight.

-Hydrogel 4: Cab-o-sil M5

Cab-o-sil M5 10 g was added to a known concentration of $ZnSO_4$ solution (0, 0.01, 0.1 and 1M) with constant agitation, pH adjusted by the addition of NaOH: and cooled to 4°C overnight.

-Hydrogel 5: Pluronic F 127

A control formulation used the cold method following a revised version of that stated in Valenta and Schultz (2004). 20 mg of PF127 was slowly added to 100ml of a known concentration $ZnSO_4$ solution (0, 0.01, 0.1 and 1M) at 5–10°C with gentle mixing until complete dissolution of the polymer, then stored overnight at 4°C .

-Hydrogel 6: Methocel 856 N Hydroxypropyl Methylcellulose

Using the hot/cold method stated in Chapter 2 section 2.2.7. 2.5g Methocel 856N was added to 40 mL DI H_2O at 80 °C with constant stirring until all particles are thoroughly wetted. 60 mL cold or iced DI H_2O was then added to the solution with constant agitation for 30 min. This enables the hydration of the powder and the increase in the hydrogels viscosity. The resulting hydrogel was cooled to 4°C. The addition of PRE 0.01 and a series of $ZnSO_4$ concentrations 0.01, 0.1, 1, 10 g mL^{-1} and $ZnSO_4$ 0.01, 0.1 and 1 M and their combinations were added to 60 ml of cold or iced DI H_2O.

9.2.3. Aesthetic properties

The aesthetic tests outlined in Chapter 2 section 2.2.7.1 (aesthetic tests) were conducted on the formulations following the methodology for appearance, odour and tactile properties.

9.2.4. Rheology

Rheological properties were examined according to the methodology stated in Chapter 2 section 2.2.4.6 out on a Bohlin CS10 Rheometer (Figure 9-5), which uses the 'cone and plate' technique where a metal cone spins above a plate covered with test material. The hydrogels analysed via this method are shown in the table below

Named Formulation	Methocel 856N (w/w)	PRE (mg ml^{-1})	$ZnSO_4$ (M)
Un-named	1%	0	0
	2%	0	0
	2.5%	0	0
	2.5%	0	0.1
	2.5%	0	0.125
	2.5%	0	0.2
	2.5%	0	0.25
	2.5%	1.25	0
	2.5%	50	0
Hydrogel A	2.5%	0.05	0.01
Hydrogel B	2.5%	0.1	0.02
Hydrogel C	2.5%	0.5	0.1
Hydrogel D	2.5%	1	0.2
Hydrogel E	2.5%	1.25	0.25
Hydrogel F	2.5%	0	0

Table 9-2 The formulation of hydrogels used for rheological analysis.

Figure 9-5 Bohlin CS10 Rheometer used in this study.

9.2.5. Spontaneous Diffusional Release

The methodology used to examine the spontaneous diffusional release follows that stated in Chapter 2 section 2.2.3.2.

9.2.6. Stability

The stability of PRE and $ZnSO_4$ within the Methocel 856 N hydrogel matrix was analysed by the spontaneous release of punicalagin and Zn^{2+} from Hydrogel 6 C and Hydrogel 6 E through CTEM following the methodology stated in Chapter 2 section 2.2.3.3. after 0, 3, 6, and 12 months of storage at room temperature with occlusion from light and air.

9.3. **Results**

9.3.1. PRE and $ZnSO_4$ formulations

9.3.1.1. Emulsion 1 and 2

PRE 5 mg mL^{-1} and $ZnSO_4$ 0.5 M resulted in similar thick emulsions in comparison to the control, however the emulsion was orange in colour. The emulsion had a smooth texture and left no residue after application. This is in contrast to emulsion 2,

which formed a thick white emulsion as a control and on the addition of $ZnSO_4$; however the addition of PRE even at all concentrations resulted in separation of the phases, with no emulsion forming.

9.3.1.2. Hydrogel 1; Carbopol C971P

C971P formed a thick clear hydrogel with the addition of $ZnSO_4$ this is in accordance with Justin-Temu *et al.* (2004) following their assessment of a C971PNF $ZnSO_4$ hydrogel. However on the addition of PRE (± $ZnSO_4$) to the C971PNF it is appears that a reaction between one or two components of PRE and the C971PNF occurred, causing the separation of the gel and liquid forming a very thick hydrophobic substance.

Formulation	Zinc Concentration (M)	PRE concentration (mg mL^{-1})	Appearance
Hydrogel 1 C971PNF	0	0	Thick gel
	0.01	0	Thick gel
	0.1	0	Thick gel
	1	0	Thick gel
	0	0.1	Separation of gel/liquid
	0	1	Separation of gel/liquid
	0	10	Separation of gel/liquid
	0.01	0.05	Separation of gel/liquid

Table 9-3 The formulation and analysis (visual, macroscopic) of a Carbopol 971 Hydrogel 1 containing $ZnSO_4$ and PRE.

9.3.1.3. Hydrogel 2; C942P

The addition of C942P to DI H_2O produced a thick gel at the pH range formulated. On addition of $ZnSO_4$ solutions a similar gel was formed, however if the formulation exceeded a pH of 3.5 then the C942P precipitated out of solution.

Formulation	Zinc Concentration (M)	pH	Appearance
Hydrogel 2 C942P	0	2	Thick gel
		3.5	Thick gel
		5.5	Thick gel
	0.01	2	Thick gel
		3.5	Thick gel
		5.5	No gel
	0.1	2	Thick gel
		3.5	Thick gel
		5.5	No gel
	1	2	Thick gel
		3.5	Thick gel
		5.5	No gel

Table 9-4 The formulation and analysis (visual, macroscopic) of a Carbopol 942 Hydrogel 2 containing $ZnSO_4$.

9.3.1.4. Hydrogel 3; hydroxymethyl cellulose

The appearance of Hydrogel 3 containing 5% (w/v) methylcellulose is detailed in Table 9-5. The formation of thick clear gel was attained with the addition of

hydroxymethyl cellulose to DI H_2O however, upon the addition of $ZnSO_4$ the formation of a white precipitate and clear liquid solution was observed.

Formulation	Zinc Concentration (M)	Appearance
Hydrogel 3	0	Thick gel
	0.01	White ppt , clear liquid
	0.1	White ppt , clear liquid
	1	White ppt , clear liquid

Table 9-5 The formulation and analysis (visual, macroscopic) of a hydroxymethyl cellulose Hydrogel 3 containing zinc.

9.3.1.5. Hydrogel 4 Cab-o-sil M5

Table 9-6 describes the visual and macroscopic analysis of hydrogel 4 containing 10% (w/v) Cab-o-sil M5. A thick non-translucent white gel was formed on the formulation of Cab-o-sil M5 alone and with the addition of $ZnSO_4$, however the addition of $ZnSO_4$ gel left a white powder residue after application and after macroscopic evaluation had an unwanted grainy tactile property.

Formulation	Zinc Concentration (M)	Appearance
Hydrogel 4 Cab-o-sil M5	0	Thick gel
	0.01	Thick gel
	0.1	Thick gel
	1	Thick gel

Table 9-6 the formulation and analysis (visual, macroscopic) of a Carbosil M5 Hydrogel 4 containing zinc

9.3.1.6. Hydrogel 5: Pluronic F127

The visual and macroscopic properties of hydrogel 5 containing 20% (w/v) Pluronic F127 is shown in table 9-7. As stated previously (Valenta and Schultz 2004), pluronic F127 formed a thick clear hydrogel; on the addition of $ZnSO_4$ a hydrophobic film formed on top of a clear liquid which contained a thick white precipitate.

Formulation	Zinc Concentration (M)	Appearance
Hydrogel 5 Pluronic F127	0	Thick gel
	0.01	Thick gel
	0.1	Thick gel
	1	Thick gel

Table 9-7 The formulation and analysis (visual, macroscopic) of a Pluronic F127 Hydrogel 5 containing zinc.

9.3.1.7. Methocel 856N

2.5% w/w Methocel 856N formed a thick, clear hydrogel on the addition of $ZnSO_4$ up to the concentration of 0.1 M. As the $ZnSO_4$ concentration increased, the gel became thinner until the concentration exceeded 0.3M whereupon the gel phase separated forming a clear liquid and solid hydrophobic film. There was no observed difference to the control gel on the addition of PRE >50 mg ml^{-1} apart from a slight discoloration of the gel. A Methocel 856N hydrogel was formulated containing 1.25 mg ml^{-1} PRE and 0.25M $ZnSO_4$, the gel was translucent with a slight orange tinge. The gel felt smooth and left no residue after application.

Formulation	Zinc Concentration (M)	PRE concentration (mg mL^{-1})	Appearance
Hydrogel 6 Methocel 856N	0	0	Thick gel
	0.01	0	Thick gel
	0.1	0	Thick gel
	0.3	0	Thin gel
	1	0	Separation of gel liquid
	0	0.1	Thick gel
	0	1	Thick gel
	0	10	Thick gel
	0.01	0.05	Thick gel
	0.25	1.25	Thick gel

Table 9-8 The formulation and analysis (visual, macroscopic) of a Methocel 865N Hydrogel 6 containing $ZnSO_4$ and PRE.

The overriding factors of emulsion and hydrogel formulation appear to be the interaction between polymers and zinc ions or compounds within PRE. Of the two emulsions tested, the addition of PRE and or zinc to emulsion formulation 1 appears to have no effect on the formation of a formulation that has acceptable aesthetics and tactility, however the addition of PRE to emulsion 2 separated the oil and water phases, rendering it useless - the reason for this is not known.

Methocel 856N was selected for further study.

9.3.2. Rheological properties of Methocel gels

Figure 9-6 shows shear rate vs shear stress profiles for aqueous Methocel 856N, at 1, 2 and 2.5% and demonstrates the significant effect of the level of Methocel 856N on the shear stress observed.

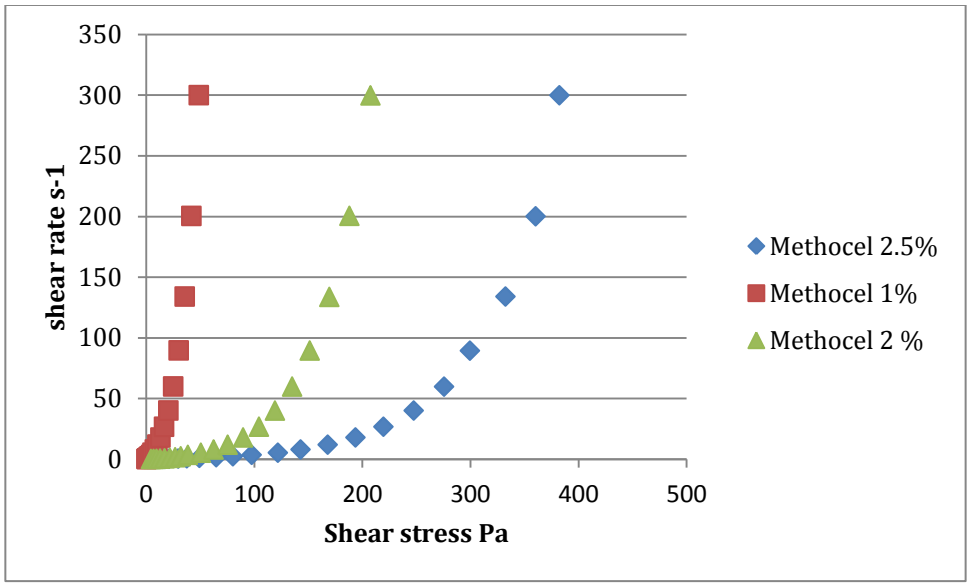

Figure 9-6 Shear stress vs shear rate of Methocel 856N at 1%, 2% and 2.5%

As the concentration progressed from 1% to 2% to 2.5% the relevant shear stress increased: at a shear rate of 300 s^{-1} the shear stress increased from 48.63 Pa to 207.5 Pa and 382.3 Pa respectively, ergo the higher the concentration of Methocel the greater the viscosity.

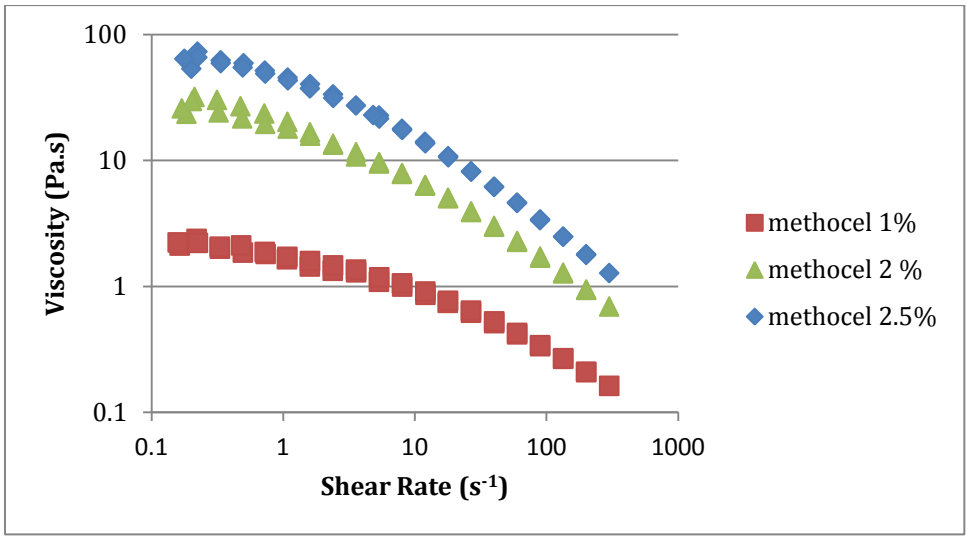

Figure 9-7 Shear rate vs viscosity of Methocel 856N at 1%, 2% and 2.5%.

Figure 9-7 shows the viscosity trend vs shear rate of the hydrogels in a steady state flow test. The plots concur with Figure 9-6 and demonstrate the increased viscosity with respect to concentration of Methocel 856N. The two curves (forward and reverse) overlap, meaning that the material morphology had not changed following the stress induced by the rheometer. This indicated the pseudoplastic nature of the hydrogels at all the concentrations analysed. Due to the acceptable macroscopic analysis of the hydrogel at 2.5% with the resulting level of viscosity stated above, this concentration was maintained for further analysis with the addition of PRE and $ZnSO_4$ alone, and in combination.

Figure 9-8 shows shear rate versus shear stress for the 2.5% Methocel gel with the addition of different amounts (0, 0.1, 0.125, 0.2 and 0.25 M) of zinc sulphate.

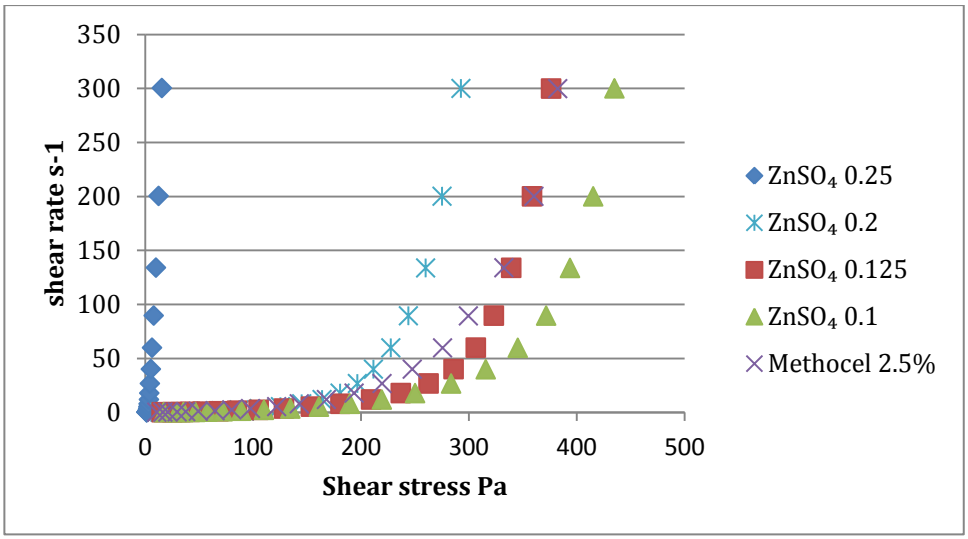

Figure 9-8 Shear rate vs shear stress for Methocel 2.5% following the addition of $ZnSO_4$.

The formulation containing 0.1 M $ZnSO_4$ slightly increased the shear stress observed for that of the blank gel from 382.3 Pa to 434.9 Pa at a shear rate of 300 s^{-1}, indicating a rise in the viscosity of the gel. However as the concentration of $ZnSO_4$ increased to 0.125 M and 0.2 M the shear stress decreased to 376.2 and 292.6 Pa. The shear stress was greatly altered when the hydrogel contained 0.25M $ZnSO_4$ resulting in a shear stress of 15.37 Pa at a shear rate of 300 s^{-1}.

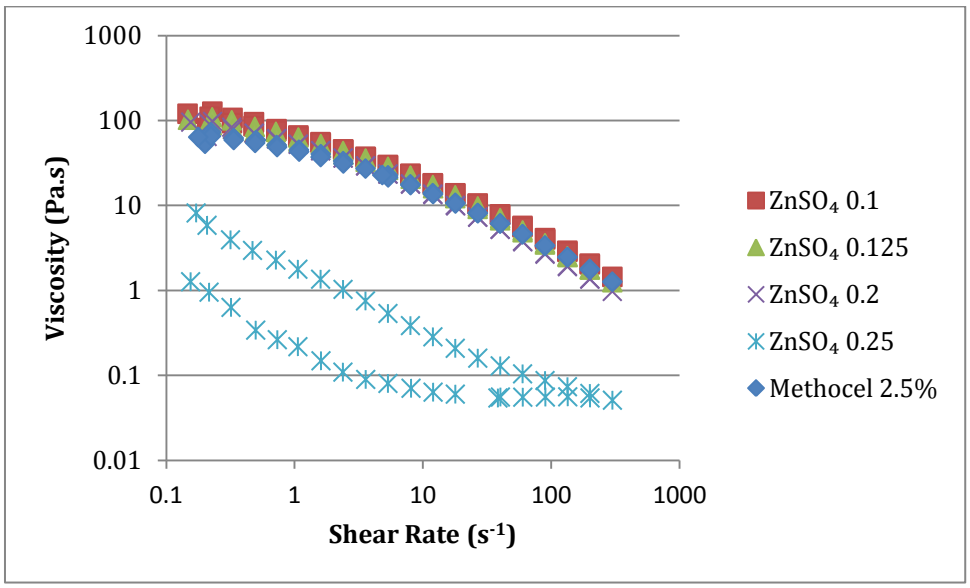

Figure 9-9 Viscosity vs shear rate of 2.5% Methocel 856N following the addition of $ZnSO_4$ at 0.1, 0.125, 0.2 and 0.25 M.

Figure 9-9 demonstrates that the viscosity of the Methocel 856N is similar on the addition of $ZnSO_4$ up to the concentration of 0.2 M at either the beginning or end of both the forward and backwards curves of the steady state flow test. The curves overlap for the blank hydrogel and for the formulations containing 0.1, 0.125, and 0.2 M $ZnSO_4$, showing that the pseudoplastic nature of the hydrogel is not altered. However at a concentration of 0.25 M $ZnSO_4$ the viscosity has decreased and the two curves (forward and backward) did not overlap, meaning that the material morphology had changed after the rheometer stress. The area within the two curves (the hysteresis loop) is representative of the energy loss required to obtain the solution gel transition. The presence of the hysteresis-loop demonstrates that the addition of 0.25 M $ZnSO_4$ changes the gel from pseudoplastic to thixotropic in nature.

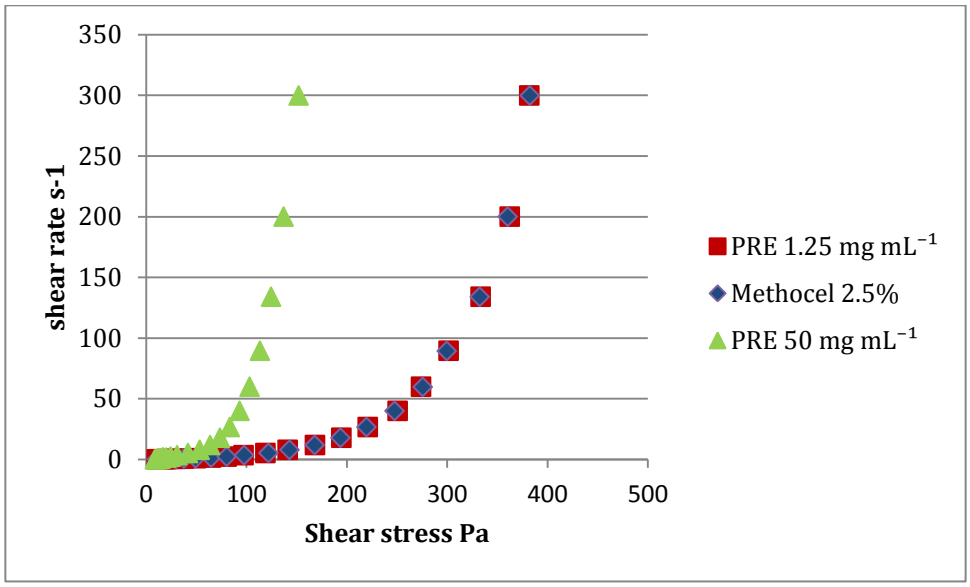

Figure 9-10 Shear rate vs shear stress of 2.5% Methocel 856N loaded with 0, 1.25 and 50 mg mL^{-1} PRE.

Figure 9-10 shows that the shear stress of the Methocel hydrogel was not significantly affected at any given shear rate. At a shear rate of 300 s^{-1} the control hydrogel had a shear stress of 382.3 Pa, the 1.25 mg mL^{-1} PRE loaded gel had a shear stress of 381.8 Pa. When the hydrogel was loaded with PRE 50 mg mL^{-1} the shear stress decreased to 151.9 Pa.

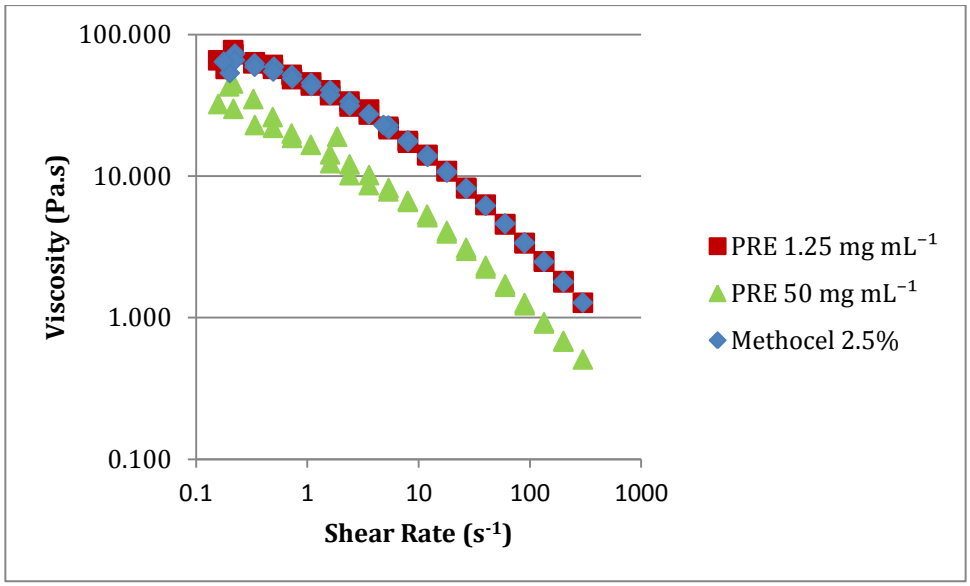

Figure 9-11Viscosity vs shear rate in the steady state flow test for 2.5% Methocel 856N loaded with 0, 1.25 and 50 mg mL^{-1} PRE.

The pseudoplastic nature of the hydrogel remained unaffected with the addition of PRE at 1.25 mg mL^{-1} or 50 mg mL^{-1} as shown by the overlapping forward and backward curves in Figure 9-11.

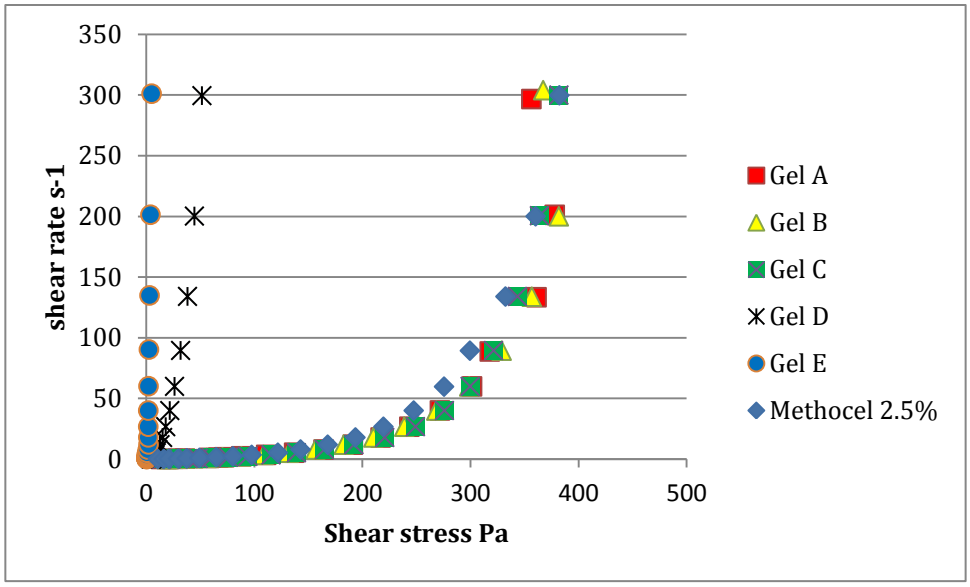

Figure 9-12 The change in shear stress with respect to shear rate on the addition of PRE + $ZnSO_4$ to Methocel 856N 2.5% Hydrogel 6 A-E (Table 9-2).

Figure 9-12 illustrates that the shear stress was unaffected upon addition of PRE and $ZnSO_4$ at the lower concentrations in Hydrogel 6 A, B and C with a shear stress ~370

Pa at a shear rate of 300 s^{-1}. However, on the addition of the more concentrated mixture the shear stress was greatly reduced to 51.54 Pa and 4.98 Pa for Hydrogel 6 D and E respectively.

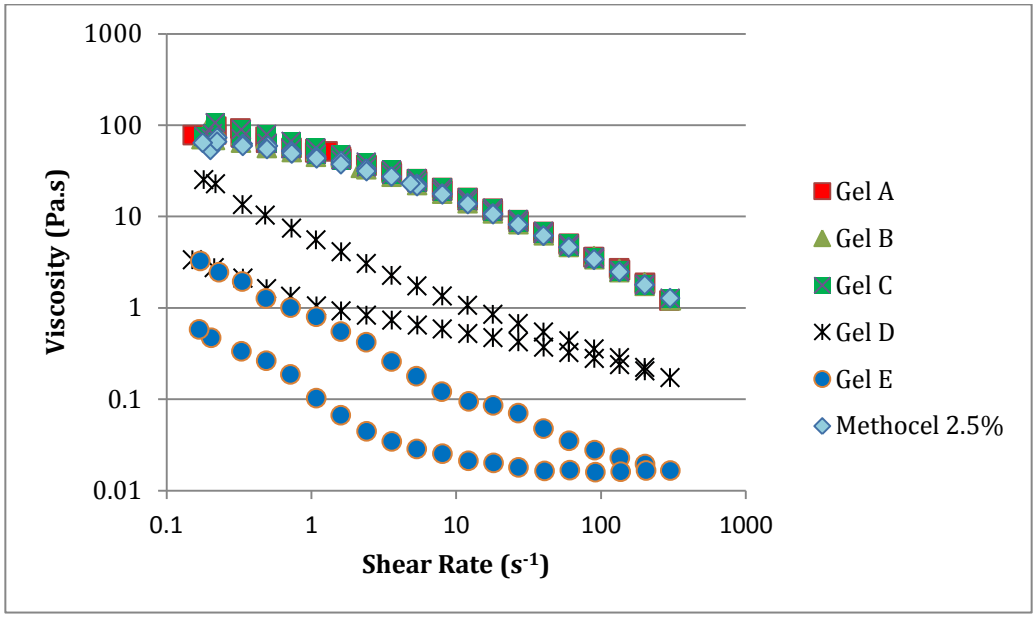

Figure 9-13 Viscosity vs shear rate in the steady state flow test for 2.5% Methocel 856N loaded with PRE and $ZnSO_4$. Hydrogel A-E (Table 9-2)

It is apparent from Figure 9-13 that low concentrations of PRE and $ZnSO_4$ loaded into the 2.5% Methocel did not alter the pseudoplastic nature of the matrix, as shown by the overlapping of the forward and reverse curve of Hydrogel 6 A, B, and C in comparison to the control gel. However, as the PRE and $ZnSO_4$ combination increased in concentration, the hydrogel became thixotropic, as shown by the prominent hysteresis loop for both Hydrogel 6 D and E. Also, the viscosity of both these gels was greatly reduced. The cause of the change of gel from pseudoplastic to thixotropic is unknown, it is expected that a greater release of constituents over a longer time after applied stress will be seen from the Hydrogel 6 D and E, however the stability of the gel and its matrix due to the change in nature could affect the chemical stability and/or the permeation of the analytes from the formulation.

9.3.3. Spontaneous Release of Punicalagin and Zinc

Figure 9-14 shows that after 30 min the spontaneous release of punicalagin from all the formulations was statistically similar ($p > 0.05$) at roughly 2 nM cm^{-2}. The highest

average mass of punicalagin permeation at 24 h was from Emulsion 1 and Hydrogel 6 E when compared with each other ($p > 0.05$). Emulsion 1 has a statistically greater release in comparison to Hydrogels A, B, C, D and E. However, Hydrogel E was not significantly different from Hydrogel D ($p > 0.05$) but was significantly different from Hydrogel C ($p < 0.05$). The spontaneous release data at 24 h was expected with a graduated rise in punicalagin release from hydrogels proportional to the concentration within the formula. Emulsion 1, containing 4 times the concentration of PRE in comparison to Hydrogel 6 E, did not, however, release a substantially greater amount of punicalagin.

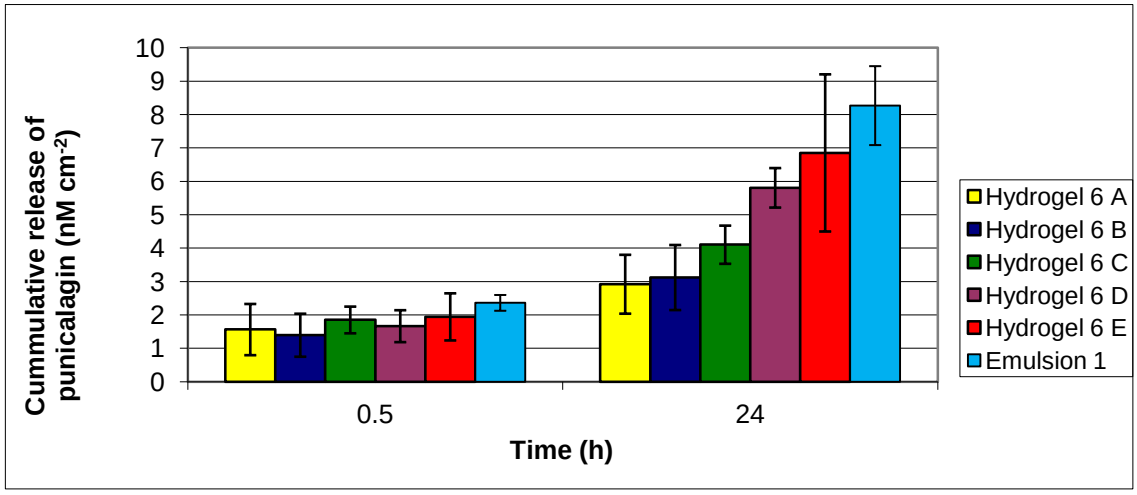

Figure 9-14 Spontaneous release of punicalagin from 6 test Hydrogels and Emulsion 1 at 0.5 and 24 h. (n = 3 ± SD)

Figure 9-15 graphically illustrates the analysis for the spontaneous release of zinc from the different formulations, which were analysed via ICP MS. To minimise analytical costs it was decided that the three samples at each time point of Hydrogel 6 C, 6 E, 6 F and Emulsion 1 would be pooled together and analysed. Figure 9-15 shows that the release of zinc from the formulations was greatest at both 0.5 and 24 h from Emulsion 1 releasing 2.04×10^{-5} M cm^{-2} and 4×10^{-5} M cm^{-2} (6×10^{-5} M cm^{-2} cumulative) respectively. After 0.5 h, Hydrogel 6 C released 1.4×10^{-5} M cm^{-2} and E released 1.24×10^{-5} M cm^{-2} - these are similar levels of zinc release; however due to the necessity for pooling of samples no statistical analysis could be undertaken. It is apparent that Hydrogel 6 E released greater concentrations of zinc after 24 h in

comparison to Hydrogel 6 C, this result is expected as the continued release offered by the thixotropic nature of Hydrogel 6 E and the increase in loading will result in longer and greater release time. However, it would be expected that a greater concentration was released after 0.5 h. The increased release from Emulsion 1 was expected due to the increase in loading. As expected no zinc was released from the control Hydrogel F.

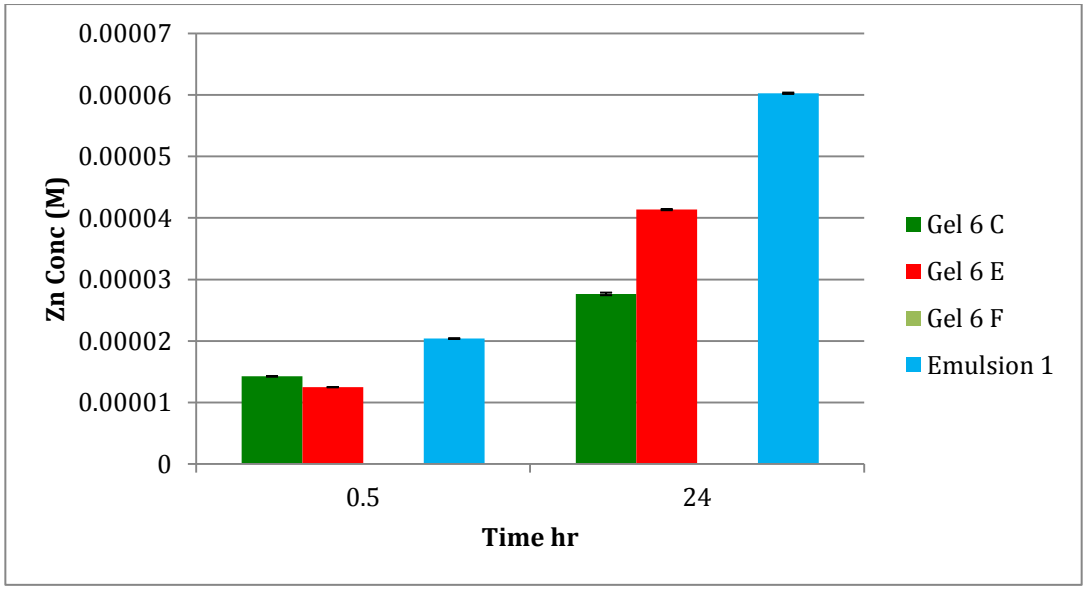

Figure 9-15 Spontaneous release of zinc from hydrogel 6 C, E and F and Emulsion 1 at 0, 0.5 and 24 h (n=3 ± SD).

The ratio required between punicalagin and Zn^{2+} to potentiate the virucidal activity of PRE and Zn^{2+} shown in Chapter 5 is that 1M punicalagin and between 50-10000M Zn^{2+} were released simultaneously – a very important feature in this type of formulation. As shown by the release data of Hydrogel 6 C, E and Emulsion 1 after 30 min ~ 2 x 10^{-9} M cm^{-2} of punicalagin was released and 1 x 10^{-5} M of Zn^{2+} was released, giving a ratio of 1:5000 which lies well within the required level for activity between Zn^{2+} and punicalagin; the release of punicalagin and zinc observed in Figures 9-14 and 9-15 show that the three formulations, Hydrogel 6 C, 6 E, and Emulsion 1 released zinc and punicalagin at concentrations that were within the synergistic virucidal ratio.

9.3.4. Stability of Prototype Methocel 846N Hydrogel

The stability data acquired for Hydrogel 6 C and 6 E was based upon the release of punicalagin and zinc from Methocel 846N hydrogel matrix at 0, 3 6 and 12 months through CTEM, and follows the methodology previously described (9.2.6.) and guidelines set out by the US Food and Drug Administration (Food and Drug Administration 2009).

Figures 9-16 and 9-17 show the punicalagin and zinc release data from Hydrogel 6 C at 0.5 and 24 h. At 0.5 and 24 h the release of the virucidally active agents, punicalagin and zinc, over the 12 month analysis period from the hydrogel matrix was not significantly different ($p > 0.05$) from that released upon the date of formulation. At 0.5 h the release of punicalagin was 1.95 ± 0.3 nM cm^{-2} and the release of Zn^{2+} was 1.37 x 10^{-5} ± 5.76 x 10^{-7} M cm^{-2}. The cumulative release of punicalagin after 24 h of application at time of formulation was 4.1 ± 0.5 nM cm^{-2}, and after a period of 3 months 4.3 ± 0.8 nM cm^{-2}, 6 months 4.45 ± 1.03 nM cm^{-2} and 12 months 4.62 ± 1.28 nM cm^{-2}, with an average release of 4.74 ± 0.92 nM cm^{-2}. It is important to note that at 24 h the release of punicalagin had a larger standard deviation, the reason for this is not entirely clear. The release of Zn^{2+} after 24 h over the 12 month period of stability analysis was 2.75 x 10^{-5} ± 5.01 x 10^{-7} M cm^{-2}.

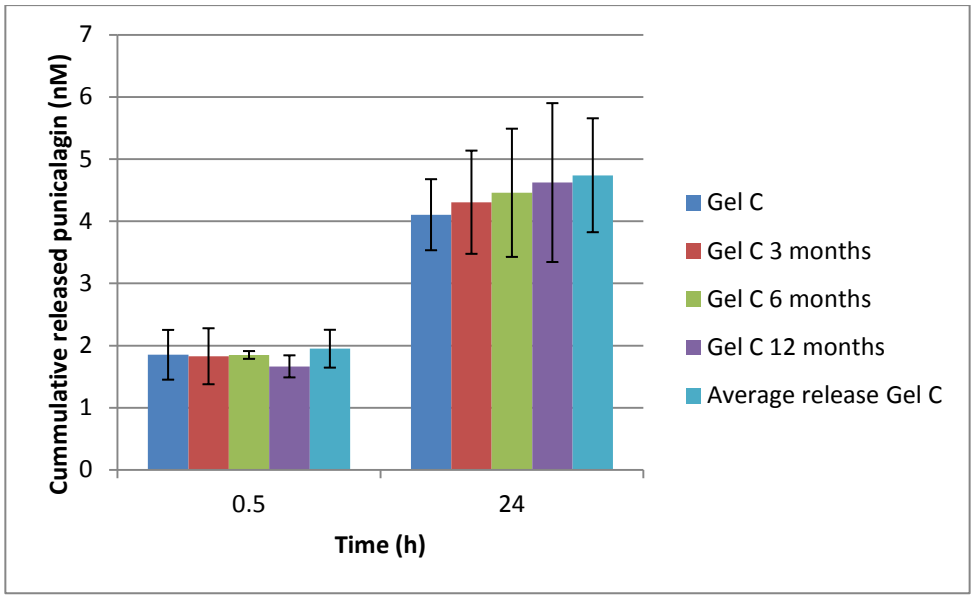

Figure 9-16 The spontaneous release of punicalagin from Hydrogel 6 C at 0.5 and 24 h after storage at room temperature and occlusion from light at 0, 3 6 and 12 months after formulation (n=3), and the average release over the 12 month time points (n=12 ± SD).

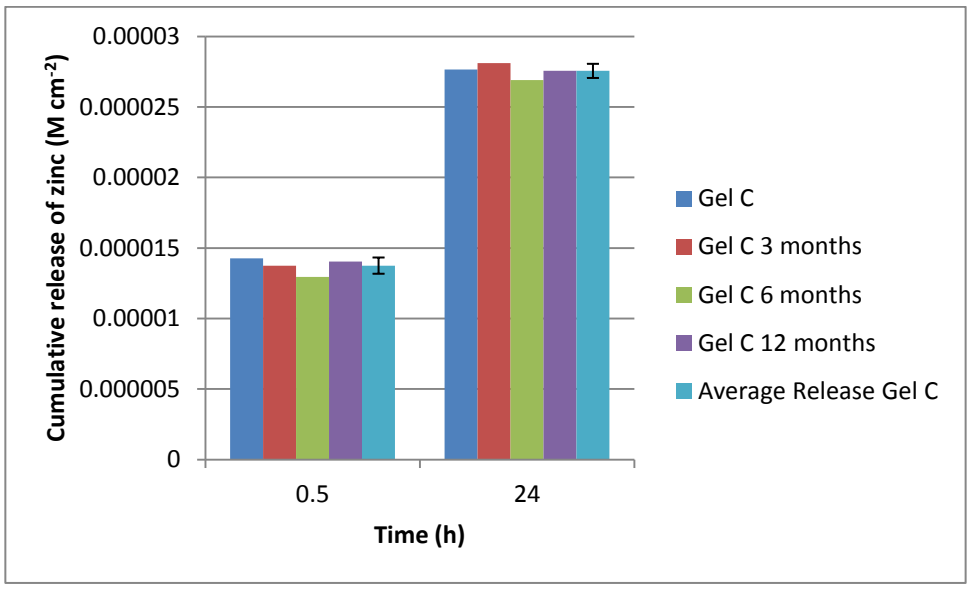

Figure 9-17 The spontaneous release of zinc from Hydrogel 6 C at 0.5 and 24 h after storage at room temperature and occlusion from light at 0, 3 6 and 12 months after formulation, and the average release over the 12 month time points (n = 4 ± SD).

Figures 9-18 and 9-19 show the release data of punicalagin and zinc from Hydrogel 6 E over a 12-month stability analysis. At 0.5 and 24 h the release of both punicalagin and zinc was maintained and not significantly different (p >0.05). Over the 12-month period the average release of punicalagin and zinc from Hydrogel 6 E was 2.3 ± 0.07 nM cm^{-2} and 1.42 x 10^{-5} ± 1.71 x 10^{-6} M respectively. The average 24 h release of punicalagin was 6.94 ± 1.29 nM cm^{-2}, the high standard deviation of the average release value resulted from the large variation of released punicalagin at the point of formulation. The average release of zinc was 4.18 x 10^{-5} ± 2 x10^{-6} M.

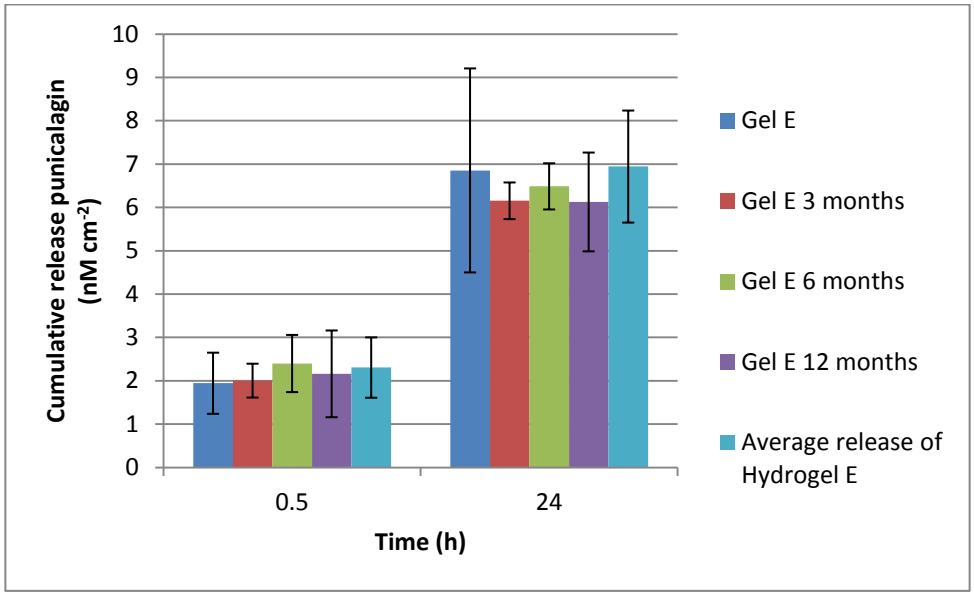

Figure 9-18 The spontaneous release of punicalagin from Hydrogel 6 E at 0.5 and 24 h after storage at room temperature and occlusion from light at 0, 3 6 and 12 months after formulation (n=3), and the average release over the 12 month timepoints (n = 12 ± SD).

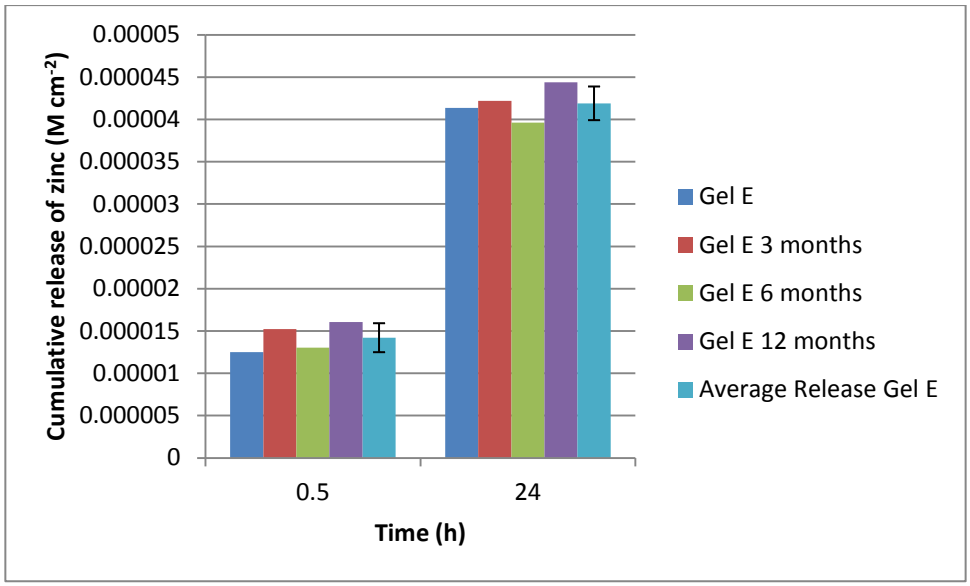

Figure 9-19 The spontaneous release of zinc from Hydrogel 6 E at 0.5 and 24 h after storage at room temperature and occlusion from light at 0, 3 6 and 12 months after formulation, and the average release over the 12 month time points (n = 4 ± SD).

The stability of the Hydrogels C and E from the above release data shows that both formulations are unaffected over a 12-month storage time. There is no decrease in the level of punicalagin released enabling the deduction that over 12 months the punicalagin content within the PRE + $ZnSO_4$ hydrogel matrix stored at room temperature was maintained and that no breakdown has occurred. Due to the instability of the punicalagin anomers as a pure extract and the readiness for its breakdown due to ester hydrolysis within the PRE mixture it is safe to assume that concentration of the majority of phytochemicals present in PRE remains constant over 12 months within the formulation of PRE, $ZnSO_4$ and Methocel 856N when stored at room temperature and occluded from light and oxygen.

9.4. **Discussion**

All of the hydrogel and emulsion formulations without the addition of PRE or zinc resulted in thick gels which are appropriate for topical administration, having both positive aesthetic and tactile properties. However, the addition of either zinc ($ZnSO_4$), PRE or a combination of the two appeared to affect the gelling properties of the polymers in varying ways. The addition of PRE to Hydrogel 1 prevented the

formation of a gel with a thick white semisolid at the base of the container and an orange liquid above. Hydrogel 2 with the inclusion of $ZnSO_4$ did not form a gel above a pH of 3. On the addition of $ZnSO_4$ to Hydrogels 3 and 5 a white precipitate formed with a clear liquid, and with respect to Hydrogel 5 a hydrophobic solid film formed on the top of the liquid after cooling. Although Hydrogel 5 did form a thick and clear hydrogel, a white residue was left on the skin after application, and on palpable examination the addition of $ZnSO_4$ led to a grainy feel. Hydrogel 6 formed a very promising gel on the addition of PRE to high concentrations (50 mg ml^{-1}) however the gel would not form above a concentration of 0.3 M $ZnSO_4$. A greater concentration of $ZnSO_4$ resulted in the formation of a white precipitate and clear hydrophobic layer similar to Hydrogels 3 and 5. Emulsion 1 was unaffected by the addition of both PRE and $ZnSO_4$, apart from slight discolouration and Emulsion 2 was unable to form after the addition of PRE.

From the literature, it is a recognised phenomenon that the addition of zinc and or PRE to many common formulations results in a chemical interaction between the polymer matrix of gels and emulsions. It is common for ionic polymers to lose viscosity in the presence of metal ions and other ionic species (Kawakami, et al. 2006); however the complete dissolution and formation of hydrophobic compounds on addition to common gel forming polymers is not widely disclosed. Common water soluble polymers such as carbopol, hydroxyethyl cellulose and hydroxypropyl cellulose have been reported to have little or no influence on the addition of salts (Keegan, et al. 2007) (Abzaeva, et al. 2009).

Emulsion 1 and Hydrogel 6, with the addition of both PRE and $ZnSO_4$, appeared to have acceptable aesthetic and tactile properties. The investigation into formulation was by no means exhaustive and there is a possibility that other simple or more complex emulsions or hydrogels may be formulated with higher concentrations of active ingredients that are both aesthetically acceptable and with a satisfactory tactility. However, it was deemed acceptable to proceed with release and permeation experiments with both a hydrogel and an emulsion to investigate.

The preference of a hydrogel formulation over an emulsion formulation, which led to the research for a wider range possible hydrogels, was due to the range of possible applications of hydrogels and the very high biocompatibility that hydrogels possess.

It should also be noted that due to the possible application of any formulation to the buccal cavity, the formulation must be harmless upon consumption due to the possibility of ingestion (Methocel 856N has been used as a thickening agent within the food industry).

The rheological properties of the Methocel 856N hydrogel as expected showed that as the Methocel content increased, the viscosity of the gel increased; an unloaded 2.5% Methocel 856N hydrogel (Hydrogel 6 F) acted as a typical non-Newtonian pseudoplastic hydrogel throughout rheological examination and was chosen for further analysis due to palpable and viscosity analysis. On the addition of $ZnSO_4$ to the formulation at 0.125 and 0.2 M to the hydrogel a decrease in viscosity was observed and pseudo-plastic behaviour maintained, however upon the addition of 0.25 M of $ZnSO_4$ the formulation showed a large decrease in viscosity with a shear stress change from 382.3 Pa for Hydrogel 6 F to 15.37 Pa at a shear rate of 300 s^{-1}; the gel also changed from pseudo-plastic to thixotropic, showing an hysteresis loop (Figure 9-9) upon the analysis of viscosity vs shear rate. The addition of PRE at 1.25 mg ml^{-1} to the Methocel 856 N hydrogel showed no change in the viscosity or pseudo-plastic nature of the gel.

The formulations Hydrogel 6 A-E with a Methocel content of 2.5% were analysed for any rheological changes occurring on the addition of both PRE and $ZnSO_4$ at a range of concentrations, in accordance with the potentiated virucidal data and concentration of punicalagin within PRE, the ratio 5:1 PRE mg ml^{-1}: $ZnSO_4$ M (concentrations in Table 9-2) was maintained. Hydrogel 6 A (PRE 0.05 mg mL^{-1}, $ZnSO_4$ 0.01 M), B (PRE 0.1 mg mL^{-1}, $ZnSO_4$ 0.02 M) and C (PRE 0.5 mg mL^{-1}, $ZnSO_4$ 0.1 M) were shown not to affect the pseudo-plastic nature or viscosity of the blank hydrogel, however Hydrogel 6 D (PRE 1 mg mL^{-1}, $ZnSO_4$ 0.2 M) and E (PRE 1.25 mg mL^{-1}, $ZnSO_4$ 0.25 M) both decreased the viscosity in comparison to the blank gel and changed the nature of the blank gel from pseudo-plastic to thixotropic with Hydrogel 6 E having the greater effect. It is apparent that the introduction of PRE and zinc in combination has a greater effect on the viscosity and properties of the gel than when introduced separately.

The spontaneous release data of punicalagin from Hydrogels 6 A-E and Emulsion 1 show that after 0.5 h there is no significant difference in the release from any of the

formulations, after 24 h it is apparent that Emulsion 1 and Hydrogel E release more. The release of permeant from a formulation usually dictates the maximum amount available to be taken up by the skin and permeate. The stability data showed that the formulation performed equitably across the 12-month test period, and thus it can be assumed no detrimental changes (eg phase separation) took place over this period – i.e. the formulation is stable under the conditions used.

9.5. **Conclusion**

A simple hydrogel has been developed which has acceptable properties, in terms of aesthetics, spontaneous release and rheology. This will be used as a prototype gel formulation in further investigation into the topical delivery of PRE and Zn^{2+}.

Chapter 10 Permeation Of Punicalagin And Zinc (II) Across Epithelial Membranes Prone To HSV Infection

10.1. **Introduction**

In Chapter 9, a simple prototype formulation was produced that was stable and which allowed the spontaneous release of the two major components in the system: punicalagin and zinc. In the current chapter, the performance of the formulation was determined in terms of its ability to deliver both punicalagin and zinc (II), following dosing onto a number of anatomical membranes that are prone to infection by HSV.

Cold sores mainly affect the perioral region in which case normal skin can be used as a model for determining penetration. HSV lesions also occur on the lips and in the mucous membranes of the buccal cavity, where the inner cheeks and gums can be the site of lesions, as shown in Figure 10-1. Ano-genital infections of HSV, commonly referred to as 'herpes', can involve the areas of normal skin or mucous membranes.

Figure 10-1 Manifestations of HSV-1 and 2 as lesions on perioral and normal skin, within the buccal cavity and the mucus membrane of the vagina (X Herpes 2011).

Depending on the progression of the lesion, the precise location of the viral load can vary from deep within the skin to near or on the surface. By using native or normal membranes, the levels of permeation would represent minimal deliverable amounts. Advanced lesions would have compromised barriers and so the amounts deliverable would be expected to be greater, particularly given the hydrophilic nature of the actives and the hydrated state of the buccal and vaginal mucosal membranes.

10.1.1. Objective and Aims

The objective of this chapter was to determine the extent of *in vitro* delivery of punicalagin and zinc (II) to models for HSV-1 and -2 vesicular specific sites, from topically applied hydrogel formulations loaded with PRE and $ZnSO_4$. The aims were:

- to determine delivery across heat separated porcine epidermis (HSE)

- to determine delivery across heat separated porcine buccal membrane (HSBM)

- to determine delivery across scalpel dissected porcine vaginal membrane (SDVM)

10.2. **Materials & Methods**

10.2.1. Materials

The materials used within this chapter are given in Chapter 2 section 2.1.

10.2.2. Formulation Preparation.

10.2.2.1. Emulsion 1

The formulation of Emulsion 1 to be analysed for permeation through the epidermal membrane followed that described in Chapter 9 section 9.2.2.1., with a PRE content of 5 mg mL^{-1} and $ZnSO_4$ concentration of 0.5 M.

10.2.2.2. Hydrogel 6 C, 6 E and 6 F Formulation

Hydrogel 6 C, E and F were prepared following the hot cold method stated in Chapter 9 section 9.2.2.3.6., using 2.5 % Methocel 856N. The use of Hydrogels 6 C and E was due to the comparative spontaneous release data after 0.5 h and the difference in the rheological properties, i.e. Hydrogel 6 C is pseudo-plastic in nature maintaining its viscoelastic properties whereas Hydrogel 6 E is thixotropic, resulting in a decreased viscosity after shear thinning. Hydrogel 6 C containing 0.5 mg mL^{-1} PRE and 0.1 M $ZnSO_4$ and Hydrogel 6 E with 1.25 mg mL^{-1} PRE and 0.25 M $ZnSO_4$. Hydrogel 6 F was used as a control and contained no PRE or $ZnSO_4$.

10.2.3. Preparation of Isolated Membranes

10.2.3.1. Heat separated epidermis

This membrane was used to model drug delivery to HSV-1 and -2 vesicular clusters which form in the early stages of a HSV or “cold sore” lesion formation, where the

skin and barrier function are still essentially intact. This could represent surrounding non-labial regions either of the mouth or vagina. The methodology for heat separated epidermal membrane followed that described in Chapter 2 section 2.2.2.2.

10.2.3.2. Heat Separated Buccal Membrane (HSBM)

Due to the fact that HSV-1 and -2 most commonly transverse the trigeminal nerve which enables the virus to present not only on the prolabium (lip) but also within the buccal cavity, it was important to determine the delivery of both punicalagin and zinc through the buccal mucosa. The preparation of this membrane follows the methodology in Chapter 2 section 2.2.2.3.

10.2.3.3. Scalpel Dissected Vaginal Membrane (SDVM)

Scalpel dissected vaginal membrane was used to model the presentation of HSV-1 and -2 vesicular clusters within and around the vaginal cavity soft tissue in female *Herpes simplex* infection. Porcine vaginal mucosal membrane (Figure 10-2) was excised via blunt dissection of the vagina and the slow removal of overlying fat and muscle until a thin semi transparent membrane remained, following the method stated in Chapter 2 section 2.2.2.4.

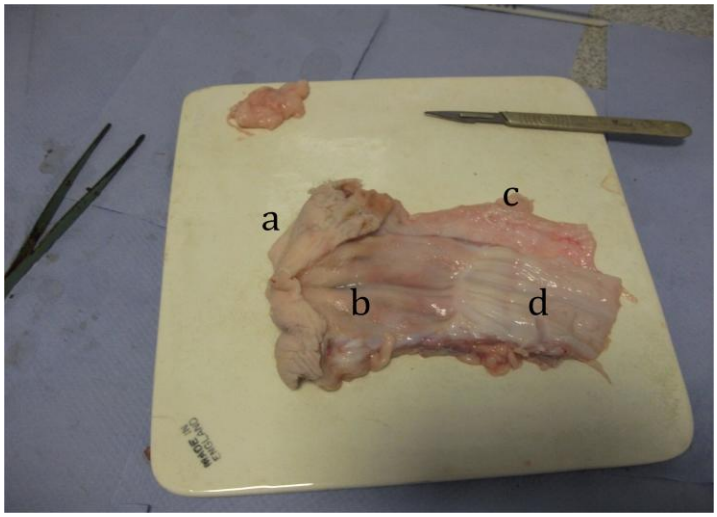

Figure 10-2 Dissected porcine vagina; a - urogenital opening, b - vaginal mucosal membrane, c - fat and muscle surrounding tube, d – uterus.

10.2.4. Membrane Permeation, *In Vitro*

Within the literature, methodology for the dosing of formulations onto membranes within a Franz diffusion cell (FDC) varies greatly but generally falls into 2 categories:

finite, representing in-use conditions

infinite, representing maximal effect (Corbo, et al. 1993).

For assessment of permeation in the current work it was decided that an infinite dose of 300 mg aliquot of formulation would be applied, and thus allow determination of maximal levels of delivery. The methodology for FDC experiments with each membrane followed that stated in Chapter 2 section 2.2.3.

Following the formulation and spontaneous release of punicalagin and zinc data obtained in Chapter 9, Emulsion 1 and Hydrogels 6 C, and E were analysed for the permeation of punicalagin and zinc through the epidermal membrane using Hydrogel F as a control. The 2.5 % Methocel 856N formulations Hydrogel 6 C (PRE 0.5 mg mL^{-1} and $ZnSO_4$ 0.1 M), E (PRE 1.25 mg mL^{-1} and $ZnSO_4$ 0.25 M) and F (control) were used to analyse the delivery of both punicalagin and zinc through the vaginal and buccal mucosal membranes. The use of these formulations was because Hydrogel 6 E contained the highest concentration of PRE and zinc, and release and delivery data showed that Hydrogel 6 E was the most effective. The unaffected pseudo-plastic nature and the benefit for the comparison of a loaded formulation led to the use of Hydrogel 6 C. Emulsion 1 was not analysed for permeation delivery of zinc through the epidermal membrane or the analysis of punicalagin or zinc through either the buccal or vaginal membrane due to the non-permeation of punicalagin from Emulsion 1 through the epidermal membrane.

After 0.5, 1, 2, 3, 6, 9, 12, 15, 18, 21 and 24 h the receptor fluids were removed via a sterile pipette and stored in 10 mL glass vials until further use. The receptor chamber was then refilled with DI H_2O using another sterile pipette.

10.2.5. Reverse Tape Stripping

To allow a comparative determination of the levels of actives in the basal layer areas of the 3 test membranes, reverse tape stripping was conducted after 24 h (Searby 2011). The membrane was removed from the FDC and carefully dabbed clean of excess formulation detailed in Chapter 2 section 2.2.3.5.

10.2.6. Recovery of Penetrants in FDC Receptor Phases

The methodology for the collection of the penetrants after the application of Hydrogel 6 E for Western blot and virucidal testing followed that stated in Chapter 2 section 2.2.5.12.

10.2.7. Virucidal Analysis

The virucidal analysis of reconstituted freeze dried receptor phase followed the methodology stated in Chapter 2 section 2.2.5.9. of the plaque reduction assay. Whereby HSV-1 was incubated with the test material for 30 min before serial dilution and plating onto 24 WP of confluent Vero cells for a 3 day incubation, at which point the plaques were counted.

10.2.8. Western Blot Analysis

The analysis of the test material, Hydrogel 6 E, on COX-2 levels after application to porcine skin for 6 h was done by SDS-PAGE and Western blotting following that stated in Chapter 2 section 2.2.4.4. using β-actin as the loading control.

10.2.9. Data Processing

Samples were analysed by HPLC or ICPMS as described in Chapter 2 sections 2.2.4.1. and 2.2.4.2., and plotted as cumulative permeation ± standard deviation. Where appropriate, flux was determined by linear fit to the linear part of permeation profile.

Statistical tests were performed using Instat 3 for Macintosh. A one way analysis of variance test was applied with a confidence interval of 95%, and a p value of <0.05

was considered significant. If values were found to be of significance a Turkey-Kramer multiple comparison test was applied.

10.3. **Results and Discussion**

10.3.1. Permeation of Punicalagin and Zinc (II) across HSE

10.3.1.1. Punicalagin

Figure 10-3 shows the levels of punicalagin permeated across heat separated epidermis from Hydrogel 6 C, E and Emulsion 1. Hydrogel 6 F was run as a control, no punicalagin penetration was observed. Although previous release data (Chapter 9 section 9.3.3.) showed that punicalagin was released at a high rate from Emulsion 1, it is apparent from the results that no recordable permeation has occurred. This may be due to the oleaginous nature of the emulsion preventing permeation of punicalagin through the epidermis. The graphical analysis obtained a J_{max} for Hydrogel 6 C and E giving fluxes of 0.3900 ± 0.0048 nM cm^{-2} hr^{-1} and 2.01 ± 0.25 nM cm^{-2} hr^{-1} respectively. The spontaneous release data of punicalagin from both Hydrogel 6 C and E is very similar to the penetration of punicalagin through the epidermal membrane. This is due to the pressure applied during application to the epidermal membrane, which in both cases will decrease the viscosity of the hydrogel resulting in a greater release of punicalagin. The data shows that the permeation of punicalagin from Hydrogel 6 E was the greatest. This is likely to be due to the increased concentration within Hydrogel 6 E and the fact that after application, and shear thinning, the thixotropic nature of Hydrogel 6 E will result in a gel of decreased viscosity during and after the shear thinning caused by application. Therefore a greater release and permeation of punicalagin from the hydrogel matrix is expected, and observed, at the time of application and afterwards.

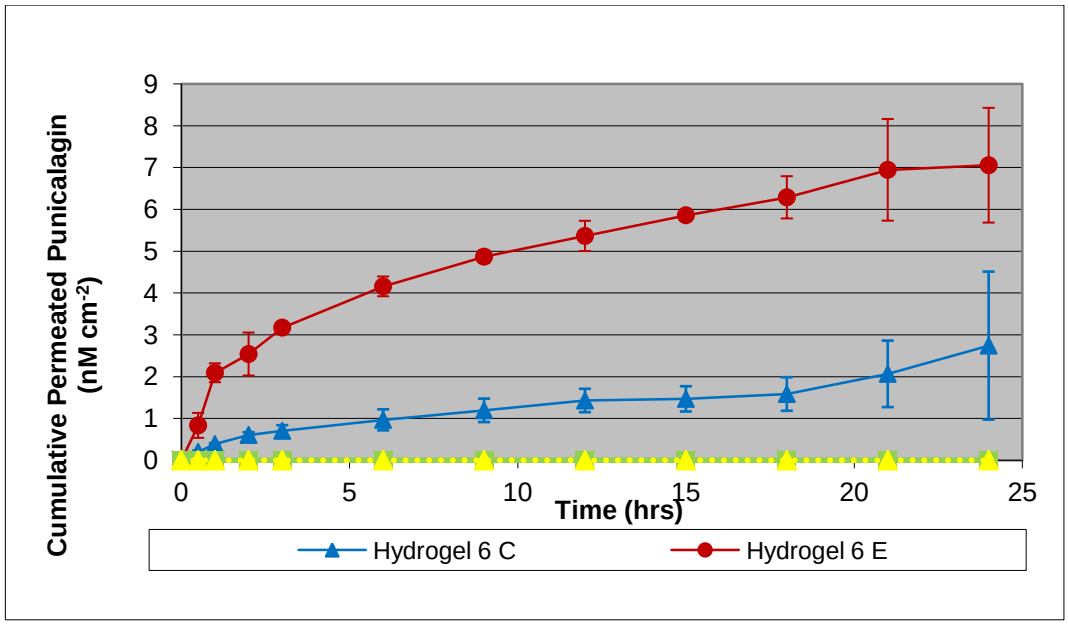

Figure 10-3 Cumulative permeation of punicalagin across HSE after infinite topical delivery of PRE and $ZnSO_4$ loaded Hydrogels 6 C, E, F (blank control) and Emulsion 1. (n= 4, ± SD).

10.3.1.2. Zinc (II)

Zinc analysis was conducted via ICP MS. Due to reasons previously described, it was necessary to pool the repeat samples. It was also deemed unnecessary to evaluate the permeation of zinc from Emulsion 1 due to the lack of punicalagin permeation.

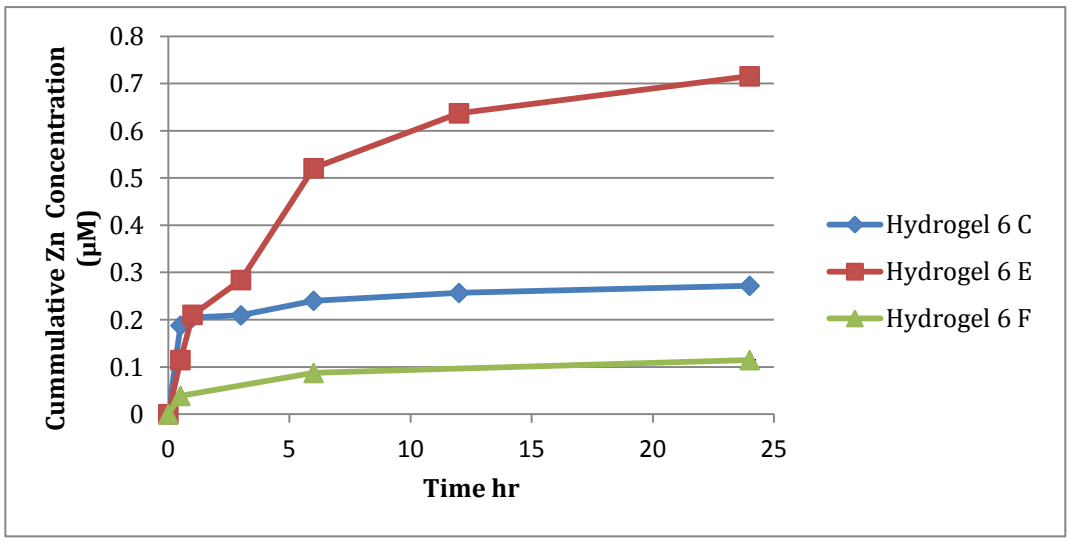

Figure 10-4 Cumulative permeated zinc through HSE After infinite dosing of Hydrogel 6 C, E and F (n=4, ± SD).

The zinc permeation analysis illustrated in Figure 10-4 reveals that a low level of zinc is present after application of the control Hydrogel 6 F. This is due to a leaching of zinc which is naturally found in porcine epidermis and observed in the analyses conducted within Chapter 6. Flux calculations subtracted this concentration from the results.

It is observed that permeation across HSE is similar to that across CTEM Hydrogel 6 C and E: both permeate with high concentrations of zinc over the first hour, Hydrogel 6 C plateauing after this period and Hydrogel 6 E continuing to deliver zinc over the 24h period.

The graphical analysis of the first three data points allowed for the flux calculation of zinc delivery from Hydrogel 6 C and E after subtraction of the control, the flux was 0.23 µM cm^{-1} hr^{-} and 0.21 µM cm^{-1} hr^{-1} respectively.

The penetration of zinc through the epidermal membrane from both Hydrogel 6 C and E show that the applied force during application has led to similar penetration concentration in comparison to release concentration. The thixotropic nature of Hydrogel 6 E has shown to be beneficial as a greater concentration of Zn^{2+} penetrated over a greater time.

The Figures 10-3 and 10-4 above show that after application of Hydrogel 6 C and E to HSE both biologically active compounds, punicalagin and zinc, permeate through the membrane. Hydrogel 6 E allows for a greater permeation of both compounds, in comparison to Hydrogel 6 C, with over 5 times the flux value of punicalagin and 3 times the flux obtained for zinc. This supports the hypothesis in Chapter 9 that the thixotropic nature of Hydrogel 6 E would allow for a greater permeation over a longer time.

10.3.1.3. Localisation of Punicalagin in HSE Basal Layer Region

Figure 10-5 represents the punicalagin which remained at the basal layer, i.e. the site of vesicular clusters in the interior region of the epidermis. All epidermal membranes were reverse tape stripped, three strips were used each time.

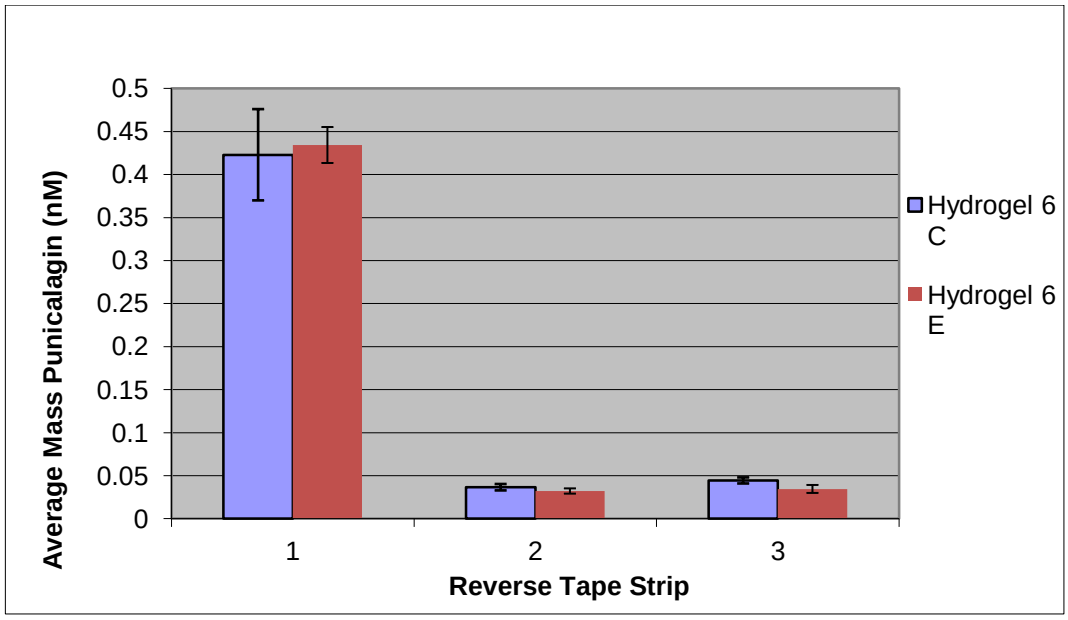

Figure 10-5 The mass of punicalagin recovered after reverse tape stripping epidermal membrane that had been dosed with Hydrogel 6 C and E (n=4, ± SD).

Reverse tape strip analysis shown in Figure 10-5 of HSE after a 24h application period of Hydrogel 6 C and E revealed that delivery of punicalagin was greatest to the lowest area of the epidermis. The second and third tape strip revealed only a very low level of punicalagin delivery by both gels. The results demonstrate that punicalagin was successfully delivered to the site of HSV-1 and -2 vesicular clusters.

10.3.2. Virucidal Testing on the Penetrants in FDC Receptor Phases

The HSV-1 virucidal analysis of the penetrants after a 24 h application of Hydrogel 6 E and Hydrogel 6 F to the epidermis is shown in Figure 10-6. The penetrants from Hydrogel 6 E caused a 2.57 ± 0.36 log reduction of HSV-1 pfus. The penetrants from Hydrogel 6 F, the control, show a negligible log reduction.

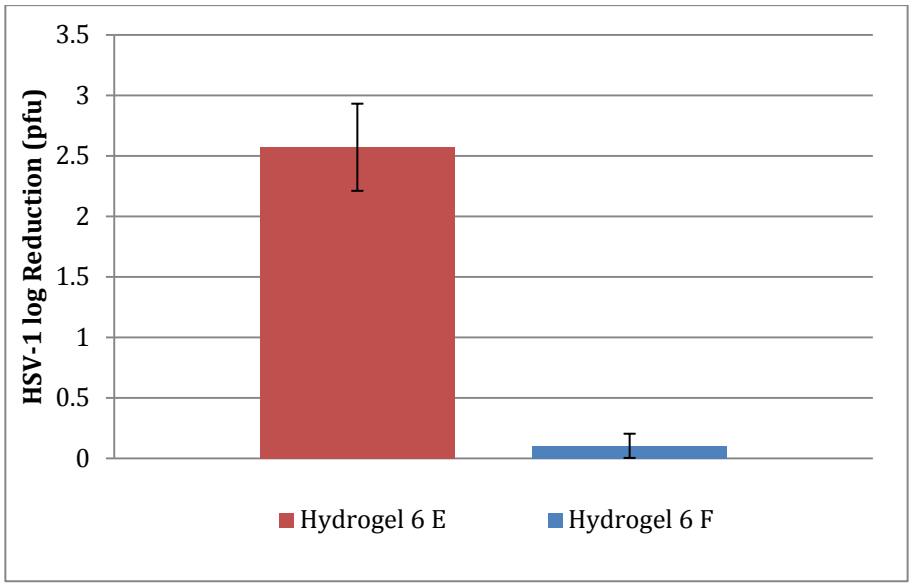

Figure 10-6 The log reduction of HSV-1 after the incubation with the reconstituted penetrants after the 24 h application of Hydrogel 6 E and 6 F to the epidermis (n=4, ± SD).

10.3.3. Western Blotting

To verify if the release of PRE from Hydrogel 6 E maintained similar anti-inflammatory levels as that stated for the application of the liquid formulation in Chapter 7, Western blot analysis was carried out. Hydrogel 6 E and control were applied to *ex vivo* full thickness porcine skin within a Franz diffusion cell for 6 h. After this time SDS PAGE and Western blotting was carried out for COX-2, as an inflammatory marker, and β-Actin, as the protein loading control.

Figure 10-7 shows the shows the bands produced by Western blot analysis for COX-2 expression at ~ 72 kDa and the protein loading control of β-actin at ~42 kDa. Densitometric results of the bands for COX-2 were normalised using β-actin, levels of COX-2 expression in the control were arbitrarily assigned a value of 100%. Test solutions were shown as a percentage of the control and graphically displayed as a histogram in Figure 10-7.

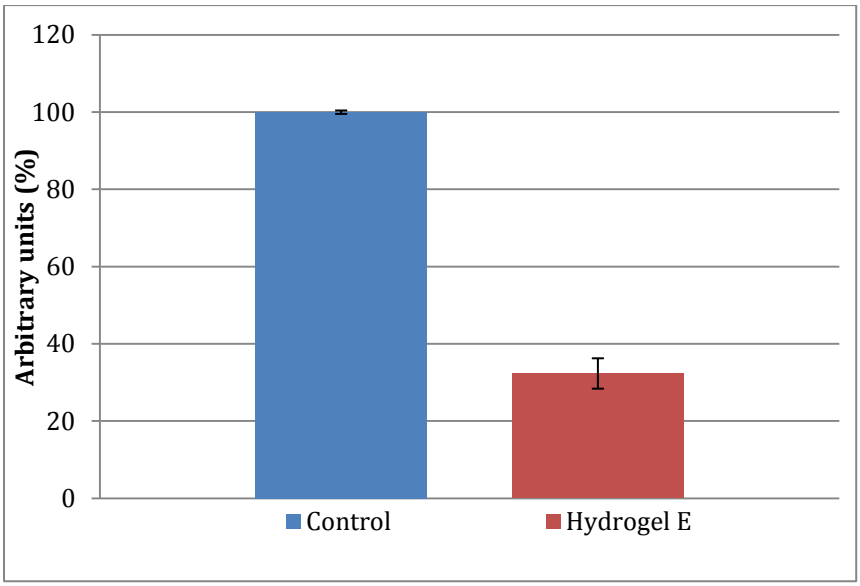

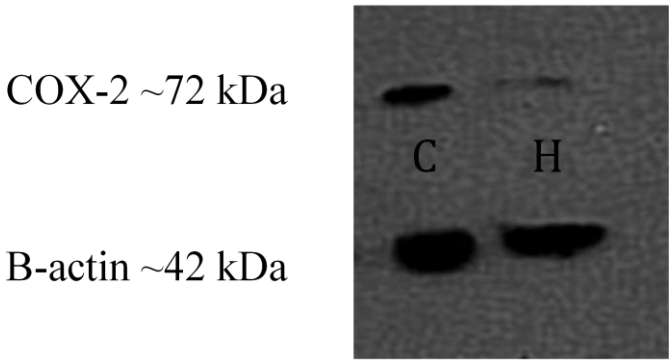

Figure 10-7 Analysis of COX-2 protein expression by Western blot. Full thickness porcine skin was treated with topical Hydrogel 6 E (H) and phthalate buffer as a control (C) for 6 h, protein was extracted and 30 µg was loaded and separated through SDS-PAGE. The histogram represents numerical data of COX-2 normalised using β-actin. Levels in control were arbitrarily assigned a value of 100%. (n=4, ± SD).

The application of Hydrogel 6 E caused the statistically significant reduction of COX-2 expression by 67.69 ± 3.93% (p<0.01).

There was not a significant difference (p>0.05) of the reduction of COX-2 after the application of the hydrogel in comparison to that of either the application of PRE (1 mg mL^{-1}) alone or in combination with $ZnSO_4$ (1M) (data given in Chapter7 section 7.3.2.).

10.3.4. Permeation of Punicalagin and Zinc (II) Across Heat Separated Buccal Membrane (HSBM) from Three Formulations

10.3.4.1. Punicalagin

Hydrogel 6 E and F were applied to HSBM following the same method used for HSE application and analysis. HSBM was used as a model for the presentation of HSV-1 and -2 lesions within the buccal cavity.

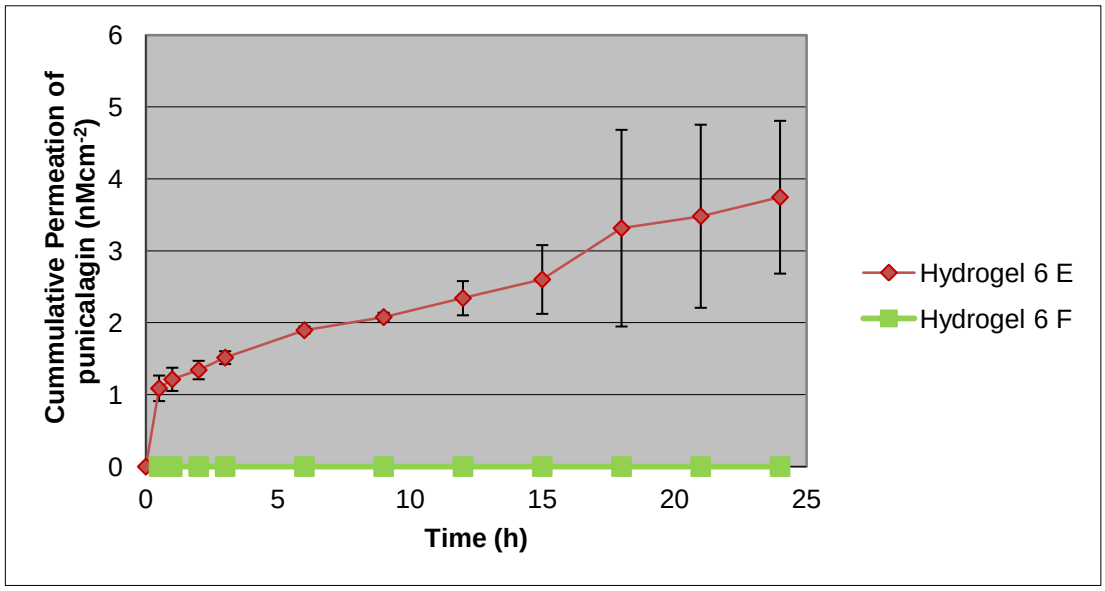

Figure 10-8 Permeation profile of punicalagin from Hydrogel 6 E and F (control) across the buccal membrane (n=4, ± SD).

Figure 10-8 demonstrates that the permeation of punicalagin within the first 0.5 h was comparable to epidermal permeation at 1.09 ± 0.18 nM cm^{-2} and 0.83 ± 0.3 nM cm^{-2} respectively, resulting in a statistically similar flux of 2.17± 0.16 nM cm^{-2} hr^{-1} for the buccal membrane and 2.01 ± 0.25 nM cm^{-2} $hr^{-1}$for the epidermal membrane. However, the level of permeation through the buccal membrane plateaued after 0.5 h. After 16 h of application it appears that the normal barrier function of the buccal membrane is inconsistent resulting in large error. It is hypothesized that receptor fluid which will be absorbed has greatly altered the membrane by this time point.

10.3.4.2. Zinc (II)

The samples collected after application of Hydrogel 6 E and F were pooled and analysed via ICP MS.

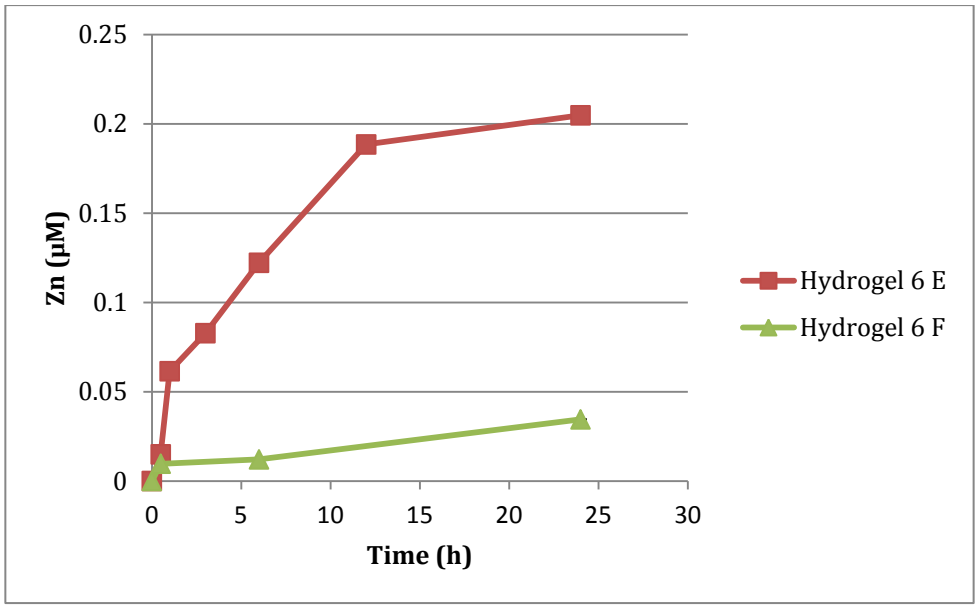

Figure 10-9 Permeation profile of zinc across HSBM after Application of Hydrogels 6 E and F (n=4, ± SD).

Figure 10-9 shows the permeation of zinc through the buccal membrane from Hydrogel 6 E and F, it is noted that a low level of zinc has leached from the buccal membrane after application of Hydrogel 6 F. This is at a much lower concentration in comparison to epidermal membrane.

The permeation of zinc from Hydrogel 6 E through the buccal membrane results in a flux 0.055 x 10^{-6} M cm^{-2} h^{-1}, which is much lower in comparison to the flux of zinc through the epidermal membrane at 0.21 x 10^{-6} M cm^{-2} h^{-1}. The large decrease could be due to an increase of zinc absorption by the buccal membrane cells. The permeation of profile of zinc over the 24 h period is similar to that through HSE; a plateau is observed after 1 h, maintained up to 12 h. and tailing off.

10.3.4.3. Localisation of Punicalagin in HSBM Basal Layer Region

The fragility of the buccal membrane after 24 h allowed for only one tape strip sample to be conducted. The average punicalagin concentration of the reverse tape strip was 0.52 ± 0.052 nM cm^{-2} (n=3), demonstrating the delivery of punicalagin to the site of buccal membrane vesicular clusters.

10.3.5. Permeation across Porcine Vaginal Membrane

10.3.5.1. Punicalagin

Hydrogels 6 E and F were applied to the vaginal membrane following similar methods of application to both other membranes to allow for comparable results.

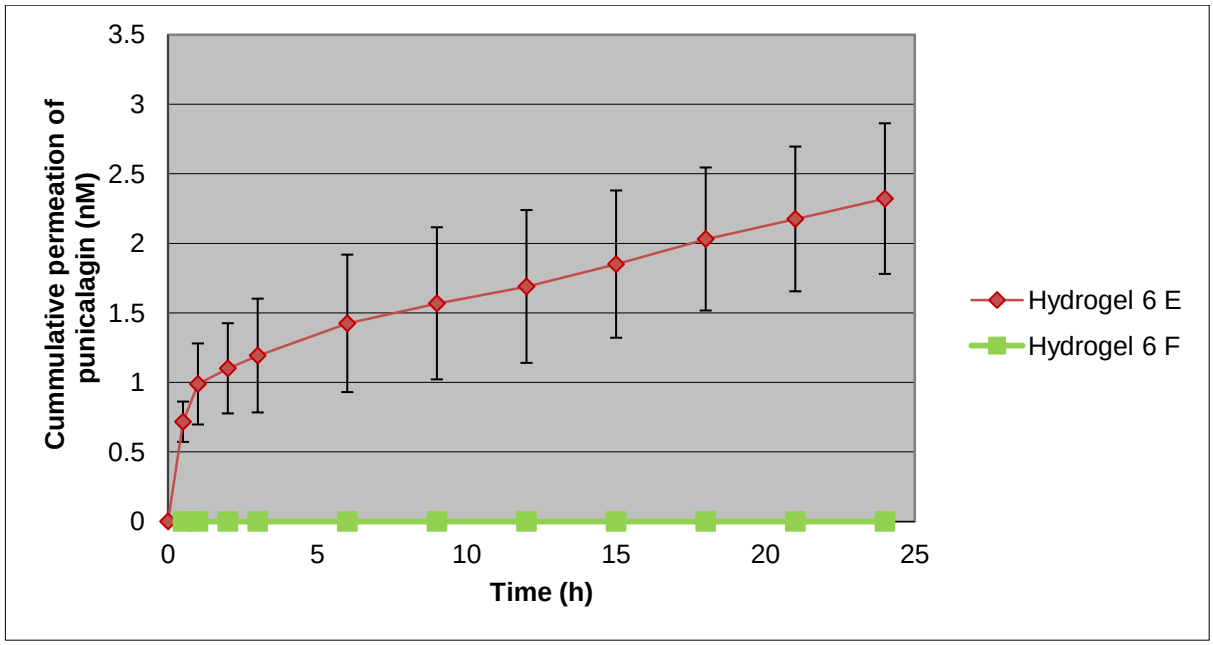

Figure 10-10 Permeation profile of punicalagin through the vaginal mucous membrane after application of Hydrogel 6 E and F (control) (n=4, ± SD).

The permeation of punicalagin through the vaginal membrane is illustrated in Figure 10-10. Within 30 min of application a large percentage of the total permeation of punicalagin is reached. After 1 h the permeation plateaus. The permeation of punicalagin across the vaginal mucosal membrane quickly reaches equilibrium after the topical application of Hydrogel 6 E, the resultant flux of which is 1.08 ± 0.26 nM cm^{-2} h^{-1}. The flux of punicalagin through the vaginal membrane is about half of that through the buccal and epidermal membranes.

10.3.5.2. Zinc (II)

The samples collected after application of Hydrogel 6 E and F to SDVM were pooled and analysed via ICP MS.

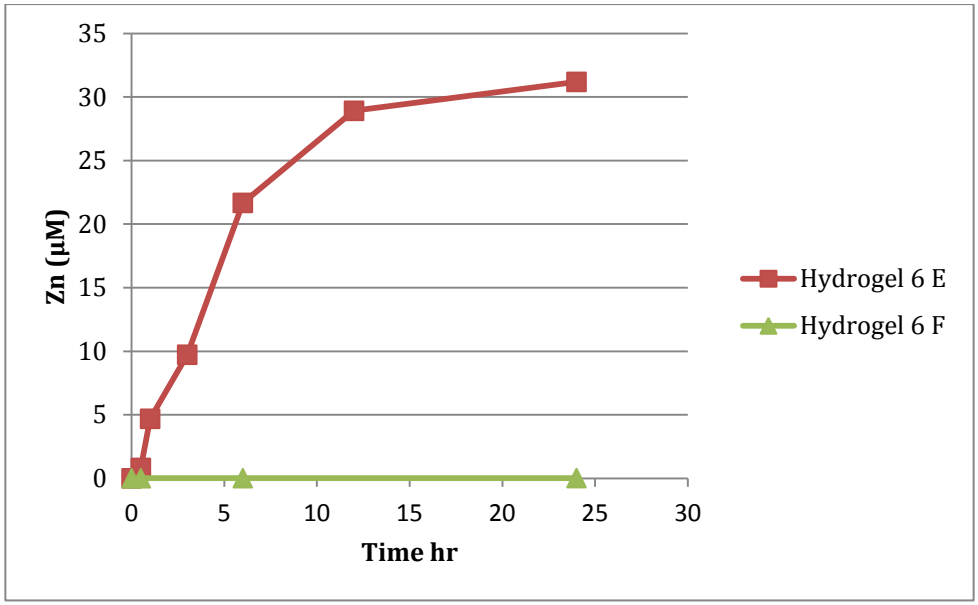

Figure 10-11 Cumulative permeation of zinc though the vaginal mucosal membrane after application of Hydrogel 6 E and F (control) (n=4, ± SD).

Figure 10-11 graphically illustrates the permeation of zinc through the vaginal mucosal membrane from Hydrogels 6 E and F. The leaching of zinc from the vaginal membranes after application of Hydrogel F was not significantly different ($p>0.05$) to that leached from the buccal membrane but was a lot less than that from the epidermis. The permeation profile reveals that zinc continues to permeate at high concentration for 12 h, reaching a plateau after this time point. This is very different to the permeation through the epidermal and buccal membranes which both plateaued after 1 or 2 h.

The permeation through this membrane was also much greater at 4 µM cm^{-2} h^{-1} than through the other tested membranes, suggesting that there is a much greater permeation of Zn through the vaginal mucosal in comparison to the epidermal and buccal membranes; however, the greatest permeation of punicalagin was through the epidermal membrane.

10.3.5.3. Localisation of Punicalagin in SDVM basal layer region

The fragility of the membrane once again prevented repeat stripping, as with the buccal membrane only one tape strip was performed on each membrane. The average punicalagin concentration of the reverse tape strip was 0.46 ± 0.048 µM cm^{-2} (n=3). This was directly comparable to the first tape strip removed from buccal membrane, demonstrating the delivery of punicalagin to the site of all membrane vesicular clusters.

10.3.6. The Comparison of Tape Stripping 3 Porcine Membranes after 24 h Application of Hydrogel 6 E.

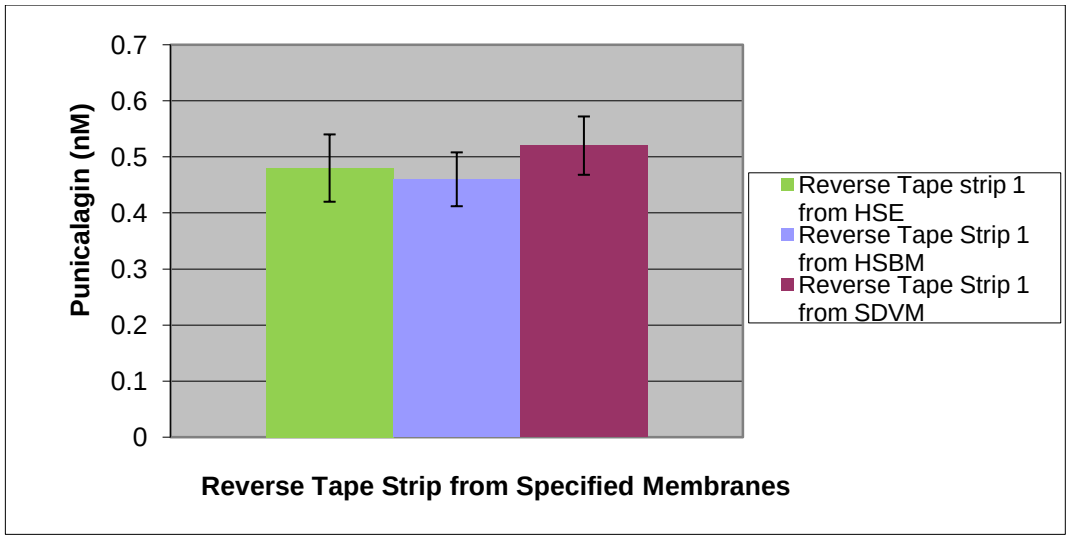

Figure 10-12 Comparison of punicalagin recovered from lowest reverse tape strip after 24 h application of hydrogel 6 E to three porcine membranes (n=4, ± SD).

The concentration of punicalagin recovered after 1 tape strip is shown in Figure 10-12. The concentration recovered from the basal layer of each membrane tested are shown to be directly comparable ($P>0.05$). The results indicate that punicalagin is being delivered to the intended site of vesicular clusters through all three membranes.

10.4. **Discussion**

The decrease in permeation through HSE in comparison to the release data obtained using CTEM was expected to be due to the greater barrier provided by the epidermis (Davidson, et al. 2010). The permeation of punicalagin from the PRE $ZnSO_4$ formulations analysed, Hydrogel 6 C and E and Emulsion 1, was best achieved after application of Hydrogel 6 E. This result was expected due to the increased loading and release of Hydrogel 6 E. Emulsion 1 proved not to overcome the epidermal barrier and no punicalagin permeated from this formulation.

The permeation of Zn from both Hydrogel 6 C and E was observed through the epidermal membrane with a greater permeation from Hydrogel 6 E.

Both Hydrogel 6 C and E facilitated the permeation of punicalagin and Zn through HSBM with a greater delivery from Hydrogel 6 E. The permeation profiles of both punicalagin and Zn were similar over the 24h period, however a much greater concentration of both analytes permeated the epidermal membrane.

The delivery of punicalagin from Hydrogel 6 E through the SDVM was comparable to that through HSBM however a greater permeation of Zn was achieved through this membrane. The comparison of the permeation data through the 3 membranes allows for the conclusion that with respect to punicalagin the permeability of the membranes follows HSE>SDVM>HSBM and with respect to Zn^{2+} the permeability of the membranes follows SDVM>HSE>HSBM. The delivery of the bioactive analytes through each susceptible membrane and to the site specific areas as shown by the reverse tape stripping of each membrane results in the conclusion that both punicalagin and zinc were sufficiently delivered to the site of vesicular cluster formation on recurrence of herpetic lesions in the epidermis, buccal mucosa, and vaginal cavity. Hydrogel E therefore has the potential as a viable treatment for HSV-1 and -2 herpetic lesions resulting in cold sores throughout all common areas in which they present.

10.5. **Conclusion**

Punicalagin and Zn^{2+} from the formulation Hydrogel 6 E are able to penetrate through epidermal, vaginal mucosal and buccal membranes at concentration ratios for which potentiated virucidal activity has been observed. Application of Hydrogel 6 E to *ex vivo* full thickness skin also showed that the punicalagin released from the gel penetrated the epidermis maintaining a statistically similar reduction in COX-2 expression to that of PRE in a liquid formulation.

Overall, Hydrogel 6 E containing 2.5% Methocel, 1.25 mg mL^{-1} PRE and 0.25 M $ZnSO_4$ is able to topically deliver, from a stable formulation, the bioactive compounds within PRE and Zn^{2+} to the site specific region of *Herpes simplex* vesicular clusters, maintaining antiviral, anti-inflammatory and potentiated virucidal properties. A possible, novel therapeutic system for the treatment of HSV-1 and HSV-1 lesions has been identified.

It is important to note: the experimental data have been collected under *ex vivo* conditions, and while the epidermal membrane of the porcine is a well recognised and accepted model for the epidermal penetration in humans, the use of the porcine scalpel dissected vaginal membrane and porcine heat separated buccal membrane has not been previously reported, and therefore its validity as a model for human extrapolation should not be assumed.

Chapter 11 **General Discussion**

11.1. **General Discussion**

The medicinal use of the extracts taken from various parts of the plant *Punica granatum L,* has been of interest for many centuries and remains so to the present day. Aligned with a greater understanding of the chemical nature of these extracts in recent times, has been heightened appreciation of the breadth of potential pharmacological activities. In particular, interest has focussed upon the high concentration of polyphenolic tannins, most notably punicalagin, contained within such extracts. The impetus for the current research was the finding by Stephen Denyer and colleagues at the University of Nottingham a decade or so ago. They noted that the phagicidal activity of PRE was markedly enhanced or potentiated by the co-administration of ferrous sulphate. Intriguingly, such potentiated activity was short-lived (approximately 3 minutes) and resulted in the development of a black byproduct. However, there seemed to be the basis of a therapeutic antimicrobial system, given further development. This view was supported by the Welsh Office of Research and Development who funded the current work following a competitive call for proposals.

The object of this thesis was therefore to probe the virucidal activity of PRE in respect to HSV-1 and to investigate any potentiation with the addition of metal salts, including $FeSO_4$. A key aim was working towards the development of a therapeutic system, particularly for the treatment of orofacial and ano genital HSV-1 and HSV-2 lesions.

The work commenced by revisiting the PRE + $FeSO_4$ combination, only the focus was on HSV, as this is a major infective agent involved in skin infections. Chapter 3 concluded that the potentiated activity previously observed in bacteriophage was essentially reproduced in virucidal experiments involving HSV-1 and -2 where the combination of PRE and $FeSO_4$ led to a 600 fold increase in activity. However, also reproduced was the transient timescale of the potentiation and the development of the black byproduct, post mixing. These factors were considered to be significantly detrimental in the context of a therapeutic product.

In Chapter 4 I attempted to examine the kinetics of the PRE/$FeSO_4$ reaction, and potentially identify an alternative to the metal salt with better properties. The results

indicated that the rapid oxidation of Fe II to Fe III as the basis for, not only the development of the black byproduct, but also the transient nature of the biological activity. This was a clue that a metal ion that remained in the +II oxidation state, resisting further oxidation, may provide a longer-lived system with no discolouration. Consequently, our attention turned to zinc, and in particular salts of Zn II. The addition of $ZnSO_4$ to the PRE produced no colour change, no redox change and no new compound, due to the stability of the Zn^{2+} ion, in terms of its resistance to further oxidation. This was therefore chosen for use in further potentiated virucidal experiments.

In Chapter 5 the potentiated virucidal activity of PRE, when added to $ZnSO_4$ was comparable to the *initial* addition of $FeSO_4$. However, unlike with $FeSO_4$, there was no evidence of any diminishing activity. There was a biphasic potentiated virucidal response to $ZnSO_4$ added to PRE. The unknown complex interplay between the mixture of phytochemicals and the addition of $ZnSO_4$ upon the virus and the precise mechanism of action has not been fully elucidated. The range of PRE : $ZnSO_4$ ratios for which a greater than 1000 fold reduction in viral count is:

PRE 1 : 2.8-575 $ZnSO_4$ (mg mL^{-1}).

The ratios PRE 1 : 28.8 $ZnSO_4$ (mg mL^{-1}) and PRE 1 : 287.6 $ZnSO_4$ (mg mL^{-1}) had the greatest potentiated reduction of viral load: over a 9000 fold reduction in comparison to either agent alone.

Examination of alternative Zn (II) salts established that it was indeed Zn^{2+} that provided the potentiation, rather than the sulphate counterion. Interestingly ZnO, a common ingredient in topical formulations, demonstrated minimal activity due (almost certainly) to low dissociation and solubility in water. Punicalagin, the most abundant polyphenol within PRE, was highly virucidally active and potentiation by $ZnSO_4$ was observed. At lower concentrations this was only at a very specific ratio (punicalagin 1 : 14 $ZnSO_4$ (mg mL^{-1})). At concentrations outside of this ratio (lower than and including punicalagin 1 : 288 $ZnSO_4$ (mg mL^{-1})) the addition of $ZnSO_4$ was deleterious to the virucidal activity of punicalagin. Similarities between the potentiated virucidal activity of the higher concentration ratios of: $ZnSO_4$ to punicalagin (above and including, punicalagin 1 : 1438 $ZnSO_4$ (mg mL^{-1})), and $ZnSO_4$ to PRE (above and including, PRE 1 : 287.6) are observed.

From this data a hypothesis was developed that a dual effect was occurring whereby upon the addition to PRE of $ZnSO_4$ at:

Lower concentrations

-An as yet unidentified viral envelope glycoprotein(s) is/are first compromised by the punicalagin enabling the absorbtion of and or interaction of free Zn^{2+} molecules to the viral tegument resulting in the combined destruction of the virus.

Higher concentrations

-The Zn^{2+} ions may act first allowing the punicalagin to then combine with the protein envelope thus destroying it.

There is evidence of some viral destruction for each of the chemicals separately and it is likely that a different mechanism of damage exists for each chemical. The combination of PRE and $ZnSO_4$ is creating a system in which free Zn^{2+} ions, irrespective of the anion, are significantly potentiating the virucidal effect of punicalagin. Punicalagin alone appears to be inhibited by components of PRE.

In terms of antiviral activity, the IC_{50} of PRE demonstrated impressive comparability to Aciclovir by weight with respect to HSV-1. Furthermore, an even lower IC_{50} was observed with respect to HSV-2 ACR. Overall the data suggested that PRE is comparable to the established cold sore treatment and that as Aciclovir resistant strains become ever more prevalent PRE may have a major role in future HSV therapeutic strategies. $ZnSO_4$ appeared to have no antiviral effect (>100 µM) alone or in combination with PRE.

Taken together, these *in vitro* results supported the development of an unprecedented product within the HSV treatment market that could not only inhibit virus intracellular replication at eruption outbreak, but could also kill any extracellular virus that was able to emerge from the host cell. Pivotal to this development is the finding that there was no cytotoxicity in the models used. However, these *in vitro* data did not take account of the location of the viral load, i.e. the viable epidermis. Therefore the next step was to determine whether the main actives could penetrate skin in order to deliver the required doses to the skin.

Initially the work concentrated on a simple aqueous solution, which was the subject of Chapter 6. Finite dosing of PRE and $ZnSO_4$ to freshly excised porcine epidermis, modelling *in situ* conditions, showed that punicalagin from PRE and Zn^{2+} both penetrated to the site of HSV-1 vesicular clusters (the formation of a cold sore). Tape stripping of full thickness porcine epidermis showed that all levels of the stratum corneum contained the actives, indicating reservoir formation.

Knowing that a simple solution of PRE and $ZnSO_4$ possessed such remarkable activity against HSV *and* was deliverable across skin, the attention turned to probing the anti-inflammatory properties of the combination. Using modulation in the expression of COX-2 in *ex vivo* skin as a marker, Chapter 7 used the techniques of Western blotting and IHC to demonstrate that the topical application of PRE to full thickness *ex vivo* skin downregulates the expression of COX-2 within 6 h and was maintained over at least 24 h. As COX-2 expression is an important mediator for inflammation in the arachidonic acid pathway, it was concluded that the topical application of PRE (with or without $ZnSO_4$) has a substantial anti-inflammatory effect in *ex vivo* skin. The inference of this finding is that a product based on PRE would be expected to result in the amelioration of inflammation and pain associated with *Herpes simplex* lesions which would be highly advantageous within a therapeutic system, as no current treatment for cold sores utilises a system which incorporates the combined benefits of anti-inflammation and pain relief.

Therefore it is clear that if $ZnSO_4$ was used in combination with PRE to potentiate the virucidal activity, its inclusion would not jeopardise the antiviral or anti-inflammatory activity of PRE

The next step was to examine the biological activity of PRE in greater detail. Successful separation of PRE yielded fractions either devoid of tannins or containing only total pomegranate tannins (TPT). The further isolation of 3 distinct fractions from TPT was also achieved, one comprising almost entirely of punicalagin and two containing a mixture of other tannins present in PRE, although not containing punicalagin. Further COX-2 analysis showed that a degree of COX-2 modulation observed by PRE was within the TPT fraction and the punicalagin fraction. However, the level of COX-2 downregulation diminished with each fractionation. The diminished biological activity due to fractionation was also observed with

respect to antiviral activity, TPT the only antivirally active fraction with an IC_{50} lower than 100 µg mL^{-1}. The fractionation processes showed that the only virucidally active component of PRE was punicalagin. However, overall the data shows that biological activity is greatest when PRE remains as a whole entity.

In the following Chapter, a semi-solid formulation was sought, suitable for further study. Chapter 9 consequently pinpointed a prototype hydrogel formulation comprised of 2.5 % Methocel 856 n, 1.25 mg mL^{-1} PRE and $ZnSO_4$ 0.25 M, that spontaneously released both punicalagin and Zn^{2+}, was aesthetically acceptable and which had suitable rheological properties for a topical application. It was further determined that the gel and the phytotchemicals within PRE remained stable over a 12 month period, retaining statistically similar spontaneous release of punicalagin and $ZnSO_4$ over this time period. The next step was to determine the delivery of punicalagin and Zn^{2+} from the gel across membranes that were representative of the tissues prone to the development of HSV-induced lesions.

The penetration of punicalagin and Zn^{2+} through epidermal, vaginal mucosal and buccal membranes was established in Chapter 10. Both analytes penetrated at sufficient concentrations through the epidermal membrane to maintain virucidal activity; similar levels of penetration were observed through the vaginal mucosal and buccal membranes. The comparison of the permeation through: heat separated epidermis (HSE), heat separated buccal membrane (HSBM) and scalpel dissected vaginal mucosal membrane (SDVM) allows for the conclusion that permeability of the membranes

-with respect to punicalagin HSE > SDVM > HSBM

-with respect to Zn^{2+} SDVM > HSE > HSBM

It must be stated that this order was not expected, as HSE with its stratum corneum barrier would be expected to give the lowest permeation.

The application of the 2.5% Methocel Hydrogel 6 E (1.25 mg mL^{-1} PRE and 0.25 M $ZnSO_4$) to *ex vivo* full thickness skin showed that PRE released from the gel penetrated the epidermis maintaining a statistically similar reduction in COX-2 expression to that of PRE in a liquid formulation.

In conclusion, the main objective of this research has been realised, in that a potentially potent therapeutic system has been developed. Based on a hydrogel matrix containing PRE and $ZnSO_4$ the prototype gel:

1. is non-cytotoxic
2. produces high potentiated virucidal activity against HSV-1
3. has antiviral activity, comparable to the Gold Standard compound, Aciclovir, against HSV-1
4. has even greater antiviral potency against Aciclovir-resistant HSV-2
5. possesses potent innate anti-inflammatory activities
6. maintains the activities above after the release, penetration, and permeation of the bioactive compounds, to the area of HSV vesicular clusters at the epidermal dermal interface, through all common epithelial membranes where the *Herpes simplex* virus presents.
7. has good aesthetic and rheological properties
8. demonstrates good stability

11.2. **Further work**

The therapeutic potential for this system are manifest. However, there are many ways in which the system could be further explored.

Prior to any human trials, standardisation of PRE needs to account for the variation of content between batches by TPT concentration within predefined limits of each molecule i.e. punicalagin between 80-85%. We believe this not to be an issue given the large dilutions that occur in the preparation of PRE.

The continuation of this work for the progression of the therapeutic system to be used within the community must analyse the observed *in vitro* effects in an *in vivo* situation. This would first be done by the HSV-1 virucidal, antiviral and anti-inflammatory analysis within a mouse model. Followed by a human trial "scratch test" testing the biological response to the topical application of the therapeutic system. Ideally this would be followed by a full human trial for the *in situ* use of the formulation as a therapeutic system for the treatment of HSV-1 and HSV-2 lesions.

The potentiated virucidal activity of the PRE + $ZnSO_4$ combination with regards to HSV-1 must be further tested against a range of virion, with specific interest in enveloped virion which are transmitted sexually i.e. HIV followed by Hepatitus B, HPV and MCV.

I propose that due to the similarities between the viral glycoproteins of the envelope of HSV and HIV it is conceivable that comparable virucidal activity could be observed, and that the formulation could be used as a lubricant on condoms, as a lubricating gel and or as a vaginal suppository for the prevention of the spread of HIV through sexual contact. The prevalence of HSV lesions within the mucous membrane of the vaginal cavity also greatly increases the level of infectious HIV virions within vaginal secretions (Baeten, et al. 2004).

Lastly, we believe it is worth revisiting the bactericidal potential of this system. Although it had been specifically stated in a previous patent application that PRE and $ZnSO_4$ were *not* active, there are grounds to believe that further work involving better *in vitro* models could prove otherwise.

REFERENCES

Abdalla, S I, I R Sanderson, and R C Fitzgerald. “Effect of inflammation on cyclooxygenase (COX)-2 expression in benign and malignant oesophageal cells.” *Carcinogenesis* 26, no. 9 (2005): 1627-1633.

Abzaeva, K A, M G Voronkov, L V Zhilitskaya, G G Belozerskaya, and V A Makarov. “Pharmacological Properties of Poly(zinc acrylate) Ziacryl.” *Doklady Akademii Nauk* 424, no. 1 (2009): 135-137.

Adams, L S, N P Seeram, B B Aggarwal, Y Takada, D Sand, and D Heber. “Pomegranate Juice, Total Pomegranate Ellagitannins, and Punicalagin Suppress Inflammatory Cell Signaling in Colon Cancer Cells.” *Journal of Agricultural Food Chemistry* 54 (2006): 980-985.

Afaq, F, M Saleem, C G Krueger, J D Reed, and H Mukhtar. “Anthocyanin- and hydrolyzable tannin-rich pomegranate fruit extract modulates MAPK and NF-kappaB pathways and inhibits skin tumorigenesis in CD-1 mice.” *International Journal of Cancer* 113, no. 3 (2005): 423-433.

Aggarwal, B B, et al. “From traditional Ayurvedic to Modern Medicine: Identification of Therapeutic Targets for Suppression of Inflammation and Cancer.” *Expert Opinion Therapeutic Targets* 10, no. 1 (2006): 87-118.

Aggarwal, G. “Development, Fabrication and Evaluation of Transdermal Drug Delivery System - A Review.” *Pharmaceutical News* 7, no. 5 (2009): 50-62.

Agren, M S, M Chvapil, and L Franzen. “Enhancement of Re-epithelialization with Topical Zinc Oxide in Porcine Partial- Thickness Wounds.” *Journal of Surgical Research* 50 (1991): 101-105.

Akbarpour, V, K Hemmati, and M Sharifani. “Physical and Chemical Properties of Pomegranate (Punica granatum L.) Fruit in Maturation Stage.” *American-Eurasian Journal of Agriculture and Environmental Science* 6, no. 4 (2009): 411-416.

Ammendolia, G M, M Marchetti, and F Superti. “Bovine lactoferrin prevents the entry and intercellular spread of herpes simplex virus type 1 in Green Monkey Kidney cells.” *Antiviral Research* 76 (2007): 252-262.

Andjelkovic, M, et al. “Iron-chelation properties of phenolic acids bearing catechol and galloyl groups.” *Food Chemistry*, 2006: 23-31.

Aranha-Creado, H, and H Brandwein. “Application of Bacteriophages as Surrogates for Mammalian Viruses: A Case for Use in Filter Validation Based on Precedents and Current Practices in Medical and Environmental Virology.” *Journal of Pharmeceutical Science and Technology* 53, no. 2 (1999): 75-82.

Aviram, M, and L Dornfeld. “Pomegranate juice consumption inhibits serum angiotensin converting enzyme activity and reduces systolic blood pressure.” *Atherosclerosis* 158, no. 1 (2001): 195-198.

Bacon, T H, M J Levin, J L Leary, R T Sarisky, and D Sutton. “Herpes Simplex Virus Resistance to Acyclovir and Penciclovir after Two Decades of Antiviral Therapy.” *Clinical Microbiology Reviews* 16, no. 1 (2003): 114-128.

Baeten, J M, et al. “Vitamin A Supplementation and Genital Shedding of Herpes Simplex Virus among HIV-1-Infected Women: A Randomized Clinical Trial.” *Journal of Infectious Diseases* 189, no. 8 (2004): 1466-1471.

Balfou, H H Jr. “Antiviral drugs.” *New England Journal of Medicine* , no. 340 (1999): 1255-1268.

Baltimore, D. “Expression of animal virus genomes.” *Bacteriological reviews* 35 (1971): 235-241.

Barbucci, R, D Pasqui, R Favaloro, and G Panariello. “A Thixotropic Hydrogel from Chemically Cross-linked Guar Gum: Synthesis, Characterization and Rheological Behaviour.” *Carbohydrate Research* 343, no. 18 (2008): 3058-3065.

Barnes, H A, J F Hutton, and K Walters. “Linear Viscoelasticity.” In *An Introduction to Rheology*, by H A Barnes, J F Hutton and K Wlaters, 37-54. oxford: Elsevier, 1989.

Barry, B W. “Rheology of Dermatological Vehicles.” In *Dermatological Formulations*,, by B W Barry, p351-407. New York: Marcel Dekker, 1983.

Berridge, M V, and A S Tan. “Characterization of the Cellular Reduction of 3-(4,5-dimethylthiazol-2-yl)-2,5-diphenyltetrazolium bromide (MTT): Subcellular Localization, Substrate Dependence, and Involvement of Mitochondrial Electron Transport in MTT.” *Archives of Biochemistry and Biophysics*, no. 303 (1993): 474-482.

Brant, R C, L M Coakley, and D R Grau. “A murine model of herpes simplex virus-induced ocular disease for antiviral drug testing.” *Journal of Virology* 36, no. 3 (1992): 209-222.

Brown, Robert, and Jerome Setloff. Composition for a topical cream for curtailing bleeding and treating skin disorders . United States Patent 4331653. 5 May 1982.

Browne, H, B Bruun, and T Minson. “Plasma membrane requirements for cell fusion induced by herpes simplex virus type 1 glycoproteins gB, gD, gH and gL.” *Journal of General Virology* 82 (2001): 1419-1422.

Buhler, V. “Oral and Topical Suspensions.” In *Generic Drug Formulations*, by V Buhler, 422-432. BSAF, 2001.

Bundar, M, et al. “Analysis of iron gall inks by PIXE.” *Nuclear Instruments and Methods in Physics Research Section B: Beam Interactions with Materials and Atoms* 243, no. 2 (2006): 407-416.

Carvalho, D N. “djmcadam.com/medieval-ink.” *D.J.Macadam Where the world goes for free information.* http://www.djmcadam.com/medieval-ink.html (accessed 08 08, 2011).

—. “djmcadam.com/medieval-ink.” *D.J.Macadam Where the world goes for free information.* 9 September 2008. http://www.djmcadam.com/medieval-ink.html (accessed 08 08, 2011).

Chadwar, V, and J Shaji. “Microsponge Delivery |System.” *Current Drug Delivery* 4, no. 2 (2007): 123-129.

Clercq, E D. “Antiviral drugs in current clinical use .” *Katholieke Universiteit Leuven*, 2004.

Corao, G M D. “Antiviral effects of ingredients in the fruit rind of punica granatum L.” School of Pharmacy and biomolecular Sciences. Brighton, University of Brighton., 2001.

Corbo, M, T W Schults, G K Wong, and G A Van Buskirk. “Development and Validation of In Vitro release Testing Methods for Semisolid Formulations.” *Pharmeceutical Technology*, 1993: 112-126.

Cross, S E, B Innes, S M Roberts, T Takuya, T, A Robertson, and P McCormick. “Human Skin penetration of Sunscreen Nanoparticles: In-vitro Assessment of a Novel Micronized Zinc Oxide Formulation.” *Skin Pharmacology and Physiology* 10 (2007): 148-154.

Davidson, Z, N I Nicholson, S P Denyer, and C M Heard. “A novel diffusion cell model for the in vitro assessment of transcutaneous breast cancer therapeutics: Effect of permeants on MCF-7 cells cultured within the receptor compartment.” *European Journal of Pharmaceutics and Biopharmaceutics* 75, no. 3 (2010): 411-417.

Dimmock, N J, and S B Primrose. *Introduction to Modern virology.* 2007.

DOW Chemical Company. *METHOCEL Cellulose Ethers Technical Hand Book.* Technical Hand Book, Philedelphia: DOW Chemical Company, 2002.

Eckhart, L, et al. “Eckhart L Declercq W Ban J, Rendl M, Lengauer B, Mayer C, Lippens S, Vandenabeele P, Tschachler E : Terminal Differentiation on Keratinocytes and Stratum Corneum Formation is Associated with caspase-14 activation.” *Journal of Investigative Dermatology* 115 (2000): 1148-1151.

El-Ashtoukhya, E S Z, N K Amina, and O Abdelwahabb. “Removal of lead (II) and copper (II) from aqueous solution using pomegranate peel as a new adsorbent.” *Desalination*, 2008: 162-173.

Enquist, L W, P J Husak, B W Banfield, and Smith G A. “Infection and spread of alphaherpesviruses in the nervous system.” *Advanced Virus Research* 51 (1999): 237-347.

Epstein, A L, M Yvonne, and B Jacquemont. “In vitro divergence of HSV-1 populations propagated in different cell lines.” *Archives of Virology* 111, no. 1 (1990): 133-140.

Erlich, Kim S, et al. “Acyclovir-Resistant Herpes Simplex Virus Infections in Patients with the Acquired Immunodeficiency Syndrome.” *New England Journal of Medicine*, no. 320 (1989): 293-296.

Escobar-Chávez, J J, et al. “The Tape-Stripping Technique as a Method for Drug Quantification in Skin.” *Journal of Phatreceutical Science* 11, no. 1 (2008): 104-130.

Flint, S J. “Principles of Virology: Molecular Biology, Pathogenesis, and Control.” 18. ASM Press, 2000.

Food and Drug Administration. “U.S. Department of Health and Human Services.” *U.S. Food and Drug Administration.* 26 May 2009. http://www.fda.gov/RegulatoryInformation/Guidances/ucm128179.htm (accessed June 3, 2011).

Gallagher, S J, and C M Heard. “Solvent content and macroviscosity effects on the in vitro transcutaneous delivery and skin distribution of ketoprofen from simple gel formulations.” *Skin Pharmacology and Physiology* 18, no. 4 (2005): 186-194.

Gamer, A O, E Leibold, and B Ravenzwaay. “The in vitro Absorption of Microfine Zinc Oxide and Titanium Dioxide Through Porcine Skin.” *Toxicology in Vitro* 20 (2006): 301-307.

Garner, J A. “Herpes simplex virion entry into and intracellular transport within mammalian cells.” *Advanced Drug Delivery Reviews 55 (2003) 1497– 1513* 55 (2003): 1497-1513.

Gil, A, L M Gutierrez, C Carrasco-Serrano, M T Alonso, S Viniegra, and M Criado. “Modifications in the C Terminus of the Synaptosome-associated Protein of 25 kDa (SNAP-25) and in the Complementary Region of Synaptobrevin Affect the Final Steps of Exocytosis.” *Journal of Biological Chemistry* 227 (2002): 9904-9910.

Gil, M I, F A Tomas- Barberan, B Hess-Pierce, D M Holcroft, and A A Kader. “Antioxidant Activity of Pomegranate Juice and Its Relationship with Phenolic Composition and Processing.” *Journal of Agricultural Food Chemistry* 48 (2000): 4581-4589.

Gil, M I, R Sanchez, J G Marin, and F Artes. “Qualtiy changes in pomegranates during ripening and cold storage.” *European Food Research and Technology* 202, no. 6 (1996): 481-485.

Gould, S w, M D Fielder, A F Kelly, and D P Naughton. “Anti-microbial activities of pomegranate rind extracts: enhancement by cupric sulphate against clinical isolates of S. aureus, MRSA and PVL positive CA-MSSA.” *Complementary alternative medicine,* 2009: 23.

Grolier, J-P E, and J M Rio. “On the Physical Meaning of the Isothermal Titration Calorimetry Measurements in Calorimeters with Full Cells.” *International Journal of Molecular Science* 10, no. 12 (2009): 5296-5325.

Gulsen, D, and A Chauhan. “Dispersion of Microemulsion Drops in HEMA Hydrogel: a Ptential Ophthamlmic Drug Delivery Vehicle.” *International Journal of Pharmeceutics* 292, no. 1-2 (2004): 95-117.

Gunther, R, T. *The Greek Herbal of Dioscorides.* Hafner Publishing Company, 1934.

Guo, J, Y Zhank, and X Q Yang. “A novel enzyme cross-linked gelation method for preparing food globular protein-based transparent hydrogel.” *Food Hydrocolloids* 26, no. 1 (2012): 277-285.

Haidari, M, M Ali, S 3rd Ward Casscells, and M Madjid. “Pomegranate (Punica granatum) purified polyphenol extract inhibits influenza virus and has a synergistic effect with oseltamivir.” *Phytomedicine* 16, no. 12 (2009): 1127-1136.

Hamidi, Mehrdad, Amir Azadi, and Pedram Rafiei. “Hydrogel nanoparticles in drug delivery.” *Advanced Drug Delivery Reviews* 60 (2008): 1638-1649.

Heard, C M, J L Bowen, and S P Denyer. Novel therapeutic delivery system. Great Britain Patent 2 437 806. 1 October 2008.

Heldwein, E E, and C Krummenacher. “ Entry of herpesviruses into mammalian cells.” *Cellular and Molecular Life Sciences* 65 (2008): 1653-1668.

Hoffman, Allan S. “Hydrogels for Biomedical Applications.” *Annals New York Academy of Sciences* 944 (2001): 62-73.

Hoogenraad, T U, J Van Hattum, and C J A Van den Hamer. “Management of wilsons disease with Zinc Sulphate.” *Neurological sciences* 77 (1987): 137-146.

Houben, E. “A Keratinocyte’s Course of Life.” *Skin Pharmacology and Physiology* 20 (2007): 112-132.

Jana Kolara, , , Andrej Štolfaa, Matija StrličbPompeb, M, B Pihlarb, M Budnarc, J Simčičc, and B Reisslandd. “Historical iron gall ink containing documents —

Properties affecting their condition." *Analytica Chimica Acta* 555, no. 1 (2006): 167-164.

Jassim, S A A, G S A B Stewart, and S P Denyer. Antiviral and antifungal composition and method. World Patent 22254. 1995.

Jeans, C W, and C M Heard. "A therapeutic dose of primaquine can be delivered across excised human skin from simple transdermal patches. ." *International journal of Pharmacy*, 1999: 189.

Jingjing, L, W Yun, and Y Qipeng. "Preparative separation of punicalagin from pomegranate husk by high-speed countercurrent chromatography." *Journal of Chromatography*, 2007: 175-179.

Justin-Temu, M, F Damian, R Kinget, and G Van Der Mooter. "Intravaginal Gels as Drug Delivery Sustems." *Journal of Womens Health* 13 (2004): 834-844.

Kawakami, K, T Ihara, T Nishiok, T Kitsuki, and Y Suzuki. "Salt Tolerance of an Aqueous Solution of a Novel Amphiphilic Polysaccharide Derivative." *Langmuir* 22 (2006): 3337-3343.

Keegan, G, J Smart, M Ingram, L Barnes, Rees. G, and G Burnett. "An In-Vitro Assessment of Bioadhesive Zinc/Carbomer Complexes for Antimicrobial Therapy Within the Oral Cavity." *International Journal of Pharmaceutics* (International Journal of Pharmaceutics) 340 (2007): 92-96.

Kligman, A M, and E Christophers. "Preparation of Isolated Sheets of Human Stratum Corneum." *Archives of Dermatology* 88, no. 6 (1963): 702-705.

Kotamballi, N. "Studies on antioxidant activity of pomegranate (Punicagranatum) peel extract using in vivo models." *Agricultural Food Chemistry* 50 (2002): 4791-4795.

Kotwal, G, J. "Genetic diversity-independent neutralization of pandemic viruses (e.g. HIV), potentially pandemic (e.g. H5N1 strain of influenza) and carcinogenic (e.g. HBV and HCV) viruses and possible agents of bioterrorism by enveloped virus neutralizing compounds." *Vaccine*, 2008.

Kros, A, M Gerritsen, V S I Sprakel, N A J M Sommerdijk, J A Jansen, and Nolte R J M. "Silica-based hybrid materials as biocompatible coatings for glucose sensors." *Sensors and Actuators*, 2001: 68-75.

Kulkarni, A P, H S Mahal, S Kapoor, and S M Aradhya. "In Vitro Studies on the Binding, Antioxidant, and Cytotoxic Actions of Punicalagin." *Journal of Agricultural and Food Chemistry* 55 (2007): 1491-1500.

Kulkarni, A P, S M Aradhya, and S Divakar. "Isolation and identification of a radical scavenging antioxidant punicalagin from pith and carpellary membrane of

pomegranate fruit Food Chemistry 87 (2004) 551–557." *Food Chemistry 87 (2004) 551–557* 87, no. 1 (2004): 551-557.

Lamb, Robert A, and Robert M Krug. "Orthomyxoviridae: The Viruses and Their Replication." In *Feilds Virology*, 1370. Lippincott-Raven Publishers, 1996.

Lansdown, A B G, and A Taylor. "Zinc and Titanium Oxides: Promising UV-absorbers but what Influence do they have on the Intact Skin." *International Journal of Cosmetic Science* 19 (1997): 167-172.

Laouini, D, A Elkhal, A Yalcindaq, S Kawamoto, H Oettgen, and R S Geha. "COX-2 inhibition enhances the TH2 immune response to epicutaneous sensitization." *Journal of Allergy and Clinical Immunology* 116, no. 2 (2005): 390-396.

Lardos, A. "The Botanical Materia Medica of the Iatrosophikon. A Collection of Prescriptions From a Monastery in Cyprus." *Journal of Ethnopharmacology* 104, no. 3 (2006): 387-406.

Larrosa, M, et al. "Anti-inflammatory properties of a pomegranate extract and its metabolite urolithin-A in a colitis rat model and the effect of colon inflammation on phenolic metabolism." *The Journal of Nutritional Biochemistry* 21, no. 8 (2010): 717-725.

Lau, W M, A W White, and C M Heard. "Topical delivery of a naproxen-dithranol co-drug: in vitro skin penetration, permeation, and staining." *Pharmaceutical Research* 27, no. 12 (2010): 2734-2742.

Lee, W J, et al. "Ellagic acid inhibits oxidized LDL-mediated LOX-1 expression, ROS generation, and inflammation in human endothelial cells." *Journal of Vascular Surgery* 52, no. 5 (2010): 1290-1300.

Lev, E. "Drugs Held and Sold by Pharmacists of the Jewish Community of Medieval (11-14th Centuries) Cairo According to lists of Materia Medica Found at the Taylor-Schechter Genizah collection Cambridge." (Journal of Ethnopharmacology) 110, no. 2 (2007): 2775-293.

Li, P, et al. "A polycationic antimicrobial and biocompatible hydrogel with microbe membrane suctioning ability." *Nature Materials*, no. 10 (2011): 149-156.

Li, Y, L S Ooi, H Wang, P P But, and V E Ooi. "Antiviral activities of medicinal herbs traditionally used in southern mainland China." *Phytotherapy Research* 18, no. 9 (2004): 718-722.

Lia, G, D Barnes, D Butzb, D Bjorling, and M E Cook. "10t, 12c-Conjugated Linoleic Acid Inhibits Lipopolysaccharide-induced Cyclooxygenase Expression in vitro and in vivo." *Journal of Lipid Research* 46 (2005): 2134-2142.

London Health Sciences Centre. 11 1 2003. http://www.lhsc.on.ca/wound/intro/structure.htm (accessed 1 6, 2008).

Matrosovich, M, T Matrosovich, W Garten, and H-D Klenk. "New low-viscosity overlay medium for viral plaque assays." *Virology Journal* 3 (2006): 63.

McCarrell, E M, S W J Gould, M D Fielder, A F Kelly, W E Sankary, and D P Naughton. "Antimicrobial activities of pomegranate rind extracts:enhancement by addition of metal salts and vitamin C." *Complementary and Alternative Medicine*, no. 8 (2008): 64.

Mettenleiter, T C. "Herpes virus Assembly and Egress." *Journal of Virology* 76, no. 4 (2002): 1537-1547.

Meyera, M, J Kaczab, N Zschemischc, S Godynicki, and J Seeger. "Observations on the Actual Structural Conditions in the Stratum Superficiale Dermidis of Porcine Ear Skin, With Special Reference To Its Use As Model For Human Skin." *Annals of Anatomy* 189 (2007): 143-156.

MHRA. *MHRA.GOV.* 1 04 2011. http://www.mhra.gov.uk/Howweregulate/Medicines/Licensingofmedicines/Clinicaltrials/index.htm (accessed 08 3, 2011).

Murray, M, and M, J Snowden. "The preparation, characterisation and applications of colloidal microgels." (Colloid Interface Science) 54, no. 73 (1995).

Mustafa, C, H Yaşar, and D Gökhan. "Classification of eight pomegranate juices based on antioxidant capacity measured by four methods." *Food Chemisrty* 112, no. 3 (2009): 721-726.

N, Fields. B, D M Knipe, and P M Howley. *Fields Virology.* 5th Edition. Lippincott Williams & Wilkins, 2007.

Nagai, T, Y Miyaichi, T Tomimori, Y Suzuki, and H Yamada. "In vivo anti influenza virus activity of plant flavonoids possessing inhibitory activity for influenza virus sialidase." *Antiviral research*, no. 21 (1993): 289-299.

Nagar, R. "Syntheses, characterization, and microbial activity of some transition metal complexes involving potentially active O and N donor heterocyclic ligands." *Inorganic Biochemistry*, no. 4 (1990): 349-356.

NASA. *http://www.nasa.gov/mission_pages/station/science/experiments/Latent-Virus.html 05/01/2009.* 05 01 2009. http://www.nasa.gov/mission_pages/station/science/experiments/Latent-Virus.html .

Naughton, D. Antimicrobial Composition. United States of America Patent 20100068297. 6 December 2007.

Negi, P, S, and G, K. Jayaprakasha. “Antioxidant and Antibacterial Activities of Punicagranatum Peel Extracts.” *Food Microbology and Safety* 68 (2003): 1136-1553.

Neudeck, A, A Petr, and L Dunsch. “The Redox Mechanism of Polyaniline Studied by Simultaneous ESR-UV-vis SPectroelectrochemistry.” *Synthetic Metals* 107 (1999): 143-158.

Neurath, A R, N Strick, Y Y Li, and A K Debnath. “Punica granatum (Pomegranate) juice provides an HIV-1 entry inhibitor and candidate topical microbicide.” *Infectious Diseases*, 2004: 41.

Newcomb, W W, and J C Brown. “Uncoating the Herpes Simplex Virus Genome.” *Journal of Mollecular Biology* 370, no. 4 (2007): 633-642.

Nigrisa, F, et al. “Effects of a Pomegranate Fruit Extract rich in punicalagin on oxidation-sensitive genes and eNOS activity at sites of perturbed shear stress and atherogenesis.” *Cardiovascular Research* 73, no. 2 (2011): 414-423.

Nikon. *MicroscopyU The Source For Microscopy Education.* 2011. www.microscopyu.com/moviegallery/livecellimaging/rk13/ (accessed 08 11, 2011).

Ojala, P M, B Sodeik, M W Embersold, U Kutay, and Helenius A. “Herpes Simplex Virus Type 1 Entry into Host Cells: Reconstitution of Capsid Binding and Uncoating at the Nuclear Pore Complex In-vitro.” *Molecular and Cell Biology*, no. 20 (2000): 4922-4931.

Osborne, D W, and A H Amann. *Topical Drug Delivery Formulations.* Vol. 42. M. Dekker, 1990.

Panichayupakaranant, P, A Itsuriya, and A Sirikatitham. “Preparation method and stability of ellagic acid-rich pomegranate fruit peel extract.” *Pharmaceutical Biology* 48, no. 2 (2010): 201-205.

Parkinson, I J, and J A Pearce. “Peridotites from the Izu–Bonin–Mariana Forearc (ODP Leg 125): Evidence for Mantle Melting and Melt–Mantle Interaction in a Supra-Subduction Zone Setting.” *Journal of Petrology* 39 (1998): 1577-1618.

Patel, C, P Dadhaniya, L Hingorani, and M G Soni. “Safety assessment of pomegranate fruit extract: Acute and subchronic toxicity studies.” *Food and Chemical Toxicology* 46, no. 8 (2008): 2728-2735.

Poires, W J, J H Henzel, C G Rob, and W H Strain. “Acceleration of Wound Healing in Man With Zinc Sulphate Given by Mouth.” *The Lancet*, 1967: 121-124.

Reddy, M K, S K Gupta, M R Jacob, S I Khan, and D Ferreira. “Antioxidant, antimalarial and antimicrobial activities of tannin-rich fractions, ellagitannins and phenolic acids from Punica granatum L.” *Planta Medica* 73, no. 5 (2007): 461-467.

Rigby, C, and C M Johnson. “Immuno-electron microscopy of herpes simplex virus.” *Canadian Journal of Microbiology* 18 (1972): 1337-1341.

Roizman, B. “Herpesviridae.” In *Feild`s Virology*, by D M Knipe, et al., 2221-2230. Philadelphia: Lippincott Williams & Wilkins, 2007.

Roselli, M, A Finamore, I Garaguso, M S Britti, and E Mengheri. “Zinc Oxide Protects Cultured Enterocytes from the Damage Induced by Escherichia coli.” *Journal of Nutrition* 133 (2003): 4077-4082.

Rosiak, Janusz M, et al. *Radiation Formation of Hydrogels for Biomedical Applications.* The International Atomic Energy Agency's report © 2002, 2002.

Sartorelli, P, et al. “Percutaneous penetration studies for risk assessment .” *The Environmental Toxicology and Pharmacology* 8 (2008): 133-152.

Satomi, H, K Umemura, A Ueno, T Hatano, and T Noro. “Carbonic Anhydrase Inhibitors from the Pericarps of Punica granatum L.” *Biological and Pharmaceutical Bulletiin* 16 (1993): 787-790.

Satomi, H, K Umemura, A Ueno, T Hatano, T Okuda, and T Noro. “Carbonic anhydrase inhibitors from the pericarps of Punica granatum L.” *Biolgical Pharmaceutical Bulletin*, 1993: 787-790.

Scheuplein, R J, and I H Blank. “Permeability of the skin.” *Physiological Review* 51 (1971): 702-742.

Schuhmacher, A, J Reichling, and P Schnitzler. “Virucidal effect of peppermint oil on the enveloped viruses herpes simplex virus type 1 and type 2 in vitro.” *Phytomedicine* 10, no. 6 (2003): 504-510.

Searby, C. “Development of a Topical Formulation for the Treatment of Basal Cell Carcinoma.” PhD Thesis, Welsh School of Pharmacy, Cardiff University, 2011.

Seeram, N P. “Pomegranates Ancient Roots to Modern Medicine.” In *Pomegranates Ancient Roots to Modern Medicine*, by N P Seeram, R N Schulman and D Heber, 20-34. Taylor Francis Group, 2006.

Seeram, N P. “Pomegranates Ancient Roots to Modern Medicine.” In *Pomegranates Ancient Roots to Modern Medicine*, by N P Seeram, R N Schulman and D Heber, 193-195. Taylor Francis Group, 2006.

Seeram, N P, R Schulman, and D Herber. *Pomegranates: Ancient Routes to Modern Medicine.* CRC press, 2006.

Seeram, N, P, L, S Adams, S, M Henning, y Niu, Y Zhang, and M, G Nair. “In vitro Antiproliferative, Apoptopic and Antioxidant Activities of Punicalagin, Ellagic acid and a Total Pomegranate Tannin Extract are Enhanced in Combination with Other

Polyphenols as Found in Pomegranate Juice." *Nutritional Biochemistry* 16 (2005): 360-367.

Seeram, N, R Lee, M Hardy, and D Heber. "Rapid Large Scale Purification of Ellagitannins from Pomegranate Husk, a by-product of the Commercial Juice Industry." *Separation and Purification Technology* 41 (2005): 49-55.

Sekkat, N, Y N Kalia, and R H Guy. "Porcine ear skin as a model for the assessment of transdermal drug delivery to premature neonates." *Pharmaceutical Research* 21, no. 8 (2004): 1390-1397.

Sestili, P, M Chiara, and S Vilberto. "Cytoprotective Effect of Preparations from Various Parts of Punica Granatum L. Fruits in Oxidatively Injurred Mammalina Cells in Comparison with their Antioxidant Capacity in Cell Free Systems." *Pharmacological Research* 56 (2007): 18-26.

Sheets, R. *History and Characterization of the Vero Cell Line.* Vaccines and Related Biological Products Advisory Committee Report, Food and Drugs Administration, 2000.

Sherris, J. In *Medical Microbiology an Introduction to Infectious Diseases*. 1990.

Shogan, B, L Kruse, G B Mulamba, A Hu, and D M Coen. "Virucidal Activity of a GT-Rich Oligonucleotide against Herpes Simplex Virus Mediated by Glycoprotein B." *Journal of Virology*, 2006: 4740-4747.

Simon, G A, and H I Maibach. "The pig as an experimental animal model of percutaneous permeation in man: Qualitative and quantitative observations – an overview." *Skin Pharmacology Applications* 13 (2000): 229-234.

Singh, V P, and A Katiyar. "Synthesis, spectral characterization and antimicrobial activity of some transition metal(II) complexes with acetone p-amino acetophenone benzoylhydrazone." *Pesticide Biochemistry and Physiology* 92, no. 1 (2008): 8-14.

Slusarczyk, S, M Hajnos, K Skalicka-Wozniak, and A Matkowski. "Antioxidant activity of polyphenols from Lycopus Lucidus Turcz." *Food Chemistry*, 2009.

Smith, J S, A Melendy, R K Rana, and J M Pimenta. "Age-Specific Prevalence of Infection with Human Papillomavirus in Females: A Global Review." *Journal of Adolescent Health* 43, no. 4 (2008): 5-62.

Song, J M, K H Lee, and B L Seong. "Antiviral effect of catechins in green tea on influenza virus." *Antiviral research*, no. 64 (2005): 66-74.

Staniforth, J. "Rheometers." In *Pharmeceutics*, by Staniforth, edited by M E Aulton, 197. New York: Churchil Livingston, 2002.

Stewart, G S A B, S A A Jassim, and S P Denyer. “The Specific and sensitive detection of bacterial pathogens within 4 h using bacteriophage anmplification.” *Applied Microbiology*, 1998: 777-783.

Stewart, G S A B, S A A Jassim, S P Denyer, P Newby, K Linley, and V K Dhir. “The specific and sensitive detection of bacterial pathogens within 4 h using bacteriophage amplification.” *Journal of Applied Microbiology* 84 (1998): 777-783.

Subramanian, R P, and R J Geraghty. “Herpes simplex virus type 1 mediates fusion through a hemifusion intermediate by sequential activity of glycoproteins D, H, L, and B.” *Proceedings of the National Academy of Sciences* 104, no. 8 (2007): 2903-2908.

Sundararajan, A, R Ganapathy, L Huan, R J Webby, R J Dunlap, G J Kotwald, and Y M Sangstera. “Influenza virus variation in susceptibility to inactivation by pomegranate polyphenols is determined by envelope glycoproteins.” *Antiviral Research* 88 (2010): 1-9.

Swierksz, E M, R L Hodinka, B M Moore, S Sacks, D R Scholl, and D K Wright. “Antiviral Susceptibility Testing: Herpes Simplex Virus by Plaque Reduction Assay; Approved Standard.” *Clinical Laboratory Standards Institute*, 2004: 1-39.

Thomas, C P, Z Davidson, and C M Heard. “Probing the skin permeation of fish oil/EPA and ketoprofen-3. Effects on epidermal COX-2 and LOX.” *Prostaglandins, Leukotrienes and Essential Fatty Acids* 76, no. 6 (2007): 357-362.

Tonic-Ribarska, J, S Trajkpvic-Jolvska, K Milenkova, K Goracinova, M Glavas-Dodov, and A Dimitrovska. “Simultaneous Determination of Diazepam and Preservativesin HPMC Hydrogel by HPLC.” *Bulletin of the Chemists and Technologists of Macedonia* 24, no. 2 (2005): 103-108.

Topley, W W C, and G S Wilson. *Topley & Wilson's Principles of bacteriology, virology and immunity.* Vol. four, edited by M T Parker and B I Duerden, 419. B.C. Decker, 1990.

Turk, G, et al. “Effects of Pomegranate Juice Consumption on Sperm Quality, Spermatogenic Cell Density, Antioxidant Activity and Testosterone Level in Male Rats.” *Clinical Nutrition* , 2008.

Valenta, C, and K Schultz. “Influence of Carrageenan on the Rheology and Skin Permeation of Microemulsion Formulations.” *Journal of Controlled Release* 95, no. 2 (2004): 257-265.

Wagner, E K. *Herpes simplex virus research.* 1 10 2003. http://www.dbc.uci.edu/~faculty/wagner/hsv4f.html (accessed 04 05, 2011).

Wang, R, Y Ding, R Liu, L Xiang, and L Du. “Pomegranate: Constituents, Bioactivities and Pharmacokinetics.” *Fruti, Vegetable and Cereal Science and Biotechnology* 4, no. 2 (2010): 77-87.

Ward, Cheryl. “Pomegranates in eastern Mediterranean contexts during the Late Bronze Age.” (World Archeaology) 34, no. 3 (2003): 529-541.

Watson, D G. *Pharmaceutical Analysis: A Textbook for Pharmacy Students and Pharmaceutical Chemists.* 2nd Edition. Edinburgh: Elsevier, 2005.

Weatherall, J, J G Gledingham, and D A Warrell. *Oxfrod Text Book of Medicine.* Vol. 1, 343. Oxford University Press, 1996.

Weerheim, A, and M Ponec. “ Determination of stratum corneum lipid profile by tape stripping in combination with high-performance thin-layer chromatography.” *Archives of Dermatological Research* 293 (2001): 191-199.

Weerheim, A, and M Ponec. “Determination of stratum corneum lipid profile by tape stripping in combination with high-performance thin-layer chromatography.” *Archives of Dermatological Reseach* 293 (2001): 131-199.

Whitley, R J, and J W Jr Gnann. “Acyclovir: a decade later.” *New England Jounral of Medicine*, 1992: 782.

Whitley, R J, and R Roizman. “Herpes simplex virus infections.” *The Lancet* 357, no. 9267 (2001): 1513-1518.

Wichterle, O, and D Lim. “Hydrophilic Gels for Biological Use.” *Nature* 185 (1960): 117-118.

Williams, A C. “The Structure and Function of th Skin.” In *Transdermal and Topical Drug Delivery*, by A C Williams, 1-13. London: Pharmeceutical Press, 2003.

Williams, A C, and W Barry. “The enhancement index concept applied to terpene penetration enhancers for human skin and model lipophilic (oestradiol) and hydrophilic (5-fluorouracil) drugs.” *International Journal of Pharmacy* 74 (1991): 157-168.

Wilson, K, and J Walker. *Principles and Techniques of Biochemistry and Molecular Biology.* Cambridge University Press, 2010.

Wu, X, Y, and Y Zhou. “Studies of diffusional release of a dispersed solute from polymeric matrixes by finite element method.” (Journal Pharmaceuticle science), no. 10 (1999): 1050-1057.

X Herpes. *XHERPES.com.* 16 March 2011. http://www.xherpes.com/herpespictures.php (accessed August 22, 2011).

Zandi, K, et al. “Evaluation of antiviral activities of curcumin derivatives against HSV-1 in Vero cell line.” *National Product Communications* 12 (2010): 1935-1938.

Zhang, J, B Zhan, X Yao, Y Gao, and J Shong. “Antiviral activity of tannin from the pericarp of Punica granatum L. against genital Herpes virus in vitro.” *Zhongguo Zhong Yao Za Zhi* 20, no. 9 (1995): 556-558.

Zulfakar, M H, N Abdelouahab, and C M Heard. “Enhanced topical delivery and ex vivo antiinflammatory activity from a betamethasone dipropionate formulation containing fish oil.” *Inflammatory Research* 59, no. 1 (2010): 23-30.

Zulfakar, M H, N Abdelouahab, and C M Heard. “Enhanced topical delivery and ex vivo anti-inflammatory activity from a betamethasone dipropionate formulation containing fish oil. Inflammation Research, 59 (2010)23-30.” *Inflammation Research* 59, no. 1 (2010): 23-30.